Coláiste na hOllscoile Corcaigh, Éire
University College Cork, Ireland

Microbes for Life; Investigating the effects of oral administration of *Lactobacillus mucosae* DPC 6426 on cardiometabolic parameters

A Thesis Presented to the National University of Ireland for the Degree of

Doctor of Philosophy

By

Aoife O Donovan, BSc.

(116224273)

School of Microbiology, University College Cork, Ireland

APC Microbiome Institute, University College Cork, Ireland

Food Biosciences, Teagasc Food Research Centre, Moorepark, Fermoy, Co. Cork, Ireland

June 2021

Under the Supervision of:

Professor Catherine Stanton and Professor R. Paul Ross

Head of School of Microbiology: Professor Paul O'Toole

Table of Contents

List of Tables and Figures

Chapter 1

Chapter 2

Chapter 3

Chapter 4

Chapter 5

List of Abbreviations

CVD – cardiovascular disease

SCFA – Short-chain fatty acids

TMAO – trimethylamine-N-oxide

CHD – coronary heart disease

MetS – metabolic syndrome

BMI – body mass index

TIMI – thrombolysis in myocardial infarction

HDL – high-density lipoprotein

LFL – low-density lipoprotein

VLDL – very low-density lipoprotein

LDLr-/- - lipoprotein receptor deficient

apoE-/- - apolipoprotein E-deficient

E3L – ApoE*3-Leiden

NC – normal chow

HFHC – high fat, high cholesterol

LDLr – lipoprotein receptor

LRPs – LDLr related proteins

LFLC – low fat, low cholesterol

CNS – central nervous system

FD – familial dysbetalipoproteinemia

LPL – lipoprotein lipase

angptl4 – angiopoietin-like protein 4

WHHL – Watanabe Heritable Hyperlipidemic

FH – familial hypercholesterolemia

WHHLMI – Watanabe Hyperlipidemic Myocardial Infarction

SMC – smooth muscle cells

TMA – trimethylamine

NAFLD – non-alcoholic fatty liver disease

MI – myocardial infarction

Bas – bile acids

DCA – deoxycholic acid

LPS – lipopolysaccharide

TLRs – toll like receptors

NF-κB – nuclear factor kappa-light-chain-enhancer of activated B cells

TC – total cholesterol

LDL-C – low-density lipoprotein-cholesterol

HDL-C – high-density lipoprotein-cholesterol

CRP- C-reactive protein

GLP-1 – glucagon like peptide-1

PYY – peptide YY

ACE – angiotensin-covering enzyme

RCT – randomised control trial

SBP – systolic blood pressure

DBP – diastolic blood pressure

IL- -interleukin

TNF-α – tumour necrosis factor-alpha

sVCAM-1 – soluble vascular cell adhesion molecule-1

NO – nitric oxide

LcS – *Lactobacillus casei* Shirota

lFAAP – lactofermented Annurca apple puree

FAO – The Food and Agricultural Organisation of the United Nations

WHO – World Health Organisation

EPS – exopolysaccharide

MFRC – Moorepark Food Research Centre

IBD – inflammatory bowel disease

IBS – irritable bowel syndrome

DPC – Dairy Product Culture Collection

LAB – lactic acid bacteria

mMRS – modified de Man, Rogosa and Sharpe

MRD – maximum recovery diluent

BHI – brain heart infusion

IPAQ – international physical activity questionnaire

AEs – adverse events

SAEs – severe adverse events

FFQ – food frequency questionnaire

GMP – good manufacturing practice

LBS – *Lactobacillus* selection

ACN – acetonitrile

LLE – liquid-liquid extraction

UHPLC-ESI-QqQ-MS – ultra high performance liquid chromatography-electrospray ionisation-triple quadrupole-mass spectrometry

MS – mass spectrometry

IS – internal standard

DOPAC – 3,4-Dihydroxyphenylacetic acid

DOPAC-d5 - 3,4-Dihydroxyphenylacetic acid-d5

HVA – Homovanillic acid

RP – reverse phase

MeOH – methanol

HILIC – hydrophilic interaction liquid

LOCF – last observation carried forward

ITT – intention to treat

PP – per protocol

TFLs – tables, figures and listings

TEAE – treatment-emergent adverse events

PLS-DA – partial least squared-discriminate analysis

HFD – high fat, salt and sugar diet

FLASH- fast length adjustment of short reads to improve genome assemblies

QIIME – quantitative insights into microbial ecology

GC-MS – gas chromatography-mass spectrometry

QC – quality control

LVED – left ventricular end-diastolic pressure

KCs – Kupffer cells

NASH – non-alcoholic steatohepatitis

FXR – farnesoid X receptor

TGR5 – Takeda G protein-coupled receptor 5

CAD – coronary artery disease

FMT – faecal microbiota transplant

HOMA – homeostatic model assessment

HOMA-IR - homeostatic model assessment of insulin resistance

HF-pEF – heart failure with preserved ejection fraction

BSH – bile salt hydrolase

HPRA – Health Products Regulatory Authority

DOCA – deoxycorticosterone acetate

RBB+C – repeat bead beating plus column

PyNAST – Python Nearest Alignment Space Termination

PCoA – principal co-ordinate analysis

FDR – false discovery rate

LVH – left ventricular hypertrophy

LA – left atrium

LV – left ventricle

PCA – principal component analysis

ISAPP – International Scientific Association for Probiotics and Prebiotics

FOS - fructooligosaccharides

GOS - galactooligosaccharides

XOS – xyloseoligosaccharides

LB – *Lactobacillus*

Fib – Fibre

PD – Phylogenetic Distance

Declaration

This is to certify that the work I am submitting is my own and has not been submitted for another degree, either at University College Cork or elsewhere. All external references and sources are clearly acknowledged and identified within the contents. All of the work herein was performed independently by the author, with the following exceptions:

Chapter 1. Aoife O Donovan is joint-first author with Dr. Kiera Murphy. Published in part in MDPI Metabolites

Chapter 3. Noel Caplice, Catherine Stanton, Paul Ross and the Atlantia Food CRO team designed the study, Lis London performed microbiological analysis, Dr. Fiona Fouhy performed bioinformatic analysis and Aoife O Donovan carried out all analysis relating to the gut microbiome. Dr. Andrea Anesi performed plasma and urine metabolite analysis.

Chapter 4. Aoife O Donovan is joint-first author with Dr. Florence Herisson in the published manuscript 'Gut microbiome of a porcine model of metabolic syndrome' Dr. Fiona Fouhy performed bioinformatic analysis

Chapter 5. Noel Caplice, Catherine Stanton and Paul Ross designed the study, Dr. Florence Herisson performed body weight analysis, Aoife O Donovan and Dr. Florence Herisson performed microbiome analysis together, Dr. Kiera Murphy performed bioinformatic analysis.

Signed Aoife O Donovan

Aoife O Donovan, June 2021

ABSTRACT

Metabolic syndrome (MetS) is a cluster of cardiometabolic risk factors, including obesity, dyslipidaemia, hypertension and insulin resistance, with a range of secondary conditions such as non-alcoholic fatty liver disease (NAFLD) and heart failure and has been identified as one of the major global health challenges of the 21st century. This thesis outlines the role the gut microbiome has in the progression of the associated risk factors and alternative therapeutic approaches for cardiovascular disease prevention. In Chapter 1, the importance of the gut microbiome and use of clinical scale models are discussed with a view towards identifying key gut microbiota which are associated with the risk factors for cardiovascular disease development, and how different pre-clinical animal models can assist in understanding the underlying mechanisms of disease, test procedures and develop appropriate therapeutic interventions that will yield the highest reproducible results. In Chapter 2, a method was developed in order to optimise cultivation and freeze-drying of *Lactobacillus mucosae* DPC 6426, an exopolysaccharide (EPS)-producing lactic acid bacteria (LAB), previously shown to reduce serum cholesterol in the apoE model of lipid driven atherosclerosis [1] at a minimum concentration of 10^9 CFU/g in order to achieve a minimum concentration of 10^{10} CFU/g following freeze-drying and subsequent storage at -30°C. In Chapter 3, the efficacy of oral supplementation with *Lactobacillus mucosae* DPC 6426 at a minimum concentration of 10^9 CFU/g on reducing cholesterol levels in mildly hypercholesterolaemic (≥5mmol/L and <7.5mml/L) adults over a 12-week period was investigated. Results indicated that supplementation with *Lb. mucosae* DPC 6426 had no significant effects on the serum lipid profiles (total cholesterol, LDL-cholesterol, HDL-cholesterol and triglycerides). Additionally, there were no

significant changes observed in the gut microbiota diversity between the placebo group and probiotic group. These results suggest that a minimum concentration of 10^9 CFU/g may be insufficient to have a significant effect on serum lipid profiles and gut microbiota diversity, prompting future investigations to be carried out. In Chapter 4, a porcine model of diet- and mineralocorticoid-induced metabolic syndrome (MetS) and heart failure with preserved ejection fraction (HF-pEF) was developed, in which this model closely mimicked the cardiovascular, metabolic, gut microbiome and metataxonomic phenotype observed in human studies. Following feeding of a high fat diet (HFD) for a period of 12 weeks, all animals developed obesity, hyperlipidaemia, insulin resistance, hypertension, fatty liver disease, structural cardiovascular changes and also a reduction in α-diversity and specific microbiota changes, in particular increased abundances of pro-inflammatory bacteria, *Fusobacteriaceae*, *Enterobacteriaceae*, and *Veillonellaceae* at family level and *Fusobacterium*, *Methanosphaera*, and *Acidaminococcus* at genus level, and a reduction in short-chain fatty acid-producing bacteria *Lachnospiraceae*, *Rikenellaceae* and *Akkermansia* in the porcine gut. In Chapter 5, using the previously established porcine model of MetS, the efficacy of daily oral supplementation of *Lb. mucosae* DPC 6426 and fibre, singly, or in combination, on the gut microbiome composition was investigated. Animals were fed a high fat, sugar and salt diet over 12 weeks combined with either *Lb. mucosae* DPC 6426 (10^{10} CFU/g/day) and fibre, alone, or in combination. All animals developed obesity, however the percentage of weight gained was reduced from week 6 and was significantly decreased at week 12 in animals supplemented with *Lb. mucosae* DPC 6426 and fibre compared to animals receiving *Lb. mucosae* DPC 6426 and fibre, singly, or no dietary supplementation. Overall results of this study have indicated

that supplementation with fibre alone and in combination with *Lb. mucosae* DPC 6426 has a significant effect on the composition of the gut microbiota. Furthermore, results have indicated that fibre acts in combination with *Lb. mucosae* DPC 6426 to increase existing anti-inflammatory gut microbiota, suggesting that supplementation of a combination of *Lb. mucosae* DPC 6426 and fibre could provide a new, novel therapeutic approach in the treatment of the gut microbiota compositions alterations associated with MetS.

In conclusion, this thesis has shown that the use of larger pre-clinical animal models are paramount in order to translate reproducible results from a pre-clinical animal model to a human clinical setting, with regards to understanding the underlying mechanisms of disease, in particular Mets, and the potential advantages of using novel gut microbiota targeted therapeutics, such as probiotics and combination therapies, on MetS-associated risk factors.

Chapter 1.

Exploring Cardiovascular Disease Mechanisms; Animal Models and Gut Microbiota

Dr. Kiera Murphy contributed to the section on ‘Probiotics and Cardiovascular Disease’

1.1 Abstract

Cardiovascular disease (CVD) has been classified as one of the leading causes of morbidity and mortality worldwide. CVD risk factors include smoking, hypertension, dyslipidaemia, obesity, inflammation and diabetes. Pre-clinical animal models are crucial for understanding disease mechanisms and guiding the improvement of current diagnostic and treatment methods for cardiovascular pathologies. Here we describe several small and large animal models of CVD including mice, rabbits and pigs and their associated strengths and limitations. The gut microbiota can influence human health through multiple interactions and community changes are associated with the development and progression of numerous disease states, including CVD. The gut microbiota are involved in the production of several metabolites, such as short-chain fatty acids (SCFA), bile acids (BAs) and trimethylamine-N-oxide (TMAO). These products of microbial metabolism are important modulatory factors and have been associated with an increased risk of CVD. Due to its association with CVD development the gut microbiota has emerged as a target for therapeutic approaches particularly probiotics. In this review, we discuss the current knowledge on the function of the gut microbiome in human health, its links to CVD, and probiotic interventions aimed at ameliorating gut microbiome changes and prevention of CVD.

1.2 Introduction

Cardiovascular disease (CVD) is a general term for a number of pathologies including coronary heart disease (CHD), cerebrovascular disease, peripheral artery disease, congenital and rheumatic heart disease and venous thromboembolism [2]. CVD has been classified as one of the leading causes of morbidity and mortality worldwide, which in turn has led to extensive health and economic burdens [3], accounting for approximately one in every three deaths in the United States and one in every four deaths in Europe [4]. The World Health Organisation (WHO) has estimated that over 75% of premature CVD is avoidable and risk factor improvement can help in the reduction of the growing incidence of CVD on both individuals and healthcare systems [5].

As CVD is a chronic progressive condition, its development often begins with risk factors such as smoking, hypertension, dyslipidaemia, obesity and inflammation, which leads to irreversible damage to vascular structures in the form of atherosclerosis and often detrimental clinical outcomes such as arterial thrombosis, myocardial infarction and stroke [6]. Assessment and treatment of several modifiable risk factors which have been established by evidence-based guidelines, to optimally manage patients with or at high risk of developing CVD are needed [7]. These modifiable risk factors include use of tobacco, lack of physical exercise, and a number of interrelated interruptions of vascular and metabolic functions, commonly referred to as metabolic syndrome (MetS). It has also been reported that some risk factors for developing CVD vary by race, ethnicity and gender. Obesity for example is particularly common in non-Hispanic black women [8]. Chinese and South Asian individuals may develop type II diabetes, hypertension or dyslipidaemia at a lower body mass index (BMI) compared with individuals of European descent [9]. One

possible explanation suggested is that non-European individuals have been shown to have a higher body fat percentage or a lower lean body mass compared to European individuals [10, 11].

Investigating the mechanisms of human disease is a complex and often difficult task. The use of pre-clinical animal models allows researchers to fully investigate and manipulate a number of pathophysiological processes as well as aiding in understanding the underlying mechanisms of disease onset and progression [12]. Although no "gold-standard" animal model of CVD exists, there are several advantages to using large animal models over small animal models for *in vivo* studies. These include (i) they are most physiologically similar to humans compared to small animal models such as mice and rats (ii) they allow for chronic studies to be performed, (iii) they allow for cardiac functions and responses to be assessed and (iv) they are considered to be the most suitable model for new drug discovery, screening and toxicity testing, due to their similarity to humans in terms of molecular mechanisms [13]. The use of large animal models can be extended further through the use of genetically modified animals in which specific disease states can be induced [14]. There are disadvantages attached to the use of large animal models as these models are more expensive to purchase, house and care for in animal facilities, as well as limitations associated with follow-up period and the availability of biomarkers to study specific histology [14, 15].

The human body harbours trillions of microbial cells that form a complex microbial community in the intestine known as the gut microbiota. The gut microbiota works in conjunction with the host's defence and immune systems to protect against pathogen infiltration and colonisation, as well as performing essential metabolic functions, serving as a source of essential nutrients and vitamins and assisting in

energy and nutrient extraction, such as short chain fatty acids (SCFAs) and amino acids, from food [16, 17]. Shifts in the composition of the gut microbiota disrupts homeostasis and have been associated with long-term consequences leading to disorders including CVD. 16S rRNA gene sequencing and whole shotgun metagenomic sequencing have added to the growing evidence which suggests that alterations of the gut microbiome composition effects the pathogenesis of CVD [18-21]. In addition to the composition of the gut microbiota, metabolites produced by these microbes can enter into the circulation and act as a modifier of gut microbial effects on the host [22, 23]. A number of microbiome studies have shown a potential link between microbial metabolites including SCFAs, BAs and TMAO and CVD [24-26]. Given the growing evidence linking the gut microbiota with the development with CVD, therapies such as probiotics aimed at modulating the gut microbiota have been suggested among the most promising strategies to prevent CVD.

1.3 Cardiovascular Disease Risk Factors

Two major studies conducted in the latter half of the 20th century, the Framingham Heart Study [27] and the Seven Countries Study [28], made substantial contributions in identifying the major risk factors for the developing CVD. Risk factors identified as being implicated in the initiation and progression of CVD include inflammation, hypertension, dyslipidaemia, type-2 diabetes, insulin resistance, metabolic syndrome (MetS), obesity and health behaviours, such as smoking, lack of exercise and poor dietary habits [29, 30]. With the steady increase in the incidence of risk factors for CVD more effective approaches are needed to prevent and/or modify the course of CVD and risk reduction is considered critical. The large international study,

INTERHEART [31], carried out between 1990 and 2010, found that traditional risk factors account for over 75% of CVD risk factors, with smoking and dyslipidaemia considered two of the most important risk factors globally, closely followed by abdominal obesity, diabetes and hypertension. The study also found that subjects with no identifiable risk factors, were at a higher risk of mortality, based on a higher Killip class and TIMI (thrombolysis in myocardial infarction score) [32]. The Killip classification is used in individuals with an acute myocardial infarction to predict and stratify their risk of mortality [33]. The TIMI risk score is used to determine the likelihood of ischemic events or mortality in patients with unstable angina or non–ST-segment elevation myocardial infarction [34]. Therefore, it is important to remember that the absence of risk factors should not be seen as encouraging in terms of a favourable prognosis.

A study carried out by Khot et al. [35] found that in patients with CHD, traditional risk factors were present at a much higher prevalence than previously thought, with only between 15 and 20% of patients presenting with none of the traditional risk factors for the disease. At least 25% of future events will occur in individuals that only have one of the traditional risk factors. This study reported that the prevalence of risk factors associated with CHD was higher in women than men, due to the disease typically presenting in females up to 10 years later than men. This finding suggests that higher risk factor prevalence is needed to lead to the development of the disease at the same age as seen in men [35]. The Rancho Bernardo Study, carried out by Barrett-Connor et al. [36] found that the prevalence of diabetes is higher in women compared to men and has been shown to be a significant risk factor for the development of CHD in women, thus reversing the usual protection women are thought to have against CVD [36]. The single risk factor that appeared to have a

lower prevalence in women was cigarette smoking, however it has been shown that women under the age of 65 smoked at a nearly identical rate to men, demonstrating that smoking has similar effects on the increased risk of CHD in both men and women [37].

It has also been seen that specific ethnic groups experience a disproportionally higher incidences of CVD, including CHD and stroke. A Westernised lifestyle has been shown to have different effects on the vascular and metabolic functions across different populations. South Asian individuals have been seen to have a higher incidence of CHD and coronary mortality compared to European individuals. African-American individuals have higher incidences of CHD while African/Caribbean individuals residing in the UK have lower incidences of CHD and higher incidences of stroke than British Europeans [38]. It was also reported that Chinese and Japanese individuals have higher incidences of stroke but not CHD. Mexican Americans have a higher incidence rate of both CHD and stroke, and North American native Indians also have higher incidences of CHD. The obvious and significant differences seen across both racial and ethnic groups in terms of disease risk are likely attributed to, host genetics, host susceptibility and response to treatment [38].

1.4 Animal Models of Cardiovascular Disease

Animal models have proven to be an invaluable tool for investigating the multifactorial pathologies associated with CVD development, including both genetic and environmental factors. Described here is a summary of the most well-known animal models of CVD, including both small and large animal models. Table 1 shows a summary of the advantages and limitations associated with the most common animal models of CVD.

Table 1. Strengths and Limitations of Animal Models of CVD

	Strengths	Limitations
Mouse	1. Rapid atherosclerotic plaque development 2. Short reproductive cycle and produce large litters 3. Genome is well-known 4. Easy to manipulate the genome 5. Low cost 6. Useful for non-invasive imaging studies 7. Extensive knowledge surrounding use of mouse models	1. Genetically only partially mimic human disease 2. Extremely high blood lipid levels 3. Atherosclerotic model rather than atherothrombosis model 4. Size related systemic effects not translatable to humans
Rabbit	1. Medium sized model 2. Fibroatheroma lesions (lipid-rich core surrounded by collagen-rich fibrous tissue) 3. Useful for studying stenosis 4. Low cost/affordable	1. Absence of plaque rupture model 2. Neointima formation model rather than atherosclerotic model 3. Requires high blood cholesterol levels
Pig	1. Anatomy, lipid profiles and lipoprotein metabolism similar to humans 2. Atherosclerotic plaques similar to those In humans 3. Verified for use in stenosis studies	1. Expensive 2. Difficult to handle 3. Few genomic tools available

1.4.1 Mouse Models

Mouse models have proven to be a useful resource to study and evaluate the development and progression of CVD particularly atherosclerotic lesions [39-41]. Knockout and transgenic mouse models for atherosclerosis have played a key role in

understanding the mechanisms that are involved in atherosclerosis. These models have also been useful in studying the effectiveness of new and existing drug therapies aimed at the treatment of CVD risk factors such as hypercholesterolemia, hypertriglyceridemia, hypertension and inflammation [42]. Wild-type mice display resistance to development of atherosclerotic lesions, due to high levels of antiatherosclerotic high-density lipoproteins (HDL) and low levels of proatherogenic low-density lipoproteins (LDL) and very low-density lipoproteins (VLDL) [42]. Moreover, mice are nocturnal herbivores unlike humans who are omnivores. As such mouse models used to study atherosclerosis are typically based on the genetic modifications of lipoprotein metabolism combined with dietary changes. The most commonly used are the low-density lipoprotein receptor deficient mouse model (LDLr -/-), where it has been demonstrated that feeding a lipid-rich diet resulted in the development of atherosclerosis, and the apolipoprotein E-deficient mouse model (apoE -/-), where the targeted deletion of the apoE gene led to high cholesterol and atherosclerosis. Atherosclerotic lesions in these models are aggravated and worsened by risk factors such as hypertension and diabetes [43]. Another mouse model that has emerged as a novel transitional disease model for atherosclerosis is the ApoE*3-Leiden (E3L) transgenic mouse. Here a mutation of the human apoE3 genes was introduced which resulted in the development of a hyperlipidemic phenotype, and the development of atherosclerosis when fed cholesterol. This model is also more sensitive to exposure to lipid-lowering drugs, compared to the ApoE -/- and LDLr -/- mouse models [42, 44].

As seen in human subjects, a mutation in the LDLr gene results in familial hypercholesterolemia. Mice lacking the LDLr gene exhibit a moderate increase in plasma cholesterol concentrations (5 mmol/L vs 2 mmol/L in wild-type animals) and

develop atherosclerosis slowly when fed a normal chow (NC) diet. However when fed a high fat, high cholesterol (HFHC) diet, cholesterol levels elevate rapidly (>25 mmol/L) and the onset of atherosclerosis is rapid [45, 46]. LDLr-/- mice also display a large increase in plasma LDL cholesterol concentrations and also develop atherosclerosis when fed a low-fat diet when they are coupled with an ApoB-editing deficiency (LDLr-/-/ApoBEC-/-) or combined with human ApoB100 transgenic mice (LDLr-/-/ApoB+/+) [42, 47]. Studies have shown that the LDLr-/- and the LDLr and apoE double-deficient (LDLr-/-apoE-/-) mouse models vary in their responses to lipoprotein lowering drugs, from lowering of plasma cholesterol concentrations without a decrease in atherosclerosis incidence to a reduction of weak atherosclerotic lesions with or without lowering plasma cholesterol concentrations [42, 43, 48]. ApoE has numerous important antiatherogenic functions within the host. As a component of plasma lipoproteins, such as VLDL and HDL, it acts as a ligand for the cell-surface lipoprotein receptors such as LDL-receptor (LDLr) and LDLr-related proteins (LRPs) assisting in the clearance of these atherogenic particles from circulation [45]. It also plays a key role in transporting cholesterol through interactions with the LDL receptor [49]. In 1992, studies by Zhang et al.[50] and Plump et al. [51] resulted in the apoE-/- mouse model through homologous recombination in embryonic stem cells [50, 51]. Both studies showed that deletion of the apoE gene in mice resulted in dramatically increased plasma concentrations of VLDL and LDL, and correlated with the failure of LDLr- and LPR- mediated clearance of these atherogenic lipoproteins from circulation. Plump et al. observed that the apoE-/- mice consuming a low fat, low cholesterol (LFLC) diet had a plasma cholesterol level of 494 mg/dL compared with 60 mg/dL in the control animals. When the apoE-/- mice were fed a HFHC diet, the plasma cholesterol level

dramatically increased to 1821 mg/dL compared to 132 mg/dL in the control. It was also observed that by ten weeks of age, the apoE-/- mice had already developed atherosclerotic lesions in the aorta and the coronary and pulmonary arteries [51]. Similar results were observed by Zhang et al., which also showed that the spontaneous lesions which developed by three months of age caused severe blockage of the coronary artery opening by eight months of age [50]. Results from these studies demonstrated that the apoE-/- mouse is a valuable model for investigating genetic and environmental factors that affect the development and progression of atherosclerosis. There are some limitations attached to this model, particularly that it is dominated by high levels of cholesterol in the plasma. For example, when consuming an NC diet, plasma cholesterol levels are around 8 mmol/L, compared to 2 mmol/L for the parent C57B1/6 mouse, and can increase to >70 mmol/L when consuming a HFHC diet [42, 48]. Another limitation of this model is that most of the cholesterol in the plasma is VLDL, compared to LDL in humans. Additionally, there is growing evidence that apoE proteins have additional antiatherogenic properties to the regulation of lipoprotein clearance, including coagulation, oxidative processes, macrophage, neuronal and non-neuronal cell homeostasis, adrenal function, central nervous system (CNS) physiology, inflammation and cell proliferation [52].

Familial dysbetalipoproteinemia (FD) or type III hyperlipoproteinaemia [53] is an uncommon lipoprotein metabolism disorder. It is characterised by the accumulation of remnants of triglyceride-rich lipoproteins such as chylomicrons and VLDL in the plasma as a result of impaired clearance of these atherogenic lipoproteins and premature CVD [54]. FD results in hypercholesterolemia and hypertriglyceridemia, increasing predisposition to coronary artery disease and peripheral artery disease. A

mutation in the ApoE gene is associated with FD and an ApoE*3-Leiden (E3L) transgenic mouse containing the human APO3Leiden and APOC1 genes is used as model of FD [55]. Binding of APOC1 to triglyceride-rich lipoproteins has been shown to block binding to the lipid/water interface, resulting in decreased lipolytic activity. APOC1 also negatively affects the protective effects of lipoprotein lipase (LPL) which is essential in preventing activating factors such as the angiopoietin-like protein 4 (angptl4), a key regulator of LPL [56]. In humans, a mutation in the ApoE gene has been shown to result in a dysfunctional protein with reduced receptor binding ability, thus impairing clearance of lipoproteins, in particular chylomicrons and VLDL [49, 57]. E3L mice are a more moderate model for hyperlipidaemia, than the ApoE-/- and LDLr-/- models with cholesterol levels remaining around 2 mmol/L with a NC diet and not exceeding 25 mmol/L with a HFHC diet [42]. The lipoprotein profile displayed in this model is comparable to that seen in patients with FD, where the plasma total cholesterol and triglycerides are restricted to VLDL [58]. A study by Leppänen et al. [59] found that when E3L mice were fed an atherogenic diet, plasma cholesterol levels increased dramatically from 2 mmol/L to 36 mmol/L in a four month period. The onset of atherosclerotic lesions was also observed which ranged from early fatty streaks in the thoracic and abdominal aorta, and more advanced atherosclerotic lesions in the aortic arch. It has been reported, that E3L mice when fed a HFHC diet for a period of six months, mimic the changes in the lipid profiles of humans with MetS [60]. Taken together these findings indicate that the E3L transgenic model may act as a practical model for investigating the pathogenesis and genetics of atherosclerosis, and also to study changes in lipid metabolism and their association with age.

1.4.2 Rabbit Models

Rabbit models have been used for over a century to investigate the pathogenesis of atherosclerosis. In 1908, a study by the Russian physician Ignatowski, fed rabbits a diet enriched with animal proteins and found intimal lesion build-up within the aorta [61]. In 1913, Anitschkow demonstrated that feeding cholesterol dissolved in sunflower oil led to the development of atherosclerotic lesions which were similar to those seen in humans and thus proposed that cholesterol had a causal role in the development atherosclerosis [62]. To this day the general consensus is that dietary cholesterol does in fact lead to the development of atherosclerosis. Both these studies provided the first evidence and basis for establishing the "lipid hypothesis" in relation to atherosclerosis [63]. Since the establishment of the "lipid hypothesis", the rabbit model has been used extensively to investigate atherosclerosis and the effect of lipid lowering on atherosclerotic plaque formation and stabilisation [64, 65]. Zaragoza et al. [43] conducted a study with a novel rabbit model to investigate the influence of inflammation on atherosclerotic plaque. The study also examined the mechanisms by which atherosclerosis appears to be more severe in rheumatoid arthritis patients. This model consisted of femoral injury in hyperlipidemic rabbits combined with induced acute knee arthritis. These rabbits displayed more intensive atherosclerotic lesions compared to control animals without inflammation, and therefore it was proposed that this model could represent a novel way to study inflammation-associated atherosclerosis [43, 66]. In 2009, Shimizu et al. [67] developed a rabbit model of plaque rupture, through vascular injury and the feeding of a high-cholesterol diet. Histological results revealed that the aortic plaque had the three requirements to be classed as "vulnerable plaque"; a lipid rich core, accumulation of macrophages and a thin fibrous cap. A LDLr-/- rabbit model, the

Watanabe Heritable Hyperlipidemic (WHHL) model, was developed by Dr. Yoshio Watanabe [68]. In this model, it was observed that the function of the LDL receptors on the cell membranes was almost completely absent, and this resulted in delayed clearance of LDL from circulation [68]. These characteristics of the WHHL rabbit closely mimic those seen in human familial hypercholesterolemia (FH), which spontaneously develops, and was therefore identified as the first pre-clinical model of this disease. Kita et al. [69, 70] used the WHHL rabbit model to validate their hypothesis of the LDL receptor pathway for lipoprotein metabolism and showed that the lipoprotein metabolism of WHHL rabbits closely mimicked that of human FH [69, 70]. As a result, WHHL rabbits were subsequently used as an animal model for the development of cholesterol-lowering therapeutics, such as statins [68].

Despite the smaller diameter of their aortic arteries compared to the human carotid artery, rabbits serve as useful models for the use of endovascular therapeutic devices, such as stents and drug-coated balloons. They have also been successfully utilised for the quantification of fibrotic and lipid components of atherosclerosis by MRI and may also allow for the repeated analysis of therapeutic approaches for atherosclerotic plaque stabilisation [71]. A limitation of this model is that the incidence of coronary atherosclerosis in the WHHL model was initially very low compared to the incidence in humans. Following years of selective breeding, a new strain of the WHHL model was developed; the myocardial infarction-prone WHHL (WHHLMI) rabbit model, where it was observed that spontaneous MI occurred by the progression of coronary atherosclerosis, followed by blockage of the coronary arteries (over 90% of the lumen area) [72]. Using the WHHLMI model, differences in the composition of the atherosclerotic plaques found in the aorta and coronary arteries were observed.

Coronary atherosclerotic plaques had a low number of macrophages and were rich in smooth muscle cells (SMC), with the opposite observed in aortic atherosclerotic plaques [73]. The WHHLMI rabbit model became the primary model used for investigating the inhibitory effects of drugs for coronary atherosclerosis but given time related effects of atherosclerosis in humans and the lifespan of these rabbits, it can only partially mimic complex atheroma [68].

1.4.3 Pig Models

Prevention of CVD is dependent on the identification of vulnerable plaques however recreation of vulnerable plaques has proved difficult when developing suitable animal models [43]. While the aged Ossabaw pig model of vulnerable plaque exists, the porcine model has been shown to also be an excellent model for CVD studies. This is largely due to the similarities shared between the porcine and human cardiovascular systems, including heart anatomy and tri-layered aortic valve leaflets, as well as similar lipid profiles and lipoprotein metabolism [74]. Several studies investigating advanced coronary atherosclerosis have been carried out using porcine models to evaluate the development and verification of different coronary imaging technologies, and the use of porcine models has proved invaluable in the area of interventional cardiology [75] and drug-eluting stents [76], as well as the effects of diet on the development of MetS, as seen in the study by O'Donovan et al. [77]. In a study carried out by Alviar et al. [78], the use of porcine models of coronary atherosclerosis allowed for the investigation of the effects of adventitial neovascularisation on the composition of atherosclerotic plaques and vascular remodelling, in which it was found that adventitial neovascularisation was more pronounced in positively remodelled segments and is shown to be associated with

the loss of SMC, increased deposition of collagen and localised macrophage invasion [78].

1.5 Gut Microbiota in Human Health

The human body is home to a vast amount of bacteria, archaea and viruses collectively known as the microbiota. The microbiota primarily colonise the gastrointestinal tract, in particular the colon, a primarily anaerobic and nutrient rich environment in which gut microbes thrive [4]. The gut is predominantly inhabited by two phyla, Bacteriodetes and Firmicutes, which account for 90% of the total inhabiting microbes. The remaining 10% consists of Actinobacteria, Cyanobacteria, Fusobacteria, Proteobacteria and Verrucomicrobia [20, 79]. The ratio of Bacteriodetes to Firmicutes is considered as significant in terms of the composition of the human gut microbiota [80]. A study carried out by Ley et al. investigating the correlation between weight and the microbial ecology of the gut showed that the microbiota of obese participants displayed an increase in Firmicutes and a reduction in the Bacteroides populations, whilst also demonstrating that a decrease in the Firmicutes/Bacteroidetes ratio was linked directly to weight loss [81].

Beginning at birth, there are multiple factors that can influence how the gut is colonised, such as mode of birth (vaginal vs caesarean), feeding method (breast feeding vs infant formula), exposure to antibiotics, hygiene standards and geographical locations [82, 83]. It has been shown that the gut microbiota of infants who were vaginally delivered predominantly consists of *Bifidobacterium* whereas those infants born via caesarean section predominantly consisted initially of maternal skin microbiota, mainly *Staphylococcus* [84]. As the infant ages, the dominant aerobic gut environment matures and evolves to form an anaerobic environment

resulting in greater abundances of *Bifidobacterium* and Clostridia [20]. The gut microbiota begin to stabilize by the second year of life and play a role in a) controlling nutrient absorption and fermentation of food, b) host immune system stimulation and maturation of immunological tissues, c) establishment and regulation of the intestinal mucosal barriers, thus protecting against pathogens, and d) synthesis of a variety of vitamins and energy metabolism through the production of SCFAs [21, 80, 85, 86]. The gut microbiota remains relatively stable throughout adulthood, however recent studies have indicated that compositional changes occur in the elderly including a reduction in the numbers *of Bifidobacterium*, *Bacteroides* and *Lactobacillus* [80, 87]. A reduction in amylolytic activity and total SCFAs, has also been observed along with increases in facultative anaerobes, *Fusobacteria*, *Clostridia* and *Eubacteria*, and proteolytic activity [88]. The gut microbiota are involved in the digestion of food through two catabolic pathways, (1) the saccharolytic pathway or (2) the proteolytic pathway. The saccharolytic pathway, uses the gut microbiota to help break down sugars in the ingested foods leading to SCFA production. The proteolytic pathway is characterised by the fermentation of ingested proteins, leading to SCFA production as well as formation of other metabolites including ammonia, thiols, amines, phenols and indoles.

Host diet has been shown to affect the composition and the functionality of the gut microbiota [19, 89]. The gut microbiome of herbivores have an increased abundance of enzymes that have the ability to hydrolyse plant polysaccharides and synthesize amino acids, whilst a carnivore's gut microbiome is enriched with proteases, which help with protein digestion [90]. Individuals who consume high levels of fibre in their diet have been shown to have increased abundances of *Prevotella* and *Xylanibacter*, which are known to contain bacterial genes that breakdown cellulose

and xylan [91]. An increased abundance of *Bacteroides* was associated with high fat and protein intake [92]. It has also been shown that the lack of fibre in animal-based diets has led to the growth of bile-resistant bacteria such as *Bacteroides*. Plant-based diets which are high in fibre, have been shown to encourage the growth of bacteria involved in the fermentation of polysaccharides, such as *Roseburia* sp., *Eubacterium rectale* and *Ruminococcus bromii* [93].

1.6. Gut Microbiota in Cardiovascular Disease

Metagenomic sequencing and analysis have revealed that the composition of the gut microbiota in subjects with stable atherosclerotic plaques is significantly different to the microbiota of subjects with unstable atherosclerotic plaques. In particular, a reduced abundance of butyrate-producing *Roseburia* was identified in unstable subjects, indicating changes in the metabolic activities of the gut microbiota, shifting towards a pro-inflammatory state in subjects with unstable plaques [18, 94]. Oral pathogens, such as *Aggregatibacter actinomyetemcomitans, Porphyromonas gingivalis, Tennerella forsythia, Treponema denticol* and *Fusobacterium nucleatum* [95], may also influence the composition of the atherosclerotic plaques accompanied by an increased risks for CVD [96]. *Proteobacteria* have been identified as the most abundant phylum found in atherosclerotic plaques, combined with members of the Firmicutes phylum, such as *Anaeroglobus, Clostridium, Eubacterium, Lactobacillales*, and *Roseburia*, which are found predominantly in the oral cavity as well as in the atherosclerotic plaques [97]. There is also evidence of other bacteria that have been shown to be altered in the gut of patients with atherosclerosis, including significant increases in Lactobacillales, the Firmicutes/Bacteroidetes ratio and members of the Enterobacteriaceae family including *Escherichia coli, Klebsiella*

spp. and *Enterobacter aerogens* [98]. The relative abundances of other commonly associated oral bacteria such as *Streptococcus, Solobacterium moorei,* and *Atopobium parvulum* also appeared to be higher in subjects with atherosclerotic CVD [99]. Furthermore, a study by Emoto et al. suggests that specific gut microbiota, such as *Bacteroides, Clostridium* and Lactobacillales could have the potential to be used as diagnostic markers in subjects with coronary artery disease [100]. However it remains unclear whether these bacteria are active or passive participants in plaque erosion/rupture.

There is growing evidence supporting the relationship between gut-derived metabolites such as SCFA, BAs and TMAO and the development of CVD [23, 101]. In addition to influencing several host metabolic pathways, these metabolites may be absorbed into the bloodstream through the intestinal epithelium, which in turn influences the function of several organs and body systems [102]. These products of microbial metabolism play a crucial role in the development and regulation of the mucosal immune system and boosting intestinal barrier function, however they can also have destructive effects on the host. Trimethylamine (TMA) is metabolized by the gut microbiota from dietary choline, phosphatidylcholine and L-carnitine. TMA is further converted to TMAO via the hepatic enzyme flavin-containing monooxygenase 3 [103, 104]. TMA has been seen to contribute to the development of non-alcoholic fatty liver disease (NAFLD) in mice susceptible to the disease [105]. In a study by Wang et al, associations were observed between coronary artery disease, peripheral vascular disease and myocardial infarction (MI) and the gut metabolites choline, TMAO and betaine [25]. A high abundance of SCFAs has been associated with a decreased risk of developing type 2 diabetes, chronic kidney disease and CVD [106, 107]. While an increased risk of disease development is

associated with a higher abundance of TMAO [26]. The conversion of primary BAs to secondary BAs is also dependent on the gut microbiota and has been shown to be linked with increased hydrophobicity and enhanced membrane lipid binding [108]. The type of secondary BAs produced is also dependent on diet and the gut microbiota composition [19]. A high intake of saturated fat in the diet leads to increased BA secretion and the presence of BAs in the intestine, resulting in the production of hydrophobic secondary BAs, such as deoxycholic acid (DCA). In turn these hydrophobic secondary BAs can cause changes in the gut microbiota composition and structure [109]. Secondary BAs that have entered the circulation have been implicated in the development of atherosclerosis, diabetes and other cardiometabolic diseases [4, 109].

Lipopolysaccharide (LPS) is an endotoxin and a component of the Gram-negative bacterial cell membrane. LPS has the ability to induce expression of inflammatory mediators and activate an immune response through toll-like receptors (TLRs) and the nuclear factor kappa-light-chain-enhancer of activated B cells (NF-κB) pathway [110]. It has been shown that endotoxemia (elevated levels of endotoxins in the blood) has been associated with the pathogenesis of several diseases such as atherosclerosis, diet-induced obesity, insulin resistance, fatigue and MetS [111]. In particular, endotoxemia has been shown to be associated with a three-fold increased risk of developing atherosclerosis, especially in current and ex-smokers. Endotoxin levels of >50 pg/ml has emerged as a significant risk predictor for atherosclerosis and this association was shown to be more evident in smokers and subjects with infectious disease [112]. Disruption of the intestinal mucosal barrier is likely to result in bacterial translocation, increasing the risk of exposure of immune cells to bacterial derived products [21].

1.7 Probiotics and Cardiovascular Disease

Probiotics are defined by the FAO/WHO as "live microorganisms which, when administered in adequate amounts, confer a health benefit on the host" [113]. A growing body of evidence demonstrates the beneficial health impacts of probiotic supplementation and they could be considered as a potential therapeutic tool for CVD. Elevated levels of cholesterol, particularly LDL are a risk factor for CVD and probiotic bacteria have been studied as a therapeutic to improve lipid profiles. Probiotic bacteria with bile salt hydrolase activity may reduce serum cholesterol levels through deconjugation of BAs and increasing their excretion [114, 115]. This increases the need for de novo bile synthesis leading to circulating cholesterol converting its molecules to BAs thus reducing serum cholesterol levels. SCFA, another end product of certain probiotic bacteria, have been shown to regulate cholesterol metabolism and reduce hepatic cholesterol synthesis [116]. Other potential mechanisms of action include probiotic driven cholesterol assimilation and increasing cholesterol binding to cell walls of probiotics in the small intestine, thereby decreasing the amount absorbed by the body [117].

Ahn et al. evaluated the triglyceride-lowering effect of supplementation with *Lactobacillus curvatus* HY7601 (5×10^9 CFU) and *Lactobacillus plantarum* KY1032 (5×10^9 CFU) [118]. The RCT was performed over 12 weeks and involved 92 participants with hypertriglyceridemia. Probiotic supplementation resulted in a significant 20% reduction in serum triglycerides ($p=0.001$) and a 25% increase in apolipoprotein A-V ($p=0.001$). Another RCT studied the effect of a fermented soy product containing *Enterococcus faecium* CRL 183 and *Lactobacillus helveticus* 416 (10^{10} CFU/day) and isoflavone on CVD risk markers in moderately hypercholesteraemic men for 42 days [119]. Consumption of the probiotic soy

product with isoflavone improved total cholesterol (TC), low-density lipoprotein-cholesterol (LDL-C) and electronegative LDL concentrations. The levels of high density lipoprotein-cholesterol (HDL-C) was unaffected and the level of fibrinogen and C-reactive protein (CRP) levels were not improved. The effect of a combination of *Lactobacillus acidophilus* and *Bifidobacterium bifidum* (10^9 CFU/capsule) three times a day or placebo for six weeks on lowering serum cholesterol in 70 hypercholesteraemic patients was evaluated [120]. The probiotic group exhibited decreases in TC (212.7 vs 252.8 mg/dL, $p<0.001$), HDL-C (52.0 vs 59.1 mg/dL, $p=0.04$) and LDL-C (153.9 vs 182.1 mg/dL, $p<0.01$) levels compared with the control at the end of treatment.

Obesity has been associated with an increased risk of CVD development and supplementation with probiotic bacteria is of interest as an approach to prevent obesity. Probiotic bacteria can regulate energy utilisation from the diet and influence genes responsible for energy storage and expenditure [121]. Probiotics may have an anti-obesity effect through modulation of the gut microbiota with obesity associated with an increase in Firmicutes and reduced proportions of *Bacteroidetes* [81]. Increased abundances of genera such as *Staphylococcus aureus* and *Escherichia coli* and decreased abundances of *Bifidobacterium* have been reported to be associated with obesity [122, 123]. Studies have shown that faecal transplantation in germ free mice results in an increase in body fat by 60% and insulin resistance [124]. The production of SCFAs is also of importance due to their role in energy metabolism, regulation of inflammation and homeostasis [123, 125]. SCFAs can induce satiety by stimulating the secretion of the gut hormones glucagon like peptide-1 (GLP-1) and peptide YY (PYY) [126, 127]. Probiotics have also been studied for their putative antihypertensive effect. Probiotics may exert this antihypertensive effect through

reducing blood glucose levels, insulin resistance and by improving cholesterol levels and endothelial dysfunction [128, 129]. It has also been demonstrated that bioactive peptides may inhibit angiotensin-converting enzyme (ACE) whose activity leads to an increase in blood pressure through the production of vasoconstrictor angiotensin II and the inactivation of the vasodilator bradykinin [130, 131].

A three week RCT involving 25 obese hypertensive participants investigated if a hypocaloric diet (1500 kcals/day) supplemented with a probiotic cheese containing *Lactobacillus plantarum* TENSIA could reduce symptoms of MetS [132]. BMI was reported to be significantly reduced ($p=0.031$) in the participants that received probiotic cheese versus the control group. Another 12 week RCT examined the effect of a multispecies probiotic Ecologic® Barrier on endothelial dysfunction in obese postmenopausal women [131]. The probiotic preparation contained *Bifidobacterium bifidum* W23, *Bifidobacterium lactis* W51, *Bifidobacterium lactis* W52, *Lactobacillus acidophilus* W37, *Lactobacillus brevis* W63, *Lactobacillus casei* W56, *Lactobacillus salivarius* W24, *Lactococcus lactis* W19, and *Lactococcus lactis* W58. 81 women participated in the trial and were randomised to receive either a low dose (2.5×10^9 CFU) of probiotic, a high dose (1×10^{10} CFU) or placebo daily. The trial revealed a significant reduction in systolic blood pressure (SBP), vascular endothelial growth factor, interleukin-6 (IL-6), tumor necrosis factor alpha (TNF-α), and thrombomodulin following high dose probiotic supplementation. Decreased SBP and IL-6 were observed with low doses of probiotic supplementation. A 12 week RCT randomised 210 healthy Japanese adults with large amounts of visceral fat to receive fermented milk containing with 10^7, 10^6, or 0 (control) CFU/g of *Lactobacillus gasseri* SBT2055 (LG2055) [133]. Participants who received 10^7 or 10^6 CFU/g of LG2055 exhibited a significant lowering in abdominal visceral fat (-

8.5% and -8.2% respectively), waist and hip circumference, BMI and body fat mass when compared with those in the control group. Another RCT investigated the impact of daily supplementation of two capsules of 1.6 x 10^8 CFU/g *Lactobacillus rhamnosus* CGMCC1.3724 (LPR) with oligofructose and inulin for 24 weeks in 125 obese adults combined with an energy-restricted diet for the first 12 weeks [134]. LPR supplementation did not significantly affect weight loss compared to placebo. However, a significant reduction in body weight was observed in the female participants compared with the placebo.

Pregnancy is associated with elevated levels of lipid concentrations. In a RCT conducted by Hoppu et al. 256 pregnant women were randomised into three study groups: dietary counselling with probiotics (*Lactobacillus rhamnosus* GG and *Bifidobacterium lactis*) or dietary counselling with placebo or control at the first trimester of pregnancy [135]. Similar lipid levels were observed in all groups during pregnancy, however, postpartum LDL-C and TC were lower in both the probiotic ($p=0.027$) and placebo ($p=0.012$) dietary counselling groups compared with controls. Another RCT examined the effects of daily supplementation of a probiotic yoghurt containing *Streptococcus thermophilus, Lactobacillus bulgaricus, Lactobacillus acidophilus* LA-5, and *Bifidobacterium animalis* BB12 among 70 pregnant women in the third trimester for 9 weeks [136]. Consumption of the probiotic yoghurt resulted in a significant reduction in TC (-53.7 mg/dL, $p=0.001$), LDL (-35.2 mg/dL, $p=0.006$) and HDL (-9.8 mg/dL, p-0.002) levels, as well as serum triglyceride concentration (-42.8 mg/dL, $p=0.029$). However, no significant differences were found in serum lipid profiles.

The anti-inflammatory effects of probiotics has also been studied in relation to CVD. The 2019 PROSIR study evaluated the effect of *L. reuteri* V3401 on the gut

microbiota composition, biomarkers of inflammation, CVD risk and hepatic steatosis in obese adults with MetS [137]. The RCT included 60 participants (aged 18 to 65 years) who were randomised to receive daily dose of 5 x 10^9 CFUs of L. reuteri V3401 or placebo for 12 weeks. Consumption of *L. reuteri* V3401 was associated with lower levels of inflammatory biomarkers IL-6 and soluble intercellular adhesion molecule-1 (sVCAM-1). Malik et al. examined whether oral *L. plantarum* 299v supplementation for six weeks in 24 men with stable coronary artery disease improves vascular endothelial function and decreases systematic inflammation [138]. Lp299v supplementation resulted in improvements in endothelium-dependant vasodilation and increased nitric oxide (NO) bioavailability. In addition, a decrease in systemic inflammation with reduced IL-8, IL-12 and leptin levels measures observed. It was also found that the SCFA propionate increased with Lp299v supplementation.

As previously discussed, TMAO has been reported to be a risk factor in the development of CVD. A 2015 RCT examined *Lactobacillus casei* Shirota (LcS) supplementation on TMAO levels in 13 patients with MetS [139]. There were no significant differences observed in TMAO levels between subjects receiving LcS and controls. Tenore et al. tested the effects of lactofermented Annurca apple puree (lfAAP) containing *Lactobacillus rhamnosus* LRH11 and *Lactobacillus plantarum* SGL07 on plasma lipid profiles and TMAO levels in 90 individuals with CVD risk factors [140]. lfAAP supplementation significantly increased HDL-C levels by 61.8% (p=0.0095) and lowered TMAO levels by 63.1% (p=0.00442) at the end of the intervention period. It remains unclear whether TMAO is simply an indicator of increased risk rather than a direct participant in CVD and atherosclerosis.

1.7.1 Meta-analysis Studies

A 2015 meta-analysis included 15 studies totalling 788 adults to examine the effect of probiotics on the reduction of CVD risk factors [141]. The authors reported a statistically significant pooled effect reduction in TC, LDL, BMI, waist circumference and inflammatory markers. A significant reduction in LDL was reported when *Lactobacillus* acidophilus ($p<0.001$) was used in a trial compared to other strains. Subgroup analysis revealed that probiotics were most effective on TC and LDL when consumed in the form of fermented milk or yoghurt ($p<0.001$) compared to capsule, consumption was at least 8 weeks ($p<0.001$), and were multi strain ($p<0.001$) rather than a single strain. Mo et al. assessed the efficacy of probiotics in lowering serum lipid concentrations in a meta-analysis of 19 RCTs including 967 hypercholesterolaemic adults [142]. The meta-analysis indicated that the use of probiotics can lower TC (-0.25 mmol/L) and LDL-C (-0.17 mmol/L) compared to controls. These effects were greatest for longer intervention times, certain probiotic strains, and in younger mildly hypercholesterolaemic subjects. No significant effects on TG and HDL-C levels were observed. The effects of probiotics on decreasing TC and LDL-C levels were greater for longer intervention times and in younger mildly hypercholesterolaemic subjects. With regard to strain specific effects, *L. acidophilus, L. plantarum*, and *L. reuteri* significantly decreased TC. *L. plantarum, L. helveticus* and *E. faecium* significantly reduced LDL-C. No significant beneficial effects were observed for L. *fermentum, L. rhamnosus* and mixtures of *L. acidophilus and Bifidobacterium*.

A more recent and larger 2020 systematic review and meta-analysis examined the efficacy of probiotics on lowering CVD risk factors (obesity, high blood pressure, high cholesterol and triglycerides, elevated HbA1c and serum glucose) in patients

with CVD or co-morbidities, such as hypertension, obesity, type II diabetes, MetS and hypercholesterolaemia [143]. A total of 34 RCTs with 2177 adults who received probiotic intervention (1176) or control (1001) were included in the analysis. An overall statistically significant reduction of SBP and diastolic blood pressure (DBP), TC, LDL-C, serum glucose, HbA1c and BMI with probiotic intake was reported. Subgroup analysis revealed that the statistically significant effects of probiotics on the lowering of risk factors may be related to patient morbidity. Diabetic patients displayed the greatest reduction in SBP (-5.82 mmHg, p=0.02), DBP (-3.81 mmHg, p<0.001), triglycerides (-14.17 mg/dL, p=0.02), HDL-C (-2.03 mg/dL, p=0.01) and fasting glucose (-12.94 mg/dL, p<0.001). While hypercholesterolaemic patients displayed the greatest reduction in TC (p<0.001) and LDL-C (p=0.001), and obese patients in reducing BMI (p=0.001). Female populations were reported to have more significant reduction in fasting glucose (− 5.63 mg/dL, p = 0.001), TC (− 5.59 mg/dL, p = 0.002), LDL-C (− 9.87 mg/dL, p=0.001), HbA1c (− 0.18%, p = 0.007) and BMI (−0.35 kg/m2, p = 0.001) compared to males. The authors hypothesize that the oestrogen-gut microbiome axis may contribute to this observed reduction in CVD risk factors. With regards to probiotic formulation, the use of probiotics in yoghurt was statistically favoured for reduction of TC, HbA1c, fasting glucose and LDL-C. Kefir and powder formulations demonstrated significant reductions in BMI. Results favoured a longer duration of > 1.5 months for reductions in SBP and DBP while shorter duration favoured significant reductions in TC, LDL- C HbA1c and fasting glucose. Dosage of probiotics was also important as higher daily doses (>1 x 10^9 CFU) were reported to be more effective in reducing TC, BMI, HbA1c and fasting glucose. Limitations of this meta-analysis include small population sizes and the use of different probiotic strains in the various studies.

1.8. Conclusions

Prevention of CVD is dependent on understanding the mechanisms underlying disease development and targeting this with appropriate therapeutic intervention. Pre-clinical animal models are essential for studying these mechanisms and are often used to represent human diseases. Developing suitable models has been shown to be very challenging and there is no "gold-standard" model that exactly replicates human disease. Therefore when moving from bench to bedside, it is important to test procedures and treatment methods in the most relevant model that will yield the highest reproducible results. Increasing evidence points to an association between alterations in the composition of the gut microbiota and microbial metabolites with the development of CVD. Probiotic interventions hold promise as a therapeutic strategy in CVD risk prevention, though larger multicentre trials, with information on doses, frequencies of administration and specific strains must be performed to generate more convincing data.

The overall objectives of this thesis were to investigate the use of larger pre-clinical animal models for human MetS and whether the results obtained are translatable to a human clinical setting, in particular with regards to understanding the underlying mechanisms of disease, specifically, MetS, and the potential benefits of using gut microbiota-targeted therapeutics, such as probiotics, prebiotics and combination therapies in the treatment of MetS-associated risk factors.

1.9 Acknowledgements

The authors are supported in part by Science Foundation Ireland in the form of a centre grant for APC Microbiome Ireland Grant No. SFI/12/RC/2273-P2 and VistaMilk Grant No. SFI/16/RC/3835.

Chapter 2.

Optimising Cultivation and Pilot Scale Freeze-Drying Methods of *Lactobacillus mucosae* DPC 6426

2.1 Abstract

Probiotics have been widely advertised and consumed, mainly as dietary supplements and functional foods, and have been shown to be involved with manipulating the intestinal microbiome, suppressing the growth of pathogenic bacteria, immunomodulation and reinforcing the intestinal barrier. It has also been shown that modification of the gut microbiome has resulted in the amelioration of gastrointestinal disorders as well as a number of systemic disorders. Freeze-drying is considered an important and commonly used process for the preservation of bacteria, allowing for long-term storage at sub-zero temperatures, whilst also minimising the losses in viability and functionality of the bacterial culture. The aim of the chapter was to devise an optimised method of cultivation and pilot scale freeze-drying of *Lactobacillus mucosae* DPC 6426, a lactic acid, exopolysaccharide (EPS)-producing bacteria, originally isolated from bovine faecal samples at Teagasc, Moorepark Food Research Centre (MFRC), Fermoy, Cork, Ireland. It was determined that the use of a 1% inoculum combined with a reduced anaerobic incubation period of 6.5 hours for 10mls and 200mls and ~16-18 hours for 5L inoculation resulted in an average of between 10^9 and 10^{10} CFU/ml prior to the addition of 10% trehalose and initiation of the freeze-drying process. Following freeze-drying using an extended program of 90-95 hours, the resulting concentration of the freeze-dried powder was ~10^{10} CFU/g.

2.2 Introduction

The Food and Agricultural Organisation (FAO) of the United Nations and the World Health Organisation (WHO) have defined probiotics as “live microorganisms, which when administered in adequate amounts, confer a health benefit on the host” [144]. The concept of probiotics was first introduced by Metchnikoff, in which he published a report which linked the increased life span of Bulgarians with the consumption of fermented milk products which contained viable *Lactobacillus* [145]. It was suggested that, based on the observations of this report, when certain microbes are consumed, they could have beneficial effects of human health, and since then, probiotics have been widely advertised and consumed, mainly as dietary supplements or as functional foods [146]. Currently, the two most common microorganisms used as probiotics are lactic acid bacteria (LAB), such as *Lactobacillus*, and *Bifidobacterium* [147, 148] and it has been shown that a probiotic mechanisms of action include intestinal microbiota manipulation, suppression of growth of pathogenic bacteria in the gastrointestinal and urogenital tract, immunomodulation, epithelia cell stimulation and differentiation and reinforcement of the intestinal barrier [149]. Furthermore, it has been shown in several studies that modification of the gut microbiota has resulted in ways to prevent and treat gut disorders including inflammatory bowel disease (IBD) and irritable bowel syndrome (IBS), as well as a number of systemic disorders such as eczema, allergies, asthma and diabetes, and metabolic disorders such as obesity [150-154].

There is increasing evidence, from both experimental and clinical investigations, demonstrating that consumption of probiotics promotes beneficial effects on cardiometabolic disorder parameters, including i) dyslipidaemia improvement, ii) glycaemic profile improvement and iii) reduce blood pressure in hypertensive

conditions. Even though there is evidence showing that probiotic consumption helps alleviate cardiometabolic disorders, the underlying mechanisms of action remain to be fully understood [155]. Several studies have proposed that the benefits of probiotic consumption may be linked to their anti-inflammatory properties [156, 157], antioxidant properties [158-160] and gut modulating properties [161].

It has also been shown that a wide range of LAB have the ability to produce exopolysaccharides (EPS), which are polysaccharides that are produced outside the bacterial cell wall [162]. EPS has the ability to be either strongly or weakly bound to the bacterial cell surface and are segregated into either capsular or secreted forms [163]. EPS is thought to play a role in the protection of the bacterial cells against extreme conditions such as temperature, light intensity, pH and osmotic stress [164]. It has also been shown that EPS can be involved in the adhesion to surfaces and biofilm formation and to cell adhesion and recognition mechanisms [165, 166]. Furthermore, there have been studies that show that EPS has been associated with several health benefits, such as the lowering of blood cholesterol, blood pressure and blood glucose levels [167, 168], immune stimulations [169, 170] and phosphorylated EPS from *Lactococcus lactis* subsp. *cremoris* has shown anti-tumour effects [171]

The strain of interest in this study, *Lactobacillus mucosae* Dairy Product Culture Collection (DPC) 6426, is a lactic acid, EPS producing bacteria, which was originally isolated from bovine faecal samples at Teagasc, Moorepark Food Research Centre (MFRC), Fermoy, Ireland [172]. Following screening for EPS production using the loop touch test, as described by Ruas-Madiedo and de los Reyes-Gavilan [173], this strain exhibited the ropy phenotype associated with EPS production. Furthermore, it was demonstrated that the EPS produced was comprised of mannosyl residues, with

mannose, glucose and galactose found to be the dominant sugar residues present in an estimated ratio of 3:2:2. Additional characterisation of this EPS producing strain demonstrated its survival following exposure to salt, bile, acid and heat stresses. When compared with *Lactobacillus mucosae* DPC 6420, a non-EPS producer, *Lactobacillus mucosae* DPC 6426 showed a two-fold increase in survival following a 120 minute exposure to 5 mol NaCl, a three-fold increase in survival following a 90 minute exposure to 0.7% (w/v) bile, a three-fold increase in survival following a 10 minute exposure to simulated gastric juice, pH 2 and a five-fold increase in survival following a 60 minute exposure to 1 mol HCl, pH 2. Furthermore, following a 30 minute exposure to 55°C, *Lactobacillus mucosae* DPC 6426 was found to be more heat tolerant compared to *Lactobacillus mucosae* DPC 6420 [174].

In order to recover high amounts of viable microorganisms that could be used in an environment such as the gut, it is highly dependent on their methods of acquisition and storage [175]. The most common techniques used to stabilise probiotics are low temperature (refrigeration or freezing) and dehydration (spray-drying and freeze-drying (lyophilisation), however, lyophilised bacterial cultures are considered more suitable compared to frozen bacterial cultures due to their lower transport and storage costs [176]. A study carried out by Zamora *et al.* [177] investigated the effects of two dehydration techniques, spray-drying and freeze-drying, on the viability of LAB. Observations from this study showed that cellular damage had occurred due to freeze-drying directly after drying, whereas cellular damage due to spray-drying did not appear until the storage period. Furthermore, there was an observed faster decrease in viability of spray-dried cultures compared to freeze-dried cultures, however this was compensated by the higher percentage of viable cells obtained after dehydrations, resulting in comparable survival rates at the end of the storage period of 60 days at 20°C and 5°C. Results from this study showed that spray-drying is as suitable as

freeze-drying for the preservation of LAB strains during a 2 month storage period [177]. Freeze-drying also helps in the preservation of bacteria through the reduction of water activity, allowing for storage at sub-zero temperatures for long periods of time, while also decreasing the chance of losses in viability, integrity and functionality of the bacteria [178].

Freeze-drying employs three simple steps; (i) freezing of the bacteria and cryoprotectant solution, (ii) primary drying step in order to eliminate ice through vaporisation and condensation (sublimation), by-passing the intermediate liquid phase formation, and (iii) secondary drying step in order to remove any unfrozen water through applying heat to the freeze-dried product at moderate temperatures of between 20°C and 30°C, thus reduction of water content to <5% dry weigh and water activity of less than 0.2. However, the stages involved in the freeze-drying process can result in irreversible damages to the components of the bacterial cell wall, and ultimately lead to cell death, but this can be rectified through the addition of a cryoprotectant to the bacterial culture prior to initialising freeze-drying. The most commonly used cryoprotectants are skimmed milk and disaccharides such as sucrose, lactose and trehalose, and also alternatives such as polyalcohols, amino acids and proteins, and have been shown to help reduce the incidence of viability loss in freeze-dried probiotic cultures [147].

The aim of this current work was to optimise cultivation and pilot-scale freeze-drying methods for the preparation and production of freeze-dried *Lactobacillus mucosae* DPC 6426.

2.3 Methods

2.3.1 Bacterial Strains and Media

Lactobacillus mucosae DPC 6426 was originally isolated from mammalian intestine and deposited in the DPC collection (Teagasc, MRFC). It was confirmed to be a potent EPS-producing strain, when grown in the presence of 5% (w/v) glucose [174].

2.3.2 Cultivation of Bacterial Culture

Through multiple attempts at growing *Lactobacillus mucosae* DPC 6426 on modified (addition of 0.5g of L-cysteine hydrochloride (Sigma Aldrich, Germany) per 1L) de Man, Rogasa and Sharpe (mMRS) agar and in broth (Difco Laboratories), in order to achieve optimal growth, a method was developed which resulted in a minimum growth of ~10^{10} CFU/ml prior to freeze-drying the bacterial cultures. Table 1 provides a summary of the cultivation parameters for each cultivation method.

Table 1: Summary of Cultivation Methods

	Method 1	**Method 2**	**Method 3**
Media	mMRS	mMRS	mMRS
Percentage Inoculated	2%	0.5%, 1%	1%
Incubation Conditions	37°C, Aerobic, Shaking	37°C, Anaerobic, Shaking	37°C, Anaerobic
Incubation Time	10ml & 200ml Broths - 24hrs	10ml & 200ml Broths - 24hrs	10ml & 200ml Broths - 6.5hrs
	5L Broths - ~60hrs	5L Broths - ~60hrs	2 x 5L Broths - ~16-18hrs
EPS Loop Touch Test	Yes	Yes	Yes
OD600nm Measurement	No	Yes	Yes
Serial Dilution	Yes in duplicate	Yes in duplicate	Yes in duplicate
Enumeration & CFU/ml Calculation	Yes	Yes	Yes

Method 1:

Lactobacillus mucosae DPC 6426 was cultivated anaerobically on mMRS agar at 37°C for 48 hours. One colony was inoculated into 10mls of mMRS broth and incubated aerobically at 37°C for 24 hours to check how the strain grows under aerobic conditions prior to freeze-drying. Following the 24 hour incubation, 200mls of fresh mMRS broth was inoculated with 4mls (2% inoculation) of the 24 hours culture and incubated aerobically at 37°C for 24 hours while constantly shaking. 100ml of the 200ml broth was then inoculated into 5L (2% inoculation) of mMRS broth and incubated aerobically at 37°C for ~60 hours. Following on from the ~60 hours incubation, a 1 in 10 serial dilution of the aerobic 5L culture was carried out in duplicate in Maximum Recovery Diluent (Saline Peptone Water (MRD)) (Sigma Aldrich, Germany) on mMRS agar from 10^{-2} dilution to 10^{-9} dilution and was incubated anaerobically at 37°C for 24 hours. A loop touch test was used to screen for EPS production, as previously described by Ruas-Madiedo and de los Reyes-Gavilan [172, 173] and enumeration of the bacterial colonies was carried out using the Stuart® Digital Colony Counter (Cole-Parmer, United Kingdom) and CFU/ml was calculated using the equation below.

$$CFU/ml = \frac{Plate\ Count}{Sample\ Dilution\ Factor} x\ Plating\ Dilution\ Factor$$

Method 2:

Lactobacillus mucosae DPC 6426 was cultivated anaerobically on mMRS agar at 37°C for 48 hours. One colony was inoculated into 10mls of mMRS broth and incubated anaerobically at 37°C for 24 hours, and following this, 2 x 200ml of the fresh mMRS broth was inoculated with 0.5% (1ml) and 1% (2ml) of 24 hour culture and incubated anaerobically at 37°C overnight while constantly shaking. 50mls of the

1% 200ml broth was inoculated into 5L (1% inoculation) of mMRS broth and incubated anaerobically at 37°C for ~60 hours. In order to anaerobically incubate such a large volume, the 5L Duran bottle was placed into a biohazard bag with their lids slightly open, and 2 Oxoid AnaeroGen 2.5L sachets (ThermoFisher Scientific, Ireland) were placed in the bag and the bag was tied off using a zip tie in order to keep the environment as anaerobic as possible. Following on from the ~60 hours incubation, a 1 in 10 serial dilution of the anaerobic 5L culture was carried out in duplicate in MRD on mMRS agar from 10^{-2} dilution to 10^{-9} dilution and was incubated anaerobically at 37°C for 24 hours. A loop touch test was used to screen for EPS production and enumeration of the bacterial colonies was carried out using the Stuart® Digital Colony Counter and CFU/ml was calculated using the equation above.

Method 3:

Lactobacillus mucosae DPC 6426 was cultivated anaerobically on mMRS agar at 37°C for 48 hours. Following 48 hour anaerobic incubation, fermentation of *L. mucosae* DPC 6426 was carried out by inoculating one colony in 10mls of fresh mMRS broth and incubated anaerobically at 37°C for 6.5 hours. 2mls (1%) of the 10ml culture was inoculated into 200ml of mMRS broth and incubated anaerobically at 37°C for 6.5 hours, followed by inoculation of 2 x 5L of mMRS with 50mls of 200ml culture each and incubated anaerobically 37°C for ~16-18 hours. Following each incubation, absorbance (OD) was measured at 600nm of using the Biochrom Ultrospec 10 cell density meter (Biochrom Ltd, Cambridge, England) and a 1 in 10 serial dilution was carried out in MRD in duplicate on mMRS and incubated anaerobically 37°C for 24 hours. Enumeration of bacterial colonies was carried out using the Stuart® Digital Colony Counter and CFU/ml was calculated using the equation above.

2.3.3 Freeze-Drying of Bacterial Culture

Using two different freeze-drying methods, a method was developed which resulted in a minimum growth of ~10^{10} CFU/g post freeze-drying of the bacterial culture. Table 2 provides a summary of the cultivation parameters for each freeze-drying method.

Table 2: Summary of Freeze-Drying Methods

	Method 1	**Method 2**
Media	mMRS	mMRS
Volume	5L	10L
Centrifugation	4200 x g for 40mins Final Centrifugation: 5200 x g for 1 hr	7650 x g for 45mins Final Centrifugation: 7650 x g for 1 hr
10% Trehalose Added	Yes	Yes
Final Volume	500ml (incl. 10% trehalose)	1L (incl. 10% trehalose)
% Solids Measured	Yes	Yes
Serial Dilution Prior to Freeze-Drying	Yes	Yes
Enumeration & CFU/ml Calculation	Yes	Yes
Freeze-Drying Program Length	48 hrs	90-95 hrs
Weighed Freeze-Dried Powder	Yes	Yes
Serial Dilution Post Freeze-Drying	Yes	Yes
Enumeration & CFU/g Calculation	Yes	Yes
Storage	Short Term (1 & 2 Weeks) Long Term (1 month)	Short Term (1 & 2 Weeks) Long Term (1 month)
Strain Survival Check After Storage	Yes	Yes

Method 1

Cells were harvested from the 5L culture by centrifugation in 6 x 500ml centrifuge bottles at 4200 x g at 4°C using the F12 6 x 500 LEX rotor (ThermoFisher Scientific, Ireland) for 40 minutes and as much media as possible was aspirated without disturbing the pellets. The pellets were resuspended in the remaining media and all

bottles were combined, followed by a final centrifugation step at 5200 x g at 4°C for 1 hour and as much media as possible was aspirated without disturbing the final pellet. The final pellet was resuspended in the remaining media following aspiration and 10% trehalose (Sigma Aldrich, Germany) was added to make a final volume of 500ml to act as a cryoprotectant during freeze-drying. Prior to initialising freeze-drying, the percentage solids was assessed using a handheld refractometer and 1ml of the concentrated cells and trehalose mix was removed to carry out a 1 in 10 serial dilution in MRD in duplicate on mMRS agar, which was incubated anaerobically at 37°C for 24 hours. Enumeration of the bacterial colonies was carried out using the Stuart® Digital Colony Counter and the CFU/ml was calculated using the above equation.

The mixture was split between 2 x 250ml q-trays (Molecular Devices (UK) Limited, United Kingdom) and placed into the Labconco™ FreeZone™ 12L -84°C Console Freeze dryer with stoppering tray dryer (Labconco Corporation, Kansas, USA) and freeze-dried using a 48 hour programme (shelf freeze temperature: -45°C; condenser set point: -84°C and vacuum set point; 0.02mBar). Once the program was complete, the freeze-dried powder was removed from the q-trays, combined and weighed.

Method 2

Cells were harvested from the 10L overnight culture by centrifugation in 6 x 1000ml FibreLite centrifuge bottles using the FibreLite F9 – 6 x 1000 LEX rotor (ThermoFisher Scientific, Ireland) at 7560 x g at 4°C for 45 minutes and as much media as possible was aspirated without disturbing the pellets. The pellets were then resuspended in the remaining media and all bottles were combined into 4 x 500ml

centrifuge bottles and centrifuged using the F12 6 x 500 LEX rotor at 4°C for 1 hour. The final pellets were resuspended in the remaining media following aspiration, and 10% trehalose was added to make a final volume of 1L. Prior to initialising freeze-drying, the percentage solids was assessed using a handheld refractometer and 1ml of the concentrated cells and trehalose mix was removed to carry out a 1 in 10 serial dilution in duplicate in MRD on mMRS agar, which was incubated anaerobically at 37°C for 24 hours. Enumeration of bacterial colonies was carried out using the Stuart® Digital Colony Counter and CFU/ml was calculated using the above equation.

The mixture was split between 3 x 250ml q-trays and 6 round petri dishes and placed into the Labconco™ FreeZone™ 12L -84°C Console Freeze dryer with stoppering tray dryer (Labconco Corporation, Kansas, USA) and freeze-dried using a 90-95 hour programme (shelf freeze temperature: -45°C; condenser set point: -85°C and vacuum set point; 0.02mBar). Once the programme was complete, the freeze-dried powder was removed from the q-trays and petri dishes, combined and weighed.

Statistical Analysis

Results were subjected to unpaired t-test analysis using GraphPad Prism (version 9.1.0), with a cut off p-value of 0.05 for significance.

Microbiological Analysis of Freeze Dried Powder

Microbiological analysis of the freeze-dried powder was carried out through a 1 in 10 (0.1g powder) and a 1 in 100 (0.01g powder) serial dilutions in duplicate in MRD on mMRS agar, which was incubated anaerobically at 37°C for 24 hours. Enumeration of bacterial colonies was carried out using the Stuart® Digital Colony Counter and CFU/g was calculated using the above equation. The freeze-dried powder was then stored at -30°C. A 1 in 10 serial dilution was carried out in duplicate in MRD on

mMRS media following 1 week, 2 weeks and 1 month of storage at -30°C to confirm survival of the freeze-dried strain. Using Brain Heart Infusion (BHI) granules (Sigma Aldrich, Germany) in a petri dish to simulate feed, 2g of the freeze-dried powder was sprinkled on top and left open on the bench for a period of 1 week to investigate what may happen to the freeze-dried powder when left exposed to the environment.

2.4 Results

2.4.1 Cultivation of Bacterial Culture

Method 1

This method focused on investigating the aerobic cultivation of the *Lactobacillus mucosae* DPC 6426. The initial cultivation and propagation of the strain from stock was promising as there were colonies present on the mMRS agar plates following initial anaerobic incubation. Following the inoculations of the mMRS broth, scaling up from 10mls to 5L, combined with aerobic incubation at 37°C, turbidity and gas production was not significant. Following the ~60 hour incubation of the 5L inoculated broth, there were more than 300 colonies present on the 10^{-4} plate and there was only one colony observed on the 10^{-6} plate. This indicated poor growth, and the loop touch test was negative, with no ropy phenotype observed, indicating the absence of EPS production under aerobic conditions, casting doubt on the strains ability to grow effectively and efficiently under aerobic conditions.

Method 2

This method focused on investigating the anaerobic cultivation of *Lactobacillus mucosae* DPC 6426. The initial cultivation and propagation of the strain from stock was excellent. Whilst the turbidity and gas production for the inoculations of both the 10mls and 200mls of mMRS broth with 0.5% and 1% were comparable, the CFU/ml

counts yielded slightly different results, ~ 10^7 CFU/ml for 0.5% and ~10^8 CFU/ml for the 1% inoculation, following 24 hour anaerobic incubation. Table 3 summarises the results of method 2 for the cultivation of the bacterial culture. Figure 1a shows the growth of the strain over a 24 hour period for both the 0.5% inoculation and the 1% inoculation. Additionally, there was also a significant difference observed in the OD 600nm absorbance measurements between the two inoculation percentages, 0.89 for 0.5% and 2.0 for 1%. Figure 1b below shows the OD 600nm measurements over a 24 hour period. The inoculation of the 5L mMRS media worked significantly better than method 1, with complete turbidity and gas production being observed along with an OD 600nm measurement of 2.0 following ~60 hours of anaerobic incubation. Furthermore, both percentage inoculations displayed positive EPS production, identified by the presence of a ropy phenotype when the loop touch test was carried out. However, after ~60 hours of anaerobic incubation, the calculated CFU/ml was ~10^8, suggesting cell death occurred somewhere between hour 7 and hour 24 of anaerobic incubation, which subsequently led to the development of method 3.

Table 3: Summary of results for method 2 for the cultivation of the bacterial culture. ††† indicates extreme turbidity of the mMRS media and extreme gas production at the end of the anaerobic incubation period

Method 2	**0.5% Inoculation**	**1% Inoculation**
Turbidity	†††	†††
Gas Production	†††	†††
OD 600nm	10ml 24 hr anaerobic incubation: 0.84	10ml 24 hr anaerobic incubation: 1.52
	200ml 24hr anaerobic incubation: 0.89	200ml 24hr anaerobic incubation: 2.0
	5L ~60hr anaerobic incubation: 2.0	5L ~60hr anaerobic incubation: 2.0
EPS Production	Yes - ropy phenotype observed	Yes - ropy phenotype observed
Final CFU/ml	~10^7	~10^8

a

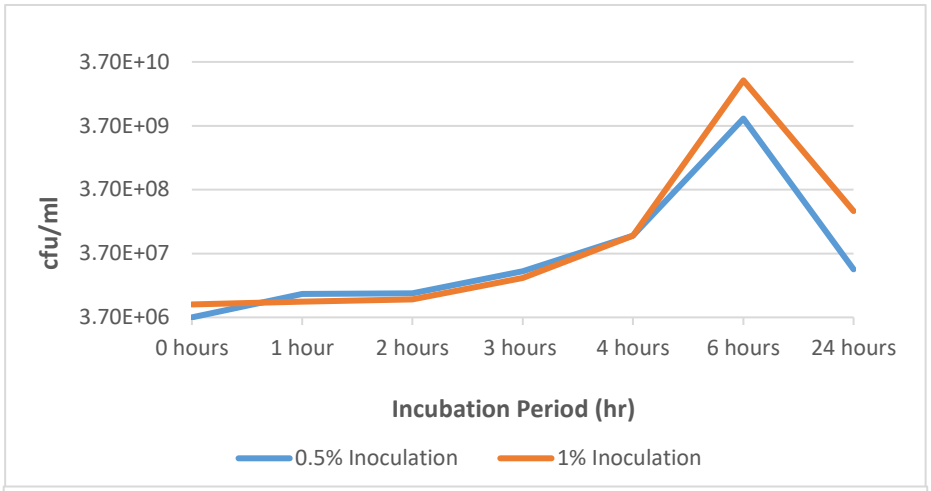

b.

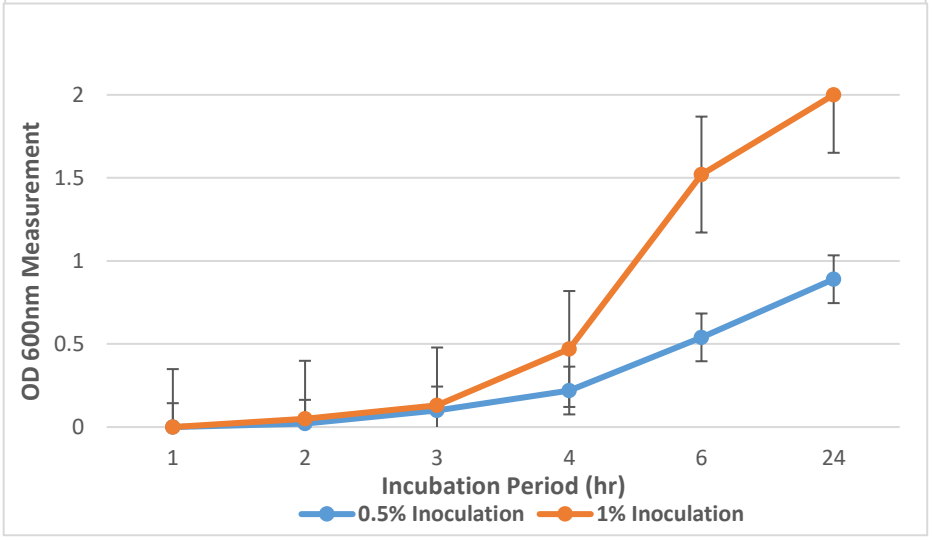

Figure 1: (a) Growth of *Lactobacillus mucosae* DPC 6426 during anaerobic incubation at 37°C in mMRS for 24 hours, (b) Absorbance measurements (OD 600nm) for *Lactobacillus mucosae* DPC 6426 during anaerobic incubation at 37°C in mMRS for 24 hours

Method 3:

This method employed the use of a 1% inoculation and a reduced anaerobic incubation period of 6.5 hours for both 10ml and 200ml inoculations and ~16-18 hours for 5L inoculations. From method 2, in which the results of a 0.5% inoculation and a 1% inoculation were compared, it was determined that a 1% inoculation resulted in better growth during the prolonged anaerobic incubation periods, however with the final CFU/ml of ~10^8, it suggests that cell death may occur somewhere between hour 7 and

hour 24 of the anaerobic incubation period, therefore resulting in a shortened incubation period of 6.5 hours for both 10ml and 200ml inoculations and ~16-18 hours for 5L inoculations for method 3. This method proved to be best way to cultivate and propagate *Lactobacillus mucosae* DPC 6426 in large volumes resulting in an average of between 10^9 and 10^{10} CFU/ml prior to the addition of 10% trehalose and initiation of the freeze-drying process. Throughout the upscaling process from 10 mls of mMRS broth to 2 x 5L mMRS broth, using 1% inoculum at each time point and volume, during cultivation and propagation, there was complete turbidity observed, an OD 600nm absorbance measurement of between 1.90 and 2, as well as extreme gas production. This is positive as this method has shown that using a 1% inoculation combined with a significant reduction in the anaerobic incubation period compared to method 1 and 2, enabled the bacterial strain to be captured at the end of the growth phase and just as it entered the stationary phase, thus maintaining cell viability and reducing the incidence of sub-optimal bacterial growth during the upscaling of media volumes. Table 4 summarises the results of method 3 for the cultivation of the bacterial culture.

Table 4: Summary of results for method 3 for the cultivation of the bacterial culture. ††† indicates extreme turbidity of the mMRS media and extreme gas production following anaerobic incubation at each volume.

Method 3	**1% Inoculation**
Turbidity	†††
Gas Production	†††
OD 600nm	10ml 6.5 hr anaerobic incubation: 1.90
	200ml 6.5hr anaerobic incubation: 2.0
	5L ~16-18hr anaerobic incubation: 2.0
EPS Production	Yes - ropy phenotype observed
Final CFU/ml	~10^9-10^{10}

2.4.2 Freeze-Drying of Bacterial Culture

Comparing the two different freeze-drying methods which were used, method 2 was deemed to be the most effective method to use as it resulted in a minimum of ~10^{10} CFU/g post freeze-drying and following short term (1 and 2 weeks) and long term (1 month) storage at -30°C the strain maintained a CFU/g of ~10^{10}. Table 5 provides a summary of the results for freeze-drying methods 1 and 2.

Table 5: Summary of results for method 1 and 2 for the freeze-drying of the bacterial culture.

	Method 1	**Method 2**
Initial Volume	5L	10L
Volume of Concentrated Cells	300mls	600ml
Volume of 10% Trehalose Added	200mls	400ml
% Solids Measurement	~8.5%	7.5%
CFU/ml Prior to Freeze-Drying	~10^8 - 10^9	~10^{10}
Mixture Completely Dried	No	Yes
Weight of Freeze-Dried Powder	39.47g	70-80g
CFU/g Post Freeze-Drying	~10^9 CFU/g	~10^{10} - 10^{11}
Strain Survival (-30°C Storage)	1 week - ~10^9 CFU/g	1 week - ~10^{10} CFU/g
	2 weeks - ~10^9 CFU/g	2 weeks - ~10^{10} CFU/g
	1 Month - ~10^9 CFU/g	1 Month - ~10^{10} CFU/g

Method 1:

Centrifugation of the 5L culture and resuspension of the pellet in remaining mMRS media following aspiration took between four and five hours in total to completes, and resulted in roughly 300mls of concentrated cells and was mixed with 200mls of 10% trehalose for a final volume of 500mls. Measurement of the % solids, using the handheld refractometer, present in the concentrated cells and 10% trehalose mixture

resulted in ~8.5% or ~42.5g prior to initialising freeze-drying, and serial dilutions carried out in duplicate on the mixture resulted in a CFU/ml of between 10^8 and 10^9.

Following the 48-hour freeze-drying program, it was seen that not all of the concentrated cells and 10% trehalose mixture had dried completely, suggesting that the program needed to be extended by a further 24 hours, possibly even 48-hours to ensure complete drying of the entire mixture. Once all of the completely freeze-dried powder was combined from the 3 q-tray, the resulting weight was 39.47g, which was not far off the predicted percentage solids based on the measurement of the handheld refractometer prior to initialising the freeze-drying program. Serial dilutions of the freeze-dried powder was carried out in duplicate and resulted in a CFU/g of ~10^9. Given that not all of the concentrated cells and 10% trehalose mixture was completely dried, it is thought that the CFU/g may be higher had it been fully dried, and this subsequently led to the development of method 2. Furthermore, following short term (1 and 2 weeks) and long term (1 month) storage at -30°C, survival of the freeze-dried strain was confirmed and resulted in a maintained CFU/g of ~10^9. The results for this method are summarised in Table 5.

Method 2:

Centrifugation of the 10L of culture and resuspension of the pellet in the remaining mMRS media following aspiration took the same time to complete as method 1 using 1000ml centrifuge bottles, due to double the volume used compared to method 1, and resulted in roughly 600mls of concentrated cells and was mixed with 400mls of 10% trehalose for a final volume of 1L. Measurement of the % solids, using the handheld refractometer, present in the concentrated cells and 10% trehalose mixture resulted in

~7.5% or ~75g prior to initialising freeze-drying, and serial dilutions carried out in duplicate on the mixture resulted in a CFU/ml of between ~10^{10}.

Following the 90-95-hour freeze-drying program, the entire concentrated cells and 10% trehalose mixture was completely dried, unlike in method 1, indicating that the extra 48-hours was essential to ensure the entire mixture was completely dried. Once all the freeze-dried powder was combined from the 3 q-trays and 6 round petri dishes, the resulting weight of the freeze-dried powder was between 70 and 80g, which was similar to the predicted percentage solids based on the measurement of the handheld refractometer prior to initialising the freeze-drying program. Serial dilutions of the freeze-dried powder was carried out in duplicate and resulted in a CFU/g of between ~10^{10} and 10^{11}. Furthermore, following short term (1 and 2 weeks) and long term (1 month) storage at -30°C, survival of the freeze-dried strain was confirmed and resulted in a maintained CFU/g of ~10^{10}. The results for this method are summarised in Table 5.

2.5 Discussion

Freeze-drying employs 3 simple steps, firstly aqueous solutions containing bacteria are frozen, followed by primary drying to convert ice into water vapour and finally, the secondary drying step which removes anyremaining unfrozen water. Freeze-drying is considered an important and effective technique in maintaining the viability, integrity and functionality of probiotic cultures, whilst also assisting in the stabilisation of extremely heat sensitive products, such as lactic acid bacteria, thus it is commonly used for the preservation of probiotic strains. However, this process can result in a proportion of cell loss due to the formation of ice crystals which results in irreversible damage to the cell [179]. The resulting freeze-dried powder contains a

combination of dead, viable and injured cells, present in varying proportions, which are dependent on the sensitivity of the strain in response to environmental stressors, such as low cooling temperatures which result in cell dehydration, brought about by the freeze-drying process itself [178]. In order to minimise the loss in viability, a variety of cryoprotectants have been developed to provide freeze-dried strains with structural support, as well as aiding in the rehydration process, ultimately aiding in the maintenance of viability of the probiotic strain during sub-zero storage, resulting in a higher level of survival [179].

Lactobacillus spp. are known to be facultative anaerobes, however there are several *Lactobacillus* species that are known to be unable to tolerate aerobic conditions. It was extremely important to understand whether *Lactobacillus mucosae* DPC 6426 could grow at an optimal rate when subjected to aerobic growing conditions. As the strain demonstrated a poor tolerance to aerobic conditions, and poor EPS production, as seen by the absence of the ropy phenotype commonly associated with positive EPS production, determined by the loop touch test previously described by Ruas-Madiedo and de los Reyes-Gavilan [173], it was established that anaerobic conditions would be required to ensure optimal growth of the strain. It was also observed that extended incubation times, 24 hours for both 10mls and 200mls, and ~60 hours for 5L volumes, used in method 1 and 2 resulted in cell death and in turn sub-optimal CFU/ml values. Resulting cell death and sub-optimal CFU/ml values are likely attributed to hindrance caused by the production and accumulation of metabolic end products such as lactic acid and acetic acid [179, 180]. Therefore, incubation times were set at 6.5 hours for both 10ml and 200ml inoculations and ~16-18 hours when scaled up to 5L volume inoculations.

The aim of this current study was to identify and formulate an optimised protocol that

would result in a minimum of ~10^{10} CFU/ml through cultivation and propagation of *Lactobacillus mucosae* DPC 6426 during the upscaling of media volumes from 10mls to 5L and ~10^{10} CFU/g of freeze-dried powder following freeze-drying. Based on the results from the methods investigating aerobic incubation conditions (method 1) and extended incubation periods (methods 1 and 2), combined with results from both freeze-drying methods, a method was developed through combining method 3 of the cultivation of the bacterial culture, which included the use of a 1% inoculum and a reduced anaerobic incubation period of 6.5 hours for both the 10ml and 200ml inoculations and ~16-18 hours for the 5L inoculation, with method 2 of freeze-drying of the bacterial culture, a 90-95 hour freeze-drying program with the following conditions shelf freeze temperature: -45°C; condenser set point: -85°C and vacuum set point; 0.02mBar in the Labconco™ FreeZone™ 12L -84°C console freeze-dryer with stoppering tray dryer. The use of 10% trehalose as a cryoprotectant worked extremely well during the freeze-drying process and storage as the concentration of the freeze-dried powder, ~10^{10} CFU/g, was maintained from prior to beginning freeze-drying and following short (1 and 2 weeks) and long term (1 month) storage at -30°C.

2.6 Conclusions

A method has been developed with regards to creating optimal cultivation and freeze-drying conditions for *Lactobacillus mucosae* DPC 6426, resulting in a high concentration of ~10^{10} CFU/g of freeze-dried powder, and included the use of a 1% inoculation, anaerobic incubation of the 10ml and 200ml inoculations for 6.5 hours, and ~16-18 hours for the 5L volumes combined with 10% trehalose as a cryoprotectant and a 90-95 hour freeze drying program. Significant changes were observed with regards to the concentration of cells when the optimised cultivation method (method 3) and freeze-drying method (method 2) were used in combination. In order to

optimise viability, it was important to keep incubation conditions as anaerobic as possible, as it was seen with method 1 for cultivation that aerobic incubation conditions resulted in the sub-optimal growth of the bacterial strain. Additionally, the use of 10% trehalose as a cryoprotectant during freeze-drying and subsequent storage at -30°C was shown to be a suitable approach for maintaining viability and aiding in the survival of the freeze-dried strain during frozen storage.

2.7 Acknowledgements

The authors wish to thank Dr. Fiona Fouhy and Dr. Claire Watkins for the assistance they provided in optimising the cultivation methods and Helen Slattery for the assistance provided with freeze-drying. The authors are supported in part by Science Foundation Ireland in the form of a centre grant for APC Microbiome Ireland Grant No. SFI/12/RC/2273-P2.

Chapter 3.

Effect of daily administration of *Lactobacillus mucosae* DPC 6426 on blood lipids and gut microbiota in mildly hypercholesterolaemic adults; A randomised, double-blind, placebo controlled trial.

Noel Caplice, Catherine Stanton, Paul Ross and the Atlantia Food CRO team designed the study, Lis London performed microbiological analysis, Dr. Fiona Fouhy performed bioinformatic analysis and Aoife O Donovan carried out all analysis relating to the gut microbiome. Dr. Andrea Anesi performed plasma and urine metabolite analysis.

3.1 Abstract

Among the recommendations to prevent heart disease is the maintenance of normal blood cholesterol levels, through the consumption of a cardioprotective diet, and if necessary the use of therapeutics such as statins. It has previously been reported that alterations in the gut microbiota have been associated with the development of obesity, insulin resistance and increased risk of developing CVD. Probiotics have since emerged as a potential therapeutic approach, aimed at reversing the alterations to the gut microbiome. In this current study, the impact of daily administration of *Lactobacillus mucosae* DPC 6426 at a minimum concentration of 10^9 CFU/g on blood lipid profiles and on the gut microbiota composition in mildly hypercholesterolaemic adults was investigated. There were no significant changes observed in blood lipid concentrations and in the gut microbiota composition between the placebo and treatment groups. As a result, further investigations need to be conducted to assess whether the dose administered was insufficient to translate from the pre-clinical apoE mouse model to humans.

3.2 Introduction

Cardiovascular disease (CVD) is the leading cause of death and morbidity worldwide, accounting for 31% of all global deaths in 2016 [181, 182]. It has previously been reported that from 1999 to 2003, hypercholesterolemia has been attributed to 45% of heart attacks in Western Europe and 35% of heart attacks in Central and Eastern Europe [31]. Those experiencing hypercholesterolemia are three times more likely to experience a heart attack when compared with those who have normal blood lipid profiles. The most important risk factors associated with the development of CVD are consumption of an unhealthy diet (high in fat, salt and sugar, and low in complex carbohydrates, fruits and vegetables), lack of physical activity, smoking and excessive, harmful use of alcohol. Other major risk factors for the development of CVD include high blood pressure, dyslipidaemia, diabetes, obesity and older age [183].

Among the many recommendations to avoid heart disease, the maintenance of normal blood cholesterol levels is one important recommendation. This can be done through the consumption of a cardioprotective diet, either as an adjunct to medication therapy, such as statins, or independently in patients where medications may be poorly tolerated, too expensive or ineffective [184]. Low consumer compliance with dietary recommendations and the expense and side effects of drug therapy for many consumers, coupled with increased consumer acceptance of foods with additional health benefits has led to an opportunity for the use of functional foods in the heart health area.

Those with hypercholesterolemia may be able to avoid the use of cholesterol-lowering medications through implementing changes to their dietary habits or

through consumption of probiotics, prebiotics or synbiotics (combination of pro- and prebiotics). Probiotics have been defined by the FAO/WHO as “live microorganisms which, when administered in adequate amounts, confer a health benefit on the host” [144], and prebiotics have been defined by The International Scientific Association for Probiotics and Prebiotics (ISAPP) as ‘a substrate that is selectively utilised by host microorganisms conferring a health benefit’ [185].

It has been previously noted that changes in the human intestinal microbiota have been involved in the development of obesity [186], insulin resistance [105] and increased risk of developing CVD [25]. Therefore based on this information, it has been previously shown that probiotics, aside from improving gut health, have demonstrated other health promoting properties such as improving the immune system, reduction in hypertension, antioxidative effects, relieving symptoms of dermatitis, mineral absorption facilitation, relieving allergy symptoms [187], as well as being studied for their potential to reduce cholesterol [115, 188].

Heart health protective bioactive components of food that have recognised cholesterol-lowering effects include phytochemicals and soluble dietary fibre. In a previous study, a novel, soluble dietary fibre (exopolysaccharide (EPS)) producing *Lactobacillus* strain (*Lactobacillus mucosae* DPC 6426), originally isolated from bovine faecal samples at Teagasc, Moorepark Food Research Centre, Fermoy, Cork, was identified [174] and demonstrated the potential to cause a significant reduction ($p \leq 0.001$) in serum total cholesterol levels by ~50%, and significantly reduced serum triglyceride ($p \leq 0.05$, ~15% reduction) *in vivo* following ingestion using the apoE mouse model, a model prone to the developing lipid rich pro-inflammatory atherosclerotic plaque, compared with un-supplemented controls. Furthermore, dietary intervention with *Lb. mucosae* DPC 6426 resulted in a significantly higher

ratio of high-density lipoprotein (HDL)-cholesterol to total cholesterol in the serum and liver ($p \leq 0.05$); while significantly increased ($p \leq 0.001$) levels of faecal cholesterol excretion were associated with daily administration of *Lb. mucosae* DPC 6426 compared with un-supplemented controls [1].

Additionally, *Lb. mucosae* DPC 6426 was compared against plant sterol esters, oat beta glucan and *Lb. reuteri* NCIMB 30242 (10^9 CFU/day, Cardioviva) and was found to be more effective than oat beta glucan and *Lb. reuteri* NCIMB 30242 (10^9 CFU/day, Cardioviva) and was found to be similar to plant sterol esters in terms of its effects on serum cholesterol reduction [189].

We hypothesise that the daily oral supplementation of *Lactobacillus mucosae* DPC 6426 will positively affect the cholesterol levels of mildly hypercholesterolaemic adults. Thus, the aim of this study was to investigate the efficacy of daily oral supplementation of *Lactobacillus mucosae* DPC 6426 [174] on reducing cholesterol levels in healthy mildly hypercholesterolaemic (≥ 5.5 mmol/L and < 8 mmol/L) adults, in which the primary efficacy objective was to investigate the impact of daily oral supplementation of *Lb. mucosae* DPC 6426, at a minimum concentration of 10^9 CFU/g, on total cholesterol, from baseline to week 12, in a randomised, double-blind, placebo controlled clinical trial. The primary efficacy endpoint was the change in the total cholesterol between baseline (Visit 2, Day 0) and the end of the trial (Visit 5, Week 12) between the two treatment groups. The secondary efficacy objectives were to compare the effect of daily oral supplementation of *Lb. mucosae* DPC 6426 on changes in total cholesterol from baseline to weeks 4 and 8, LDL-cholesterol, HDL-cholesterol and triglycerides concentrations from baseline and weeks 4, 8 and 12.

In addition to investigating the impact of daily dietary supplementation on blood

lipids, alterations in the gut microbiome were also investigated and compared between the placebo and treatment groups at baseline (week 0/Visit 2) and end of the study (week 12/Visit 5).

3.3 Materials and Methods

Ethical approval was obtained from the Cork University Hospital Research Ethics Committee.

3.3.1 Study Design and Sampling

In order to calculate the sample size required for this study, it was assumed that two populations would be tested for a statistically significant difference between the means of the two groups, using the one-tailed unpaired t-test. With the expected mean difference on 0.42 and standard deviation of 0.77, based on the previous pilot study (data unpublished), the level of significance of 2.5% and the power of 80, the total sample size is n = 81.81.

It was assumed for the sample size calculation that the samples are equal in size, resulting in the individual samples being about 81.8/2 or 40.9 in size, therefore resulting in a minimum of 41 participants per group.

A total of 174 participants were initially screened, both male and female, aged between 20 and 70 years, with mildly hypercholesterolaemic blood lipid levels (≥5.5mmol/L and <8mmol/L), where the inclusion and exclusion criteria were reviewed and blood pressure, body weight and body mass index (BMI) were measured. Out of that 174 screenings, 94 were found to be eligible and were randomised into the study for evaluation of cholesterol lowering effects of the probiotic bacterial strain *Lb. mucosae* DPC 6426 compared with the placebo. The clinical trial was conducted at Atlantia Food CRO, Cork, Ireland.

The study involved five visits over a total of an 18 to 19 week period, Figure 1 provides a summary of the study. Activities and measurements which were carried out at each visit are as follows;

Visit #1 – Screening visit (-21 to -3 days): Overall study details were explained, inclusion (Female and Male BMI of $< 25 kg/m^2$ and $\geq 25 kg/m^2$, aged between 20 and 70 years of age and a non-smoker) and exclusion criteria (consumption of antibiotics, medication and is a smoker), informed consent, demographic data, past medical history, concomitant medications, vital signs, anthropometric measurements, pregnancy test if applicable, urine sample collected for urinary protein measurements, fasting blood sample collected for haematology, biochemistry (including total cholesterol (TC), LDL-cholesterol, HDL-cholesterol and triglycerides), glucose and blood lipids. Participants were also asked to fill out an International Physical Activity Questionnaire (IPAQ).

Visit #2 – Baseline, Randomisation (Day 0): Inclusion and exclusion criteria were reviewed and eligibility for study entry was established, Adverse Events (AEs) and Serious Adverse Events (SAEs) and concomitant medications were recorded, vital signs, anthropometric measurements, pregnancy test if applicable were taken and results recorded, a stool sample was collected for microbiome analysis, a urine sample was collected for metabolomic analysis, and a fasting blood sample collected for haematology, biochemistry, glucose and blood lipids. Participants were also asked to fill out an IPAQ and a Food Frequency Questionnaire (FFQ). Participants were randomised into either treatment or placebo groups and were supplied with first batch of capsules and instructions for administration.

Visit #3 – Week 4 (+/- 4 Days): AEs and SAEs were reviewed and records updated, concomitant medications updated since visit #2, vital signs, anthropometric measurements were recorded, a stool sample was collected for microbiome analysis, a urine sample was collected for metabolomic analysis, and a fasting blood sample (12 mls) was collected for blood lipid profile analysis (TC, LDL-cholesterol, HDL-cholesterol and triglycerides). Participants were also asked to fill out and IPAQ, and capsule consumption compliance was recorded. Participants were re-supplied with their second batch of capsules.

Visit #4 – Week 8 (+/- 4 Days): AEs and SAEs were reviewed and records updated, concomitant medications updated since visit #3, vital signs, anthropometric measurements were recorded, a stool sample was collected for microbiome analysis, a urine sample was collected for metabolomic analysis, and a fasting sample collection for haematology, biochemistry, glucose and blood lipids (TC, LDL cholesterol, HDL cholesterol and triglycerides). Participants were also asked to fill out and IPAQ, and capsule consumption compliance was recorded. Participants were resupplied with their third batch of capsules.

Visit #5 – End of Treatment, Week 12 (+/- 4 Days): AEs and SAEs reviewed and records updated, concomitant medications updated since visit #4, vital signs, anthropometric measurements were recorded, a stool sample was collected for microbiome analysis, a urine sample was collected for metabolomic analysis, and a fasting sample collection for blood lipids (TC, LDL cholesterol, HDL cholesterol and triglycerides). Participants were also asked to fill out and IPAQ and FFQ, and capsule consumption compliance was recorded.

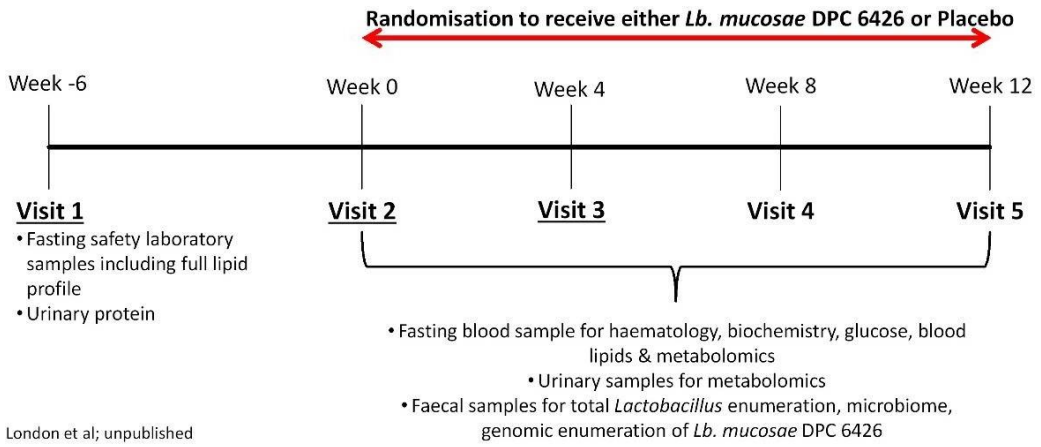

Figure 1: Summary of Study design

Table 1 lists the assessment that were carried out at each study visit.

Table 1: Summary of assessments at each visit

Study Design	**Visit #1**	**Visit #2**	**Visit #3**	**Visit #4**	**Visit #5**
Procedure	Screening	Baseline Wk 0	Week 4	Week 8	Week 12
Visit Window	Week -6	Day 0	+/- 4 Days	+/- 4 Days	+/- 4 Days
Consent	X				
Inc/Exc Criteria	X	X			
Medical History	X				
Family History	X				
Vitals (BP, HR & Temp)	X	X	X	X	X
Anthropometric Measurements (Weight, Height & BMI)	X	X	X	X	X
IPAQ	X	X	X	X	X
Urine Pregnancy Test	X	X			
Urine (20 mls) for metabolomics		X	X	X	X
Blood-safety labs (Haematology, Biochemistry & Glucose)	X				
Stool Sample Collection		X	X	X	X
Urinary Protein	X				
TC, LDL & HDL	X	X	X	X	X
FFQ		X			X
Randomisation		X			

Administer Capsules		X	X	X	
Collect Capsules/Record Compliance			X	X	X
AEs & SAEs Review & Record		X	X	X	X
Prior/Concomitant Medication	X	X	X	X	X

3.3.2 Product formulation, Manufacture and Packaging

Food grade powder containing either freeze dried *Lb. mucosae* DPC 6426, was used to produce capsules containing a minimum concentration of 10^9 CFU/g *Lb. mucosae* DPC 6426 (treatment), or placebo freeze dried powder, which contains 0 CFU/g *Lb.* mucosae DPC 6426. Both products were produced by Probiotical S.p.A (Via E. Mattei, 3 28100 Novara, Italy).

The capsule containers were labelled in accordance with good manufacturing practice (GMP) guidelines consisting of the name, address and telephone number of the study sponsor and contract research organisation. The container label also included information on dosage form (capsule), route of administration (oral) and quantity of capsule doses per container; the code number to identify the contents and packaging operation; the trial reference code (AFCRO-059) allowing for identification of the trial; the trial participant identification number (059-); the name of the investigator; directions for use; “For clinical trial use only” or similar wording; the storage conditions; period of use (use-by date, expiry date or re-test date as applicable) and “keep out of reach of children”.

3.3.3 Treatments Administered

Participants were randomised into one of two treatment groups, *Lb. mucosae* DPC 6426 or Placebo. Participants took their first dose (*Lb. mucosae* DPC 6426 or placebo) at the study site and were instructed to take one capsule with a glass of

water (approximately 200 mls) at the same time each day for the duration of the study.

3.3.4 Blood Measurements

A fasting blood sample was collected at each visit of the study. These samples were collected following an overnight fasting period of at least 10 hours, where participants were required to avoid all foods and drinks, aside from water. At the screening visit (Visit #1) 10 mls was collected for haematology, biochemistry (TC, LDL-cholesterol, HDL-cholesterol, triglycerides and glucose). At all following visits, 12 mls of blood was collected and TC, LDL-cholesterol, HDL-cholesterol and triglycerides were measured. A total of 70mls was collected from each participant throughout the course of the study.

Analysis of the blood samples was carried out by Eurofins Biomnis Ireland.

3.3.5 Stool Collection for Microbiome Analysis

Stool collection and storage: Participants were provided with a stool collection kit and were instructed to collect a sample at home. Participants were instructed to urinate prior to collecting the stool sample, and in order to avoid the stool sample coming into contact with the toilet water, which would cause degradation of the sample, to remove the lid of the container and place the container into the toilet bowl. Once participants had completed their bowel movement, they were instructed to open the anaerobic sachet attached to the lid of the stool sample collection container before closing the container, and to write the date and time on the container and keep the sample refrigerated. They were instructed to bring the sample to their next visit, and this was refrigerated until processing (less than 24 hours).

DNA Extraction: Bacterial genomic DNA was extracted from 0.25g of faecal material using the repeated bead-beating plus column (RBB+C) protocol as described by Yu et al. [190] in combination with the QIAamp DNA Stool Mini Kit (Qiagen, UK) described by Fouhy et al. [191] with slight modifications: 1.0mm and 2.3mm sterile zirconia beads were used during the homogenisation step instead of 0.5mm sterile zirconia beads to avoid sedimentation of the 0.1mm beads and the faecal material. Cell lysis was achieved through bead-beating in conjunction with the use of 1ml of lysis buffer containing 4% (w/v) sodium dodecyl sulphate (SDS) 500 mM NaCl and 50 mM EDTA. Samples were homogenised for 3 minutes at max speed (3800 strokes/min) using the Mini Beadbeater (BioSpec). Following homogenisation, samples were incubated at 70ºC for 15 minutes to lyse the cells. Samples were then centrifuged at 16,000 x g and the supernatant was removed, the bead beating steps were repeated with 300µl of lysis buffer. Once supernatant was pooled, samples were treated with 10M ammonium acetate (Sigma Aldrich, Ireland) and the DNA was pelleted, through centrifugation at 16,000 x g for 10 minutes. The DNA was precipitated using isopropanol (Sigma Aldrich, Ireland), centrifuged at 16,000 x g for 15 minutes and washed with 70% ethanol. The pellet was allowed to dry, and then re-suspended in 200µl of TE buffer. The re-suspended DNA pellet was then treated with RNase and proteinase K, combined with 37ºC for 15 minutes and 70ºC for 10 minutes heating steps. The DNA was cleaned with Qiagen AW1 and AW2 buffers using a Qiagen column (QIAmp DNA Stool Mini Kit, Qiagen, UK). The DNA was eluted using 200µl of Buffer AE (Qiagen, UK) and stored at -80°C [84].

16S rRNA Gene Sequencing and Analysis: After bacterial genomic DNA extraction, the V3-V4 regions of the 16S rRNA gene were amplified through 30 PCR reactions on the template DNA using the primer pair ‘5-TCGT CGGC AGCG TCAG ATGT

GTAT AAGA GACA GCCT ACGG GNGG CWGC AG-3' and '5-GTCT CGTG GGCT CGGA GATG TGTA TAAG AGAC AGGA CTAC HVGG GTAT CTAA TCC-3' according to the 16S Metagenomic Sequencing preparation protocol for the Illumina Miseq and as previously described by Fouhy et al. [191]. Indexed PCR products were visualised using gel electrophoresis and cleaned using AMPure XP magnetic beads before the DNA was quantified using the Qubit (BioSciences, Dublin, Ireland) combined with the Qubit High Sensitivity DNA Kit (Life Technologies). Samples were then pooled at equimolar concentrations, and high-throughput sequencing was performed on the Illumina MiSeq platform in the Teagasc sequencing facility using a 2 x 300 kit and following standard Illumina sequencing protocols.

Bioinformatic analysis: Resulting 300-bp paired-ends reads were assembled using Fast Length Adjustment of Short Reads to improve genome assemblies (FLASH). Quantitative Insights into Microbial Ecology (QIIME; version 1.8.0) was used for quality filtering of pair-end reads, which was based off a quality score of >25 and removal of mismatched barcodes [192]. Before analysis began, sequences that produced less than 40,000 reads were manually removed, which accounted for the differences in the number of participants between groups and time points. USEARCH (version 7, 64-bit) was then used for deionisation, chimera detection and clustering into operational taxonomic units (OTU 97% identity). Alignment of the OTUs was done using Python Nearest Alignment Space Termination (PyNAST) and assignment of taxonomy of 97% similar identity against the SILVA SSURef database release v123.

Statistical analysis of the microbiome was carried out using GraphPad Prism (version 9.1.0), with a cut off p-value of 0.05 for significance. Where possible,

statistical analysis of changes over time, resulting from diet, took the subject numbers into account, and facilitated alpha diversity linear modelling.

In order to assess the alpha diversity of the samples, Chao1 Index and Shannon were calculated (Supplementary Figure 1). Multiple beta diversity metrics were also calculated, including weighted and unweighted UniFrac PCoA plots, in which these plots were used to highlight the participants based on the treatment they received, and by sample time point (Supplementary Figure 2 and 3).

Enumeration of Lactobacillus mucosae DPC 6426: For each stool sample collected at every visit, 1g of faecal sample, from the middle of the sample in order to capture as many anaerobes as possible, was mixed with 9ml of sterile Maximum Recovery Diluent ((MRD), Sigma Aldrich, Germany) and placed in the stomacher machine (Seward Stomacher 400 Circulator Paddle Blender) at 260 rpm for 4 minutes.

Following stomaching, a 1 in 10 dilution, with 1ml of sample in 9ml of MRD, was carried out and 100µl of sample was plated on *Lactobacillus* Selection (LBS) agar in duplicate from neat to 10^{-6} dilution. Plates were incubated anaerobically at 37°C for 48hours and enumeration of *Lactobacillus* colonies was carried out using the Stuart® Digital Colony Counter (Cole-Parmer, United Kingdom) and CFU/ml was calculated and recorded.

3.3.6 Plasma and Urine Metabolite Analysis

Metabolomics analysis was performed on both plasma and urine samples from each study visit for both treatment and placebo groups as described by Anesi et al. [193].

Urine samples were extracted by thawing on ice and 25µl aliquots were loaded into 96-well multifilter plates (Millipore) combined with 225µl of internal standard mix (500ng/ml) in water with 0.1% formic acid (FA). Plates were shaken for 15 seconds

and then filtered using a positive pressure-96 manifold (Waters Corporation, Milan, Italy) and collected in 350µl 96-well plates.

Plasma samples were extracted through loading 50µl onto 25mg Ostro 96-well plates (Waters Corporation, Milan, Italy) and 20µl of internal standard mix in acetonitrile (ACN) 1% formic acid was added. Protein precipitation and metabolite extraction was carried out by adding 150µl of ice cold ACN 1% formic acid and vortexing for 15 seconds. Samples were then placed on an Eppendorf shaker for 10 minutes at 500 rpm and filtered using a positive pressure-96 manifold (Waters Corporation, Milan, Italy). The extraction process was repeated through addition of 150µl of ice cold ACN 1% formic acid and dried using a stream of nitrogen at 37°C in a Techne Dri-block DB-3D heater (Cole-Parmer, Staffordshire, UK) and re-dissolved in 100µl of sterile water; ACN (8:2 ratio) 0.1% formic acid and collected in 350µl 96-well plates.

Liquid-Liquid Extraction (LLE) of urine and plasma was carried out through the extraction of 100µl of urine or plasma using 200µl of ice cold ACN containing internal standards. The mixtures were shaken at 500 rpm for 30 minutes at 5°C and then stored at -20°C for one hour, in order to improve the protein precipitation, and then centrifuged at 17,968 x g at 4°C for 15 minutes**.**

Detection of metabolites was performed through Ultra High Performance Liquid Chromatography-Electrospray Ionization-Triple Quadrupole-Mass Spectrometry (UHPLC-ESI-QqQ-MS) on the Waters Xevo TQ MS Triple Quadrupole which was equipped with ESI source and combined online with an Aquity UHPLC (Waters, Milford, MA, USA). The mass spectrometer (MS) was operated in positive ionisation mode, with the capillary set at 270°C, the source set at 300°C and source voltage at 3kV. The detection of the internal standard (IS), 3,4-

Dihydroxyphenylacetic acid (DOPAC), 3,4-Dihydroxyphenylacetic acid-d5 (DOPAC-d5) and Homovanillic acid (HVA) was performed in negative ion mode in the same run by setting polarity switching. Ultra-high purity argon was used as the collision gas for the detection and the MS and MS/MS conditions were optimised using IntelliStart software (Waters, Milford, MA, USA) through infusing analytical standards.

Reverse phase (RP) C_{18} chromatography separation was carried out using a Water UPLC HSST3 column (1.8µm, 2.1 x 150mm, 100 A pore diameter) (Waters Corporation, Milan, Italy), where mobile phase A was water with 0.1% formic acid, and mobile phase B was ACN 0.1% formic acid. The gradient began with 5% Mobile phase B and was maintained at 30 seconds; then percentage of Mobile phase B was increased to 10% at 2.5 mins, 15% at 3.5 mins, 25% at 4.5mins, 35% at 5.5mins, 45% at 6.5 mins, 55% at 7 mins and then to 100% Mobile phase B at 7.5 mins. The final conditions were maintained for 3 minutes and re-equilibrated to initial conditions for 4 minutes. The total run time including re-equilibrations was 14 minutes with the flow rate of 0.3ml/min, injection volume of 2 µl, and the column oven was set at 40°C. The weak and strong solvent washes consisted of water: Methanol (MeOH) (9:1, v/v) and water: ACN: MeOH: 2-propanol (1:1:1:1, v/v/v/v) respectively. Generated data were processed using Mass Lynx 4.1 software (Waters, Milford, MA, USA).

Hydrophilic interaction liquid (HILIC) chromatography was carried out using an ACQUITY BEH AMIDE analytical column (1.7µm, 2.1 x 150mm) (Waters Corporation, Milan, Italy). The Mobile phases consisted of A) 10 mM ammonium formate and 0.2% formic acid in water: ACN (1:1, v/v) and B) 10 mM ammonium formate and 0.2% formic acid in water: ACN (5:95, v/v). The multi-step elution gradient began with a flow rate of 0.5 mL/min: at 0.0 mins, 100% Mobile phase B at

a gradient up to 4.0 mins, 90% Mobile phase B; then % Mobile phase B was decreased to 70% at 8.0 mins, 60% at mins 9.0, 50% at 9.5 mins and maintained isocratically until 11.0 mins, and finally a re-conditioning period up to 1.5 minutes at 100% Mobile phase B. The injection volume was 5µl and the temperature of the autosampler was maintained at 5°C. The weak and strong solvent washes were water: ACN: MeOH: 2-propanol (1:1:1:1, v/v/v/v) and water: MeOH (9:1, v/v) respectively [193].

3.3.7 Statistical Analysis

Statistical analysis was carried out by StatisticaMedica, Dublin, Ireland using statistical software Rx64 version 3.3.1. In the primary efficacy analysis, an unpaired two tailed t-test was performed to test the difference of the total cholesterol levels from baseline to week 12 between the two treatment groups.

In the secondary analysis, an unpaired two tailed t-test was performed to test the difference between the two treatment groups for changes in the total cholesterol from baseline to weeks 4 and 8, LDL-cholesterol, HDL-cholesterol and triglycerides concentrations from baseline to weeks 4, 8 and 12.

The last observation carried forward (LOCF) was applied to the Intention-to-Treat (ITT) populations and safety analysis was presented as the Clopper-Pearson Confidence Intervals. The data collected in the case report form (CRF), but was not used in the Efficacy analysis, was reported using the descriptive summaries and the frequency distributions where applicable. Scores for the FFQ and IPAQ questionnaires were calculated using corresponding guidelines and descriptive summaries were reported (data not shown).

3.4 Results

The main aims of this study were to investigate the efficacy of daily oral

supplementation of *Lb. mucosae* DPC 6426 for 12 weeks on blood cholesterol levels and on the gut microbiota in healthy mildly hypercholesterolaemic (≥ 5.5mmol/L and < 8 mmol/L) adults.

Analysis of serum lipid profiles (total cholesterol, LDL-cholesterol, HDL-cholesterol and triglycerides) indicated no significant changes between baseline (V2) and end of the study (V5) between the placebo and treatment groups. Furthermore there was no distinct separation in the gut microbiota composition, as well as no significant differences at phylum, family and genus levels between the placebo and treatment groups.

3.4.1 Serum Lipid Profiles

The primary efficacy analysis was the change in total cholesterol from baseline to visit 5 (end of treatment). Table 2 shows the results of this analysis for the Intention-to-Treat (ITT) population.

Table 2: Primary Efficacy Analysis: Change in Total Cholesterol for ITT Population

		N	Mean (SD)	Median	Min,Max	1Q,3Q	Missing
Baseline (V2)	Placebo	46	6.42 (0.8)	6.25	4.9,8.2	5.8,7.17	NA
	Active	47	6.08 (0.87)	6	3.9,8.2	5.6,6.4	NA
	p-value =	.054					
End of Treatment (V5)	Placebo	46	6.43 (0.78)	6.3	5.1,8.5	5.9,6.9	NA
	Active	47	6.33 (0.74)	6.3	4.7,8.8	5.85,6.65	NA
Difference Active – Placebo		0.24					
p-value =		0.148					

Cholesterol levels at baseline were slightly higher in the placebo group compared to the treatment group, however this difference was found not to be statistically significant (p = 0.054). The changes observed in the difference between the values of the placebo group and treatment group at baseline and visit 5 were 0.24 mmol/L and this was also not statistically significant (p = 0.148). These findings are similar to those of the Per Protocol (PP) population, with the difference between groups being 0.186 mmol/L, which was also not significant (p = 0.29). Results for the PP population are shown in the Table 1 in the supplementary materials.

The results for the secondary outcomes for the change in total cholesterol concentration showed no statistically significant differences between the treatment and placebo groups from baseline to visit #3 (p = 0.197; p = 0.297) or baseline to visit #4 (p = 0.51; p = 0.804) in the ITT and PP populations, respectively. Results for the secondary outcomes for the change in total cholesterol concentration in the ITT and PP populations are shown in Table 2.1. ITT and 2.1.PP in the supplementary materials, respectively.

The results for the secondary outcomes for the change in LDL-cholesterol concentration showed no significant differences between the treatment and placebo groups from baseline to visit #3 (p = 0.154; p = 0.276), baseline to visit #4 (p = 0.495; p = 0.808) or baseline to visit #5 (p = 0.194; p = 0.437) in either the ITT or PP populations, respectively. Results for the secondary outcomes for the change in LDL-cholesterol concentration in the ITT and PP populations are shown in Table 2.2. ITT and 2.2.PP in the supplementary materials, respectively.

The results for the secondary outcomes for the change in HDL-cholesterol concentration showed no significant differences between the treatment and placebo from baseline to visit #3 (p = 0.962; p = 0.756), baseline to visit #4 (p = 0.769; p = 0.782) or baseline to visit #5 (p = 0.86; p = 0.511) in either the ITT or PP

populations, respectively. Results for the secondary outcomes for the change in LDL-cholesterol concentration in the ITT and PP populations are shown in Table 2.3. ITT and 2.3.PP in the supplementary materials, respectively.

The results for the secondary outcomes for the change in triglyceride concentration showed no significant differences between the treatment and placebo groups in the change in triglyceride concentrations from baseline to visit #3 ($p = 0.255$; $p = 0.202$), baseline to visit #4 ($p = 0.805$; $p = 0.838$) or baseline to visit #5 ($p = 0.818$; $p = 0.797$) in either ITT or PP populations, respectively. Results for the secondary outcomes for the change in LDL-cholesterol concentration in the ITT and PP populations are shown in Table 2.4. ITT and 2.4.PP in the supplementary materials, respectively.

3.4.2 Safety Outcomes

Throughout the study there was only one SAE reported and although it did occur during the course of the study, it was unrelated to the study product and was resolved with therapy after a two week period.

A total of sixty one adverse events (AEs) were reported throughout the study. There was an equal number of participants that experienced at least one Treatment-Emergent Adverse Event (TEAE), with twenty three participants reporting at least one TEAE in the placebo group and the same number in the treatment group ($p = 0.516$). Others AEs that were reported were not related to the study product/treatment. There were nineteen participants from the placebo group and eighteen from the treatment group who reported experiencing one AE and four participants from the placebo group and five participants from the treatment correspondingly reported two AEs ($p = 0.500$) throughout the course of the study. No subjects reported more than two AEs throughout the course of the study.

Majority of the AEs reported were classified as “Mild intensity” (twenty five in the placebo group and twenty six in the treatment group), and two AEs in each group were classified as “Moderate intensity”, with no AE being classified as “Severe intensity” ($p = 0.681$).

It was established that none of the TEAEs reported had a definite and probable relationship to the study product, however there were more possible relationships to the study product in the treatment group (8) when compared with the placebo group (5). There were also four events in the treatment group that were unlikely to be related to the study product. Twenty two reported events in the placebo group and sixteen reported events in the treatment group ($p = 0.60$) were deemed to be unrelated to the study product.

In relation to any of the AEs reported in the placebo and treatment groups (nineteen and twenty one, respectively) no action was taken. However, treatment was discontinued for two participants in the placebo group and one in the treatment group, and therapy was required for six and four subjects in the placebo and treatment groups, respectively. Hospitalisation was not required for any participants that reported a TEAE, however, one subject from the treatment group was referred to a GP, and one action in the same group was reported as “Other” ($p = 0.598$). All TEAEs resolved ($p = 1.000$).

3.4.3 Targeted quantification of 22 metabolites in plasma samples.

Plasma samples were extracted according to the validated protocol by Anesi *et al.* [193]. For each participant, the first (V2) and last (V5) time points were selected, however for some participants V2 time points were not available and therefore the first time point available e.g. V3 was used instead. Missing values (or zero values) were replaced with an arbitrary number equal to 1/10 of the minimum value for each

multivariate metabolite. Following that, data was transformed (expressed as μmol) as log_2 and the difference between V5 and baseline was calculated, therefore ending up with one single point for each participant. Multivariate data analysis of both plasma and urine metabolites was performed using MetaboAnalyst 4.0 software (https://www.metaboanalyst.ca); no filtering, transformation and scaling were performed. Principal Component Analysis (PCA) score plots for plasma metabolites are reported in Figure 2a below. Despite the 46.3% of variation, explained by PC1 and PC2, there was no clear distinction between the treatment and placebo groups. Partial Least Square-Discriminate Analysis (PLS-DA) (Figure 2b) was also performed, but the model was not statistically significant, as shown by a resulting *p*-value of 0.6615 following permutation test (Figure 2c).

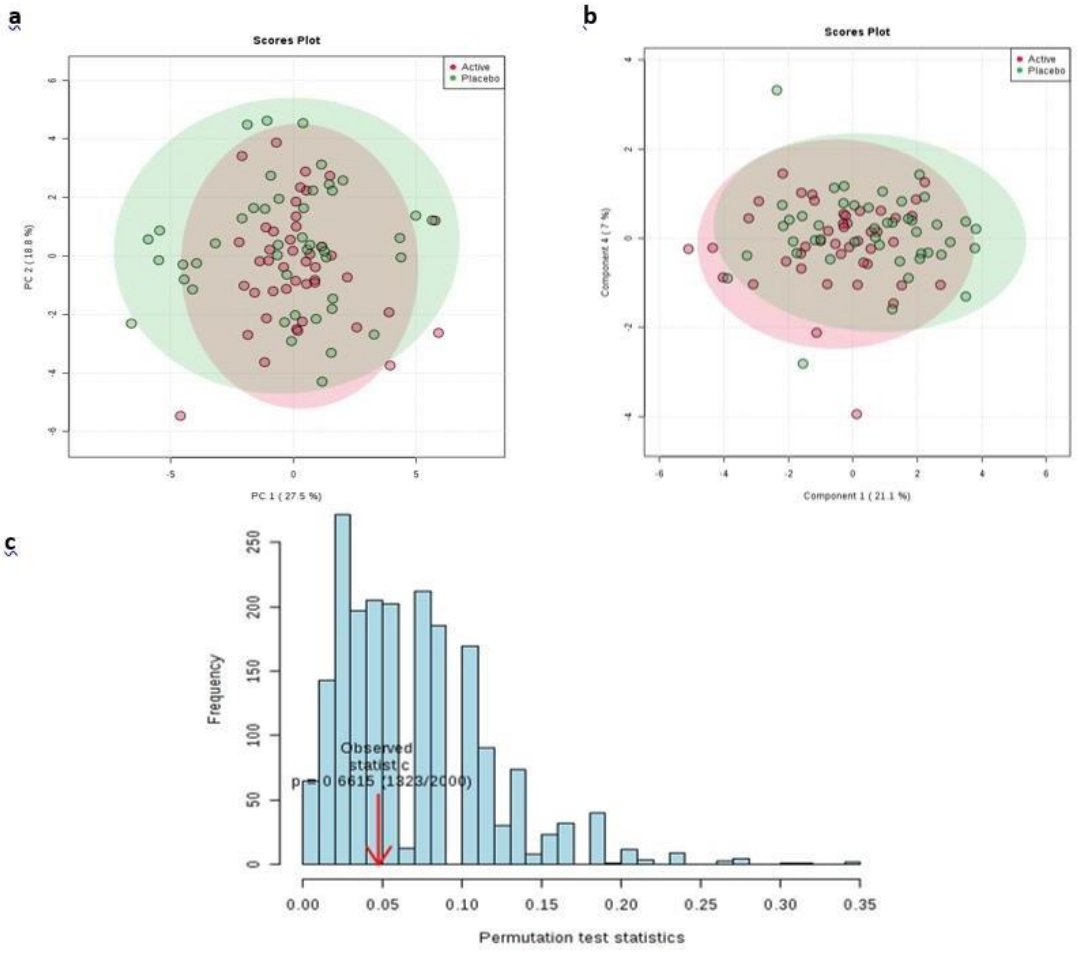

Figure 2: Plasma metabolites analysis (a) PCA score plot, (b) PLS-DA score plot of plasma samples (active (treatment) – red, placebo – green) and (c) Permutation test statistics.

Volcano plots in Figure 3 visualise the statistical significance (*p*-value, Y axis) versus the fold change (X-axis). Figure 4 (a-d) shows four metabolites, kynurenic acid, xanthurenic acid, kynurenine and tyrosine, which were significantly higher in the placebo (left) group compared to the treatment group (right). L-valine, highlighted by the blue circle, was >1.5 fold higher in the treatment group but was not considered statistically significant (p-value > 0.05). Similarly, indole-3-caroboxaldehyde, indole-3-lactic acid, tryptophan and L-isoleucine displayed a fold change of >1.5 in the placebo group by were not considered statistically significant

(*p*-value > 0.05).

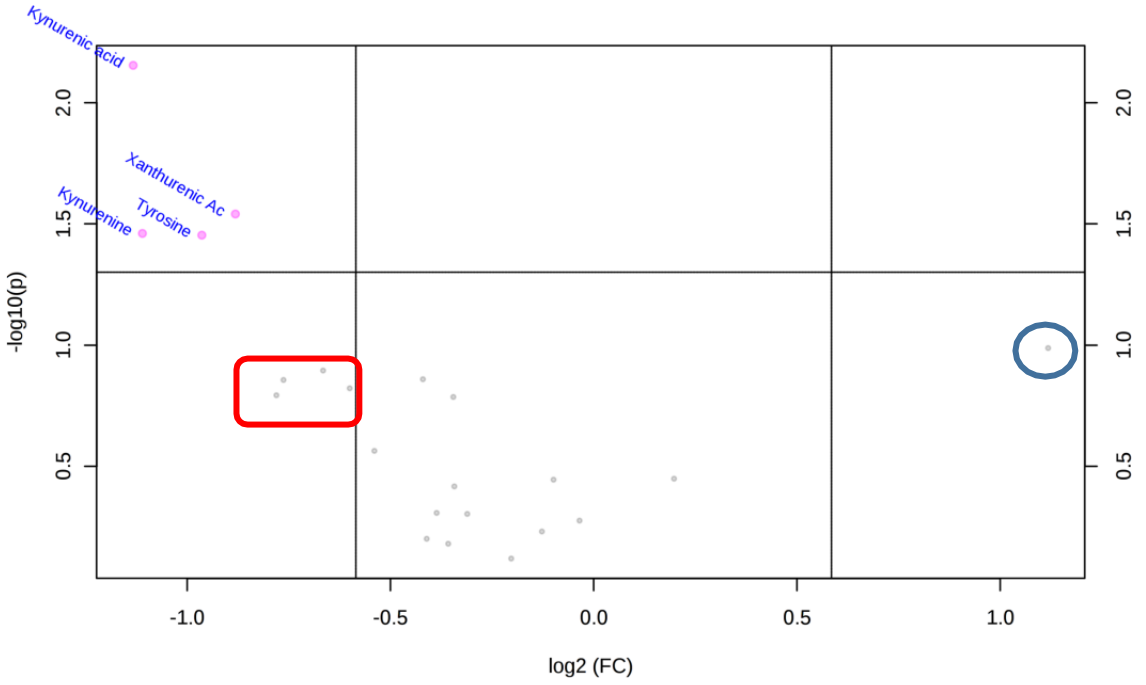

Figure 3: **Volcano plot of plasma sample analysis**. *P*-value threshold: 0.05; fold change: 1.5.

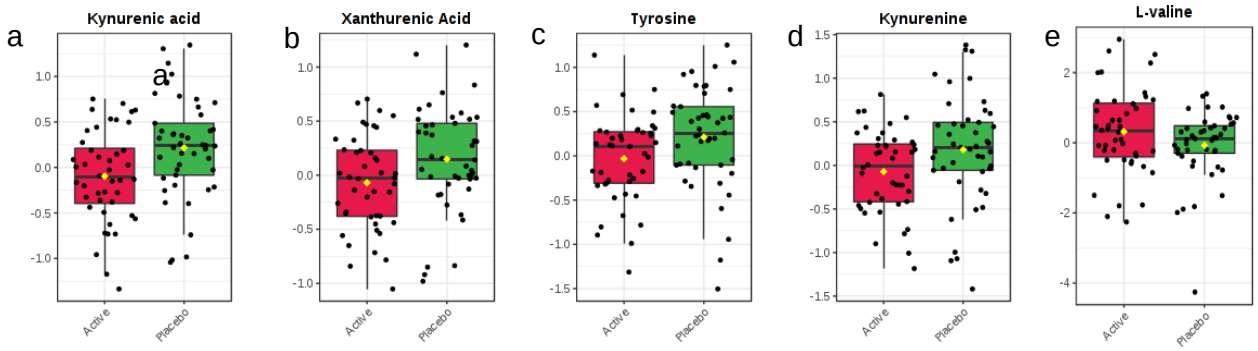

Figure 4. Box-plots of selected plasma metabolites (a-d) which were significantly higher in the placebo group (right) compared to treatment group (left), (e) Box-plot of L-valine which was >1.5 fold higher in the active group compared to the placebo, not significant (*p*-value > 0.05).

Table 3 provides a summary of the plasma biomarkers detected during analysis, where data are expressed as mean ± SEM (median (IQR)). Data were analysed using

linear mixed (normally distributed data) or generalised linear mixed models; *p*-value shown in metabolite column depicts treatment*time interaction, *p*-value in the same row depicts the difference between the two group at a specific time point. * in the same column within the metabolite depicts the differences between time points within the same group. Treatment: n: baseline (V2) = 47, 4-weeks (V3) = 28, 8-weeks (V4) = 44 and 12-weeks (V5) = 42. Placebo: n: baseline (V2) = 45, 4-weeks (V3) = 26, 8-weeks (V4) = 43 and 12-weeks (V5) = 41. Within the summary table, two metabolites, namely methionine (p = 0.03) and phenylalanine (p = 0.01) were significantly different between the active and placebo groups, Furthermore, there were significant differences identified between week 8 and the rest of the time points for methionine (p = 0.02), and between week 4 the rest of the times points for phenylalanine (p = 0.01). Graphical representation of the concentrations of plasma biomarkers are presented in supplementary material (Supplemental Figure 4).

Table 3. Concentrations of plasma biomarkers

Metabolite	**Treatment**	**Placebo**	**P-value**
Methionine			0.03
Baseline (V2)	10.47±0.41	10.06±0.35	
4-weeks (V3)	11.44±0.74	10.35±0.53	
8-weeks (V4)	9.73±0.41*	11.13±0.44	0.02
12-weeks (V5)	11.03±0.38*	11.15±0.51	
L-valine			0.21
Baseline (V2)	58.54±4.59	63.31±3.29	
4-weeks (V3)	66.25±5.81	67.72±5.19	
8-weeks (V4)	56.7±3.96	67.61±3.28	
12-weeks (V5)	66.72±4.09	62.38±4.22	
Quinolinic acid			0.59
Baseline (V2)	0.47±0.03	0.38±0.02	
4-weeks (V3)	0.42±0.03	0.37±0.04	
8-weeks (V4)	0.4±0.03	0.38±0.04	
12-weeks (V5)	0.36±0.03	0.4±0.04	
Isoleucine			0.54
Baseline (V2)	26.39±1.48	24.18±1.1	
4-weeks (V3)	27.89±2.4	27.34±1.66	
8-weeks (V4)	24.15±1.05	25.47±1.01	
12-weeks (V5)	26.08±1.21	27.61±1.48	
Leucine			0.12
Baseline (V2)	52.29±2.36	48.75±1.68	

4-weeks (V3)	54.28±3.59	52.34±2.52	
8-weeks (V4)	47.95±1.76	51.86±1.71	
12-weeks (V5)	52.58±1.97	53.23±2.29	
Dopamine			0.41
Baseline (V2)	0.04±0	0.04±0	
4-weeks (V3)	0.04±0	0.03±0	
8-weeks (V4)	0.04±0	0.03±0	
12-weeks (V5)	0.04±0	0.04±0	
Serotonin			0.51
Baseline (V2)	0.05±0.03	0.13±0.04	
4-weeks (V3)	0.08±0.05	0.02±0.01	
8-weeks (V4)	0.02±0	0.02±0.01	
12-weeks (V5)	0.05±0.02	0.04±0.01	
Tyrosine			0.11
Baseline (V2)	38.05±1.58	35.47±1.6	
4-weeks (V3)	37.76±2.74	38.38±2.35	
8-weeks (V4)	35.27±1.94	40.86±2.22	
12-weeks (V5)	36.4±1.62	40.57±1.96	
Phenylalanine			0.01
Baseline (V2)	32.57±1.25	29.86±1.21	
4-weeks (V3)	28.45±1.67	33.72±1.64	0.01
8-weeks (V4)	31.42±2.13	32.5±1.5	
12-weeks (V5)	34.33±4.11	31.32±1.29	
Tyramine			0.72
Baseline (V2)	0.03±0	0.03±0	
4-weeks (V3)	0.03±0	0.03±0	
8-weeks (V4)	0.03±0	0.03±0	
12-weeks (V5)	0.03±0	0.03±0	
3,4-Dihydroxyphenylacetic acid			0.26
Baseline (V2)	0.05±0	0.04±0	
4-weeks (V3)	0.04±0	0.05±0.01	
8-weeks (V4)	0.04±0	0.04±0	
12-weeks (V5)	0.04±0	0.04±0.01	
Kynurenic acid			0.26
Baseline (V2)	0.07±0	0.06±0	
4-weeks (V3)	0.07±0	0.07±0	
8-weeks (V4)	0.06±0	0.07±0	
12-weeks (V5)	0.07±0	0.07±0	
5-Hydroxyindole-3-acetic acid			0.30
Baseline (V2)	0.05±0	0.04±0	
4-weeks (V3)	0.04±0	0.04±0	
8-weeks (V4)	0.05±0.01	0.05±0	
12-weeks (V5)	0.04±0	0.05±0.01	
Tryptophan			0.12
Baseline (V2)	29.89±1.11	27.6±0.92	
4-weeks (V3)	30.1±1.62	28.73±1.36	
8-weeks (V4)	27.37±0.95	30.44±1.36	
12-weeks (V5)	28.62±0.95	30.54±1.42	

3-Hydroxyanthranilic acid			0.41
Baseline (V2)	0.02±0	0.02±0	
4-weeks (V3)	0.02±0	0.02±0	
8-weeks (V4)	0.01±0	0.02±0	
12-weeks (V5)	0.02±0	0.02±0	
Indole-3-Acetic acid			0.49
Baseline (V2)	2.1±0.25	1.99±0.2	
4-weeks (V3)	2.11±0.36	2.02±0.26	
8-weeks (V4)	1.78±0.12	2.35±0.39	
12-weeks (V5)	1.84±0.18	2.21±0.25	
Indole-3-Carboxaldehyde			0.61
Baseline (V2)	0.1±0.01	0.09±0.01	
4-weeks (V3)	0.1±0.01	0.09±0.01	
8-weeks (V4)	0.09±0.01	0.09±0.01	
12-weeks (V5)	0.08±0	0.09±0.01	
Indole-3-lactic acid			0.30
Baseline (V2)	1±0.07	0.89±0.05	
4-weeks (V3)	1.08±0.13	1±0.09	
8-weeks (V4)	0.88±0.04	0.97±0.06	
12-weeks (V5)	0.91±0.05	1.01±0.07	
Indole-3-Propionic acid			0.45
Baseline (V2)	1.09±0.1	1.24±0.13	
4-weeks (V3)	1.06±0.11	1.09±0.2	
8-weeks (V4)	1.2±0.09	1.18±0.13	
12-weeks (V5)	1.12±0.12	1.35±0.17	
Xanthurenic acid			0.07
Baseline (V2)	1.02±0.04	0.91±0.03	
4-weeks (V3)	1.02±0.06	0.95±0.04	
8-weeks (V4)	0.93±0.03	1.03±0.05	
12-weeks (V5)	0.95±0.03	1.03±0.05	
Kynurenine			0.11
Baseline (V2)	1.92±0.08	1.7±0.07	
4-weeks (V3)	1.87±0.12	1.88±0.12	
8-weeks (V4)	1.76±0.08	1.97±0.11	
12-weeks (V5)	1.79±0.09	1.98±0.12	
Indoxylsulfate			0.61
Baseline (V2)	9.38±0.81	8.26±0.78	
4-weeks (V3)	7.95±0.69	8.41±0.92	
8-weeks (V4)	8.48±0.66	8.58±0.61	
12-weeks (V5)	9.98±0.88	9.75±0.97	

3.4.4 Targeted Quantification of 30 metabolites in Urine Samples

Urine samples were prepared according to the validated protocol by Anesi *et al.* [193] and data analysis was performed as described above for the targeted quantification of plasma metabolites.

PCA score plot (Figure 5a) showed no clear separation between the treatment and

control groups, similar to what was described for plasma samples. Total variation, explained by PC1 and PC2, was 73%. PLS-DA (Figure 5b) was also performed, but the model was not statistically significant, as shown by a resulting *p*-value of 0.385 following permutation test (Figure 5c). Normalisation of the urine volume was not performed as the data were not available.

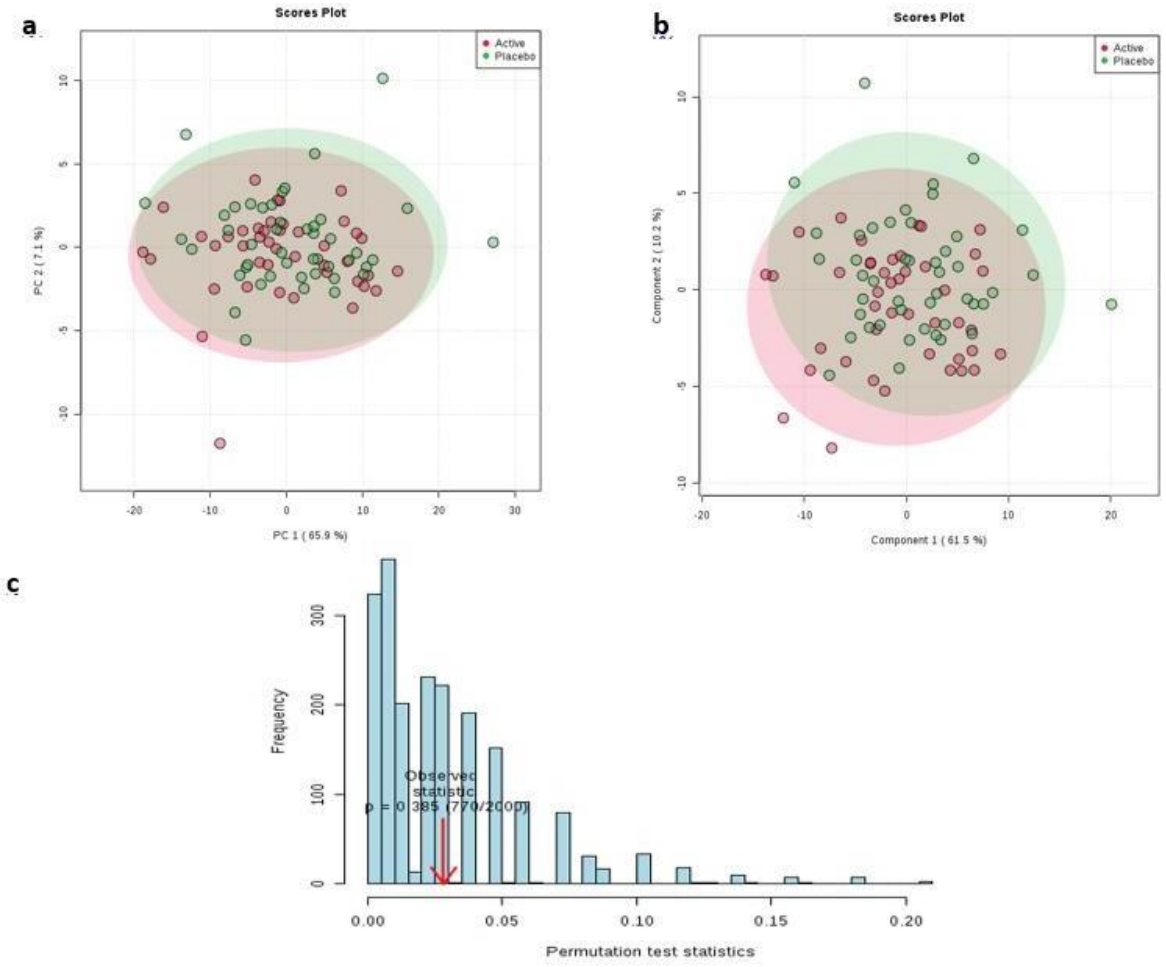

Figure 5: Urine metabolites analysis (a) PCA score plot, (b) PLS-DA score plot of plasma samples (active (treatment) – red, placebo – green) and (c) Permutation test statistics

Volcano plots in Figure 6 showed that no metabolite was statistically different between the two groups. However, three metabolites, indole-3-acetic acid, indole-3-acetamide and 3-hydyroxyanthranilic acid, highlighted by the red rectangle (Figure 6), were higher in the placebo group compared to the treatment group but were not

statistically significant (see Figure 7). Correction for urine volume may however increase the chance of detecting differences between the groups.

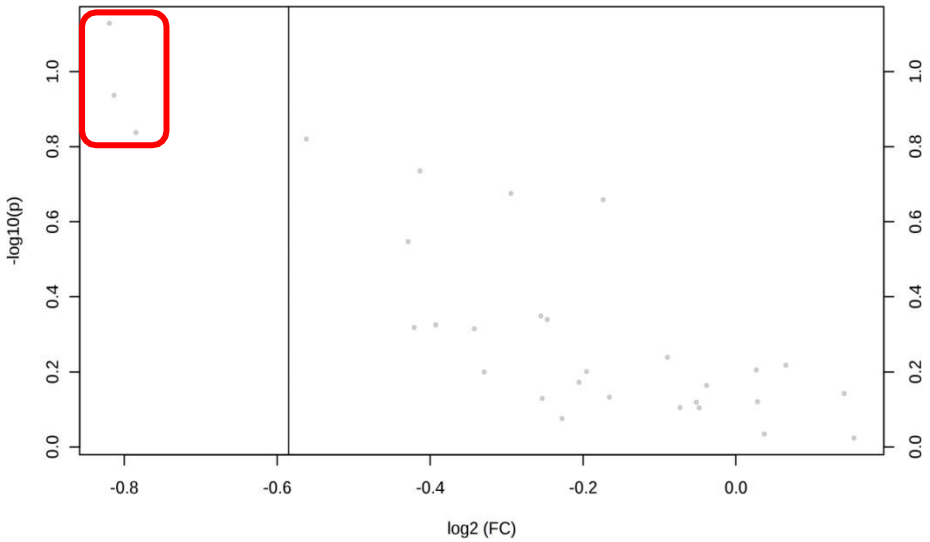

Figure 6. Volcano plot of urine sample analysis. Highlighted by red rectangle, three metabolites which were higher in placebo group compared to active group.

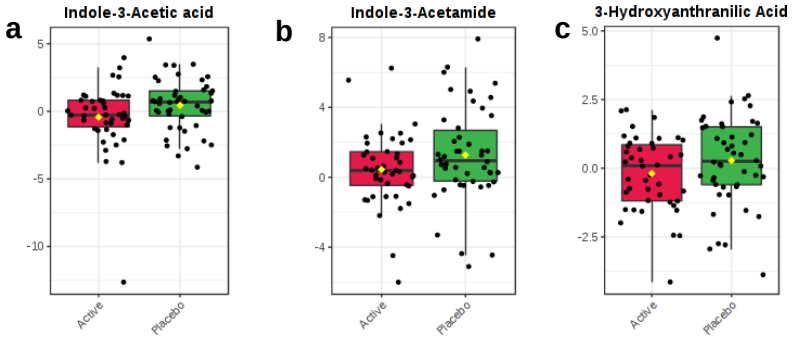

Figure 7. **Box-plots of selected urine metabolites** (a) indole-3-acetic acid, (b) indole-3-acetamide and (c) 3- hydyroxyanthranilic acid, all of which were higher in placebo group (right) compared to treatment group (left), but the differences were not significant.

Table 4 provides a summary of the urine biomarkers detected, in which data are expressed as mean ± SEM. Data were analysed as described above for plasma biomarkers. Treatment: n: baseline (V2) = 45, 4-weeks (V3) = 18, 8-weeks (V4) = 45 and 12-weeks (V5) = 44. Placebo: n: baseline (V2) = 45, 4-weeks (V3) = 20, 8-weeks (V4) = 42 and 12-weeks (V5) = 39. Within the summary table, four

metabolites, namely dopamine (p = 0.05), phenylalanine (p = 0.04), indole-3-acetamide (p = 0.04) and indole-3-acetic acid (p= 0.03) were significantly different between the active and placebo groups, Furthermore, there were significant differences identified at week 8 between the active and placebo groups for both dopamine and (p = 0.002) and phenylalanine (p = 0.04). Further, there were differences identified between baseline and week 12 and the rest of the time points for indole-3-acetamide and between weeks 4 and 12 and the rest of the times points for indole-3-acetic acid, both within the placebo group. Graphical representation of the concentrations of urine biomarkers are presented in supplementary material (Supplemental Figure 5).

Table 4. Concentrations of Urine Biomarkers

Metabolite	**Treatment**	**Placebo**	**p-value**
Methionine			0.59
Baseline	10.13±1.16	14.97±2.51	
4-weeks	9.23±2.25	10.14±2.96	
8-weeks	8.92±1.34	13.07±1.38	
12-weeks	10.36±1.48	12.41±1.49	
GABA			0.16
Baseline	0.25±0.05	0.22±0.04	
4-weeks	0.19±0.06	0.2±0.09	
8-weeks	0.22±0.04	0.31±0.06	
12-weeks	0.14±0.03	0.27±0.07	
L-valine			0.35
Baseline	35.86±3.84	51.07±7.94	
4-weeks	34.54±7.47	38.64±9.86	
8-weeks	34.58±5.15	49.4±5.6	
12-weeks	39.76±5.44	42.57±4.1	
Picolinic acid			0.77
Baseline	2.56±0.29	3.7±0.67	
4-weeks	2.91±0.66	3.28±1.09	
8-weeks	2.29±0.37	3.35±0.44	
12-weeks	2.83±0.41	3.33±0.48	
Quinolinic acid			0.33
Baseline	127.81±15.32	138.17±13.14	
4-weeks	118.58±27.19	121.98±23.13	
8-weeks	107.93±14.19	146.78±14.24	
12-weeks	113.91±12.18	140.73±13.13	

Isoleucine			0.17
Baseline	18.28±2.35	25.94±4.82	
4-weeks	18.79±5.38	18.06±4.31	
8-weeks	16.51±2.79	25.17±3.3	
12-weeks	21.8±3.59	21.76±2.82	
Leucine			0.20
Baseline	50.94±6.33	75.59±13.33	
4-weeks	56.31±17.4	53.41±12.74	
8-weeks	45.55±7.45	71.13±9.16	
12-weeks	58.03±8.91	63.32±8.45	
Dopamine			0.05
Baseline	3.13±0.37	3.98±0.53	
4-weeks	2.37±0.51	3.81±1.06	
8-weeks	2.36±0.27	4.43±0.53	0.002
12-weeks	3.26±0.45	3.35±0.37	
Serotonin			0.14
Baseline	0.89±0.09	1.3±0.17	
4-weeks	0.84±0.18	1.26±0.46	
8-weeks	0.82±0.12	1.36±0.16	
12-weeks	1.06±0.15	1.12±0.12	
Tyrosine			0.11
Baseline	186.17±20.6	296.22±48.69	
4-weeks	208.86±45.54	218.35±37.28	
8-weeks	165.05±21.49	275.64±29.77	
12-weeks	205.46±26.03	253.39±28.83	
Phenylalanine			0.04
Baseline	113.93±12.82	165.2±27.03	
4-weeks	112.76±25.18	106±16.97	
8-weeks	96.07±12.95	155.54±16.69	0.004
12-weeks	120.75±15.81	139.27±14.77	
Tyramine			0.43
Baseline	6.52±0.67	11.5±1.99	
4-weeks	7.5±1.24	10.68±2.88	
8-weeks	6.68±0.88	10.76±1.2	
12-weeks	7.85±1.01	9.82±1.13	
3-methodxy-p-tyramine			0.32
Baseline	0.39±0.05	0.58±0.09	
4-weeks	0.31±0.07	0.49±0.14	
8-weeks	0.35±0.05	0.6±0.07	
12-weeks	0.44±0.07	0.51±0.06	
3,4-Dihydroxyphenylacetic acid			0.06
Baseline	9.02±1.12	12.7±1.66	
4-weeks	8.89±2.92	10.42±2.22	
8-weeks	8.01±1.32	15.41±1.78	
12-weeks	9.13±1.1	11.3±1.32	
Kynurenic acid			0.71
Baseline	21.29±2.56	29.12±3.23	
4-weeks	21.55±4.09	35.22±12.96	
8-weeks	18.93±2.5	30.08±3.03	
12-weeks	24.04±3.27	28.96±2.81	

5-Hydroxyindole-3-acetic acid			0.27
Baseline	30.6±3.84	46.11±8.66	
4-weeks	24.55±6.61	33.9±9.23	
8-weeks	26.42±3.48	42.85±6.29	
12-weeks	29.96±3.74	39.65±9.12	
Tryptophan			0.09
Baseline	97.3±10.02	146.53±23.38	
4-weeks	100.56±22.15	126.26±31.95	
8-weeks	85.94±11	141.81±15.75	
12-weeks	110.84±15.05	122.39±12.88	
3-Hydroxantranilic acid			0.94
Baseline	6.72±0.92	8.07±1.27	
4-weeks	4.83±0.99	6.88±2.06	
8-weeks	5.39±0.91	7.35±0.98	
12-weeks	6.06±0.66	7.27±0.89	
Anthranilic acid			0.55
Baseline	0.2±0.03	0.2±0.02	
4-weeks	0.24±0.04	0.19±0.03	
8-weeks	0.24±0.03	0.23±0.02	
12-weeks	0.31±0.08	0.28±0.03	
Tryptamine			0.73
Baseline	0.33±0.04	0.66±0.12	
4-weeks	0.38±0.1	0.59±0.17	
8-weeks	0.32±0.04	0.62±0.1	
12-weeks	0.39±0.06	0.53±0.09	
Indole-3-acetamide			0.04
Baseline	0.11±0.03	0.11±0.01*	
4-weeks	0.18±0.06	0.14±0.01	
8-weeks	0.14±0.03	0.16±0.02	
12-weeks	0.17±0.03	0.27±0.07*	0.05
Indole-3-Acetic acid			0.03
Baseline	53.53±8.74	66.5±8.38	
4-weeks	42.05±6.6	32.3±5*	
8-weeks	46.32±6.22	73±11.86	
12-weeks	68.02±16.46	86.1±13.13*	
Indole-3-carboxylic acid			0.33
Baseline	0.41±0.07	0.66±0.16	
4-weeks	0.28±0.09	0.41±0.12	
8-weeks	0.33±0.07	0.65±0.17	
12-weeks	0.45±0.13	0.42±0.07	
Indole-3-carboxaldehyde			0.76
Baseline	0.56±0.05	0.75±0.1	
4-weeks	0.67±0.13	1.29±0.78	
8-weeks	0.58±0.09	0.78±0.1	
12-weeks	0.78±0.14	0.8±0.09	
Indole-3-lactic acid			0.18
Baseline	10.28±1.64	13.96±2.37	
4-weeks	7.85±2.45	38.41±31.06	
8-weeks	8.37±1.48	17.97±3.4	
12-weeks	16.01±4.02	16.41±4.5	

Indole-3-propionic acid			0.63
Baseline	0.08±0	0.09±0.01	
4-weeks	0.09±0.01	0.08±0.02	
8-weeks	0.08±0.01	0.1±0.01	
12-weeks	0.08±0.01	0.09±0.01	
Xanthurenic acid			0.53
Baseline	14.94±1.87	21.13±2.7	
4-weeks	14.7±2.9	33.9±19.67	
8-weeks	13.69±2.15	20.18±2.24	
12-weeks	18.21±2.74	20.88±2.49	
3-Hydroxkynurenine			0.17
Baseline	3.98±0.67	5.62±1.21	
4-weeks	3.05±0.69	5.7±1.92	
8-weeks	2.9±0.41	5.51±0.87	
12-weeks	3.64±0.5	4.41±0.47	
Kynurenine			0.13
Baseline	7.75±1.27	12.12±2.88	
4-weeks	8.95±2.82	10.22±2.42	
8-weeks	6.79±1.52	11.4±1.77	
12-weeks	7.63±1.29	10.36±1.66	
5-Hydroxytryptophan			0.42
Baseline	0.08±0.05	0.17±0.05	
4-weeks	0.11±0.06	0.19±0.07	
8-weeks	0.21±0.08	0.23±0.06	
12-weeks	0.12±0.04	0.08±0.03	
Indoxyl sulfate			0.10
Baseline	986.91±125.12	894.28±108.5	
4-weeks	884.02±236.1	745.25±161.25	
8-weeks	802.24±122.43	1035.56±114.61	
12-weeks	933.96±127.14	982.81±103.56	
Homovanilic acid			0.39
Baseline	49.83±5.56	69.57±8.67	
4-weeks	60.81±15.38	62.44±9.34	
8-weeks	52.56±8.28	81.86±9.64	
12-weeks	61.56±7.65	76.65±9.06	

3.4.5 Impact of daily oral supplementation of *Lb. mucosae* DPC 6426 on the gut microbiome

Enumeration of faecal bacterial counts from individual participants confirmed gastrointestinal transit and recovery of the administered *Lb. mucosae* DPC 6426 strain, with the average recovery of the strain being 1.26 x 10^7 CFU/g faeces at visit 5. There was a significant difference in CFU/g faeces between the baseline and visit

5 for the treatment group (*Lb. mucosae* DPC 6426), with baseline producing an average recovery of 1.37 x 10^6 CFU/g faeces.

Taxonomy-based analysis of the gut microbiome showed that at baseline (V2) the gut microbiota of participants in both placebo and treatment groups, were dominated by *Firmicutes* and *Bacteroidetes* (Figure 8) which is consistent with previous findings [1, 194]. The most abundant families were *Lachnospiraceae, Streptococcaceae* and *Bacteroidaceae* (Figure 9); and the most abundant genera were *Bacteroides, Faecalibacterium, Agathobacter* and *Subdoligranulum* (Figure 10). However, daily supplementation with *Lb. mucosae* DPC 6426, at a minimum concentration of 10^9 CFU/g, did not significantly alter the relative abundances of the gut microbiota between baseline (V2) and V5 of the participants in the treatment group, and appeared similar to that of the participants in the placebo group. Principal coordinate analysis (PCoA) generated using Bray Curtis, unweighted UniFrac and weighted UniFrac distances showed that there was no distinct separation between the placebo and treatment groups and between time points. (Supplementary Figure 2 and 3).

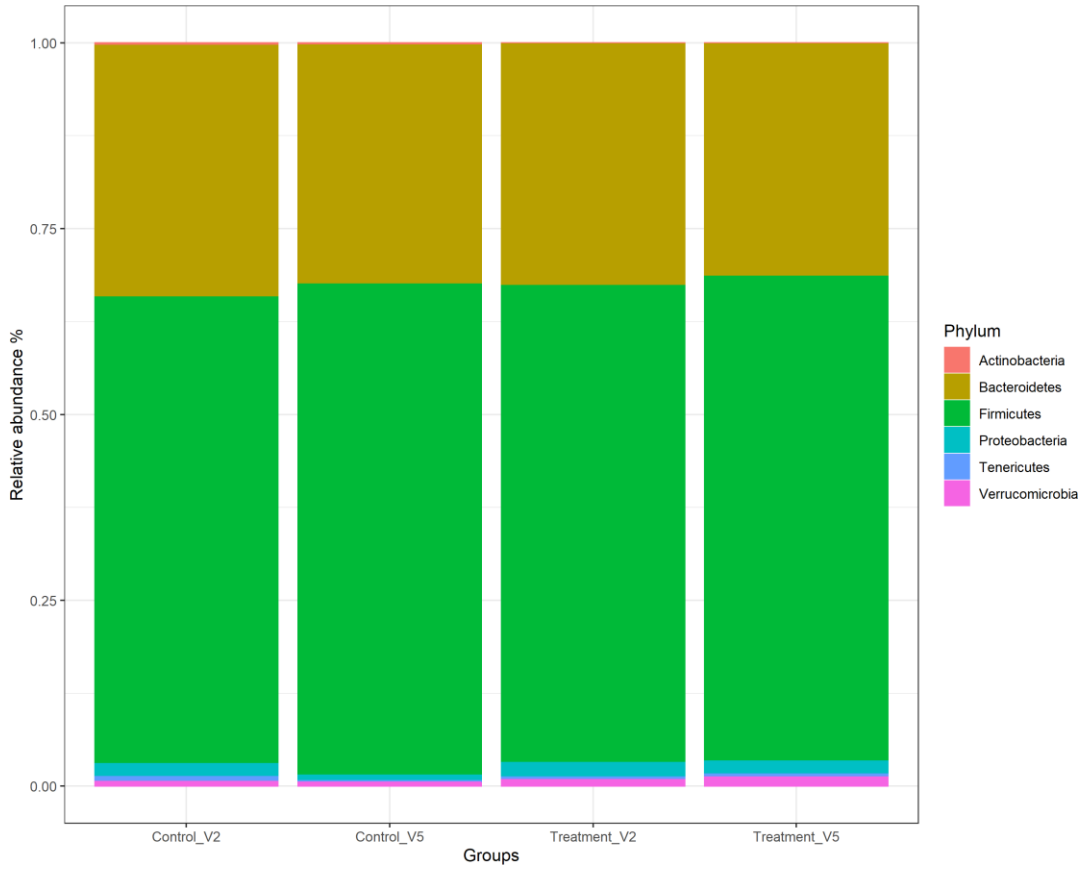

Figure 8. Phylum-level analysis Phylum-level taxonomic distribution of microbial communities in the faecal contents, expressed as a percentage of total population, in participants at baseline (V2) and end of the study (V5) for both control (placebo) and treatment groups.

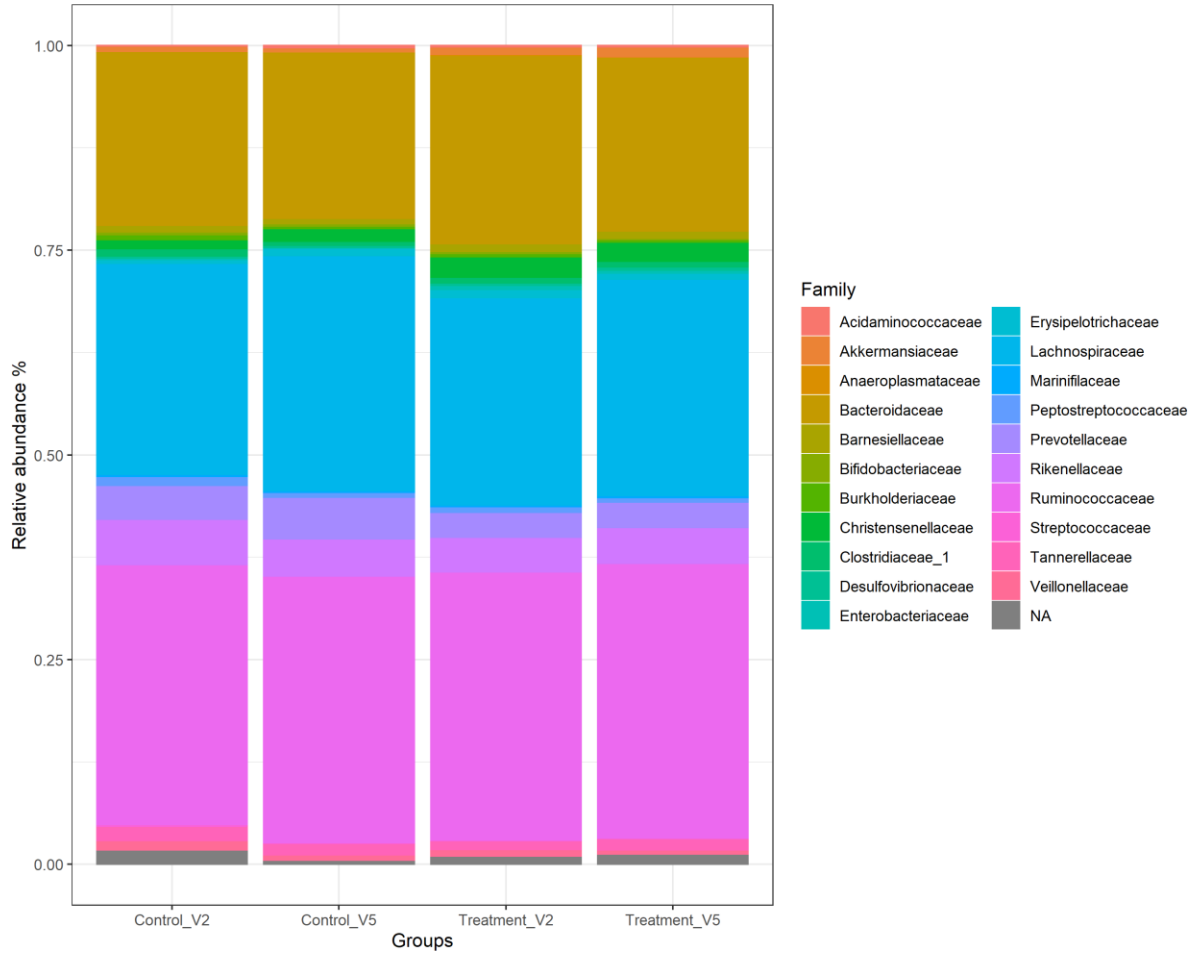

Figure 9. Family-level analysis Family-level taxonomic distribution of microbial communities in the faecal contents, expressed as a percentage of total population, in participants at baseline (V2) and end of the study (V5) for both control (placebo) and treatment groups.

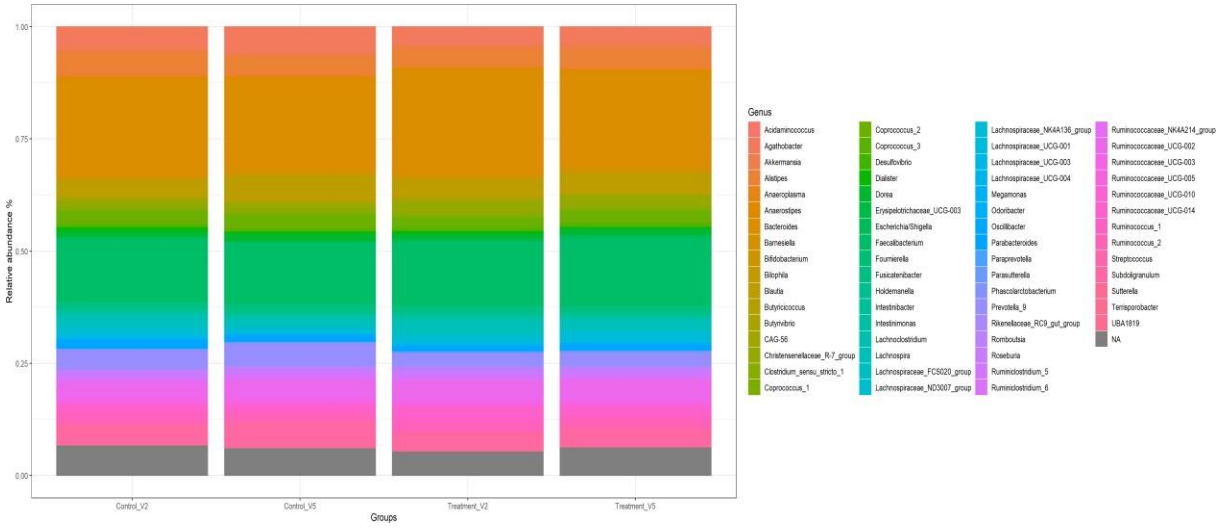

Figure 10. Genus-level analysis Genus-level taxonomic distribution of microbial communities in the faecal contents, expressed as a percentage of total population, in participants at baseline (V2) and end of the study (V5) for both control (placebo) and treatment groups.

3.5 Discussion

In this current study, the primary objective was to investigate the impact of daily dietary supplementation of the EPS producing *Lb. mucosae* DPC 6426 [174], on blood cholesterol levels and the gut microbiota composition, from baseline (V2) to week 12 (V5), in healthy mildly hypercholesterolaemic (≥ 5.5mmol/L and < 8 mmol/L) adults in a 12-week randomised, double blind, placebo controlled clinical trial. The primary efficacy endpoint was the change in total cholesterol between baseline (V2, day 0) and at the end of the trial (V5, week 12) between the treatment and placebo groups. The secondary efficacy objectives were to compare the effect of *Lb. mucosae* DPC 6426 supplementation on the changes in total cholesterol, from baseline to weeks 4 (V3) and 8 (V4), LDL-cholesterol, HDL-cholesterol and triglyceride concentrations from baseline to weeks 4, 8 and 12 (V5).

Results of the blood lipid analysis indicated that there were no statistically significant changes observed between the treatment and placebo groups from baseline to V5, baseline to V4 or baseline to V3 for total cholesterol, LDL-cholesterol, HDL-cholesterol or total triglyceride concentrations. Analysis of total cholesterol levels indicated that, on average, total cholesterol concentrations at baseline were slightly higher in the placebo group compared to the treatment group, however this difference was not considered to be statistically significant ($p = 0.054$). Furthermore, the change in the differences between the concentrations of the placebo group and treatment group at baseline and end of treatment was 0.24 mmol/L, however this was not statistically significant ($p = 0.148$). These findings were similar in the PP population, with the difference between the groups being 0.186 mmol/L with a *p*-value of 0.29. Analysis of secondary efficacy investigations indicated that there were no statistically significant differences between the placebo and treatment groups in the change in total cholesterol concentration from baseline to V3 ($p = 0.297$, $p = 0.197$) or baseline to V4 ($p = 0.804$, $p = 0.51$), in the change in LDL-cholesterol concentration from baseline to V3 ($p = 0.276$, $p = 0.154$), baseline to V4 ($p = 0.808$, $p = 0.495$) or baseline to V5 ($p = 0.437$, $p = 0.194$), in the change in HDL-cholesterol concentration from baseline to V3 ($p = 0.756$, $p = 0.962$), baseline to V4 ($p = 0.782$, $p = 0.769$) or baseline to V5 ($p = 0.511$, $p = 0.86$), and finally in the change in triglyceride concentration from baseline to V3 ($p = 0.202$, $p = 0.255$), baseline to V4 ($p = 0.838$, $p = 0.805$) or baseline to V5 ($p = 0.797$, $p = 0.818$).

There were no significant differences observed in the TEAEs reported between the placebo and treatment groups ($p = 0.516$). Furthermore, there were no significant differences observed in intensity ($p = 0.681$), relationship to product ($p = 0.060$), outcomes ($p = 1.000$) or serious adverse events ($p = 0.491$).

In this current study, analysis of the microbiota data indicated that there were no significant differences observed between the placebo and treatment groups. Taxonomy-based analysis at baseline (V2) showed that the gut microbiota of participants in both groups was dominated by *Firmicutes* and *Bacteroidetes.* The most abundant families were *Lachnospiraceae, Streptococcaceae* and *Bacteroidaceae,* and the most abundant genera were *Bacteroides, Faecalibacterium, Agathobacter* and *Subdoligranulum.* However, supplementation with *Lb. mucosae* DPC 6426 did not significantly alter the relative abundance of the gut microbiota between baseline (V2) and V5, and appeared similar to that of the participants in the placebo group.

Multivariate analysis of both plasma and urine metabolites reported that, based on the PCA scores plot and the PLS-DA scores plot, there was no clear distinction between the placebo and treatment groups and this model was deemed not to be statistically significant, based on the permutation test statistic which resulted in a *p*-value of 0.6615 for plasma metabolites and a *p*-value of 0.385 for urine metabolites. With regards to plasma metabolites, four metabolites, namely kynurenic acid, xanthurenic acid, kynurenine and tyrosine, were significantly higher in the placebo group compared to the treatment group. Additionally, L-valine was >1.5 fold higher in the treatment group compared to the placebo group, but was not statistically significant (*p*-value >0.05). Three urine metabolites, namely indole-3-acetic acid, indole-3-acetamide and 3-hydroxyanthranilic acid, were present in higher amounts in the placebo group compared to the treatment group but without statistical significance.

In conclusion, the results of this study indicate that daily supplementation with *Lb. mucosae* DPC 6426 at a minimum concentration of 10^9 CFU/g did not significantly

affect the blood lipid profiles or the gut microbiota of mildly hypercholesterolaemic adults. These data are contrary to the results previously obtained in the pre-clinical mouse trial [1]. Further investigations are necessary, using larger pre-clinical animal models and increased concentration of *Lb. mucosae* DPC 6426 to verify the efficacy of *Lb. mucosae* DPC 6426 *in vivo*.

3.6 Acknowledgments

The authors wish to thank the staff at Atlantia Food CRO, Cork, Ireland for their assistance in carrying out the trial, and Dr. Andrea Anesi for their assistance in plasma and urine metabolite analysis. We acknowledge the Teagasc Moorepark sequencing platform, Dr. Paul Cotter, Dr. Fiona Crispie and Laura Finnegan. This study was supported by an Enterprise Ireland Grant, EI Project Code: CF20133030A. The authors are supported in part by Science Foundation Ireland in the form of a centre grant for APC Microbiome Ireland Grant No. SFI/12/RC/2273-P2.

Supplemental Material

Supplementary Table 1. PP Primary Efficacy Analysis: Change in total cholesterol

		N	Mean (SD)	Median	Min,Max	1Q,3Q	Missing
Baseline (V2)	Placebo	41	6.45 (0.82)	6.3	4.9,8.2	5.8,7.2	NA
	Active	43	6.09 (0.91)	6	3.9,8.2	5.55,6.4	NA
	p-value =	.062					
End of Treatment (V5)	Placebo	41	6.49 (0.77)	6.4	5.2,8.5	6,6.9	NA
	Active	43	6.32 (0.76)	6.3	4.7,8.8	5.85,6.65	NA
Difference Active – Placebo		0.186					
p-value =		0.29					

Supplementary Table 2.1 ITT Secondary Efficacy Analysis: Change in total cholesterol

		N	Mean (SD)	Median	Min,Max	1Q,3Q	Missing
Baseline (V2)	Placebo	46	6.42 (0.8)	6.25	4.9,8.2	5.8,7.17	NA
	Active	47	6.08 (0.87)	6	3.9,8.2	5.6,6.4	NA
	p-value =	.054					
Visit 3	Placebo	46	6.4 (0.87)	6.2	5.1,9.3	5.8,6.9	NA
	Active	47	6.29 (0.71)	6.2	4.7,8.1	5.8,6.65	NA
Difference Active – Placebo		0.232					
	p-value =	0.197					
Visit 4	Placebo	46	6.47 (0.88)	6.3	5.1,8.6	5.8,7	NA
	Active	47	6.24 (0.65)	6.3	4.8,7.7	6,6.55	NA
Difference Active – Placebo		0.112					
p-value =		0.51					

Supplementary Table 2.1 PP Secondary Efficacy Analysis: Change in total cholesterol

		N	Mean (SD)	Median	Min,Max	1Q,3Q	Missing
Baseline (V2)	Placebo	41	6.45 (0.82)	6.3	4.9,8.2	5.8,7.2	NA
	Active	43	6.09 (0.91)	6	3.9,8.2	5.55,6.4	NA
	p-value =	.062					
Visit 3	Placebo	41	6.43 (0.88)	6.2	5.1,9.3	5.8,6.9	NA
	Active	43	6.27 (0.73)	6.1	497,8.1	5.8,6.65	NA
Difference Active – Placebo		0.201					
	p-value =	0.297					
Visit 4	Placebo	41	6.53 (0.87)	6.3	5.3,8.6	5.8,7	NA
	Active	43	6.22 (0.65)	6.3	4.8,7.7	6,6.55	NA
Difference Active – Placebo		0.045					
p-value =		0.804					

Supplementary Table 2.2 ITT Secondary Efficacy Analysis: Change in LDL-cholesterol concentrations

		N	Mean (SD)	Median	Min,Max	1Q,3Q	Missing
Baseline (V2)	Placebo	46	4.24 (0.84)	4.15	1.8,5.6	3.62,4.97	NA
	Active	47	4.02 (0.75)	3.9	2.2,6.2	3.5,4.45	NA
	p-value =	.080					
Visit 3	Placebo	46	4.25 (0.89)	4.15	1.8,6.7	3.73,4.78	NA
	Active	47	4.26 (0.66)	4.1	2.9,6.2	3.9,4.5	NA
Difference Active – Placebo		0.23					
	p-value =	0.154					
Visit 4	Placebo	46	4.36 (0.96)	4.15	2.3,6.3	3.73,.52	NA
	Active	47	4.25 (0.69)	4.2	3,5.9	3.85,4.8	NA
Difference Active – Placebo		0.114					
	p-value =	0.495					
Visit 5	Placebo	46	4.44 (1)	4.35	2.3,6.7	3.65,5.28	NA
	Active	47	4.43 (0.82)	4.3	2.8,7	4,4.8	NA
Difference Active – Placebo		0.213					
	p-value =	0.194					

Supplementary Table 2.2 PP Secondary Efficacy Analysis: Change in LDL-cholesterol concentrations

		N	Mean (SD)	Median	Min,Max	1Q,3Q	Missing
Baseline (V2)	Placebo	41	4.3 (0.78)	4.2	2.7,5.6	3.7,5	NA
	Active	43	4.04 (0.77)	3.9	2.2,6.2	3.5,4.5	NA
	p-value =	0.75					
Visit 3	Placebo	41	4.32 (0.87)	4.2	1.8,6.7	3.9,4.8	NA
	Active	43	4.25 (0.69)	4.1	2.9,6.2	3.9,4.5	NA
Difference Active – Placebo		0.185					
	p-value =	0.276					
Visit 4	Placebo	41	4.47 (0.89)	4.3	2.6,6.3	3.9,5.2	NA
	Active	43	4.25 (0.71)	4.2	3,5.9	3.8,4.8	NA
Difference Active – Placebo		0.043					
	p-value =	0.808					
Visit 5	Placebo	41	4.56 (0.94)	4.5	3,6.7	3.8,5.3	NA
	Active	43	4.44 (0.86)	4.3	2.8,7	3.95,4.9	NA
Difference Active – Placebo		0.134					
	p-value =	0.437					

Supplementary Table 2.3 ITT Secondary Efficacy Analysis: Change in HDL-cholesterol concentrations

		N	Mean (SD)	Median	Min,Max	1Q,3Q	Missing
Baseline (V2)	Placebo	46	1.68 (0.51)	1.55	1.05,3.09	1.32,1.91	NA
	Active	47	1.6 (0.46)	1.62	0.86,2.67	1.25,1.88	NA
	p-value =	0.533					
Visit 3	Placebo	46	1.68 (0.5)	1.52	1.03,3.2	1.34,1.8	NA
	Active	47	1.59 (0.4)	1.62	0.88,2.38	1.23,1.86	NA
Difference Active – Placebo		0.002					
	p-value =	0.962					
Visit 4	Placebo	46	1.67 (0.48)	1.51	1.1,3.13	1.34,1.9	NA
	Active	47	1.6 (0.43)	1.67	0.95,2.53	1.2,1.91	NA
Difference Active – Placebo		0.01					
	p-value =	0.769					
Visit 5	Placebo	46	1.68 (0.49)	1.6	1.03,3.13	1.3,1.87	NA
	Active	47	1.59 (0.43)	1.59	0.95,2.62	1.19,1.9	NA
Difference Active – Placebo		-0.007					
	p-value =	0.86					

Supplementary Table 2.3 PP Secondary Efficacy Analysis: Change in HDL-cholesterol concentrations

		N	Mean (SD)	Median	Min,Max	1Q,3Q	Missing
Baseline (V2)	Placebo	41	1.64 (0.47)	1.49	1.05,3.09	1.3,1.91	NA
	Active	43	1.59 (0.46)	1.62	0.86,2.67	1.25,1.86	NA
	p-value =	0.659					
Visit 3	Placebo	41	1.64 (0.45)	1.53	1.03,2.82	1.33,1.79	NA
	Active	43	1.58 (0.38)	1.62	0.88,2.387	1.23,1.84	NA
Difference Active – Placebo		-0.012					
	p-value =	0.756					
Visit 4	Placebo	41	1.64 (0.43)	1.5	1.1,2.8	1.34,1.85	NA
	Active	43	1.58 (0.42)	1.67	0.95,2.53	1.2,1.88	NA
Difference Active – Placebo		-0.01					
	p-value =	0.782					
Visit 5	Placebo	41	1.65 (0.44)	1.61	1.03,2.86	1.29,1.86	NA
	Active	43	1.57 (0.41)	1.59	0.95,2.62	1.19,1.9	NA
Difference Active – Placebo		-0.029					
	p-value =	0.511					

Supplementary Table 2.4 ITT Secondary Efficacy Analysis: Change in triglycerides concentrations

		N	Mean (SD)	Median	Min,Max	1Q,3Q	Missing
Baseline (V2)	Placebo	46	1.47 (0.75)	1.25	0.45,4.1	0.96,1.8	NA
	Active	47	1.38 (0.97)	1.13	0.56,6.05	0.9,1.48	NA
	p-value =	0.242					
Visit 3	Placebo	46	1.41 (0.87)	1.23	0.41,3.91	0.76,1.17	NA
	Active	47	1.46 (0.94)	1.22	0.61,5.63	0.91,1.58	NA
Difference Active – Placebo		0.13					
	p-value =	0.255					
Visit 4	Placebo	46	1.36 (0.7)	1.19	0.37,3.18	0.79,1.6	NA
	Active	47	1.34 (0.65)	1.19	0.52,3.37	0.88,1.53	NA
Difference Active – Placebo		0.03					
	p-value =	0.805					
Visit 5	Placebo	46	1.52 (0.85)	1.32	0.41,4.03	0.8,1.88	NA
	Active	47	1.41 (0.76)	1.23	0.51,3.5	0.84,1.68	NA
Difference Active – Placebo		-0.031					
	p-value =	0.818					

Supplementary Table 2.4 PP Secondary Efficacy Analysis: Change in triglycerides concentrations

		N	Mean (SD)	Median	Min,Max	1Q,3Q	Missing
Baseline (V2)	Placebo	41	1.49 (0.76)	1.27	0.45,4.1	1,1.81	NA
	Active	43	1.36 (0.96)	1.09	0.56,6.05	0.9,1.46	NA
	p-value =	0.156					
Visit 3	Placebo	41	1.46 (0.9)	1.23	0.41,3.91	0.8,1.76	NA
	Active	43	1.48 (0.96)	1.22	0.61,5.63	0.98,1.58	NA
Difference Active – Placebo		0.155					
	p-value =	0.202					
Visit 4	Placebo	41	1.39 (0.73)	1.18	0.37,3.18	0.8,2	NA
	Active	43	1.28 (0.59)	1.19	0.52,3.09	0.88,1.53	NA
Difference Active – Placebo		0.027					
	p-value =	0.838					
Visit 5	Placebo	41	1.57 (0.87)	1.41	0.41,4.03	0.8,1.91	NA
	Active	43	1.4 (0.74)	1.23	0.51,3.5	0.84,1.68	NA
Difference Active – Placebo		-0.037					
	p-value =	0.797					

Supplementary Figure 1. α-diversity analysis Chao1 index and Shannon compared between placebo and treatment groups between baseline (V2) and end of treatment (V5)

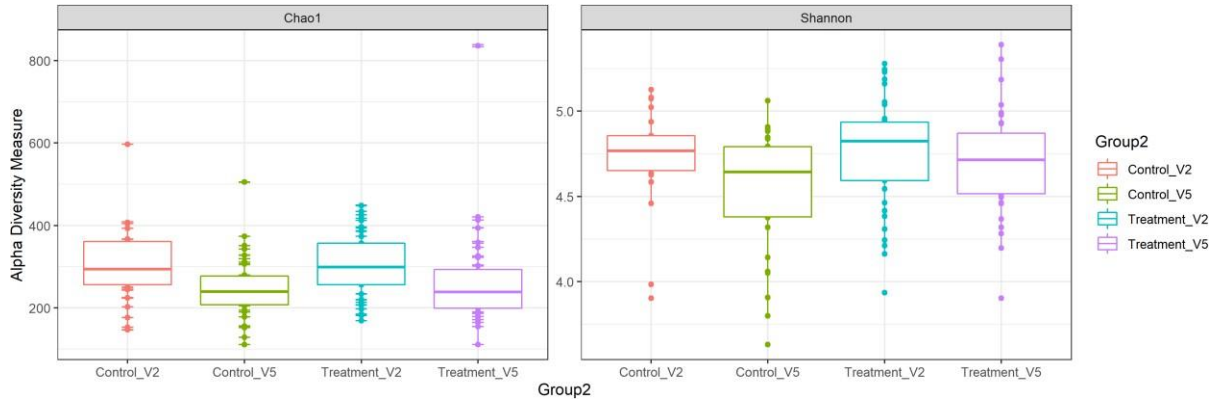

Supplementary Figure 2. Unweighted Principal coordinate analysis (PCoA), A treatment (placebo – red, active – blue) and B: time point (V2 – red, V5 – blue)

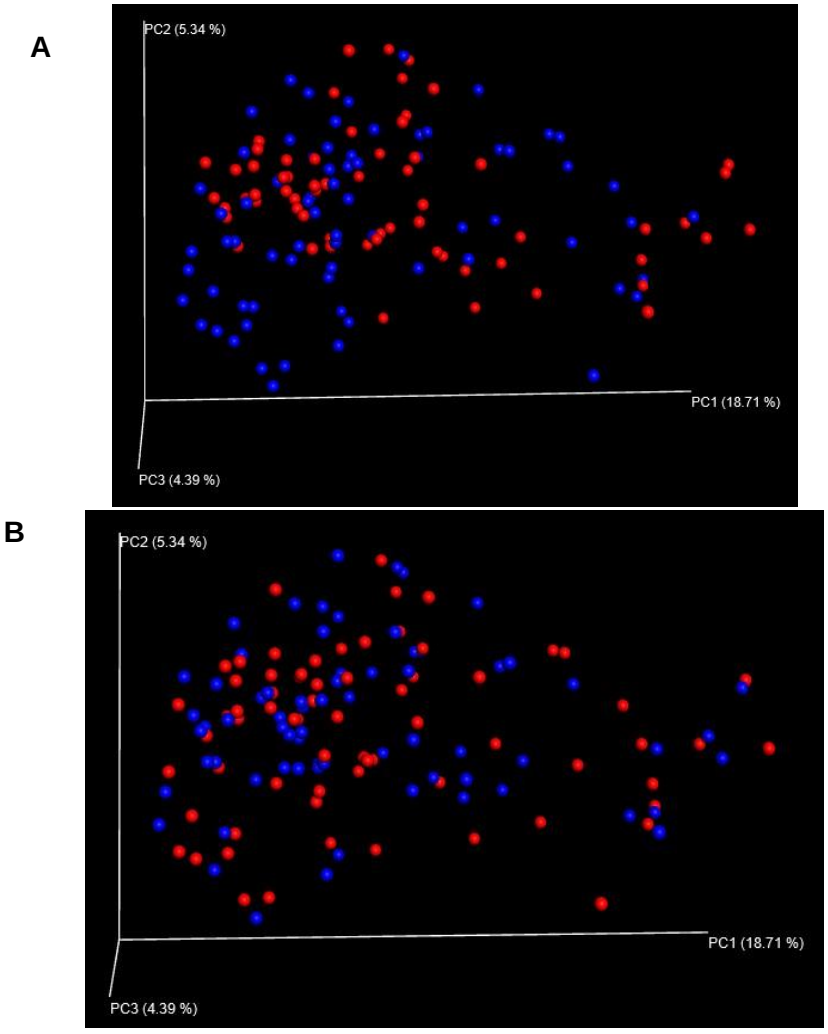

Supplementary Figure 3. Weighted Principal coordinate analysis (PCoA) A: treatment (placebo – red, active – blue) and B: time point (V2 – red, V5 – blue)

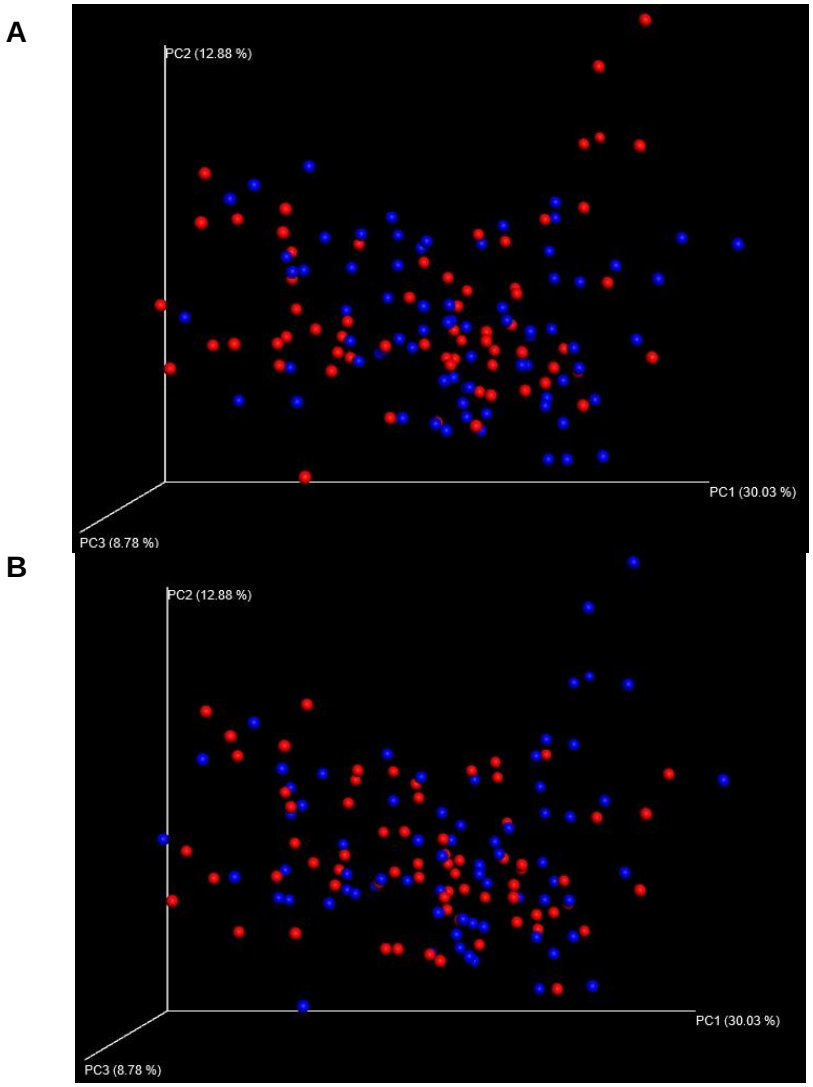

Supplementary Figure 4. Graphical representation of concentrations of plasma biomarkers

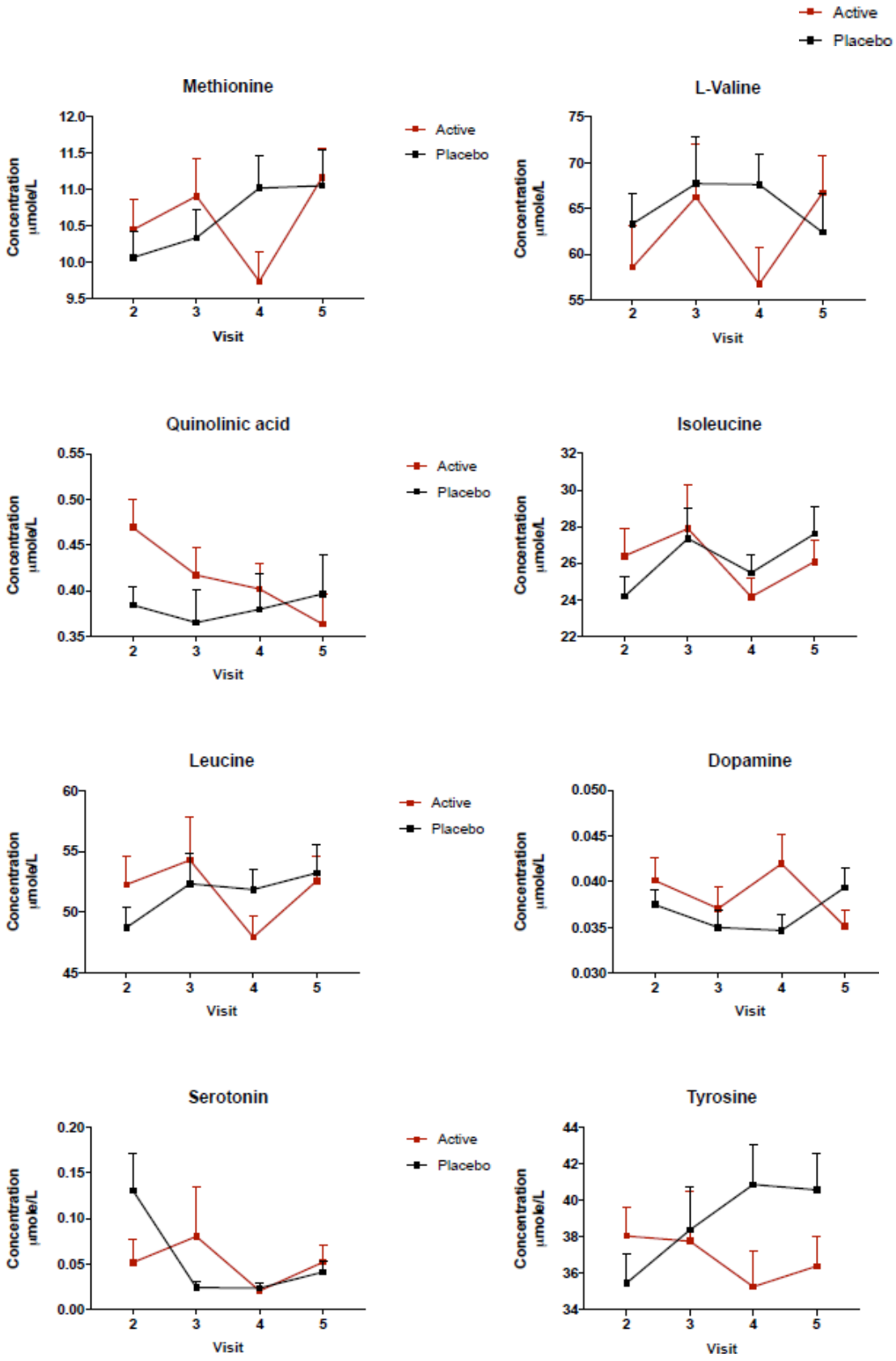

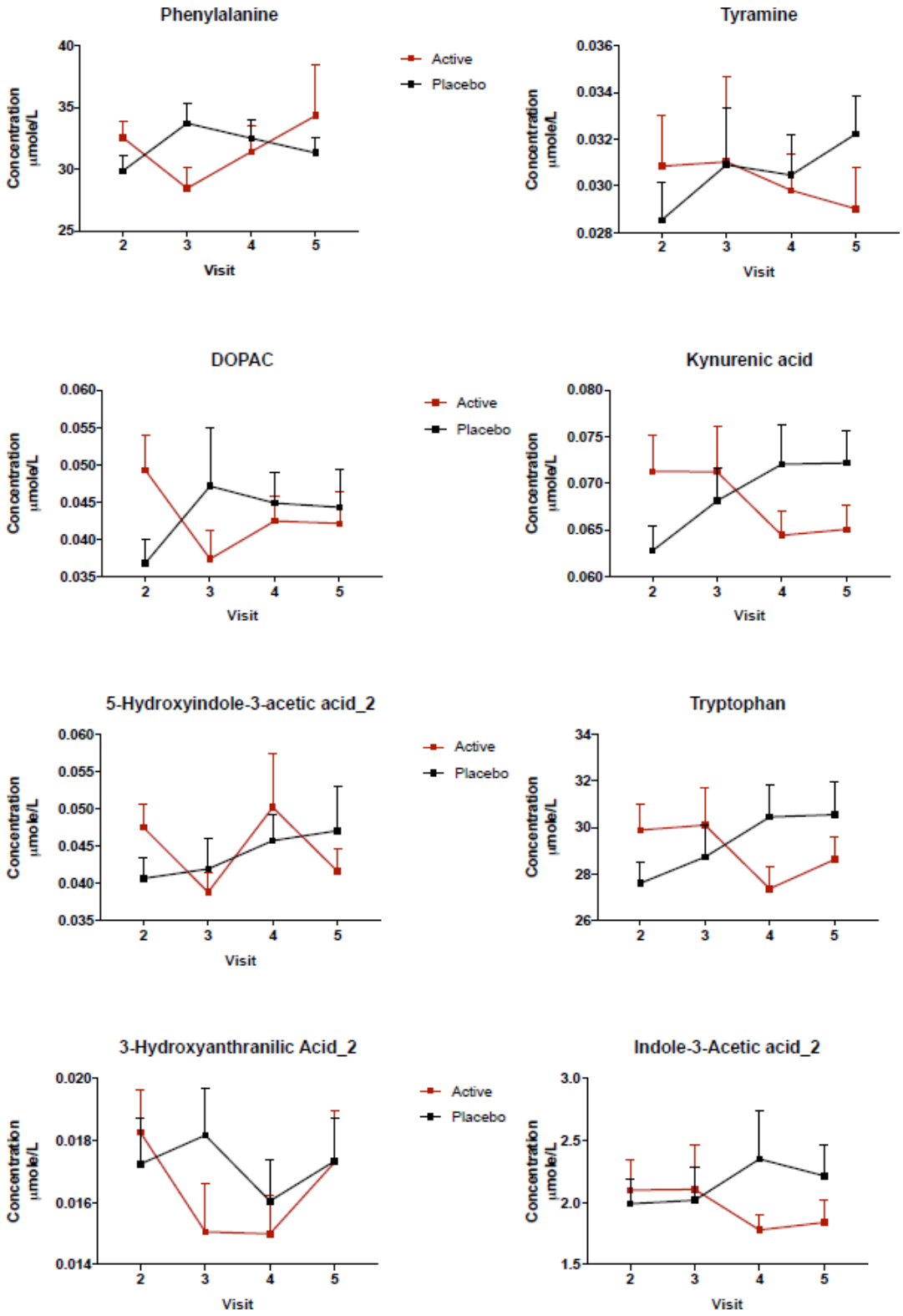
Phenylalanine
Concentration µmole/L
40
35
30
25
2
3
4
5
Visit
Active
Placebo
Tyramine
Concentration µmole/L
0.036
0.034
0.032
0.030
0.028
2
3
4
5
Visit
DOPAC
Concentration µmole/L
0.060
0.055
0.050
0.045
0.040
0.035
2
3
4
5
Visit
Active
Placebo
Kynurenic acid
Concentration µmole/L
0.080
0.075
0.070
0.065
0.060
2
3
4
5
Visit
5-Hydroxyindole-3-acetic acid_2
Concentration µmole/L
0.060
0.055
0.050
0.045
0.040
0.035
2
3
4
5
Visit
Active
Placebo
Tryptophan
Concentration µmole/L
34
32
30
28
26
2
3
4
5
3-Hydroxyanthranilic Acid_2
Concentration µmole/L
0.020
0.018
0.016
0.014
2
3
4
5
Visit
Active
Placebo
Indole-3-Acetic acid_2
Concentration µmole/L
3.0
2.5
2.0
1.5
2
3
4
5
Visit

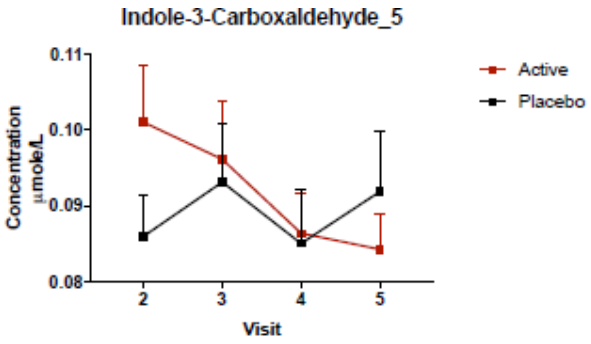
Indole-3-Carboxaldehyde_5
Concentration µmole/L
0.11
0.10
0.09
0.08
2
3
4
5
Visit
Active
Placebo

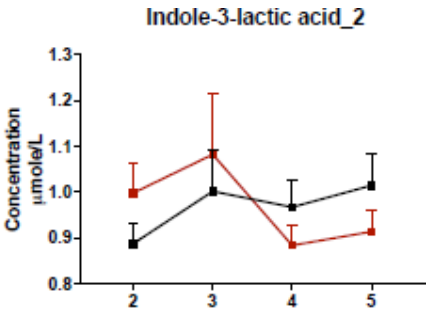
Indole-3-lactic acid_2
Concentration µmole/L
1.3
1.2
1.1
1.0
0.9
0.8
2
3
4
5

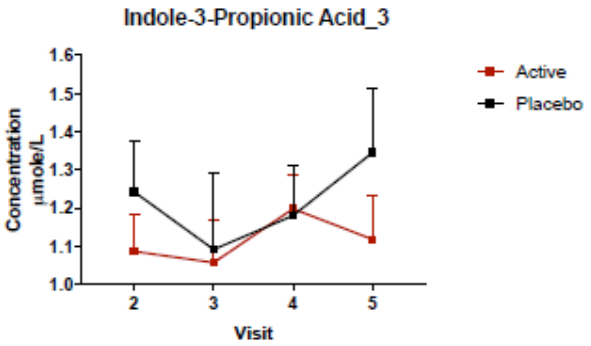
Indole-3-Propionic Acid_3
Concentration µmole/L
1.6
1.5
1.4
1.3
1.2
1.1
1.0
2
3
4
5
Visit
Active
Placebo

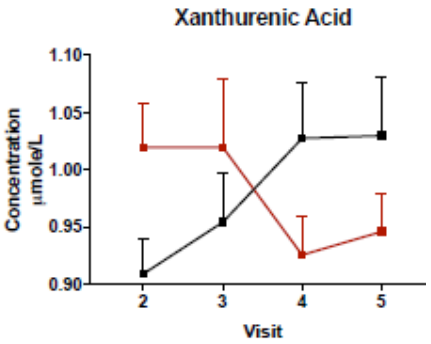
Xanthurenic Acid
Concentration µmole/L
1.10
1.05
1.00
0.95
0.90
2
3
4
5
Visit

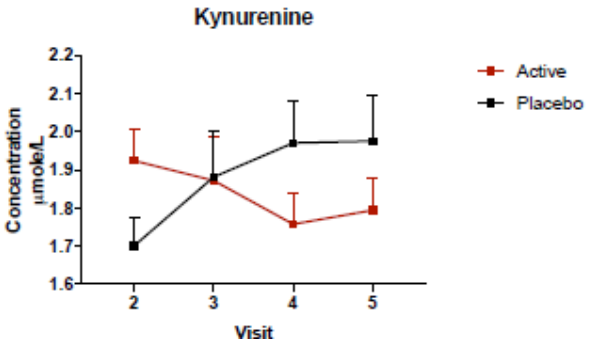
Kynurenine
Concentration µmole/L
2.2
2.1
2.0
1.9
1.8
1.7
1.6
2
3
4
5
Visit
Active
Placebo

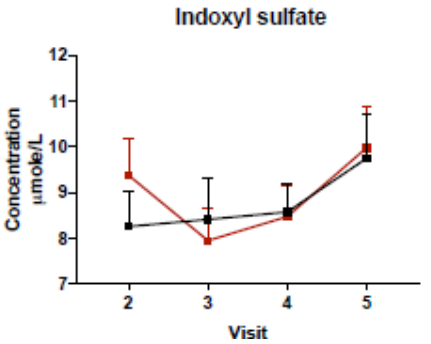
Indoxyl sulfate
Concentration µmole/L
12
11
10
9
8
7
2
3
4
5
Visit

Supplementary Figure 5. Graphical representation of concentrations of urine biomarkers

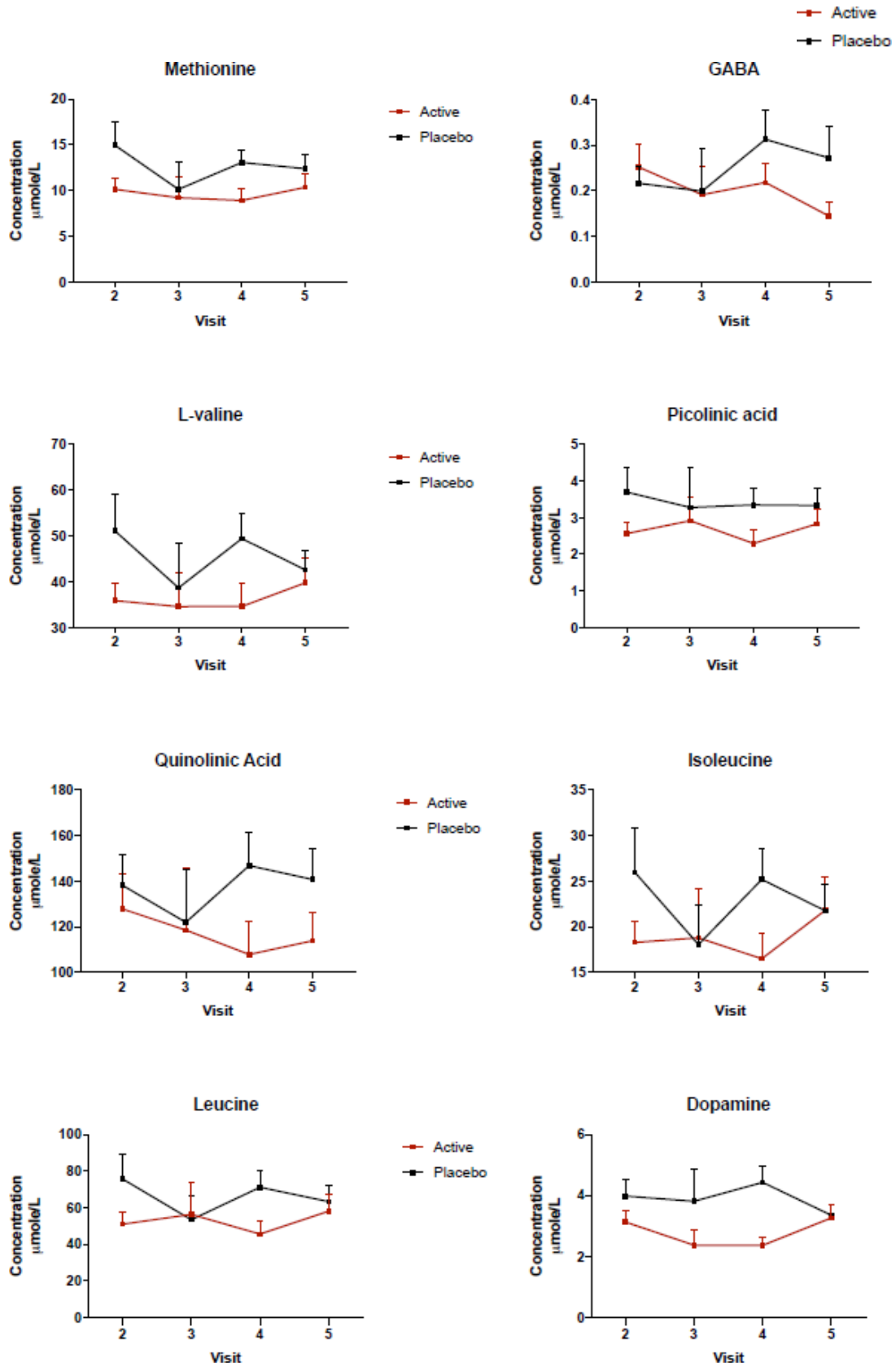

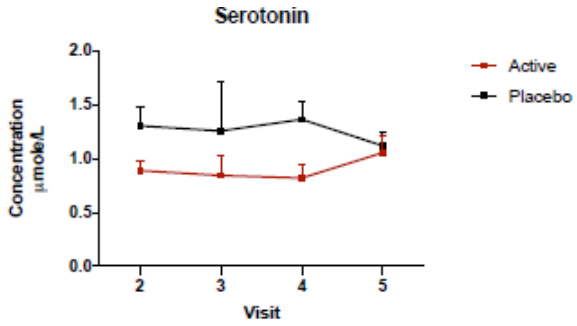
Serotonin
Concentration µmole/L
2.0
1.5
1.0
0.5
0.0
2
3
4
5
Visit
Active
Placebo

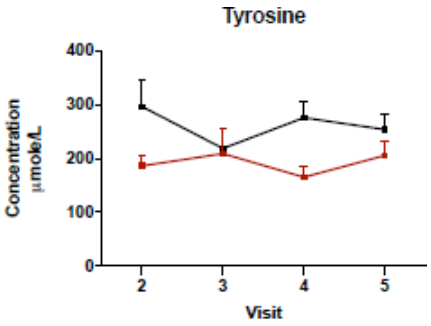
Tyrosine
Concentration µmole/L
400
300
200
100
0
2
3
4
5
Visit

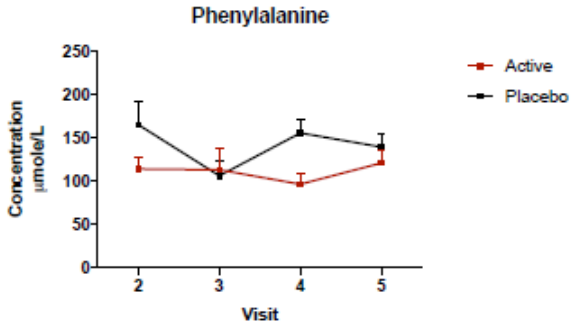
Phenylalanine
Concentration µmole/L
250
200
150
100
50
0
2
3
4
5
Visit
Active
Placebo

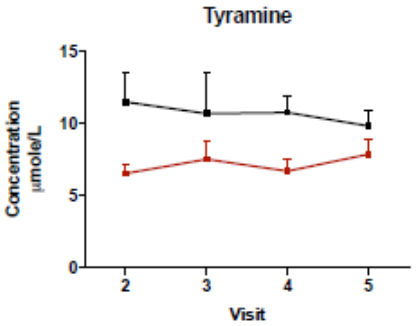
Tyramine
Concentration µmole/L
15
10
5
0
2
3
4
5
Visit

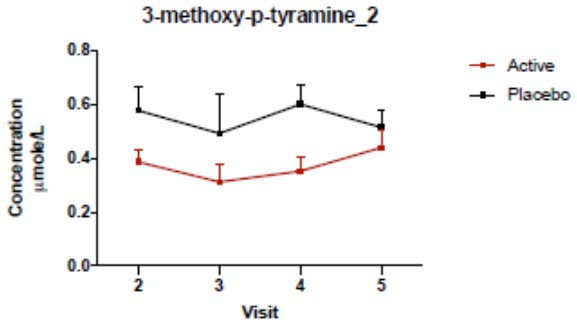
3-methoxy-p-tyramine_2
Concentration µmole/L
0.8
0.6
0.4
0.2
0.0
2
3
4
5
Visit
Active
Placebo

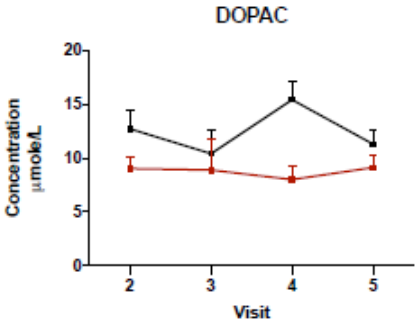
DOPAC
Concentration µmole/L
20
15
10
5
0
2
3
4
5
Visit

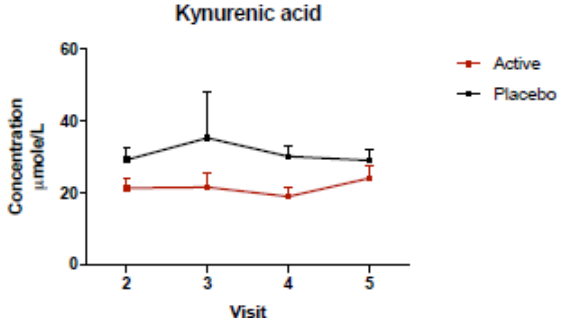
Kynurenic acid
Concentration µmole/L
60
40
20
0
2
3
4
5
Visit
Active
Placebo

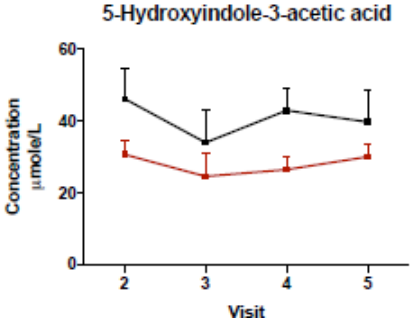
5-Hydroxyindole-3-acetic acid
Concentration µmole/L
60
40
20
0
2
3
4
5
Visit

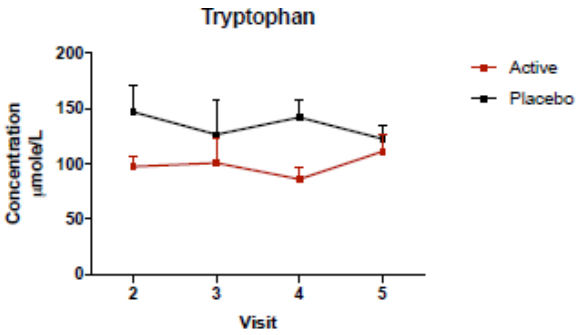
Tryptophan
Concentration µmole/L
200
150
100
50
0
2
3
4
5
Visit
Active
Placebo

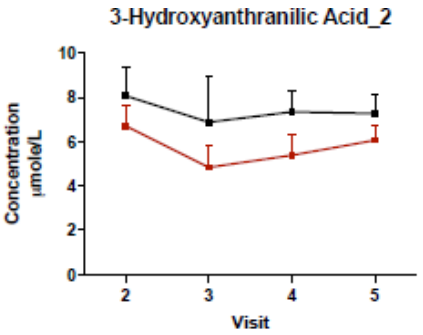
3-Hydroxyanthranilic Acid_2
Concentration µmole/L
10
8
6
4
2
0
2
3
4
5
Visit

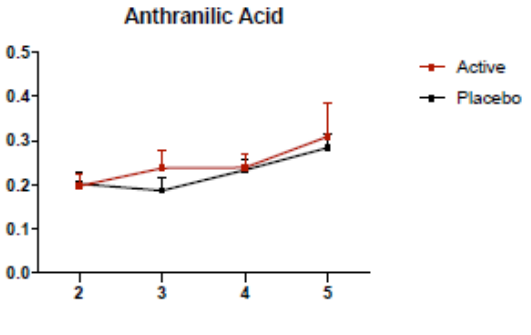
Anthranilic Acid
0.5
0.4
0.3
0.2
0.1
0.0
2
3
4
5
Active
Placebo

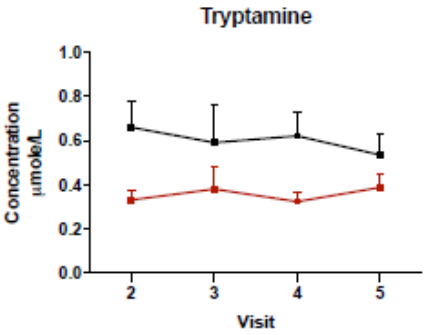
Tryptamine
Concentration µmole/L
1.0
0.8
0.6
0.4
0.2
0.0
2
3
4
5
Visit

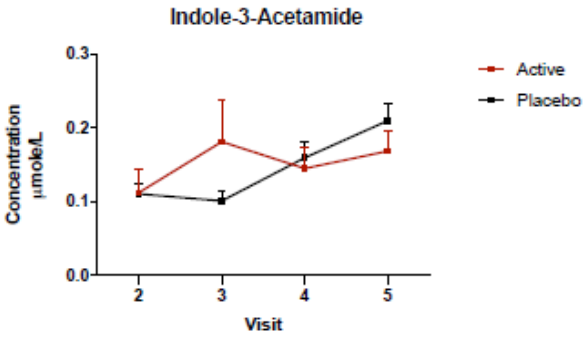
Indole-3-Acetamide
Concentration µmole/L
0.3
0.2
0.1
0.0
2
3
4
5
Visit
Active
Placebo

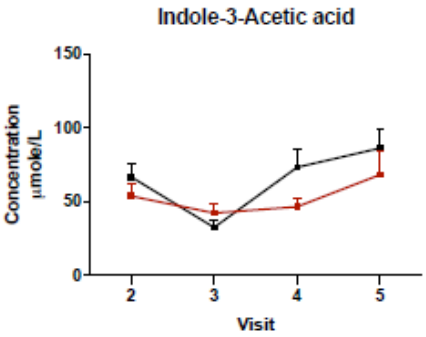
Indole-3-Acetic acid
Concentration µmole/L
150
100
50
0
2
3
4
5
Visit

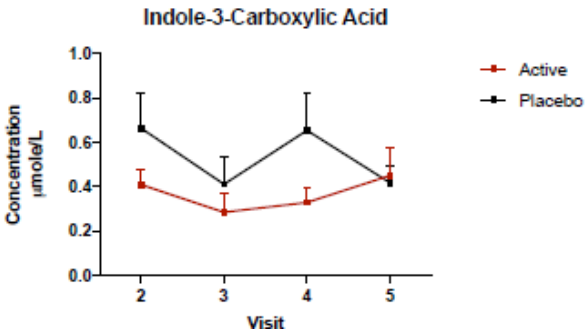
Indole-3-Carboxylic Acid
Concentration µmole/L
1.0
0.8
0.6
0.4
0.2
0.0
2
3
4
5
Visit
Active
Placebo

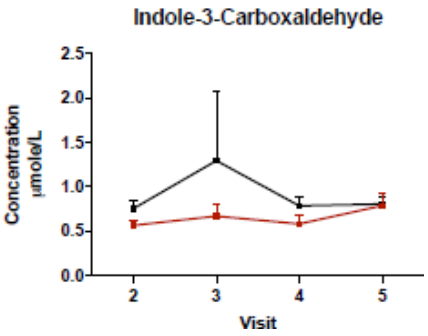
Indole-3-Carboxaldehyde
Concentration µmole/L
2.5
2.0
1.5
1.0
0.5
0.0
2
3
4
5
Visit

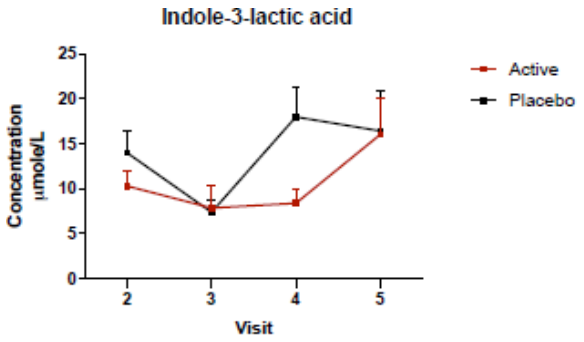
Indole-3-lactic acid
Concentration µmole/L
Visit
Active
Placebo

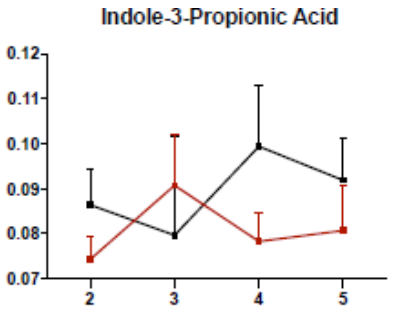
Indole-3-Propionic Acid
Visit

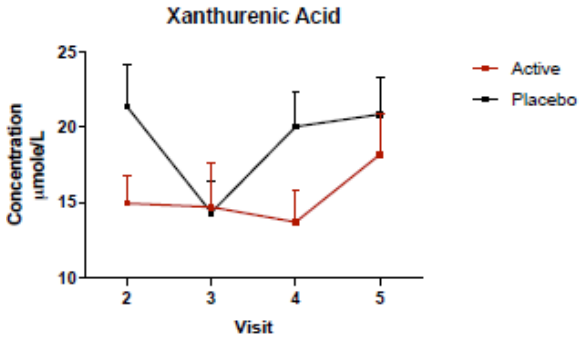
Xanthurenic Acid
Concentration µmole/L
Visit
Active
Placebo

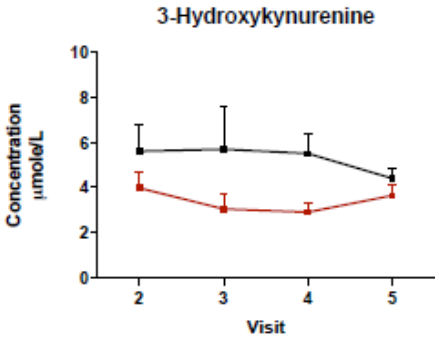
3-Hydroxykynurenine
Concentration µmole/L
Visit

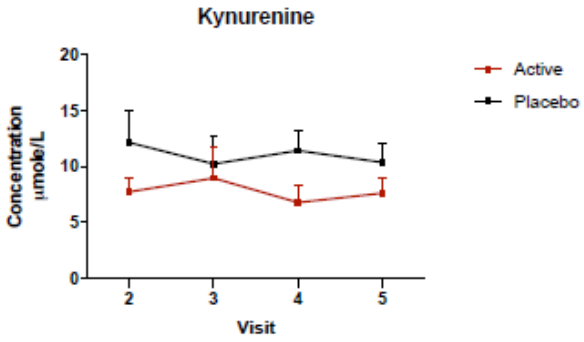
Kynurenine
Concentration µmole/L
Visit
Active
Placebo

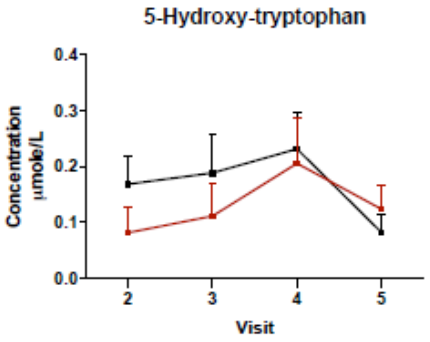
5-Hydroxy-tryptophan
Concentration µmole/L
Visit

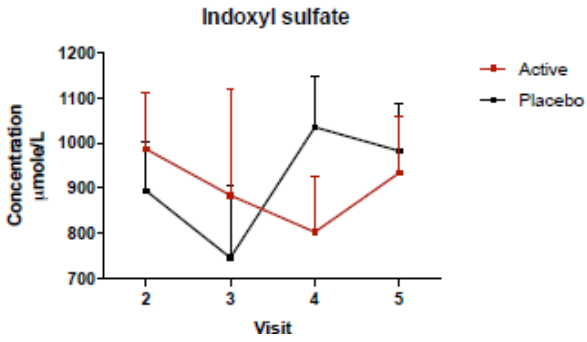
Indoxyl sulfate
Concentration µmole/L
Visit
Active
Placebo

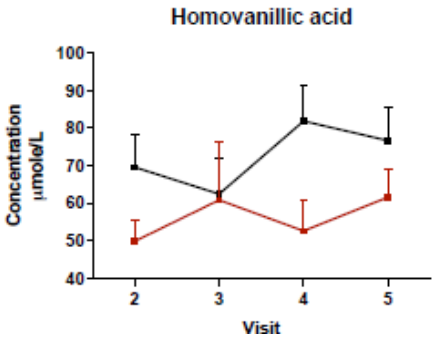
Homovanillic acid
Concentration µmole/L
Visit

Chapter 4.

Gut microbiome of a porcine model of metabolic syndrome and HF-pEF

This chapter has been published by 'American Journal of Physiology – Heart and Circulatory Physiology', March 2020

Citation: O'Donovan AN, Herisson FM, Fouhy F, Ryan PM, Whelan D, Johnson CN, Cluzel G, Ross RP, Stanton C, Caplice NM. Gut microbiome of a porcine model of metabolic syndrome and HF-pEF. *Am J Physiol Heart Circ Physiol* 318: H590 –H603, 2020

Aoife O Donovan is joint-first author with Dr. Florence Herisson, and both contributed equally to this work.

4.1 Abstract

Metabolic syndrome (MetS) is a composite of cardiometabolic risk factors, including obesity, dyslipidaemia, hypertension, and insulin resistance, with a range of secondary sequelae such as non-alcoholic fatty liver disease and diastolic heart failure. This syndrome has been identified as one of the greatest global health challenges of the 21st century. Herein, we examine whether a porcine model of diet- and mineralocorticoid-induced MetS closely mimics the cardiovascular, metabolic, gut microbiota, and functional metataxonomic phenotype observed in human studies. Landrace pigs with deoxycorticosterone acetate-induced hypertension fed a diet high in fat, salt, and sugar over 12 week were assessed for hyperlipidaemia, hyperinsulinemia, and immunohistologic, echocardiographic, and hemodynamic parameters, as well as assessed for microbiome phenotype and function through 16S rRNA metataxonomic and metabolomic analysis, respectively. All MetS animals developed obesity, hyperlipidaemia, insulin resistance, hypertension, fatty liver, structural cardiovascular changes including left ventricular hypertrophy and left atrial enlargement, and increased circulating saturated fatty acid levels, all in keeping with the human phenotype. A reduction in a-diversity and specific microbiota changes at phylum, family, and genus levels were also observed in this model. Specifically, this porcine model of MetS displayed increased abundances of pro-inflammatory bacteria coupled with increased circulating tumour necrosis factor-α and increased secondary bile acid-producing bacteria, which substantially impacted fibroblast growth factor-19 expression. Finally, a significant decrease in enteroprotective bacteria and a reduction in short-chain fatty acid-producing bacteria were also noted. Together, these data suggest that diet and mineralocorticoid-mediated development of biochemical and cardiovascular stigmata of metabolic

syndrome in pigs leads to temporal gut microbiome changes that mimic key gut microbial population signatures in human cardiometabolic disease.

NEW & NOTEWORTHY: This study extends a prior porcine model of cardiometabolic syndrome to include systemic inflammation, fatty liver, and insulin sensitivity. Gut microbiome changes during evolution of porcine cardiometabolic disease recapitulate those in human subjects with alterations in gut taxa associated with pro-inflammatory bacteria, bile acid, and fatty acid pathways. This clinical scale model may facilitate design of future interventional trials to test causal relationships between gut dysbiosis and cardiometabolic syndrome at a systemic and organ level.

4.2 Introduction

Metabolic syndrome (MetS), a cluster of metabolic disorders leading to downstream cardiovascular complications, including atherosclerosis, diastolic heart failure, and atrial fibrillation, is the fastest growing human disease with significant global implications for morbidity and mortality [195]. There is emerging scientific data to support a role for the gut microbiome in many aspects of MetS, including obesity, hyperlipidaemia, and insulin resistance in human subjects [196]. Obesity is a risk factor for heart disease, and recent studies have shown that obese individuals exhibit a significantly discordant gut micro- biome compared with lean individuals [197]. More than half of all patients with heart failure retain a preserved ejection fraction, a form of the disease that is associated with metabolic syndrome and for which there are no specific therapies at present. Clearly there is a need for new insights into the mechanisms underlying this disease, and gut microbiome re- search offers one avenue of investigation.

Currently, our understanding of the mechanistic link between the gut microbiome and biochemical or structural changes of cardiometabolic disease is limited by inadequacies of existing preclinical rodent models and restricted access to ex vivo tissue in the case of human subjects [198]. For instance, rodent and human gut microbiomes are significantly different, and rodent metabolic syndrome models require additional genetic alteration that reduces their relevance to human causes of biochemical, metabolic, and cardiovascular changes seen in this disease, most of which are diet induced [199].

The development of larger animal models that have closer structural homology to human gastrointestinal, immune, metabolic, and cardiovascular systems is paramount to further probing the microbiome-metabolic syndrome interaction. The

pig fulfils many of these criteria, having a similar body mass and physiology to humans as well as omnivorous dietary behaviour, and offers the potential to mimic human responses to diet with respect to investigating the gut microbiome and its function [200]. Previous studies already suggest that the porcine and human gut microbiome present a high degree of similarity [201]. Recently, a pig model was established [202] in which a diet high in fat, salt, and sugar, along with mineralocorticoid-induced hypertension for 12 weeks, led to hypertension, hyperlipidaemia, and cardiovascular structural changes that mimic the phenotype of heart failure-preserved ejection fraction (HF- pEF) seen in human subjects.

The aim of the current study was to determine the temporal alterations in gut microbiome (metaxonomic composition and functional changes) during evolution of biochemical and cardiovascular elements of MetS in a porcine model. Specifically, we wished to establish whether these microbiome changes mimic those observed in human subjects with cardiometabolic disease. Our detailed analyses demonstrate the potential clinical relevance of this swine model for investigating the role of gut microbiome in development of cardiometabolic syndrome.

4.3 Materials and Methods

4.3.1 Ethics Statement

All experimental procedures used during the study were reviewed and approved by the University College Cork Ethics Committee, under a license issued by the Health Products Regulatory Authority (HPRA; reference no. AE19130-P041). Effect size was calculated on G Power (version 3.1.9.2, University Kiel, Germany), and a sample- size estimation was computed. Because this was experimental work generating new data, a 10% observed difference in means was assumed with an estimated standard deviation of 6.25 for each group. This required a sample size of

10 animals in each group to detect a statistically significant difference and reject the null hypothesis. Calculations were based on an effect size of 1.6 and α error probability 0.05 with a power of 0.95.

4.3.2 Study Design and Sampling

This study model was based on previous work by Schwarzl et al. [202] that looked at the development of a porcine model of hypertensive cardiomyopathy and associated diastolic dysfunction in the setting of obesity, hyperlipidaemia, and hypertension. Three-month-old Landrace female piglets weighing 20 –25 kg were acquired and housed in individual stalls within the Biological Service Unit, University College Cork. Animals were separated into two groups. The control group (n = 10) was fed 1 kg/day Connolly's Redmills normal chow (20% protein, 3.5% fibre, 6% oil; 20% Hi-Density Weaner Pellets), and the MetS group (n = 10) was fed 0.5 kg/day Connolly's Redmills normal chow supplemented with 1 kg/day 4% salt, 4% cholesterol, 25% crude fat, 0.5% cholate, and 26% sugar [high fat, salt, and sugar diet (HFD); R8620 version 0011, SAFE, Augy, France]. All animals had free access to water at all times. In conjunction with the supplemented diet, the MetS group also underwent surgical implantation of a subcutaneous mineralocorticoid deoxycorticosterone acetate (DOCA) depot (200 mg/kg, 90-day release pellets from Innovative Research of America) in the inguinal region before trial initiation to induce sodium and water retention, ultimately resulting in hypertension. Control and MetS groups were fed with the aforementioned respective diets over a 12-wk period. Faecal samples were collected every 2 wk for a total of 7 time points: at baseline before initiation of study diet (baseline: n = 5 per group), as well as 2 wk (T2: n = 10 per group), 4 wk (T4: n = 10 per group), 6 wk (T6: n = 10 per group), 8 wk (T8: n = 10 control, n = 9 MetS), 10 wk (T10: n = 10

control, n = 9 MetS), and 12 wk (T12: n = 10 control, n = 9 MetS) after diet commencement. After 12 wk of being fed test diets, pigs were fasted for 24 h, at which point body mass, blood pressure, and hemodynamic parameters were measured. Pigs were administered propofol (3 mg/kg IV) and intubated with 1 to 2% isoflurane (Vetflurane, Virbac) to maintain anaesthesia while echocardiographic and hemodynamic examinations were performed. ECG, non-invasive blood pressure, and oxygen saturation were continuously monitored throughout hemodynamic study. Once cardiac parameters were completed, animals were euthanized via bolus intravenous injection of pentobarbitone (50 mg/kg; Dolethal, Vetaquinol). Blood, organs, and faecal samples were subsequently collected from the pigs. Whole blood was collected into serum clot activator tubes and allowed to clot by being left undisturbed at room temperature. After 15 min, the clot was removed by centrifugation at 2,000 g for 10 min in a refrigerated centrifuge, and the resulting supernatant was stored at -80°C until usage. Organs were weighed and statistical comparisons calculated between groups. Faecal samples were stored at 4°C for a maximum of 2 h before bacterial DNA extraction

4.3.3 Heart Parameter Measurements

Echocardiographic examination. Echocardiographic measurements were performed according to the recommendations of the American Society of Echocardiography guideline using an ultrasound diagnostic system (Vivid S5, GE Medical Systems) equipped with a 1.7/3.3 MHz probe [203-205]. All studies were performed with pigs lying in the left lateral decubitus position while echo variables were measured three times with average values recorded. Left atrium area, left ventricular septum, and posterior wall thickness were measured using two-dimensional image tracings on parasternal long-axis and short- axis views.

Dobutamine stress left ventricular pressure. To determine diastolic dysfunction and provide evidence of MetS-induced HF-PEF, a 6-Fr pigtail catheter was introduced through the right common carotid artery and directed to the left ventricular cavity. A standard graded- dose dobutamine stress test was performed following a modification of a previous protocol [206]. After fluid loading of 150 mL saline (Sodium Chloride 0.9%, Baxter Healthcare) via the internal jugular vein, an infusion of dobutamine (Pharmacy, Cork University Hospital, Ireland) was commenced at 2.5 $\mu g \cdot kg^{-1} \cdot min^{-1}$ with incremental increases of 2.5 $\mu g \cdot kg^{-1} \cdot min^{-1}$ every 5 min to a maximum dose of 10 $\mu g \cdot kg^{-1} \cdot min^{-1}$. Left ventricular systolic and diastolic pressures were assessed by pigtail catheter, recorded at baseline and at 5-min intervals during dobutamine stress with simultaneous ECG recording.

4.3.4 Blood Measurements

Fasted serum levels of total cholesterol (TC), LDL, triglyceride (TAG), glucose, and insulin were quantified according to manufacturer's instructions with a Cholesterol Assay Kit-TC and LDL/VLDL (ab65390, Abcam, Cambridge, MA), Triglyceride Assay Kit-Quantification (ab65390, Abcam, Cambridge, MA), Maltose and Glucose Assay Kit (ab65335, Abcam, Cambridge, MA), and Insulin ELISA Assay (Cat. No. 10-1256-01, Mercodia, Sylveniusgatan 8A, SE-754 50, Uppsala, Sweden), respectively.

4.3.5 Liver Histologic and Lipid Analysis

A small portion of liver tissue was collected and embedded with optimal cutting temperature compound (OCT) (ThermoFisher scientific, Ireland) for cryostat sectioning at 5-µm thickness. The sections were mounted on microscope slides and frozen at -80°C. The samples were subsequently thawed, fixed with 4% paraformaldehyde solution (PFA) (Sigma Aldrich, Ireland) for 10 minutes and

stained with Oil Red O (ORO, Sigma-Aldrich, St. Luis, MO, United States) to detect hepatic lipid droplets. Liver samples from 9 pigs per group were prepared, stained and 3 fragments from each liver were further analysed. Each section was photographed with bright field microscopy (Olympus BX43 microscope, Tokyo, Japan) using 40X magnification. The amounts of lipid droplets were quantified in at least six different high-power fields for each fragment using Nikon NIS-Elements BR 3.0 software. Results are presented as number of lipid droplets per pixel per μm2. Lipids in liver were analysed by t tests using PRISM (GraphPad Software, Inc.).

4.3.6 Microbiome Analysis

DNA extraction. Bacterial genomic DNA was extracted from 0.25 g of faecal material using the repeated bead-beating plus column protocol as described by Yu et al. [190] in combination with the QIAamp Fast DNA Stool Mini kit (Qiagen, UK) described by Fouhy et al. [191], with slight modifications: 1.0 and 2.3-mm sterile zirconia beads were used during the homogenizing step instead of 0.5-mm sterile zirconia beads to prevent sedimentation of the 0.1-mm beads and the faecal material. The DNA was eluted with 200 μL of Buffer AE (Qiagen) and stored at -80°C [84].

16S rRNA gene sequencing and analysis. After DNA extraction, the V3-V4 regions of the 16S rRNA gene were amplified through 30 cycles of PCR reactions on the template DNA using the primer pair 5'-TCGT CGGC AGCG TCAG ATGT GTAT AAGA GACA GCCT ACGG GNGG CWGC AG-3' and 5'-GTCT CGTG GGCT CGGA GATG TGTA TAAG AGAC AGGA CTAC HVGG GTAT CTAA TCC-3' according to the 16S Metagenomic Sequencing preparation protocol for Illumina MiSeq and as previously described by Fouhy et al. [191]. Indexed

products were visualized using gel electrophoresis and cleaned with AMPure XP magnetic-based beads before DNA quantification using the Qubit (BioSciences, Dublin, Ireland), along with the Qubit High Sensitivity DNA kit (Life Technologies). Samples were pooled at equimolar concentrations, and high-throughput sequencing was completed on the Illumina MiSeq platform in the Teagasc sequencing facility using a 2 × 300 cycle kit and following standard Illumina sequencing protocols.

***Bioinformatic analysis*.** Resulting 300-bp paired-end reads were assembled using fast length adjustment of short reads to improve genome assemblies (FLASH). Quantitative Insights into Microbial Ecology (QIIME; version 1.8.0) was used for quality filtering of pair-end reads, which is based on a quality score of >25 and the removal of mismatching barcodes [192]. Prior to the analysis as part of the quality control process, sequences that produced less than 40,000 reads were manually removed, which accounted for the difference in the number of animals between groups and between time points. USEARCH (version 7, 64-bit) was employed for deionization, chimera detection, and clustering into operational taxonomic units (OTUs; 97% identity). Alignment of OTUs was carried out using python nearest alignment space termination (PyNAST) and assignment of taxonomy of 97% similar identity against the SILVA SSURef database release v123.

Statistical analysis: In order to assess the alpha diversity of the samples, Chao1 Index and phylogenetic diversity (PD_Whole_Tree) were calculated using the diversity function from the R vegan package and ANOVA followed by Bonferroni correction and an F test in Calypso.

In order to assess phylum, family and genus level changes in the pigs, all significant taxa were analysed by Mann Whitney, were graphically represented as “relative

abundance" with the mean ± SEM, P values, and confidence intervals using PRISM (GraphPad Software Inc.). Relative abundance of Phylum, Family and Genus significantly increased and remain unchanged in Control and MetS, samples at T6 and T12 were represented in supplemental FigS5.

4.3.7 Association between gut microbial phyla and MetS-associated symptoms

Gut bacteria phylum prevalence was correlated with pig's weight (W, kg), Systolic Blood Pressure (SBP, mmHg), Diastolic Blood Pressure (DBP, mmHg), Total Cholesterol (TC, mg/dL), Triglycerides (TG, mg/dL) and Low Density Lipoproteins (LDL, mg/dL) blood concentrations. Spearman correlation test was run using pairwise "corr.test" function, adjusted according to Benjamini-Hochberg procedure, in Rstudio (Version 1.0.136 – © 2009-2016 RStudio, Inc.). Correlation plot was obtained with "corrplot" function, and only correlations resulting in p-values < 0.05 are displayed.

4.3.8 SCFAs, bile acids and inflammation markers measurement

Serum SCFAs analysis*:* Metabolomics analysis was performed on serum samples following 12 weeks feeding trial in control (N=10) and MetS animals (N=9) by MS-Omics, Denmark, where Gas Chromatography–Mass Spectrometry (GC-MS) was utilised to investigate the effect of the MetS model. Samples were prepared through derivatisation with methyl tert-butyl ether (MTBE). The samples were randomized and analysed by GC-MS, and to ensure quality control, a mixed sample (QC sample) was created by combining a small aliquot from each of the samples. This QC sample was re-analysed every 4-5 samples, and testing of the matrix effects was carried out Raw GC-MS data were processed by the proprietary software that has been designed by MS-Omics and collaborators. The software incorporated the use of the powerful PARAFAC2 model to create cleaner MS spectra compared to most other GC-MS

software. Compounds that were extracted using this software underwent extensive data curation and quality control.

Serum FGF19 and TNF alpha analysis: Serum level of FGF19 and TNF-α, were quantified according to manufacturer‘s instructions with a Pig fibroblast growth factor 19 (FGF19) ELISA Kit (EKC38180, Biomatik, DE, United States) and a Swine TNF- alpha ELISA Kit (KSC3011, Invitrogen, Invitrogen Corporation, Carlsbad, USA).

Immunofluorescence - Inflammation in liver: A small portion of liver tissue was collected and embedded with optimal cutting temperature compound (OCT) (ThermoFisher scientific, Ireland) for cryostat sectioning at 5-µm thickness. The sections were mounted on microscope slides and frozen at -80°C. Slides were fixed in methanol for 10 minutes at 4°C, incubated for 1h at RT in blocking buffer (10% serum in PBS-Tween) and incubated with the primary antibody (diluted in 1% Bovine serum albumin and PBS-Tween) over night at 4°C: CD163 for macrophages (mouse anti pig CD163 IgG1, 0.1mg, BIORAD, 1:1000). The slides were washed in PBS three times for 5mins and were then incubated with the secondary antibody (goat anti mouse IgG Alexa Fluor 488, 2mg/ml, Invitrogen, 1:1000, diluted in 1% Bovine serum albumin and PBS-Tween) for 1h at RT in the dark. After washings, slides were stained with DAPI and coverslipped using mounting media. Liver samples from 10 pigs per group were prepared, stained and 10 fragments from each liver were further analysed. Sections were observed with a confocal laser microscope (Nikon D-Eclipse) using x60 magnification and pictures were taken. Pictures were analysed using NIS-Elements BR 3.0 software.

Statistical Analysis: Acetate, Butyrate, FGF19, TNF alpha and CD163 data were presented as mean ± SEM and analysed by a nonparametric Mann-Whitney test using PRISM (GraphPad Software, Inc.), where $p < 0.05$ was used to reject the null hypothesis.

4.3.9 Serum Metabolomic Analysis

Metabolomics analysis was performed on serum samples after a 12-wk feeding trial

in control (n = 10) and MetS animals (n = 9) by MS-Omics, Denmark, where gas chromatography-mass spectrometry (GC-MS) was utilized to investigate the effect of the MetS model. Samples were prepared through derivatisation with methyl chloroformate (MCF), which converts amino acids and non-amino organic acids into volatile carbamates and esters. The samples were randomised and analysed by GC-MS. To ensure quality control, a mixed quality control (QC) sample was created by combining a small aliquot from each of the samples. This QC sample was re-analysed every 4 to 5 samples, and testing of the matrix effects was carried out through spiking/dilution of the QC samples [207]. Raw GC-MS data were processed by the proprietary software designed by MS-Omics and collaborators. The software incorporated the use of the powerful PARAFAC2 model to create cleaner MS spectra compared with most other GC-MS software. Compounds that were extracted using this software underwent extensive data curation and quality control.

4.3.10 Statistical Analysis

Body weight, serum biochemistry (lipid profile, glucose, insulin, homeostatic model assessment (HOMA), and blood pressure data were all presented as means ± SE and analysed by a two-way ANOVA followed by Tukey's multiple comparisons test using PRISM (GraphPad Software), where $P < 0.05$ was used to reject the null hypothesis. To confirm the observed trends in insulin resistance, 3 additional MetS animals were included in the statistical analysis, giving baseline and T12 a total of 8 and 12 animals, respectively. Glucose, insulin measurements, and HOMA calculations were then performed on the expanded group of animals. Lipids in liver [oil red O (ORO) staining], heart parameters, and organ-mass data were all presented as means ± SE and analysed by t-tests. Estimates of a- diversities were generated with QIIME and visualized through

principal coordinate analysis (PCoA) plots generated using the web-based software Calypso (version 8.72). Multiple β-diversity metrics were also calculated, including Bray-Curtis UniFrac PCoA plots, highlighting the alterations based on diet and time point. To assess phylum, family, and genus level changes in the pigs, all significant taxa analysed by Mann-Whitney test were graphically represented as relative abundance with the means ± SE, P values, and confidence intervals. All significant taxa analysed by a Kruskal-Wallis test were adjusted by a false discovery rate. A q value less than 0.05 was considered statistically significant. All metabolomics data underwent generalized logarithm transformation through MetaboAnalyst to permit parametric analysis. Data were found to be of a normal distribution under visualization and Shapiro-Wilk test post transformation (Supplemental FigS1) before ANOVA and multivariate analyses in the MetaboAnalyst metabolomics analysis suite [208]. To visualize clustering trends between MetS and control pigs, the unsupervised principal component analysis (PCA) tool was performed on all metabolomic data and boxplot figures of the variables of importance to the model were plotted [209].

4.4 Results

4.4.1 Metabolic Syndrome Development

To characterize the porcine model for MetS, body weight, lipid profile, and blood pressure were measured at baseline, 2 wk (T2), 6 wk (T6), and before euthanisation at 12 wk (T12). Weights of heart, liver, kidney, and spleen were also recorded after euthanisation. To evaluate the presence of insulin resistance and non-alcoholic fatty liver disease, serum biochemistry and fat deposition in the liver were measured. Additionally, heart parameters such as left ventricular (LV) septal and posterior wall thickness (PW) and left atrial

(LA) area were measured by echocardiography. Left ventricular end-diastolic pressure (LVED) pre- and post- dobutamine stress was measured by LV pigtail catheter (Table 1).

At baseline, no differences were detected between MetS and control animals regarding body weight, blood pressure, and serum biochemistry (Table 1, Supplemental Fig. S3A-I). However, animals fed a HFD over 12 wk developed obesity and demonstrated hyperlipidaemia, hyperinsulinemia and insulin resistance, hypertension, and a cardiovascular phenotype reminiscent of cardiometabolic HF-pEF observed in human subjects. After 12 wk of HFD, MetS animals had significantly increased body weight (1.16-fold increase, $P < 0.0001$); markedly increased serum lipids, including triglyceride (1.86-fold, $P < 0.01$), total cholesterol (7.92-fold, $P < 0.0001$), and LDL (10.9-fold, $P < 0.0001$); and significantly increased insulin levels ($P = 0.02$; Table 1, Supplemental Fig. S3). Fasting glucose between the two groups was not significantly different; however, calculation of HOMA insulin resistance [HOMA-IR: (fasting insulin × fasting glucose)/22.5] was significantly increased at T12 in MetS compared with control pigs ($P = 0.04$). In line with these observations, no signs of fat deposition in the liver were found in control animals, whereas significantly increased hepatosteatosis was detected in the livers of MetS animals by ORO staining at T12 (Supplemental Fig. S2). Regarding cardiac structural and hemodynamic parameters, MetS animals exhibited significantly elevated values for every measured parameter: systolic blood pressure (1.61-fold, $P < 0.0001$), diastolic blood pressure (1.66-fold, $P < 0.001$), LV septal thickness (1.67-fold, $P < 0.0001$), LV PW thickness (1.77-fold, $P < 0.0001$), LA area (1.82-fold, $P < 0.0001$), and LVED at baseline (1.54-fold, $P < 0.001$) and after dobutamine stress (1.89-fold $P < 0.001$). Organ weights were also significantly higher in MetS animals compared with control animals (heart: 1.5-

fold, $P < 0.0001$; liver: 1.64- fold, $P < 0.0001$; kidney: 2.17-fold, $P < 0.0001$), with the exception of spleen weight.

Interestingly, markers of metabolic syndrome such as blood pressure and cholesterol in serum were significantly increased in MetS compared with control pigs as early as T6: SBD 1.3-fold, DSP 1.49-fold, TC 4.89-fold, and LDL 1.7-fold. These data confirmed the establishment of robust metabolic, organ-specific (i.e., liver), and cardiovascular features (i.e., HF-pEF) of MetS in our study animals after 12 wk of HFD when compared with controls.

Table 1. *Characteristics of metabolic syndrome and control pigs*

	Control	MetS	*P* Value
N	10	9	
Body weight, kg			
Baseline	20.24 ± 0.2	19.1 ± 0.6	ns
T2	31.9 ± 0.5	31.31 ± 0.98	ns
T6	43.5 ± 0.4	43.6 ± 2.5	ns
T12	61.1 ± 0.64	70.9 ± 1.8	0.00007
Lipids, mg/dL			
TAG			
Baseline	15.28 ± 1.3	12.96 ± 1.3	ns
T2	25.97 ± 2.9	28.05 ± 3.8	ns
T6	31.87 ± 4.6	46.11 ± 8.8	ns
T12	35.84 ± 4.3	66.76 ± 7.8	0.0047
TC			
Baseline	227 ± 12	231.1 ± 13	ns
T2	212.4 ± 5.7	458.5 ± 1.357.5	ns
T6	201.9 ± 6.1	988.7 ± 39.9	<0.0001
T12	188.3 ± 32.5	1493 ± 187	<0.0001

LDL			
Baseline	71.5 ± 3.9	58.76 ± 6.9	ns
T6	39.65 ± 2.1	319.4 ± 48	0.0033
T12	70.37 ± 7.75	769.9 ± 104	<0.0001
Glucose, mg/dL			
Baseline	98.25 ± 11.4	87.43 ± 6.4*	ns
T6	76.42 ± 9.1	81.93 ± 7.1†	ns
T12	62.01 ± 8.3	81.63 ± 4.9	ns
Insulin, µIU/mL			
Baseline	6.987 ± 2.2	4.968 ± 2.8*	ns
T6	8.082 ± 2	3.333 ± 1.5†	ns
T12	5.713 ± 1.5	16.23 ± 3.5	0.02
HOMA			
Baseline	1.446 ± 0.3	1.6 ± 0.5*	ns
T6	1.693 ± 0.6	0.6094 ± 0.2†	ns
T12	1.004 ± 0.4	3.25 ± 0.6	0.04
Oil red O, pixel/µm2	0 ± 0	1,492 ± 55.71	<0.0001
Blood pressure			
SBP, mmHg			
Baseline	119.4 ± 5	121.4 ± 1.7	ns
T2	116 ± 3	128 ± 8.3	ns
T6	115.6 ± 3.7	150.9 ± 8.5	0.0311
T12	102.2 ± 3.4	165 ± 11	0.00001
DBP, mmHg			
Baseline	64 ± 4	61.8 ± 1.1	ns
T2	61 ± 6	88.6 ± 4	ns
T6	55.2 ± 4	82.6 ± 6	0.0239
T12	58.4 ± 3.5	97.28 ± 8	0.0001

Heart parameters			
LV septal thickness, cm	1.01 ± 0.031	1.689 ± 0.069	<0.0001
LV PW thickness, cm	0.94 ± 0.04	1.667 ± 0.079	<0.0001
LA area, cm2	9.4 ± 0.312	17.12 ± 0.610	<0.0001
LVED, mmHg	10.65 ± 0.85	16.44 ± 1.05	0.0004
LVED post-dobutamine stress, mmHg	18 ± 1.45	34.11 ± 3.63	0.0005
Organs, kg			
Heart	0.247 ± 0.008	0.376 ± 0.024	<0.0001
Liver	0.728 ± 0.031	1.193 ± 0.068	<0.0001
Spleen	0.342 ± 0.057	0.287 ± 0.08	ns
Kidney	0.092 ± 0.002	0.2 ± 0.016	<0.0001

Values are means ± SE; n = number of pigs. DBP, diastolic blood pressure; HOMA, homeostatic model assessment; LA, left atrial; LV, left ventricular; LVED, LV end-diastolic pressure; LV PW, LV posterior wall; MetS, metabolic syndrome; SBP, systolic blood pressure; T2, T6, and T12, 2, 6, and 12 wk after diet commencement; TAG, triglyceride; TC, total cholesterol. *For glucose, insulin, and HOMA levels, n = 8 MetS at baseline; † For glucose, insulin, and HOMA levels, n = 12 MetS at T12.

4.4.2 Reduced Microbiota Diversity during Diet-Induced MetS

α-Diversity was measured using Simpson, Chao1, Shannon, and Phylogenetic Diversity (PD Whole tree) indexes and observed species. α -Diversity was significantly reduced in MetS pigs compared with the control-fed animals over 12 wk (Fig.1A, p = 0.001, Supplemental Fig. S4: Chao1 p = 0.001, Shannon p = 0.001, and Simpson P = 0.023), an effect that was observed as early as 2 wk on the HFD and was maintained throughout the subsequent 12-wk study period (Fig. 1B, p < 0.001). A PCoA plot based on Bray-Curtis distance matrices found distinct separation in microbiota from week 2 of feeding in MetS compared with the control feeding group (Fig. 2A). This difference in microbial diversity was maintained out to week 12 (Fig. 2, B and C).

4.4.3 Microbiome Analysis at Phylum, Family, and Genus Levels

Microbiome analysis at phylum, family, and genus levels showed no differences between control (n = 5) and MetS (n = 5) groups at T0 (baseline) (Fig. 3A). The predominant phyla at T2, T6, and T12 were *Firmicutes* and *Bacteriodetes* in control animals and *Firmicutes, Bacteriodetes*, and *Actinobacteria* in MetS animals (Fig. 3A). The MetS gut microbiota displayed increases in *Actinobacteria* and *Syngergistetes* at T2, T6, and T12 and *Fusobacteria* at T6 and T12, with decreases in *Tenericutes* at T2, T6, and T12, *Spirochaetae* at T6 and T12, and *Saccharibacteria* at T12 (Fig. 3B).

At family level, there were significant increases in *Bacteroidaceae*, *Enterobacteriaceae*, and *Nocardiaceae* at T2 and T6; *Oxalobacteraceae* at T2, T6, and T12; *Synergistaceae* at T2 and T12; *Enterococcaceae* at T6; and *Fusobacteriaceae* and *Succinivibrionaceae* at T6 and T12. There were decreases in *Anaeroplasmataceae, Clostridiales_vadinBB60_group, p253418B5_gut_group*, and *Verrucomicrobiaceae* at T6, as well as *Spirochaetaceae* at T6 and T12 in MetS animals compared with control animals (Supplemental Figs. S5 and S7).

At genus level, there were significant changes in gut microbiota at 2 wk post feeding and throughout the feeding study. This included increases in *Alistipes, Bacteroides, Bilophila, Butyricimonas, Citrobacter, Salmonella*, and *Veillonella* at T2 and *Rhodococcus* and *Synergistes* at T2 and T6. *Eubacterium_brachy_ group, Ruminococcaceae UCG004*, and *Selenomonas* increased at T2, T6, and T12. There were also increases in *Oxalobacter* at T6, *Fusobacterium* at T6 and T12, and *Acidaminococcus, Catenibacterium, Megasphaera*, *Methanosphaera,* and *Pseudoflavonifractor* at T12. *Erysipelotrichaceae_UCG004, Faecalibacterium, Fibrobacter,* and *Ruminococcus 2* decreased at T2. Additionally, there were decreases in *Akkermansia, Anaeroplasma, Flavonifractor, Methanobrevibacter,*

Ruminiclostridium, and *Ruminococcaceae UCG010/014* at T6. *Anaerorhabdus, Candidatus Saccharimonas, Lachnospiraceae XPB1014 group, Peptococcus*, and *Treponema* decreased at T6 and T12, and *Megasphaera* and *Rikenellaceae RC9* gut group decreased at T12 in MetS compared with control animals (Supplemental Figs. S6 and S7).

Analysis of statistical association between gut microbial phyla and MetS parameters such as body weight, blood lipid levels, and blood pressure showed *Actinobacteria, Fusobacteria*, and *Synergistetes* to be positively associated with MetS and Cyanobacteria, *Deferribacteres, Elusimicrobia, Lentisphaerae, Saccharibacteria, Spirochaetae, Tenerictutes*, and *Verrucomicrobia* to be negatively associated with MetS. Indeed, *Actinobacteria* ($P < 0.01$, $r = 0.72$) and *Synergistetes* ($P < 0.01$, $r = 0.77$) were positively associated and *Cyanobacteria* ($P < 0.01$, $r = -0.74$), *Deferribacteres* ($P < 0.01$, $r = -0.73$), *Lentisphaerae* ($P < 0.01$, $r = -0.72$), *Saccharibacteria* ($P < 0.001$, $r = -0.88$), *Spirochaetae* ($P < 0.01$, $r = -0.75$), *Tenerictutes* ($P < 0.01$, $r = -0.70$), and *Verrucomicrobia* ($P < 0.01$, $r = -0.73$) were negatively associated with body weight. Regarding blood pressure, *Actinobacteria* ($P < 0.001$, $r = 0.81$) were positively associated and *Elusimicrobia* ($P < 0.001$, $r = -0.84$) were negatively associated with systolic pressure, and *Synergistetes* ($P < 0.01$, $r = 0.75$) was positively associated and *Elusimicrobia* ($P < 0.01$, $r = -0.72$), *Saccharibacteria* ($P < 0.01$, $r = -0.71$), and *Tenerictutes* ($P < 0.01$, $r = -0.76$) were negatively associated with diastolic pressure. Regarding lipid profile, total cholesterol and LDL were positively associated with *Actinobacteria* (TC: $P < 0.001$, $r = 0.78$, LDL: $P < 0.01$, $r = 0.73$), *Fusobacteria* (TC: $P < 0.01$, $r = 0.73$, LDL: $P < 0.001$, $r = 0.88$), and *Synergistetes* (TC: $P < 0.01$, $r = 0.77$, LDL $P < 0.01$, $r = 0.72$). Total cholesterol was mainly negatively associated with *Saccharibacteria* ($P < 0.001$, $r = -0.84$), *Spirochaetae* ($P < 0.001$, $r = -0.81$), and *Tenerictutes* ($P < 0.001$, r

= -0.78), whereas LDL was negatively associated with *Cyanobacteria* ($P < 0.001$, $r = -0.89$), *Tenerictutes* ($P < 0.01$, $r = -0.79$), and *Verrucomicrobia* ($P < 0.01$, $r = -0.71$). Triglycerides were positively associated with *Fusobacteria* ($P < 0.001$, $r = 0.88$) and negatively associated with *Saccharibacteria* ($P < 0.01$, $r = -0.76$) (Supplemental Fig. S8).

Analysis of the gut microbiome of MetS animals showed significant increases in bacteria previously associated with increased inflammation and bile acid signaling in human studies (Fig. 5), such as *Fusobacterium* ($P < 0.01$), *Acidaminococcus* ($P < 0.05$), *Actinobacteria* ($P < 0.01$), *Ruminococcacaeae_UCG004* ($P < 0.01$), *Eubacterium* ($P < 0.01$), and *Methanosphaera* ($P < 0.001$) (Fig. 4, A and B). With respect to bacteria reportedly associated with reduced inflammation, there were reductions in *Lachnospiraceae* ($P < 0.001$), *Rikenellaceae* ($P < 0.05$), and *Akkermansia* ($P < 0.005$) in MetS animals compared with controls (Fig. 4A) [210-213].

In line with microbiome results, serum TNF-α ($P < 0.001$) and hepatic inflammation in the form of CD163 immunoreactivity ($P < 0.0001$) were both significantly increased in MetS animals compared with controls (Supplemental Fig. S9). With respect to bile acid metabolism and gut-liver feedback through fibroblast growth factor (FGF) 19, there was significant reduction in serum FGF19 ($P < 0.01$) in MetS animals compared with control animals (Supplemental Fig. S9). These data are consistent with previous observations in murine models showing that excess secondary bile acids in gut of high-fat diet animals suppress FGF19 homolog-FGF15 synthesis (19). Reduction of FGF19 feedback from gut to liver is consistent with uncoupling of enterohepatic feedback of liver bile acid synthesis in our model. Finally, circulating levels of short-chain fatty acids (SCFAs) butyrate and acetate tended to be lower at

T12 in animals receiving HFD (Supplemental Fig. S9).

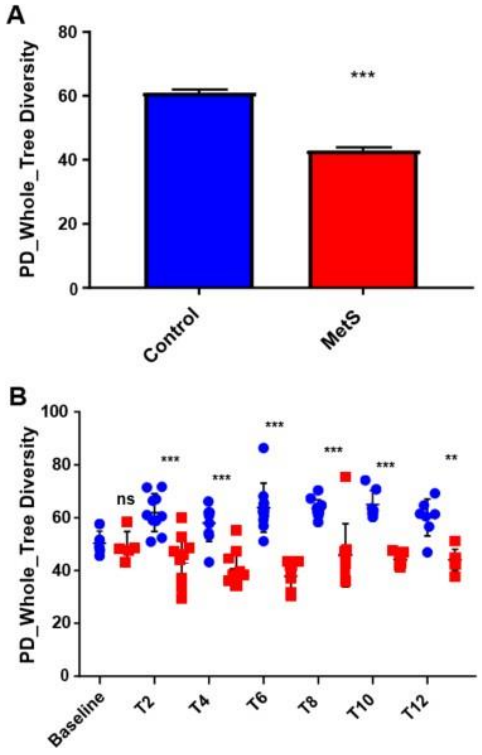

Fig. 1. Pig faecal α-diversity levels and kinetics in response to metabolic syndrome (MetS). Phylogenetic distance (PD) compared between control and MetS animals over 12 wk (*A*) and compared by sampling over time from baseline to 12 wk after diet commencement (T12; *B*). Diet: control received normal diet (blue); MetS received diet in fat, salt, and sugar (red). Significant difference was calculated using *t*-test (*A*) and ANOVA followed by Tukey's multiple comparisons test (*B*) using PRISM. $^{**}P < 0.01$, $^{***}P < 0.001$. ns, non-significant; T2, T4, T6, T8, T10, 2, 4, 6, 8, and 10 wk after diet commencement, respectively.

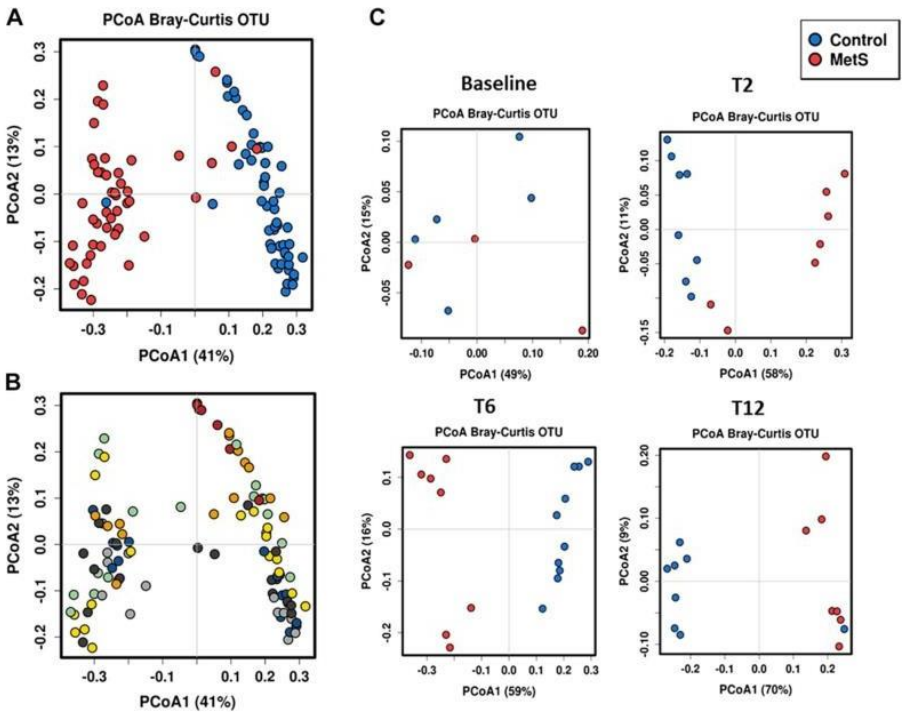

Fig. 2. Temporal shift of pig faecal microbiome β-diversity in response to metabolic syndrome (MetS). *A*: all time point Bray-Curtis β-diversity of pig faecal microbiome by diet control (blue) and MetS (red). *B*: temporal shift of pig faecal microbiome β-diversity in response to metabolic syndrome by time point. *C*: temporal evolution and separation of groups at selected time points: baseline, 2, 6, and 12 wk after diet commencement (T2, T6, and T12, respectively). Baseline: control *n* = 5, MetS *n* = 3; T2: control *n* = 8, MetS *n* = 7; T6: control *n* = 10, MetS *n* = 8; T12: control *n* = 7, MetS *n* = 7. Principal coordinate analysis (PCoA) was calculated using Bray-Curtis. OTU, operational taxonomic unit.

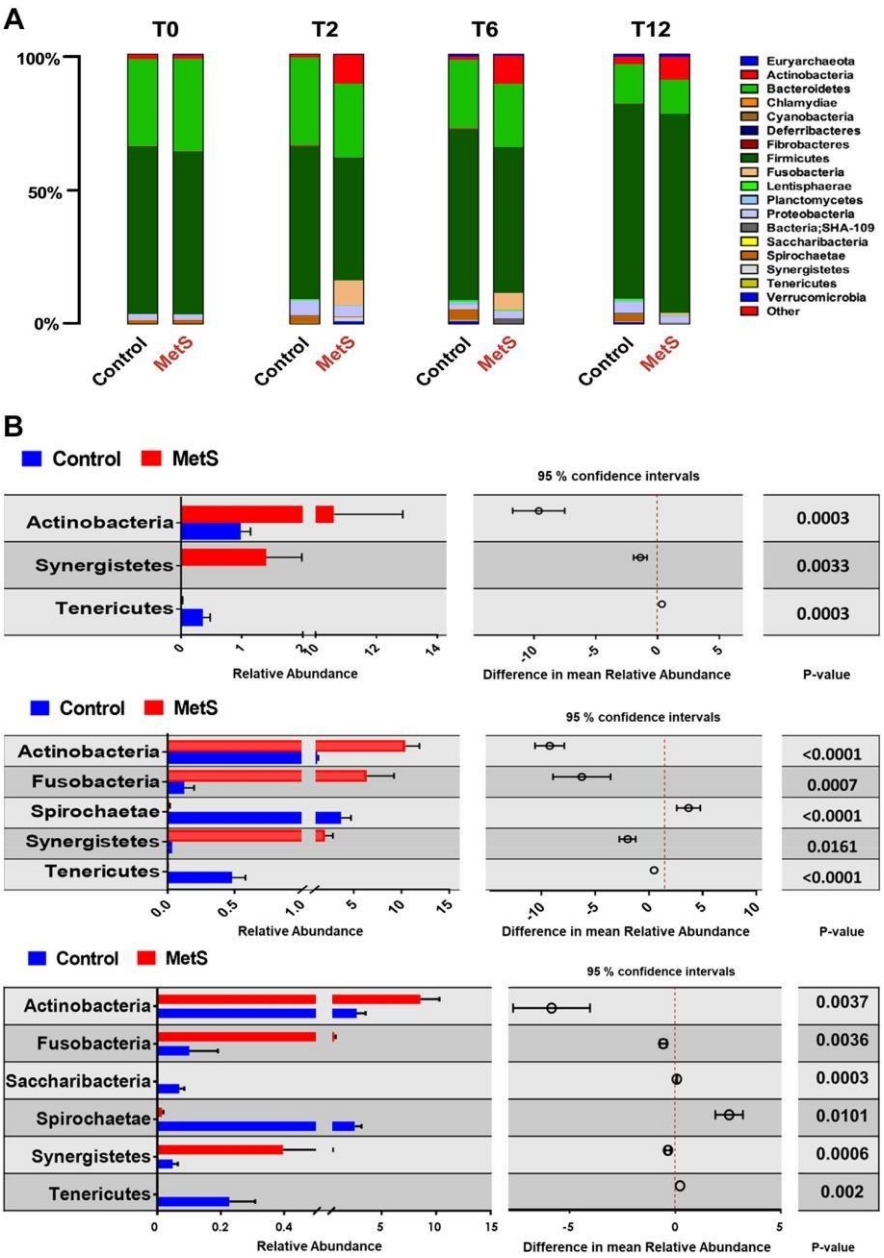

Fig. 3. Phylum level alterations in response to the development of metabolic syndrome (MetS). *A*: stacked bar plots showing relative abundance of specified phylum in pig faeces at baseline (T0) and 2, 6, and 12 wk after diet commencement (T2, T6, and T12, respectively) in control and MetS (baseline: control *n* = 5, MetS *n* = 3; T2: control *n* = 8, MetS *n* = 7; T6: control *n* = 10, MetS *n* = 8, T12: control *n* = 7, MetS *n* = 7). *B*: extended error bar plot identifying significantly different bacterial phylum between mean relative abundance at baseline, T2, T6, and T12 in

control (blue) and MetS (red) samples (T2: control *n* = 8, MetS *n* = 7; T6: control *n* = 10, MetS *n* = 8; T12: control *n* = 7, MetS *n* = 7). Significant difference was calculated using Mann-Whitney test using PRISM; *P* values are shown at right; confidence intervals = 95%.

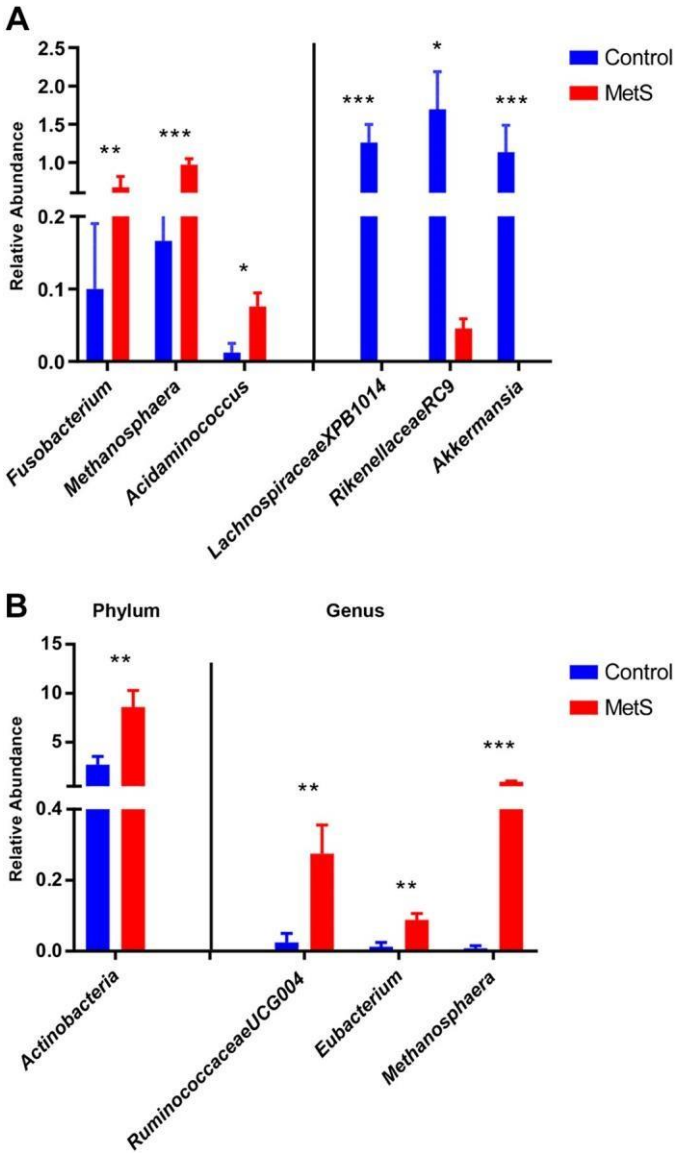

Fig. 4. Metabolic syndrome (MetS)-driven alterations in microbial taxa related to inflammation and bile metabolism. Relative abundance of bacteria related to pro-inflammation vs. anti-inflammation (*A*) and bile acids in control (blue) and MetS (red) samples (*B*). At 6 wk after diet commencement (T6): control *n* = 10, MetS *n* = 8 and 12 wk after diet commencement (T12): control *n* = 7, MetS *n* = 7. Significant

difference was calculated using Kruskal-Wallis adjusted by false discovery rate using PRISM; *$P < 0.05$, **$P < 0.01$, ***$P < 0.001$.

4.4.4 Serum Metabolomic Profile of MetS Compared with Controls

The unsupervised PCA plot showed clear separation between serum metabolomic profiles of MetS and control animals (Fig. 5*A*). Amino acid analysis indicated that significant variance in relative concentrations existed between groups, with an elevation in ornithine ($P < 0.01$) in MetS animals compared with controls (Fig. 5*B*). However, major metabolomic differences were attributable to relative concentrations of free fatty acids, specifically tetradecanoic ($P < 0.001$), hexadecanoic ($P < 0.0001$), and octadecanoic acid ($P < 0.0001$), which were significantly increased in the serum of MetS animals ($n = 9$) compared with control-fed animals ($n = 10$) at 12 wk (Fig. 5*C*).

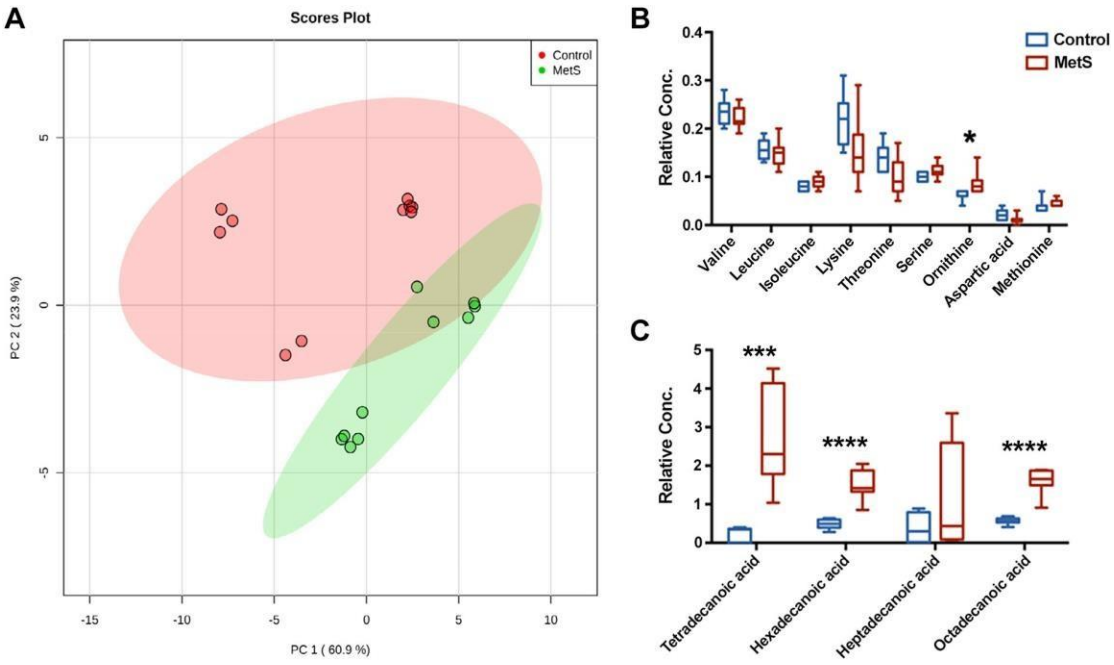

Fig. 5. Serum metabolome of metabolic syndrome (MetS) pigs is defined by increased free fatty acids. *A*: unsupervised principal component analysis (PCA) score plot demonstrating clear separation between serum metabolomic profiles of control (red; $n = 10$) and MetS (green; $n = 9$) at 12 wk after diet commencement (T12), based on all shared metabolites. *B*: box-plot demonstrating relative concentrations of amino acids outlined in the loadings plot, as well as branched-chain amino acids of interest. *C*: box plot demonstrating relative concentrations of free fatty acids at T12 in control (blue; $n = 10$) and MetS (red; $n = 9$) animals. PCA was calculated using MetaboAnalyst metabolomics analysis suite (*A*) and ANOVA followed by Tukey's multiple comparisons test (*B* and *C*) using PRISM; *$P < 0.05$, ***$P < 0.0001$; ****$P < 0.00001$

4.5 Discussion

Metabolic syndrome is a combination of risk factors, including inter alia obesity, hypertension, insulin resistance, dyslipidaemia (hypercholesterolemia, hypertriglyceridemia, and increased free fatty acids), non-alcoholic fatty liver disease

(NAFLD), and cardiovascular complications such as HF-pEF and atrial fibrillation [214-216]. To elucidate the pathophysiology of MetS in humans, a homologous animal model of similar scale and physiology that mimics the complexity of MetS is paramount. The current study confirms the cardiometabolic features of HF-pEF (including LV hypertrophy, LA enlargement, raised LVED at rest and in response to dobutamine), hypertension, and hyperlipidaemia in a porcine model first described by Schwarzl and colleagues [202]. Additionally, we have shown that this model also demonstrates fatty liver disease and early insulin resistance, thus advancing the model by recapitulating many of the key biochemical and cardiovascular aspects of human MetS.

Growing scientific evidence supports the gut microbiome as an important interface between diet and the biochemical and cardiometabolic changes that characterize obesity, insulin resistance, hyperlipidaemia, hypertension, and HF-pEF [196, 217, 218]. With respect to gut microbes, more than 95% of the functional pathways seen in pigs are also observed in the human catalogue [219]. Determination of the microbial changes that occur during MetS development in a human scale porcine model may offer additional mechanistic insight and therapeutic assessment options for future targeted interventional studies.

The changes observed in MetS Landrace pigs were similar for body weight, blood pressure, and insulin and glucose levels to those found in other porcine models of metabolic obesity using other pig breeds, but lipid and insulin levels were higher in the current model [220-222]. In human subjects with MetS, serum levels of TC, TAG, and LDL are all increased, and these lipids were also markedly elevated in the current porcine model compared with control animals [223]. In healthy nondiabetic human populations, HOMA-IR cut-off is reported to lie in the range of 1.8 –3.8 and, at 3.25 in this porcine MetS model, HOMA-IR was significantly

elevated compared with control animals, suggesting early signs of insulin resistance [224]. The development of NAFLD is an established feature of human MetS [215, 225]. In MetS pigs fed a HFD over 12 wk, increased liver weight and histopathology associated with excess hepatic lipid deposition was detected when compared with control animals. This combination of increased hepatic lipid deposition, hypercholesterolemia, and hypertriglyceridemia in MetS pigs recreates the triad observed in humans with MetS-associated NAFLD [226].

In this study, MetS pigs showed significant decreases in α-diversity in gut microbiota, which manifested as early as 2 wk of feeding HFD and stabilized over the 12-wk feeding period. These microbiome changes are consistent with those observed in previous human obesity and metabolic syndrome clinical studies [227-230]. A highly diverse microbiome builds resilience within the gastrointestinal system; thus, reduced diversity in MetS pig's microbiome supports susceptibility to intestinal and extraintestinal cardiometabolic disease development [231, 232]. Gut microbiome changes occurred at phylum, family, and genus levels in MetS animals compared with controls, with phylogenetic analysis indicating a strongly positive association at phylum level between *Actinobacteria* relative abundance and systolic hypertension and hyperlipidaemia, as well as between *Fusobacteria* and hyperlipidaemia. There were also strong negative associations at phylum level between *Cyanobacteria* and weight and hyperlipidaemia; *Saccharibacteria* and weight, diastolic blood pressure, and total cholesterol; and *Spirochaetae* and weight, systolic hypertension, and total cholesterol. With regard to specific functional microbial populations, there was 1) a reduction of SCFA-producing bacteria *Lachnospiraceae, Rikenellaceae,* and *Akkermansia* and *2*) an increase in pro-inflammatory bacteria combined with *3*) a decrease in enteroprotective bacteria

[233, 234]. Metataxonomic analysis showed increases in secondary bile acid-producing bacteria, and serum metabolomic profiles indicated increased relative circulating saturated fatty acid concentrations in MetS pigs compared with controls. Together, these results suggest that diet-induced MetS in pigs is associated with an inflammation-prone gut microbiota similar to that observed in human MetS subjects.

The reduction in α-diversity in MetS compared with the control pigs is consistent with previous studies of microbial composition in the distal gut of other mammals exposed to HFD and exhibiting MetS [91, 235, 236]. Indeed, human studies have highlighted the coexistence of low gut microbiota diversity in patients with chronic low-grade inflammation and body fat deposition in obese individuals [230]. *Actinobacteria* relative abundances were significantly elevated in MetS pigs, which is consistent with observations by Turnbaugh et al. [230] who showed a similar increase in the phylum in obese versus lean human subjects. Consistent with these findings, in the current study MetS animals had a strong correlation between *Actinobacteria* and increase in body weight. Additionally, higher relative abundances of the *Actinobacteria, Fusobacteria,* and *Synergistetes* were noted in MetS animals (Fig. 3), and these phyla were in turn associated with aggravated MetS diagnostic parameters (Supplemental Fig. S8). In contrast, *Tenericutes, Saccharibacteria,* and *Spirochaetae* were less abundant in MetS animals than controls and were associated with attenuated MetS diagnostic parameters. Fu et al. [237] showed associations between *Actinobacteria* phyla (*Eggerthella spp* and *Collinsella stercoris*) and increased blood triglycerides and body mass index in humans. Their data also suggested an association between Tenericutes phylum and reduced blood triglycerides and body mass index. Based on a human population-

level analysis, He et al. [238] published supporting results that also suggested an association between *Actinobacteria, Fusobacteria,* and *Synergistetes* phyla and metabolic-syndrome parameters. *Tenericutes phylum* was once again associated with an attenuated MetS profile, whereas Turnbaugh et al. [230] and Ferrer et al. [239] showed higher *Actinobacteria* abundance in obese human patients compared with lean counterparts. Combined, these results strengthen the association between *Actinobacteria, Fusobacteria*, and *Synergistetes* and aggravated MetS and between *Tenericutes* and attenuated MetS parameters. However, most of the phyla discussed count for less than 0.1% of the total community (*Fusobacteria* between 0.1 and 1%), with the exception of *Actinobacteria* phyla, which is more highly represented [240]. Therefore, we must be cautious and conservative in our interpretation of associations between these phyla and MetS biologic effects. Further interventional faecal microbiota transplantation (FMT), live biotherapeutic, and gain or loss-of-function studies will be required to test any causal relationship between alteration in bacterial populations and pathophysiologic cardiometabolic effects.

In previous studies, HFD and dietary intake of carbohydrates have been shown to cause shifts in gut bacterial diversity as well as alter the proportion of *Lachnospiraceae*, *Rikenellaceae*, and *Akkermansia* in humans with MetS. In the current study, the microbiome of MetS pigs exhibited a lower abundance of *Lachnospiraceae XPB1014*, *Rikenellaceae,* and the absence of *Akkermansia* compared with control animals. These organisms have each previously been associated with an enteroprotective effect within the gut and are described as SCFA producers [210, 211, 241]. Indeed, similar observations were made in inflammatory bowel disease patients where dominant genera within the *Lachnospiraceae* family were decreased and in MetS patients who exhibited lower *Rikenellaceae* abundance

[210, 242]. In line with these results, the SCFAs butyrate and acetate, which are produced by *Lachnospiraceae*, *Rikenellaceae*, and *Akkermansia*, were lower in MetS animals compared with controls in the current study [206, 241, 243]. Of those taxa previously defined as protectors against metabolic dysfunction, only *Akkermansia* was absent in MetS pigs compared with controls [244-246]. Lower abundance of *Akkermansia muciniphila* has been well described in HFD-fed mammalian models and correlated with adipose tissue inflammation, altered lipid metabolism, and insulin resistance [247]. Consistent with MetS animals displaying a pro-inflammatory profile, this study showed that the gut microbiome of MetS pigs had a higher abundance of *Fusobacteriaceae*, *Enterobacteriaceae*, and *Veillonellaceae* at family level and *Fusobacterium*, *Methanosphaera*, and *Acidaminococcus* at genus level. These bacteria have previously been correlated with intestinal barrier dysfunction and systemic inflammation (i.e., IL-23, IL-1b, IL-2, IL-4, and IL-13) and implicated in the pathogenesis of diseases such as Crohn's disease [248, 249]. Similarly, additional evidence suggests that two *Veillonellaceae* genera, namely *Acidaminococcus* and *Megasphaera*, are associated with inflammatory bowel disease, obesity, and altered blood glucose and insulin levels [250-252]. Finally, Ciubotaru et al. [253] showed a similarly elevated abundance of *Veillonellaceae* in pre-diabetic MetS African American men when compared with matched healthy controls. Thus, MetS pigs exhibited an imbalance between pro- and anti-inflammatory bacteria consistent with an emerging paradigm of low-grade inflammation promoted by gut microbiota observed in human subjects.

In line with this, the levels of TNF-α in the serum were increased in MetS pigs compared with the control animals in our study. This inflammatory marker is consistently elevated in the serum of human subjects with metabolic syndrome

[254].

Moreover, TNF-α is one of the major pro-inflammatory cytokines in heart failure and is elevated in patients with diastolic dysfunction, cardiac hypertrophy, and myocardial fibrosis [255, 256]. In the liver, CD163 is a macrophage marker of Kupffer cells (KCs) [257], and the accumulation of hepatic lipid in NAFLD can lead to the activation of KCs via the scavenger receptor [258]. Once activated, KCs produce TNF-α to promote monocyte infiltration and activation of the NF-κB pathway promoting inflammasomal activity, leading to the progression of non-alcoholic steatohepatitis (NASH) [259-261]. This link between hepatic lipid deposition and system inflammation with cardiac consequences will need to be further explored in this pig model in the future.

A prominent finding in this porcine study was the marked increase in bile acid-associated bacteria in the MetS pig microbiome compared with control animals. Bile acids are recognized as key signalling molecules implicated in modulation of glucose homeostasis, cholesterol metabolism, and energy expenditure through the activation of receptors such as farnesoid X receptor (FXR) and G protein-coupled bile acid receptor (TGR5) [262]. Moreover, multiple additional receptors for bile acids exist within the hepatic, adipose, and cardiovascular system that appear to have important regulatory functions in these organs and, thus, may have an impact on the cardiometabolic profile. Gut microbiota in pigs and humans convert primary bile acids to a number of secondary bile acids through bacterial enzymes, including hydroxysteroid dehydrogenases present in *Actinobacteria*, *Proteobacteria*, *Firmicutes*, and *Bacteroidetes* [263, 264]. In MetS pigs, the gut microbiome was found to be composed of a higher abundance of *Actinobacteria* at phylum level and *Eubacterium*, *Ruminococcaceae_UCG004*, and *Methanosphaera* at genus level.

These bacteria have previously been implicated in deconjugation of bile acids through bile salt hydrolase expression [265]. Populations of *Actinobacteria* and *Ruminococcaceae* have been shown to expand in response to HFD in human subjects, whereas the levels *Eubacterium* have been decreased [266-268]. FGF19 is produced in the ileum and secreted into the portal blood in response to microbial-modified bile acid activation of FXR in enterocytes [269-271]. In the liver, FGF19 inhibits the production of bile acids, glucose, and fatty acids by reducing the transcription of CYP7A1 [270, 272]. In MetS pigs, FGF19 serum was markedly decreased compared with control animals. Interestingly, microbial dysbiosis in germ-free mice or antibiotic-treated humans has been linked to FXR-FGF pathways [273-276]. Moreover, decreased FGF19 in the circulation may in part explain the lipid accumulation and inflammation (markers of NASH) observed in the liver of MetS animals. In mice fed a diet high in fat, fructose, and cholesterol to induce NASH, treatment with human FGF19 or engineered FGF19 abolished lipid accumulation, a key metabolic liver disease feature of this model [277]. In this same experiment, Zhou et al. [277] also showed that injection of FGF19 reduced inflammation and liver expression of monocyte/macrophage markers. Moreover, a lower level of FGF19 has been detected in the serum of patients with coronary artery disease and is significantly decreased in plasma of obese patients [278, 279], whereas circulating levels of FGF19 have been seen to increase in obese individuals after bariatric surgery [280]. However, the pathophysiologic relationship between FGF19 and MetS parameters is yet to be completely elucidated, and the current model may prove useful in exploring mechanistic insights in the future.

Serum metabolomic profiles indicated increased ornithine levels in MetS animals but no significant difference in branched-chain amino acids. In humans, MetS-increased orthinine in the circulation has been observed with respect to citrulline and

arginine [281]. Elevated levels of saturated fatty acids myristic acid, palmitic acid, and stearic acid are observed in serum of obese patients, and relative concentrations of these free fatty acids were similarly increased in MetS pigs compared with control animals in the current study [282-284]. Free fatty acids may thus form another mechanistic link between obesity, inflammation, and cardiovascular disease, and high plasma levels of myristic and palmitic acid have both been previously associated with significant risk for myocardial infarction and stroke [285]. Reduction in gut *Akkermansia* abundance, similar to that observed in MetS pigs in the current study, was previously associated with a higher level of saturated free fatty acids in the human circulation, an effect which was posited to be mediated by alteration in gut barrier permeability [286]. Our results strongly suggest that HFD in pigs influenced the gut microbiota and may have contributed to the increased saturated fatty acids levels and ornithine detected in the circulation of MetS animals. There are a number of limitations to this study. First, the present design does not address whether there is a causal relationship between the observed gut microbiome alterations and metabolic syndrome pathophysiologic changes detected. This was beyond the scope of the current study and will require more carefully designed interventional trials in the future. Indeed, placebo-controlled FMT, live biotherapeutic interventions, and gain and loss of function intervention studies that target specific pathways linking gut microbiome to liver and cardiometabolic readouts would all be appropriate methods to further explore this question. Additionally, some of the blood parameters measured in MetS, such as serum SCFAs, are likely better analysed in the faeces or portal circulation because of the short half-life of these compounds. Future analysis of colonic luminal SCFAs in this model is therefore warranted.

In conclusion, we show in a large animal model that temporal gut microbiome changes in response to diet and mineralocorticoid-induced cardiometabolic disease mimic changes previously observed for key gut microbial populations in human subjects with this disease. The current porcine MetS model provides opportunities to better understand how the gut microbiome interacts with the cardiovascular system through pathways as diverse as gut inflammation, altered bile acid, lipid, amino acid, and free fatty acid metabolism. Homologies between pigs and humans with respect to scale and physiology may offer enhanced translational opportunities for dose finding and organ targeting in the field of gut microbiome-mediated metabolic syndrome therapeutics, whether in prebiotic, probiotic, or postbiotic forms.

4.6 Acknowledgements

We thank Grace Ahern, Katríona Lyons, and Dr. Cara Hueston for technical support; MS-Omics for assistance in metabolome analysis; and Vincent Mehigan for technical support with animal husbandry and care. We acknowledge the Teagasc Moorepark sequencing team, Dr. Paul Cotter, Dr. Fiona Crispie, and Laura Finnegan. This work was supported in part by Science Foundation Ireland Research Grant SFI/12/RC/2273. APC is an SFI funded research centre.

4.7 Supplemental Material

Supplemental Fig.S1

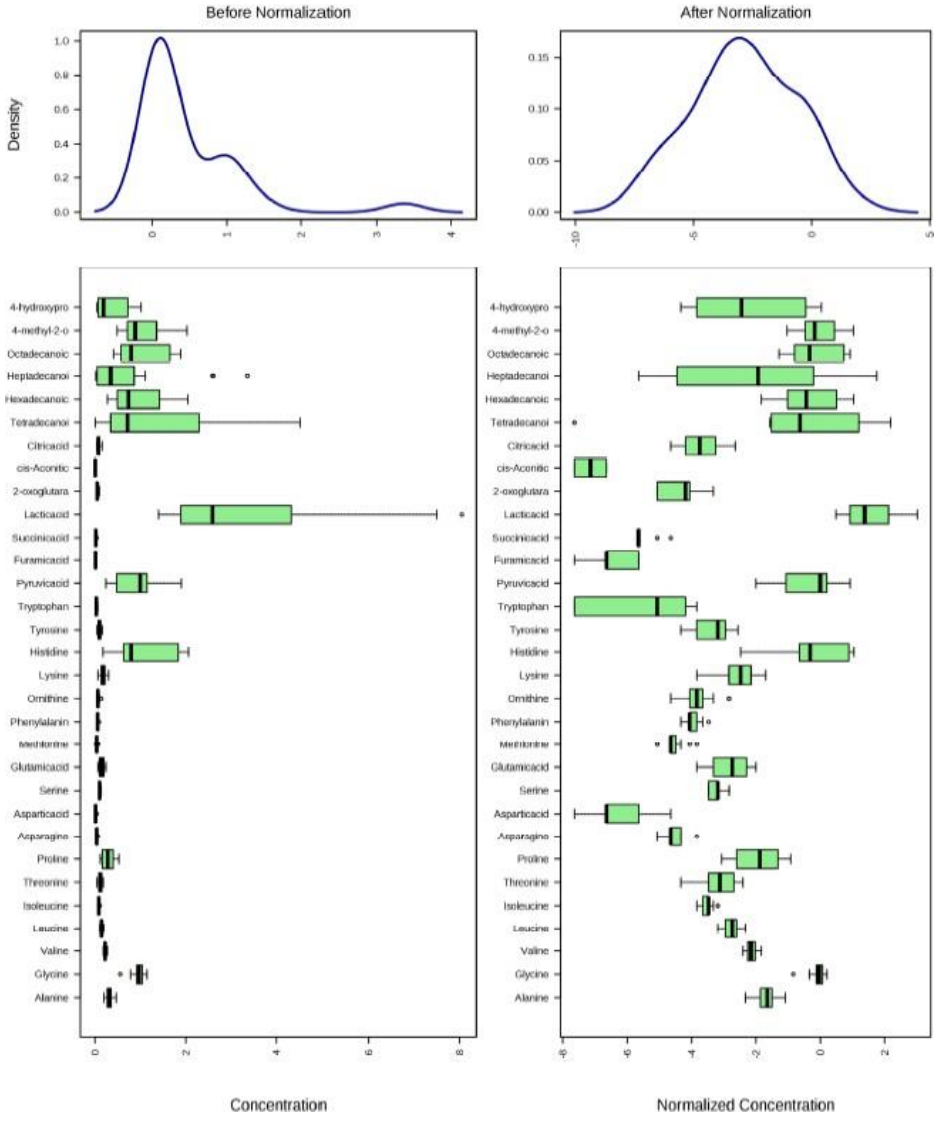

Supplemental FigS1: Metabolomic data: Pre and post logarithm normalization.

Metabolomics data underwent generalized logarithm transformation through Metaboanalyst in order to permit parametric analysis. Data was found to be of a normal distribution under visualisation and Shapiro-Wilk test posttransformation

Supplemental FigS2

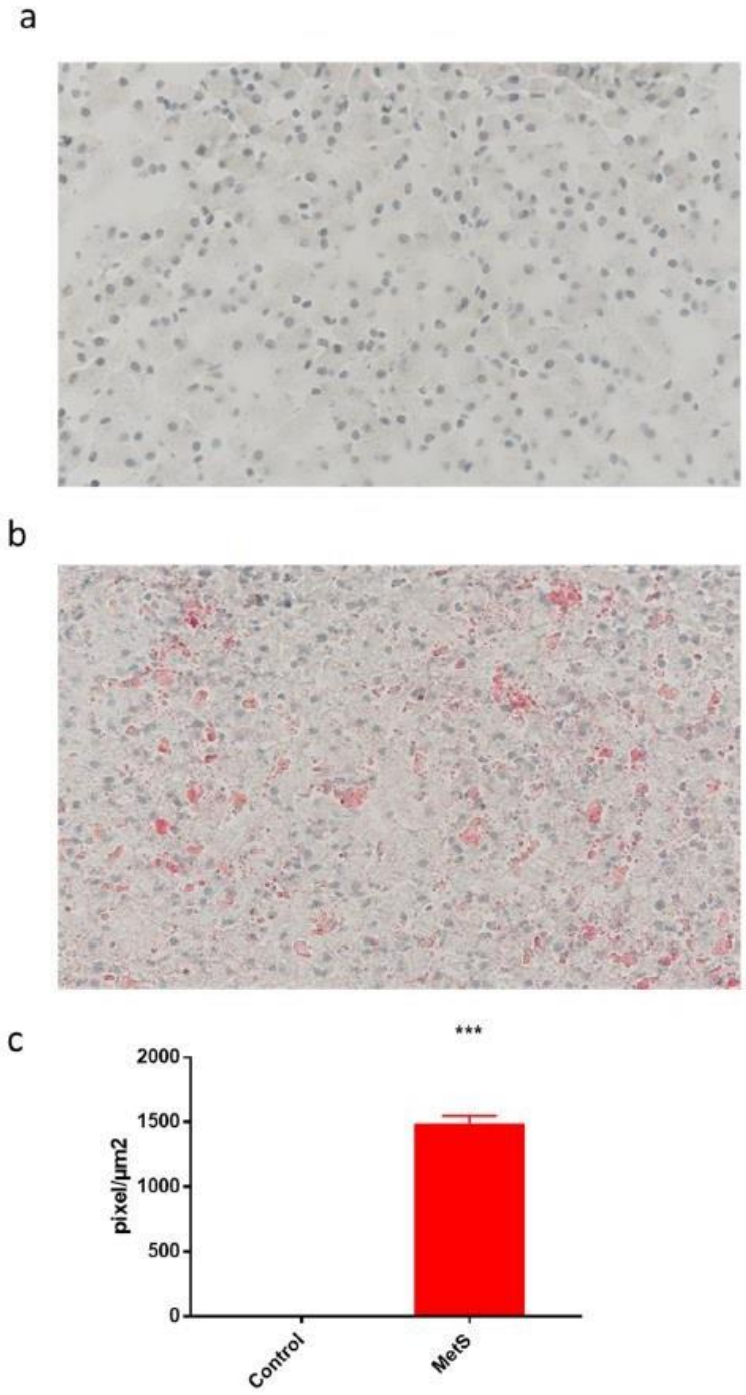

Supplemental FigS2: Fatty liver staining in MetS compared to control animals after 12weeks fed with HFD. Representative oil red O (ORO) staining of liver samples (× 40 magnification) (a) Control, N=9 (b) MetS animals, N=9 (B). Red area that consisted of lipid droplets were quantified (c). Significant difference was calculated using T-test using PRISM, $P < 0.001$(***).

Supplemental FigS3A

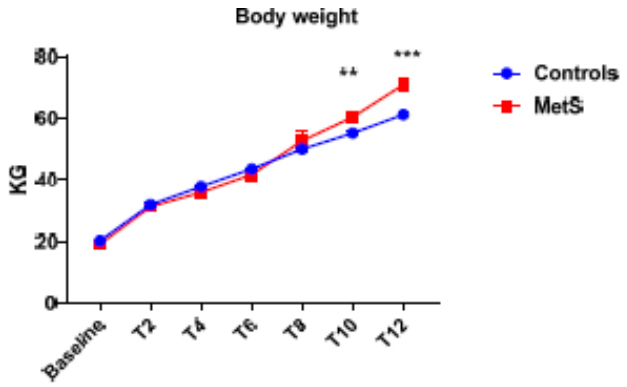

ANOVA summary	
F	222.6
P value	<0.0001
P value summary	****
Significant diff. among means (P < 0.05)?	Yes
R square	0.9641

Tukey's multiple comparisons	Mean Diff.	95.00% CI of diff.	Significant?	Summary	Adjusted P Value
Ctl Baseline vs. CtlT2	-11.70	-17.61 to -5.790	Yes	****	<0.0001
Ctl Baseline vs. Ctl T6	-23.34	-29.25 to -17.43	Yes	****	<0.0001
Ctl Baseline vs. Ctl T12	-40.93	-46.84 to -35.02	Yes	****	<0.0001
Ctl Baseline vs. MetS Baseline	1.160	-5.665 to 7.985	No	ns	0.9994
Ctl Baseline vs. MetS T2	-11.07	-16.98 to -5.160	Yes	****	<0.0001
Ctl Baseline vs. MetS T6	-23.40	-29.72 to -17.08	Yes	****	<0.0001
Ctl Baseline vs. MetS T12	-50.67	-56.69 to -44.65	Yes	****	<0.0001
CtlT2 vs. Ctl T6	-11.64	-16.47 to -6.814	Yes	****	<0.0001
CtlT2 vs. Ctl T12	-29.23	-34.06 to -24.40	Yes	****	<0.0001
CtlT2 vs. MetS Baseline	12.86	6.950 to 18.77	Yes	****	<0.0001
CtlT2 vs. MetS T2	0.6300	-4.196 to 5.456	No	ns	0.9999
CtlT2 vs. MetS T6	-11.70	-17.02 to -6.385	Yes	****	<0.0001
CtlT2 vs. MetS T12	-38.97	-43.93 to -34.01	Yes	****	<0.0001
Ctl T6 vs. Ctl T12	-17.59	-22.42 to -12.76	Yes	****	<0.0001
Ctl T6 vs. MetS Baseline	24.50	18.59 to 30.41	Yes	****	<0.0001
Ctl T6 vs. MetS T2	12.27	7.444 to 17.10	Yes	****	<0.0001
Ctl T6 vs. MetS T6	-0.06286	-5.381 to 5.255	No	ns	>0.9999
Ctl T6 vs. MetS T12	-27.33	-32.29 to -22.37	Yes	****	<0.0001
Ctl T12 vs. MetS Baseline	42.09	36.18 to 48.00	Yes	****	<0.0001
Ctl T12 vs. MetS T2	29.86	25.03 to 34.69	Yes	****	<0.0001
Ctl T12 vs. MetS T6	17.53	12.21 to 22.84	Yes	****	<0.0001
Ctl T12 vs. MetS T12	-9.741	-14.70 to -4.783	Yes	****	<0.0001
MetS Baseline vs. MetS T2	-12.23	-18.14 to -6.320	Yes	****	<0.0001
MetS Baseline vs. MetS T6	-24.56	-30.88 to -18.24	Yes	****	<0.0001
MetS Baseline vs. MetS T12	-51.83	-57.85 to -45.81	Yes	****	<0.0001
MetS T2 vs. MetS T6	-12.33	-17.65 to -7.015	Yes	****	<0.0001
MetS T2 vs. MetS T12	-39.60	-44.56 to -34.64	Yes	****	<0.0001
MetS T6 vs. MetS T12	-27.27	-32.71 to -21.83	Yes	****	<0.0001

Supplemental FigS3A: Report of ANOVA analysis for body weight (KG).

Supplemental FigS3B

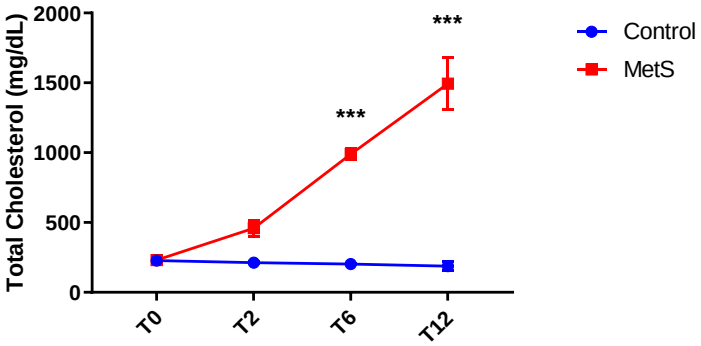

ANOVA summary	
F	37.05
P value	<0.0001
P value summary	****
Significant diff. among means (P < 0.05)?	Yes
R square	0.8250

Tukey's multiple comparisons test	Mean Diff.	95.00% CI of diff.	Significant?	Summary	Adjusted P Value
C T0 vs. MetS T0	-4.075	-468.9 to 460.8	No	ns	>0.9999
C T0 vs. Ctl T2	14.54	-430.5 to 459.6	No	ns	>0.9999
C T0 vs. MetS T2	-231.5	-641.5 to 178.5	No	ns	0.6364
C T0 vs. Ctl T6	25.09	-377.5 to 427.7	No	ns	>0.9999
C T0 vs. MetS T6	-761.7	-1164 to -359.1	Yes	****	<0.0001
C T0 vs. Ctl T12	38.67	-371.3 to 448.6	No	ns	>0.9999
C T0 vs. MetS T12	-1267	-1676 to -856.5	Yes	****	<0.0001
MetS T0 vs. Ctl T2	18.61	-426.5 to 463.7	No	ns	>0.9999
MetS T0 vs. MetS T2	-227.4	-637.4 to 182.5	No	ns	0.6567
MetS T0 vs. Ctl T6	29.16	-373.4 to 431.7	No	ns	>0.9999
MetS T0 vs. MetS T6	-757.6	-1160 to -355.1	Yes	****	<0.0001
MetS T0 vs. Ctl T12	42.75	-367.2 to 452.7	No	ns	>0.9999
MetS T0 vs. MetS T12	-1262	-1672 to -852.5	Yes	****	<0.0001
Ctl T2 vs. MetS T2	-246.0	-633.4 to 141.3	No	ns	0.4906
Ctl T2 vs. Ctl T6	10.55	-369.0 to 390.1	No	ns	>0.9999
Ctl T2 vs. MetS T6	-776.3	-1156 to -396.7	Yes	****	<0.0001
Ctl T2 vs. Ctl T12	24.13	-363.2 to 411.5	No	ns	>0.9999
Ctl T2 vs. MetS T12	-1281	-1668 to -893.7	Yes	****	<0.0001
MetS T2 vs. Ctl T6	256.6	-81.11 to 594.3	No	ns	0.2649
MetS T2 vs. MetS T6	-530.2	-867.9 to -192.5	Yes	***	0.0002
MetS T2 vs. Ctl T12	270.2	-76.30 to 616.7	No	ns	0.2359
MetS T2 vs. MetS T12	-1035	-1381 to -688.5	Yes	****	<0.0001
Ctl T6 vs. MetS T6	-786.8	-1116 to -458.1	Yes	****	<0.0001
Ctl T6 vs. Ctl T12	13.58	-324.1 to 351.3	No	ns	>0.9999
Ctl T6 vs. MetS T12	-1292	-1629 to -953.9	Yes	****	<0.0001
MetS T6 vs. Ctl T12	800.4	462.7 to 1138	Yes	****	<0.0001
MetS T6 vs. MetS T12	-504.8	-842.5 to -167.1	Yes	***	0.0004
Ctl T12 vs. MetS T12	-1305	-1652 to -958.7	Yes	****	<0.0001

Supplemental FigS3B: Results of ANOVA analysis for total cholesterol concentration.

Supplemental FigS3C

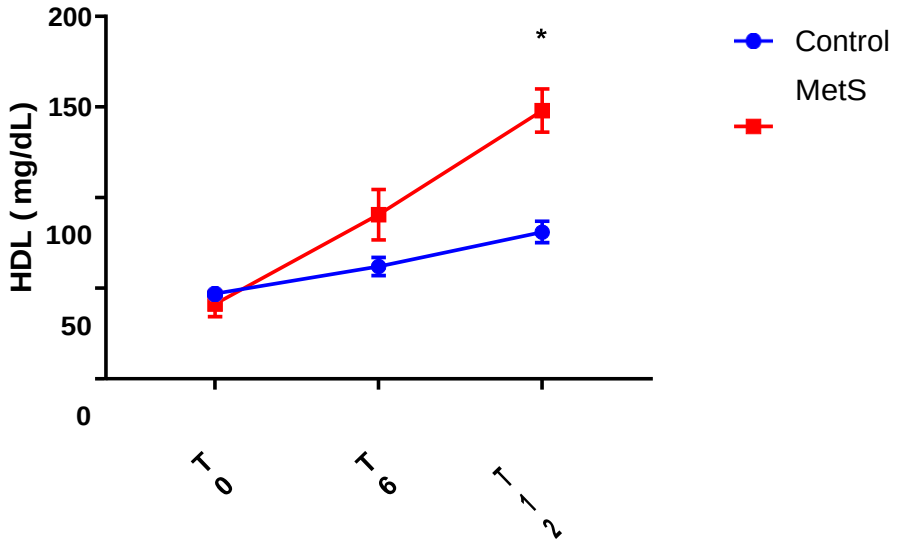

ANOVA summary	
F	5.628
P value	0.0004
P value summary	***
Significant diff. among means (P < 0.05)?	Yes
R square	0.3956

Tukey's multiple comparisons test	Mean Diff.	95.00% CI of diff.	Significant?	Summary	Adjusted P Valu
Ctl T0 vs. MetS T0	5.654	-83.50 to 94.81	No	ns	>0.999
Ctl T0 vs. Ctl T6	-14.91	-92.12 to 62.30	No	ns	0.992
Ctl T0 vs. MetS T6	-60.67	-137.9 to 16.54	No	ns	0.199
Ctl T0 vs. Ctl T12	-34.03	-111.2 to 43.17	No	ns	0.775
Ctl T0 vs. MetS T12	-101.1	-179.7 to -22.43	Yes	**	0.005
MetS T0 vs. Ctl T6	-20.57	-97.77 to 56.64	No	ns	0.967
MetS T0 vs. MetS T6	-66.32	-143.5 to 10.88	No	ns	0.129
MetS T0 vs. Ctl T12	-39.69	-116.9 to 37.52	No	ns	0.645
MetS T0 vs. MetS T12	-106.7	-185.3 to -28.08	Yes	**	0.002
Ctl T6 vs. MetS T6	-45.76	-108.8 to 17.28	No	ns	0.275
Ctl T6 vs. Ctl T12	-19.12	-82.16 to 43.92	No	ns	0.943
Ctl T6 vs. MetS T12	-86.14	-150.9 to -21.37	Yes	**	0.003
MetS T6 vs. Ctl T12	26.64	-36.40 to 89.67	No	ns	0.804
MetS T6 vs. MetS T12	-40.38	-105.1 to 24.38	No	ns	0.440
Ctl T12 vs. MetS T12	-67.02	-131.8 to -2.250	Yes	*	0.038

Supplemental FigS3C: Results of ANOVA analysis for HDL-cholesterol concentration.

Supplemental Fig3D

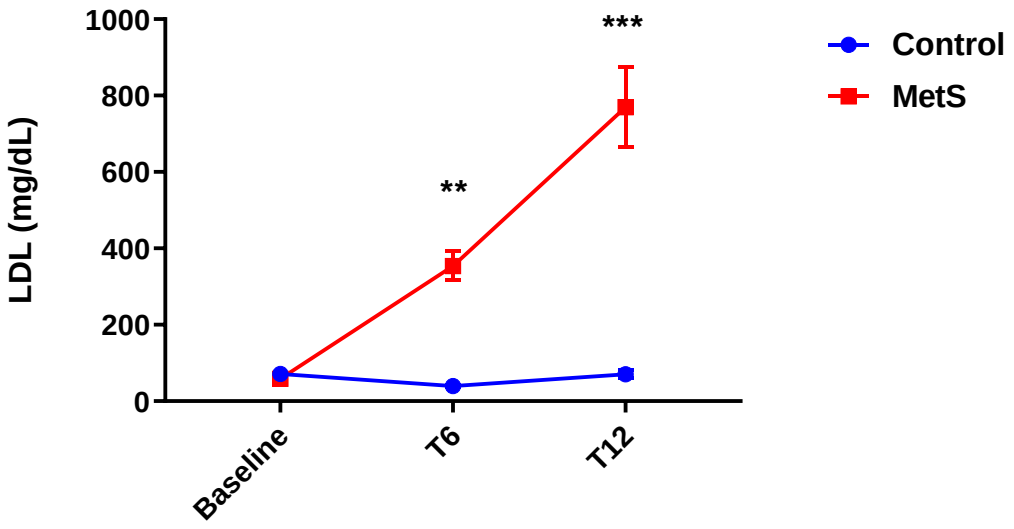

ANOVA summary	
F	27.99
P value	<0.0001
P value summary	****
Significant diff. among means (P < 0.05)?	Yes
R square	0.7777

Tukey's multiple comparisons test	Mean Diff.	95.00% CI of diff.	Significant?	Summary	Adjusted P Valu
Ctl T0 vs. MetS T0	12.74	-286.1 to 311.6	No	ns	>0.999
Ctl T0 vs. Ctl T6	31.85	-227.0 to 290.7	No	ns	0.999
Ctl T0 vs. MetS T6	-247.9	-506.7 to 10.96	No	ns	0.067
Ctl T0 vs. Ctl T12	1.133	-275.6 to 277.8	No	ns	>0.999
Ctl T0 vs. MetS T12	-698.4	-961.9 to -434.8	Yes	****	<0.000
MetS T0 vs. Ctl T6	19.11	-239.7 to 277.9	No	ns	>0.999
MetS T0 vs. MetS T6	-260.6	-519.4 to -1.776	Yes	*	0.047
MetS T0 vs. Ctl T12	-11.61	-288.3 to 265.1	No	ns	>0.999
MetS T0 vs. MetS T12	-711.1	-974.7 to -447.5	Yes	****	<0.000
Ctl T6 vs. MetS T6	-279.7	-491.1 to -68.38	Yes	**	0.003
Ctl T6 vs. Ctl T12	-30.71	-263.6 to 202.2	No	ns	0.998
Ctl T6 vs. MetS T12	-730.2	-947.3 to -513.1	Yes	****	<0.000
MetS T6 vs. Ctl T12	249.0	16.12 to 481.9	Yes	*	0.030
MetS T6 vs. MetS T12	-450.5	-667.6 to -233.4	Yes	****	<0.000
Ctl T12 vs. MetS T12	-699.5	-937.6 to -461.3	Yes	****	<0.000

Supplemental Fig3D: Results of ANOVA analysis for LDL-cholesterol concentration.

Supplemental Fig3E

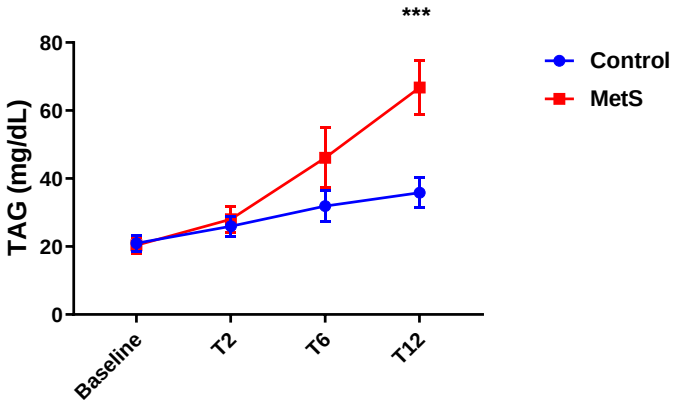

ANOVA summary	
F	7.582
P value	<0.0001
P value summary	****
Significant diff. among means (P < 0.05)?	Yes
R square	0.4612

Tukey's multiple comparisons test	Mean Diff.	95.00% CI of diff.	Significant?	Summary	Adjusted P Value
Ctl T2 vs. MetS T2	-2.079	-28.57 to 24.41	No	ns	>0.999
Ctl T2 vs. Ctl T6	-5.901	-31.72 to 19.92	No	ns	0.996
Ctl T2 vs. MetS T6	-20.13	-45.39 to 5.120	No	ns	0.214
Ctl T2 vs. Ctl T12	-9.864	-35.12 to 15.39	No	ns	0.921
Ctl T2 vs. MetS T12	-40.79	-66.61 to -14.97	Yes	***	0.000
Ctl T2 vs. Ctl Baseline	10.69	-20.65 to 42.03	No	ns	0.960
Ctl T2 vs. MetS Baseline	13.01	-18.33 to 44.35	No	ns	0.894
MetS T2 vs. Ctl T6	-3.822	-29.64 to 21.99	No	ns	0.999
MetS T2 vs. MetS T6	-18.05	-43.31 to 7.200	No	ns	0.341
MetS T2 vs. Ctl T12	-7.785	-33.04 to 17.47	No	ns	0.977
MetS T2 vs. MetS T12	-38.71	-64.53 to -12.89	Yes	***	0.000
MetS T2 vs. Ctl Baseline	12.77	-18.57 to 44.11	No	ns	0.903
MetS T2 vs. MetS Baseline	15.09	-16.25 to 46.43	No	ns	0.799
Ctl T6 vs. MetS T6	-14.23	-38.78 to 10.32	No	ns	0.610
Ctl T6 vs. Ctl T12	-3.963	-28.51 to 20.59	No	ns	0.999
Ctl T6 vs. MetS T12	-34.89	-60.02 to -9.760	Yes	**	0.001
Ctl T6 vs. Ctl Baseline	16.59	-14.18 to 47.37	No	ns	0.692
Ctl T6 vs. MetS Baseline	18.91	-11.87 to 49.69	No	ns	0.538
MetS T6 vs. Ctl T12	10.27	-13.69 to 34.23	No	ns	0.877
MetS T6 vs. MetS T12	-20.65	-45.20 to 3.896	No	ns	0.161
MetS T6 vs. Ctl Baseline	30.82	0.5190 to 61.13	Yes	*	0.043
MetS T6 vs. MetS Baseline	33.14	2.838 to 63.45	Yes	*	0.022
Ctl T12 vs. MetS T12	-30.92	-55.47 to -6.374	Yes	**	0.004
Ctl T12 vs. Ctl Baseline	20.55	-9.751 to 50.86	No	ns	0.409
Ctl T12 vs. MetS Baseline	22.87	-7.433 to 53.18	No	ns	0.275
MetS T12 vs. Ctl Baseline	51.48	20.70 to 82.25	Yes	****	<0.000
MetS T12 vs. MetS Baseline	53.80	23.02 to 84.57	Yes	****	<0.000
Ctl Baseline vs. MetS Baseline	2.319	-33.22 to 37.85	No	ns	>0.999

Supplemental Fig3E: Results of ANOVA analysis for triglyceride (TAG) concentration.

Supplemental Fig3F

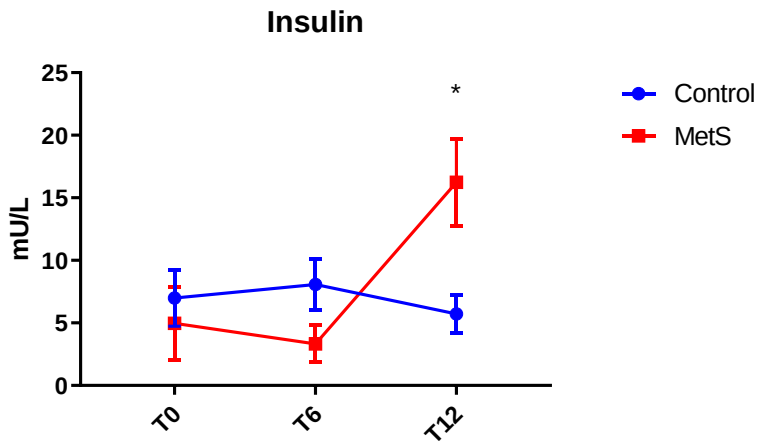

ANOVA summary	
F	3.904
P value	0.0059
P value summary	**
Significant diff. among means (P < 0.05)?	Yes
R square	0.3394

Tukey's multiple comparisons test	Mean Diff.	95.00% CI of diff.	Significant?	Summary	Adjusted P Value
Ctl T0 vs. MetS T0	2.018	-10.58 to 14.61	No	ns	0.996
Ctl T0 vs. Ctl T6	-1.095	-12.20 to 10.01	No	ns	0.999
Ctl T0 vs. MetS T6	3.654	-8.007 to 15.31	No	ns	0.933
Ctl T0 vs. Ctl T12	1.273	-9.834 to 12.38	No	ns	0.999
Ctl T0 vs. MetS T12	-9.243	-20.35 to 1.865	No	ns	0.150
MetS T0 vs. Ctl T6	-3.113	-14.22 to 7.995	No	ns	0.957
MetS T0 vs. MetS T6	1.636	-10.02 to 13.30	No	ns	0.998
MetS T0 vs. Ctl T12	-0.7446	-11.85 to 10.36	No	ns	>0.999
MetS T0 vs. MetS T12	-11.26	-22.37 to -0.1531	Yes	*	0.045
Ctl T6 vs. MetS T6	4.749	-5.287 to 14.78	No	ns	0.715
Ctl T6 vs. Ctl T12	2.368	-7.019 to 11.76	No	ns	0.973
Ctl T6 vs. MetS T12	-8.148	-17.54 to 1.240	No	ns	0.121
MetS T6 vs. Ctl T12	-2.381	-12.42 to 7.655	No	ns	0.979
MetS T6 vs. MetS T12	-12.90	-22.93 to -2.861	Yes	**	0.005
Ctl T12 vs. MetS T12	-10.52	-19.90 to -1.128	Yes	*	0.020

Supplemental Fig3F: Results of ANOVA analysis for Insulin concentration.

Supplemental Fig3G

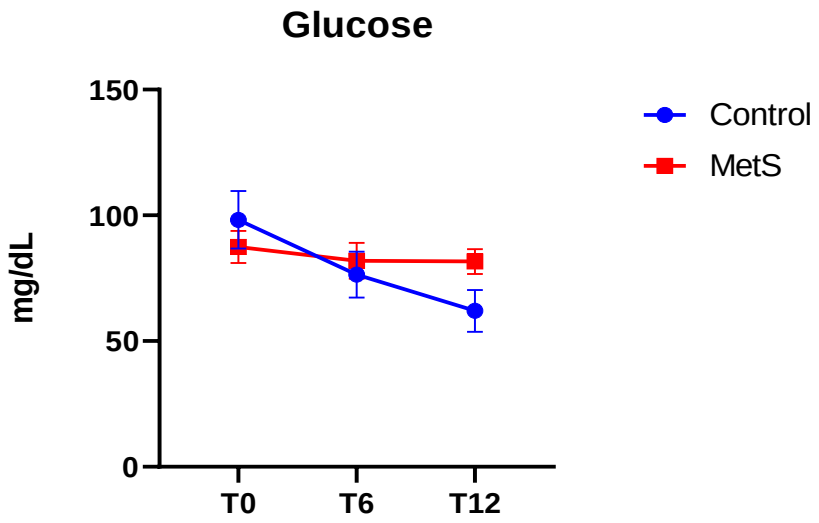

ANOVA summary	
F	1.989
P value	0.0972
P value summary	ns
Significant diff. among means (P < 0.05)?	No
R square	0.1716

Tukey's multiple comparisons test	Mean Diff.	95.00% CI of diff.	Significant?	Summary	Adjusted P Valu
Ctl T0 vs. MetS T0	10.82	-27.93 to 49.56	No	ns	0.960
Ctl T0 vs. Ctl T6	21.83	-15.40 to 59.06	No	ns	0.512
Ctl T0 vs. MetS T6	16.32	-20.91 to 53.54	No	ns	0.783
Ctl T0 vs. Ctl T12	36.24	-1.675 to 74.15	No	ns	0.068
Ctl T0 vs. MetS T12	16.61	-19.56 to 52.79	No	ns	0.748
MetS T0 vs. Ctl T6	11.02	-21.22 to 43.26	No	ns	0.911
MetS T0 vs. MetS T6	5.502	-26.74 to 37.74	No	ns	0.995
MetS T0 vs. Ctl T12	25.42	-7.606 to 58.45	No	ns	0.220
MetS T0 vs. MetS T12	5.800	-25.22 to 36.82	No	ns	0.993
Ctl T6 vs. MetS T6	-5.514	-35.91 to 24.88	No	ns	0.994
Ctl T6 vs. Ctl T12	14.40	-16.82 to 45.63	No	ns	0.745
Ctl T6 vs. MetS T12	-5.216	-34.32 to 23.89	No	ns	0.994
MetS T6 vs. Ctl T12	19.92	-11.31 to 51.15	No	ns	0.418
MetS T6 vs. MetS T12	0.2978	-28.80 to 29.40	No	ns	>0.999
Ctl T12 vs. MetS T12	-19.62	-49.59 to 10.35	No	ns	0.389

Supplemental Fig3G: Results of ANOVA analysis for Glucose concentration.

Supplemental Fig3H

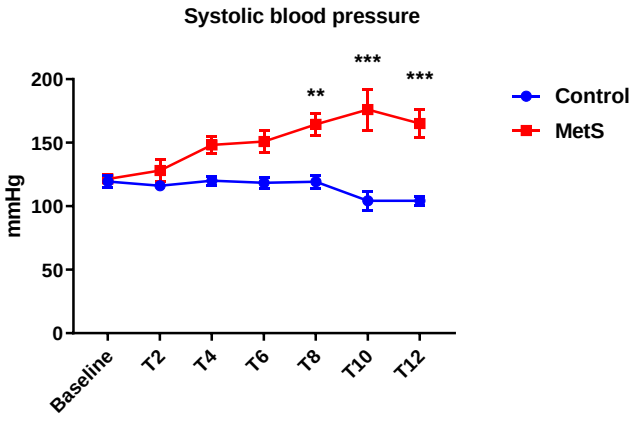

ANOVA summary	
F	10.17
P value	<0.0001
P value summary	****
Significant diff. among means (P < 0.05)?	Yes
R square	0.5596

Tukey's multiple comparisons test	Mean Diff.	95.00% CI of diff.	Significant?	Summary	Adjusted P Value
Ctl Baseline vs. Ctl T2	3.400	-37.59 to 44.39	No	ns	>0.9999
Ctl Baseline vs. Ctl T4	-0.6000	-40.85 to 39.65	No	ns	>0.9999
Ctl Baseline vs. Ctl T6	3.844	-37.14 to 44.83	No	ns	>0.9999
Ctl Baseline vs. Ctl T8	0.2000	-40.05 to 40.45	No	ns	>0.9999
Ctl Baseline vs. Ctl T10	15.21	-26.68 to 57.10	No	ns	0.9928
Ctl Baseline vs. Ctl T12	17.18	-23.81 to 58.16	No	ns	0.9747
Ctl Baseline vs. MetS Baseline	-2.000	-48.47 to 44.47	No	ns	>0.9999
Ctl Baseline vs. MetS T2	-8.600	-49.59 to 32.39	No	ns	>0.9999
Ctl Baseline vs. MetS T4	-28.80	-69.05 to 11.45	No	ns	0.4472
Ctl Baseline vs. MetS T6	-31.50	-71.75 to 8.748	No	ns	0.3009
Ctl Baseline vs. MetS T8	-44.93	-85.92 to -3.947	Yes	*	0.0183
Ctl Baseline vs. MetS T10	-56.60	-101.1 to -12.10	Yes	**	0.0023
Ctl Baseline vs. MetS T12	-45.60	-86.59 to -4.613	Yes	*	0.0153
Ctl T2 vs. Ctl T4	-4.000	-37.76 to 29.76	No	ns	>0.9999
Ctl T2 vs. Ctl T6	0.4444	-34.20 to 35.08	No	ns	>0.9999
Ctl T2 vs. Ctl T8	-3.200	-36.96 to 30.56	No	ns	>0.9999
Ctl T2 vs. Ctl T10	11.81	-23.89 to 47.52	No	ns	0.9970
Ctl T2 vs. Ctl T12	13.78	-20.86 to 48.42	No	ns	0.9837
Ctl T2 vs. MetS Baseline	-5.400	-46.39 to 35.59	No	ns	>0.9999
Ctl T2 vs. MetS T2	-12.00	-46.64 to 22.64	No	ns	0.9954
Ctl T2 vs. MetS T4	-32.20	-65.96 to 1.563	No	ns	0.0777
Ctl T2 vs. MetS T6	-34.90	-68.66 to -1.137	Yes	*	0.0357
Ctl T2 vs. MetS T8	-48.33	-82.97 to -13.69	Yes	***	0.0005
Ctl T2 vs. MetS T10	-60.00	-98.73 to -21.27	Yes	****	<0.0001
Ctl T2 vs. MetS T12	-49.00	-83.64 to -14.36	Yes	***	0.0003
Ctl T4 vs. Ctl T6	4.444	-29.32 to 38.21	No	ns	>0.9999
Ctl T4 vs. Ctl T8	0.8000	-32.06 to 33.66	No	ns	>0.9999
Ctl T4 vs. Ctl T10	15.81	-19.04 to 50.67	No	ns	0.9527
Ctl T4 vs. Ctl T12	17.78	-15.99 to 51.54	No	ns	0.8673
Ctl T4 vs. MetS Baseline	-1.400	-41.65 to 38.85	No	ns	>0.9999
Ctl T4 vs. MetS T2	-8.000	-41.76 to 25.76	No	ns	>0.9999
Ctl T4 vs. MetS T4	-28.20	-61.06 to 4.662	No	ns	0.1752
Ctl T4 vs. MetS T6	-30.90	-63.76 to 1.962	No	ns	0.0878
Ctl T4 vs. MetS T8	-44.33	-78.10 to -10.57	Yes	**	0.0013

Ctl T4 vs. MetS T10	-56.00	-93.95 to -18.05	Yes	***	0.0001
Ctl T4 vs. MetS T12	-45.00	-78.76 to -11.24	Yes	**	0.0010
Ctl T6 vs. Ctl T8	-3.644	-37.41 to 30.12	No	ns	>0.9999
Ctl T6 vs. Ctl T10	11.37	-24.34 to 47.07	No	ns	0.9980
Ctl T6 vs. Ctl T12	13.33	-21.31 to 47.97	No	ns	0.9878
Ctl T6 vs. MetS Baseline	-5.844	-46.83 to 35.14	No	ns	>0.9999
Ctl T6 vs. MetS T2	-12.44	-47.08 to 22.20	No	ns	0.9935
Ctl T6 vs. MetS T4	-32.64	-66.41 to 1.118	No	ns	0.0687
Ctl T6 vs. MetS T6	-35.34	-69.11 to -1.582	Yes	*	0.0311
Ctl T6 vs. MetS T8	-48.78	-83.42 to -14.14	Yes	***	0.0004
Ctl T6 vs. MetS T10	-60.44	-99.17 to -21.72	Yes	****	<0.0001
Ctl T6 vs. MetS T12	-49.44	-84.08 to -14.80	Yes	***	0.0003
Ctl T8 vs. Ctl T10	15.01	-19.84 to 49.87	No	ns	0.9684
Ctl T8 vs. Ctl T12	16.98	-16.79 to 50.74	No	ns	0.9014
Ctl T8 vs. MetS Baseline	-2.200	-42.45 to 38.05	No	ns	>0.9999
Ctl T8 vs. MetS T2	-8.800	-42.56 to 24.96	No	ns	0.9998
Ctl T8 vs. MetS T4	-29.00	-61.86 to 3.862	No	ns	0.1443
Ctl T8 vs. MetS T6	-31.70	-64.56 to 1.162	No	ns	0.0702
Ctl T8 vs. MetS T8	-45.13	-78.90 to -11.37	Yes	***	0.0010
Ctl T8 vs. MetS T10	-56.80	-94.75 to -18.85	Yes	***	0.0001
Ctl T8 vs. MetS T12	-45.80	-79.56 to -12.04	Yes	***	0.0008
Ctl T10 vs. Ctl T12	1.965	-33.74 to 37.67	No	ns	>0.9999
Ctl T10 vs. MetS Baseline	-17.21	-59.10 to 24.68	No	ns	0.9786
Ctl T10 vs. MetS T2	-23.81	-59.52 to 11.89	No	ns	0.5656
Ctl T10 vs. MetS T4	-44.01	-78.87 to -9.157	Yes	**	0.0026
Ctl T10 vs. MetS T6	-46.71	-81.57 to -11.86	Yes	***	0.0009
Ctl T10 vs. MetS T8	-60.15	-95.85 to -24.44	Yes	****	<0.0001
Ctl T10 vs. MetS T10	-71.81	-111.5 to -32.13	Yes	****	<0.0001
Ctl T10 vs. MetS T12	-60.81	-96.52 to -25.11	Yes	****	<0.0001
Ctl T12 vs. MetS Baseline	-19.18	-60.16 to 21.81	No	ns	0.9404
Ctl T12 vs. MetS T2	-25.78	-60.42 to 8.862	No	ns	0.3815
Ctl T12 vs. MetS T4	-45.98	-79.74 to -12.21	Yes	***	0.0007
Ctl T12 vs. MetS T6	-48.68	-82.44 to -14.91	Yes	***	0.0002
Ctl T12 vs. MetS T8	-62.11	-96.75 to -27.47	Yes	****	<0.0001
Ctl T12 vs. MetS T10	-73.78	-112.5 to -35.05	Yes	****	<0.0001
Ctl T12 vs. MetS T12	-62.78	-97.42 to -28.14	Yes	****	<0.0001
MetS Baseline vs. MetS T2	-6.600	-47.59 to 34.39	No	ns	>0.9999
MetS Baseline vs. MetS T4	-26.80	-67.05 to 13.45	No	ns	0.5682
MetS Baseline vs. MetS T6	-29.50	-69.75 to 10.75	No	ns	0.4067
MetS Baseline vs. MetS T8	-42.93	-83.92 to -1.947	Yes	*	0.0309
MetS Baseline vs. MetS T10	-54.60	-99.10 to -10.10	Yes	**	0.0040
MetS Baseline vs. MetS T12	-43.60	-84.59 to -2.613	Yes	*	0.0261
MetS T2 vs. MetS T4	-20.20	-53.96 to 13.56	No	ns	0.7294
MetS T2 vs. MetS T6	-22.90	-56.66 to 10.86	No	ns	0.5376
MetS T2 vs. MetS T8	-36.33	-70.97 to -1.693	Yes	*	0.0305
MetS T2 vs. MetS T10	-48.00	-86.73 to -9.271	Yes	**	0.0034
MetS T2 vs. MetS T12	-37.00	-71.64 to -2.360	Yes	*	0.0249
MetS T4 vs. MetS T6	-2.700	-35.56 to 30.16	No	ns	>0.9999
MetS T4 vs. MetS T8	-16.13	-49.90 to 17.63	No	ns	0.9306
MetS T4 vs. MetS T10	-27.80	-65.75 to 10.15	No	ns	0.4075
MetS T4 vs. MetS T12	-16.80	-50.56 to 16.96	No	ns	0.9081
MetS T6 vs. MetS T8	-13.43	-47.20 to 20.33	No	ns	0.9837
MetS T6 vs. MetS T10	-25.10	-63.05 to 12.85	No	ns	0.5790
MetS T6 vs. MetS T12	-14.10	-47.86 to 19.66	No	ns	0.9755
MetS T8 vs. MetS T10	-11.67	-50.40 to 27.06	No	ns	0.9988
MetS T8 vs. MetS T12	-0.6667	-35.31 to 33.97	No	ns	>0.9999
MetS T10 vs. MetS T12	11.00	-27.73 to 49.73	No	ns	0.9994

Supplemental Fig3H: Results of ANOVA analysis for systolic blood pressure.

Supplemental Fig3I

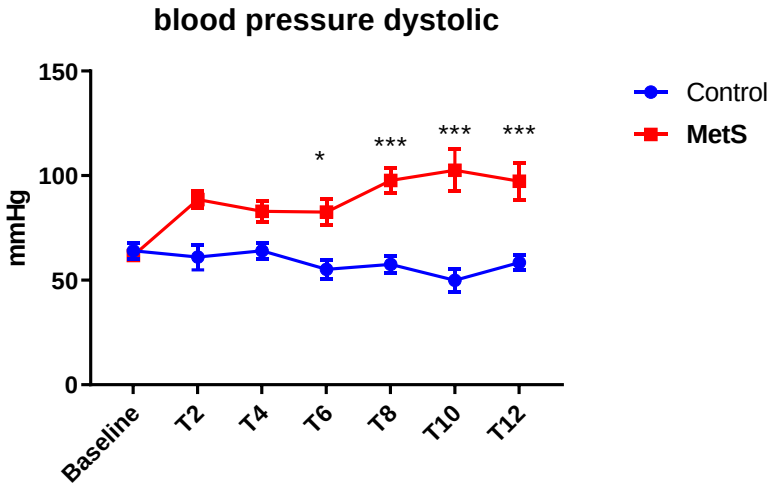

ANOVA summary	
F	9.178
P value	<0.0001
P value summary	****
Significant diff. among means (P < 0.05)?	Yes
R square	0.5490

Tukey's multiple comparisons test	Mean Diff.	95.00% CI of diff.	Significant?	Summary	Adjusted P Value
Ctl Baseline vs. Ctl T2	3.000	-33.14 to 39.14	No	ns	>0.9999
Ctl Baseline vs. Ctl T4	0.000	-31.30 to 31.30	No	ns	>0.9999
Ctl Baseline vs. Ctl T6	8.800	-22.50 to 40.10	No	ns	0.9994
Ctl Baseline vs. Ctl T8	6.400	-24.90 to 37.70	No	ns	>0.9999
Ctl Baseline vs. Ctl T10	14.13	-18.45 to 46.70	No	ns	0.9662
Ctl Baseline vs. Ctl T12	5.600	-25.70 to 36.90	No	ns	>0.9999
Ctl Baseline vs. MetS Baseline	2.200	-33.94 to 38.34	No	ns	>0.9999
Ctl Baseline vs. MetS T2	-24.60	-60.74 to 11.54	No	ns	0.5297
Ctl Baseline vs. MetS T4	-14.40	-45.70 to 16.90	No	ns	0.9466
Ctl Baseline vs. MetS T6	-18.60	-49.90 to 12.70	No	ns	0.7363
Ctl Baseline vs. MetS T8	-33.67	-65.54 to -1.791	Yes	*	0.0283
Ctl Baseline vs. MetS T10	-38.60	-73.20 to -3.996	Yes	*	0.0149
Ctl Baseline vs. MetS T12	-33.28	-65.15 to -1.402	Yes	*	0.0321
Ctl T2 vs. Ctl T4	-3.000	-34.30 to 28.30	No	ns	>0.9999
Ctl T2 vs. Ctl T6	5.800	-25.50 to 37.10	No	ns	>0.9999
Ctl T2 vs. Ctl T8	3.400	-27.90 to 34.70	No	ns	>0.9999
Ctl T2 vs. Ctl T10	11.13	-21.45 to 43.70	No	ns	0.9959
Ctl T2 vs. Ctl T12	2.600	-28.70 to 33.90	No	ns	>0.9999
Ctl T2 vs. MetS Baseline	-0.8000	-36.94 to 35.34	No	ns	>0.9999
Ctl T2 vs. MetS T2	-27.60	-63.74 to 8.543	No	ns	0.3379
Ctl T2 vs. MetS T4	-17.40	-48.70 to 13.90	No	ns	0.8149
Ctl T2 vs. MetS T6	-21.60	-52.90 to 9.701	No	ns	0.5065
Ctl T2 vs. MetS T8	-36.67	-68.54 to -4.791	Yes	*	0.0101
Ctl T2 vs. MetS T10	-41.60	-76.20 to -6.996	Yes	**	0.0055
Ctl T2 vs. MetS T12	-36.28	-68.15 to -4.402	Yes	*	0.0116
Ctl T4 vs. Ctl T6	8.800	-16.76 to 34.36	No	ns	0.9955
Ctl T4 vs. Ctl T8	6.400	-19.16 to 31.96	No	ns	0.9998
Ctl T4 vs. Ctl T10	14.13	-12.98 to 41.23	No	ns	0.8743
Ctl T4 vs. Ctl T12	5.600	-19.96 to 31.16	No	ns	>0.9999
Ctl T4 vs. MetS Baseline	2.200	-29.10 to 33.50	No	ns	>0.9999
Ctl T4 vs. MetS T2	-24.60	-55.90 to 6.701	No	ns	0.2932
Ctl T4 vs. MetS T4	-14.40	-39.96 to 11.16	No	ns	0.8005
Ctl T4 vs. MetS T6	-18.60	-44.16 to 6.957	No	ns	0.4168
Ctl T4 vs. MetS T8	-33.67	-59.92 to -7.409	Yes	**	0.0020

Ctl T4 vs. MetS T10	-38.60	-68.11 to -9.089	Yes	**	0.0015
Ctl T4 vs. MetS T12	-33.28	-59.54 to -7.020	Yes	**	0.0025
Ctl T6 vs. Ctl T8	-2.400	-27.96 to 23.16	No	ns	>0.9999
Ctl T6 vs. Ctl T10	5.325	-21.78 to 32.43	No	ns	>0.9999
Ctl T6 vs. Ctl T12	-3.200	-28.76 to 22.36	No	ns	>0.9999
Ctl T6 vs. MetS Baseline	-6.600	-37.90 to 24.70	No	ns	>0.9999
Ctl T6 vs. MetS T2	-33.40	-64.70 to -2.099	Yes	*	0.0252
Ctl T6 vs. MetS T4	-23.20	-48.76 to 2.357	No	ns	0.1165
Ctl T6 vs. MetS T6	-27.40	-52.96 to -1.843	Yes	*	0.0239
Ctl T6 vs. MetS T8	-42.47	-68.72 to -16.21	Yes	****	<0.0001
Ctl T6 vs. MetS T10	-47.40	-76.91 to -17.89	Yes	****	<0.0001
Ctl T6 vs. MetS T12	-42.08	-68.34 to -15.82	Yes	****	<0.0001
Ctl T8 vs. Ctl T10	7.725	-19.38 to 34.83	No	ns	0.9993
Ctl T8 vs. Ctl T12	-0.8000	-26.36 to 24.76	No	ns	>0.9999
Ctl T8 vs. MetS Baseline	-4.200	-35.50 to 27.10	No	ns	>0.9999
Ctl T8 vs. MetS T2	-31.00	-62.30 to 0.3009	No	ns	0.0549
Ctl T8 vs. MetS T4	-20.80	-46.36 to 4.757	No	ns	0.2424
Ctl T8 vs. MetS T6	-25.00	-50.56 to 0.5571	No	ns	0.0617
Ctl T8 vs. MetS T8	-40.07	-66.32 to -13.81	Yes	****	<0.0001
Ctl T8 vs. MetS T10	-45.00	-74.51 to -15.49	Yes	****	<0.0001
Ctl T8 vs. MetS T12	-39.68	-65.94 to -13.42	Yes	****	<0.0001
Ctl T10 vs. Ctl T12	-8.525	-35.63 to 18.58	No	ns	0.9982
Ctl T10 vs. MetS Baseline	-11.93	-44.50 to 20.65	No	ns	0.9921
Ctl T10 vs. MetS T2	-38.73	-71.30 to -6.146	Yes	**	0.0064
Ctl T10 vs. MetS T4	-28.53	-55.63 to -1.418	Yes	*	0.0295
Ctl T10 vs. MetS T6	-32.73	-59.83 to -5.618	Yes	**	0.0052
Ctl T10 vs. MetS T8	-47.79	-75.56 to -20.02	Yes	****	<0.0001
Ctl T10 vs. MetS T10	-52.73	-83.59 to -21.86	Yes	****	<0.0001
Ctl T10 vs. MetS T12	-47.40	-75.17 to -19.63	Yes	****	<0.0001
Ctl T12 vs. MetS Baseline	-3.400	-34.70 to 27.90	No	ns	>0.9999
Ctl T12 vs. MetS T2	-30.20	-61.50 to 1.101	No	ns	0.0700
Ctl T12 vs. MetS T4	-20.00	-45.56 to 5.557	No	ns	0.2997
Ctl T12 vs. MetS T6	-24.20	-49.76 to 1.357	No	ns	0.0825
Ctl T12 vs. MetS T8	-39.27	-65.52 to -13.01	Yes	***	0.0001
Ctl T12 vs. MetS T10	-44.20	-73.71 to -14.69	Yes	***	0.0001
Ctl T12 vs. MetS T12	-38.88	-65.14 to -12.62	Yes	***	0.0001
MetS Baseline vs. MetS T2	-26.80	-62.94 to 9.343	No	ns	0.3857
MetS Baseline vs. MetS T4	-16.60	-47.90 to 14.70	No	ns	0.8597
MetS Baseline vs. MetS T6	-20.80	-52.10 to 10.50	No	ns	0.5693
MetS Baseline vs. MetS T8	-35.87	-67.74 to -3.991	Yes	*	0.0134
MetS Baseline vs. MetS T10	-40.80	-75.40 to -6.196	Yes	**	0.0072
MetS Baseline vs. MetS T12	-35.48	-67.35 to -3.602	Yes	*	0.0153
MetS T2 vs. MetS T4	10.20	-21.10 to 41.50	No	ns	0.9974
MetS T2 vs. MetS T6	6.000	-25.30 to 37.30	No	ns	>0.9999
MetS T2 vs. MetS T8	-9.067	-40.94 to 22.81	No	ns	0.9993
MetS T2 vs. MetS T10	-14.00	-48.60 to 20.60	No	ns	0.9808
MetS T2 vs. MetS T12	-8.678	-40.55 to 23.20	No	ns	0.9996
MetS T4 vs. MetS T6	-4.200	-29.76 to 21.36	No	ns	>0.9999
MetS T4 vs. MetS T8	-19.27	-45.52 to 6.991	No	ns	0.4031
MetS T4 vs. MetS T10	-24.20	-53.71 to 5.311	No	ns	0.2320
MetS T4 vs. MetS T12	-18.88	-45.14 to 7.380	No	ns	0.4373
MetS T6 vs. MetS T8	-15.07	-41.32 to 11.19	No	ns	0.7797
MetS T6 vs. MetS T10	-20.00	-49.51 to 9.511	No	ns	0.5368
MetS T6 vs. MetS T12	-14.68	-40.94 to 11.58	No	ns	0.8091
MetS T8 vs. MetS T10	-4.933	-35.05 to 25.19	No	ns	>0.9999
MetS T8 vs. MetS T12	0.3889	-26.55 to 27.33	No	ns	>0.9999
MetS T10 vs. MetS T12	5.322	-24.80 to 35.44	No	ns	>0.9999

Supplemental Fig3I: Results of ANOVA analysis for diastolic blood pressure.

Supplemental FigS4

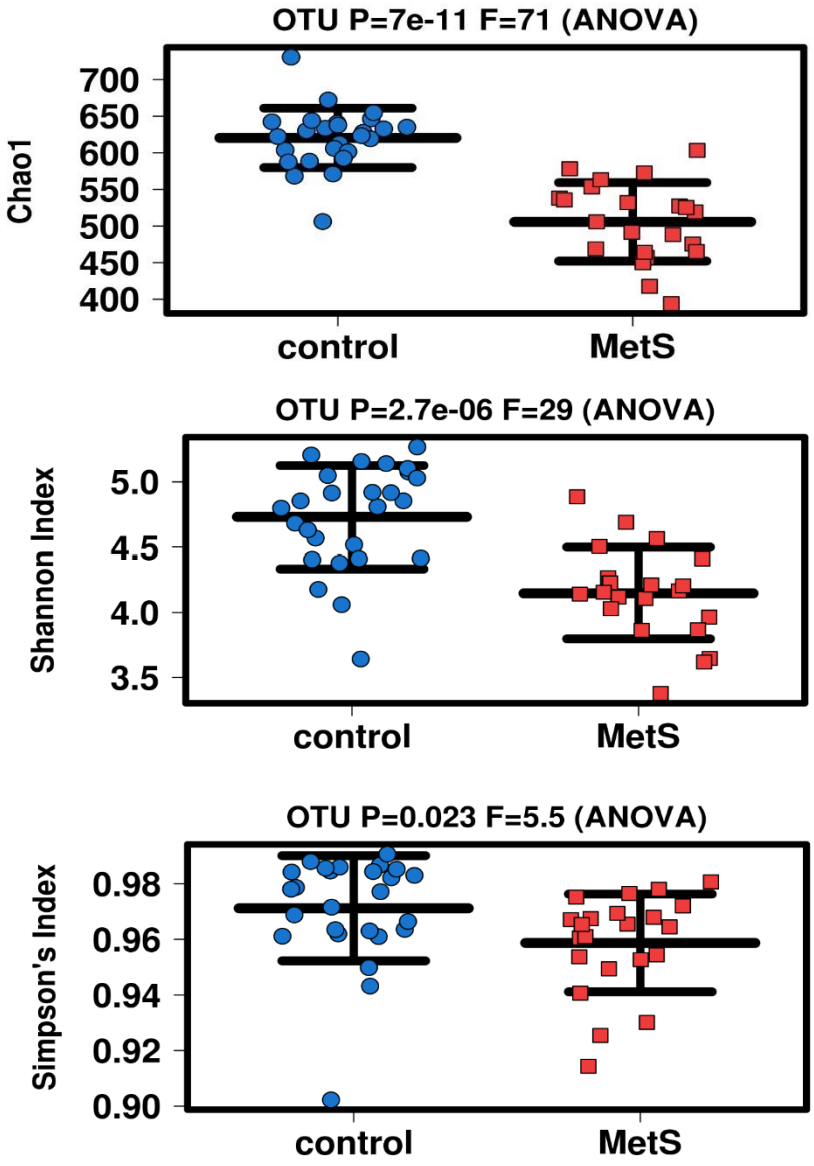

Supplemental FigS4: Community diversity represented by Chao1, Shannon and Simpson's index at an OTU level compared between diets. Diet: control (Ctl) – normal diet, MetS – High fat diet.

Supplemental FigS5

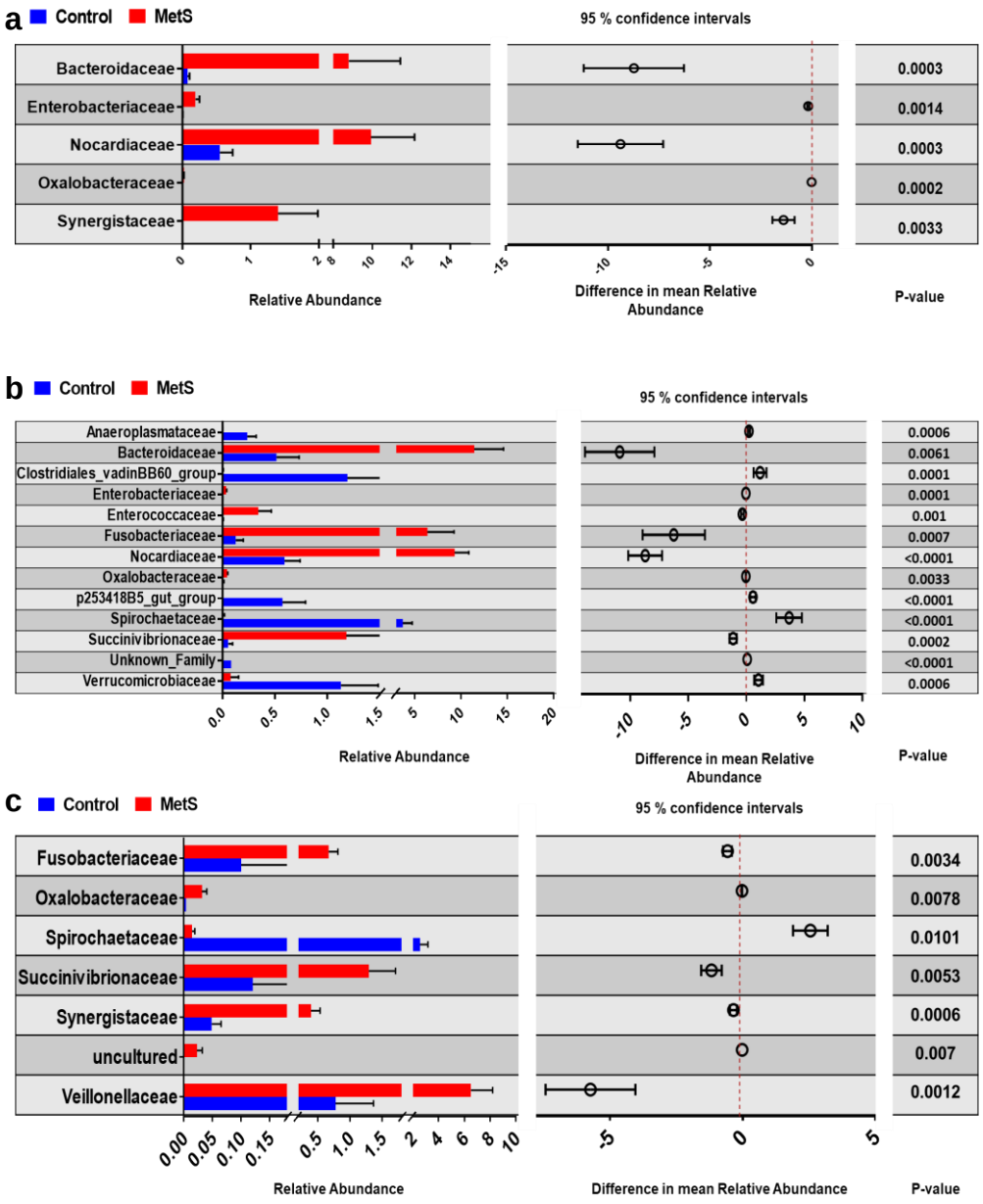

Supplemental FigS5: Family-level alterations in response to the development of metabolic syndrome (MetS). Extended error bar plot identifying significant differences between mean relative abundance of Family in Control (blue) and MetS (red) samples at (a) T2 Control N=8, MetS N=7, (b) T6 Control N=10, MetS N=8 and (c) T12 Control N= 7, MetS N=7. Significant difference was calculated using Mann Whitney test using PRISM, P-values are shown at right, confidence intervals = 95%

Supplemental FigS6

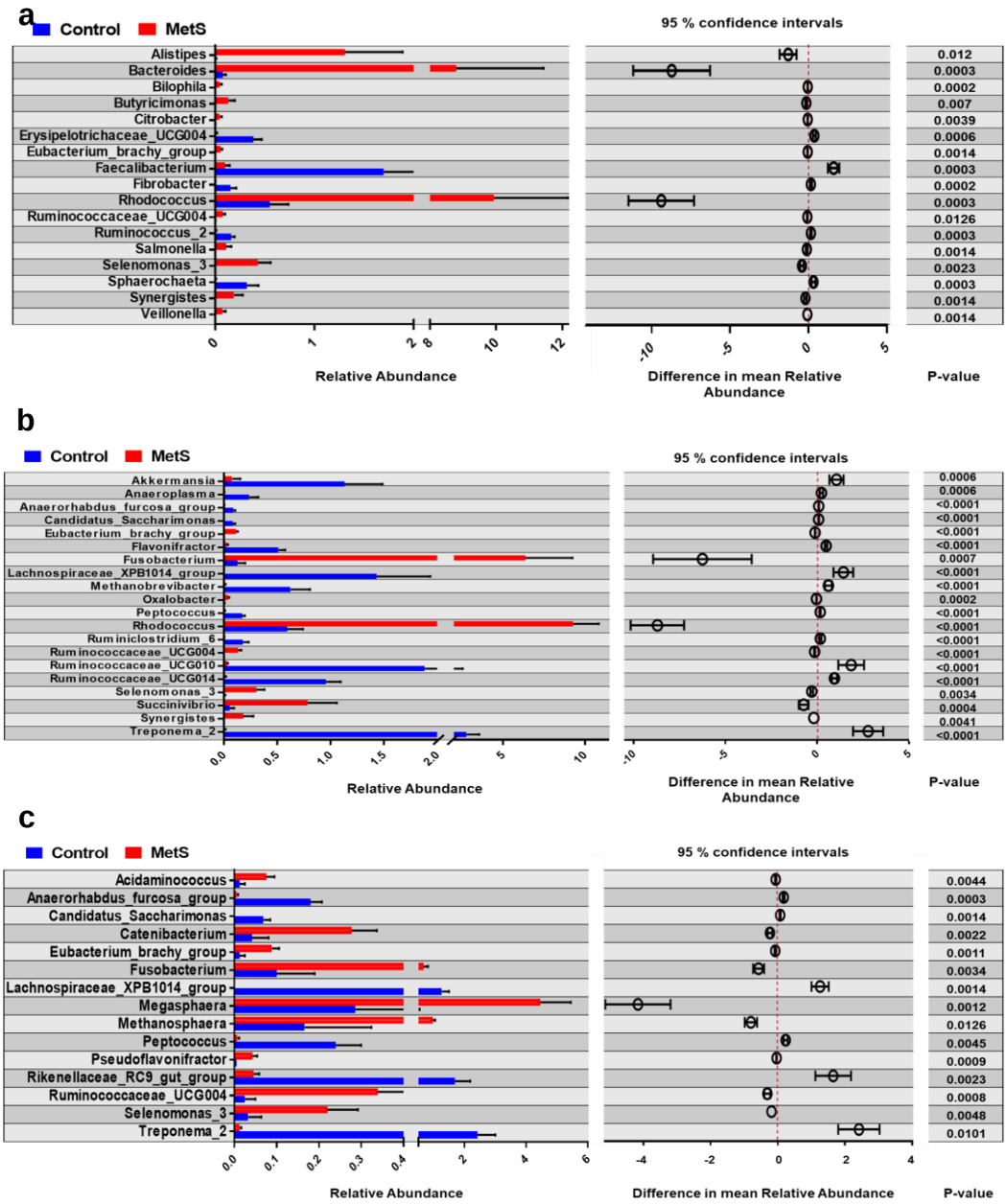

Supplemental FigS6: Genus-level alterations in response to the development of metabolic syndrome (MetS). Extended error bar plot identifying significant differences between mean relative abundance of Genus in Control (blue) and MetS (red) samples at (a) T2 Control N=8, MetS N=7, (b) T6 Control N=10, MetS N=8 and (c) T12 Control N= 7, MetS N=7. Significant difference was calculated using Mann Whitney test using PRISM, P-values are shown at right, confidence intervals = 95%.

Supplemental FigS7

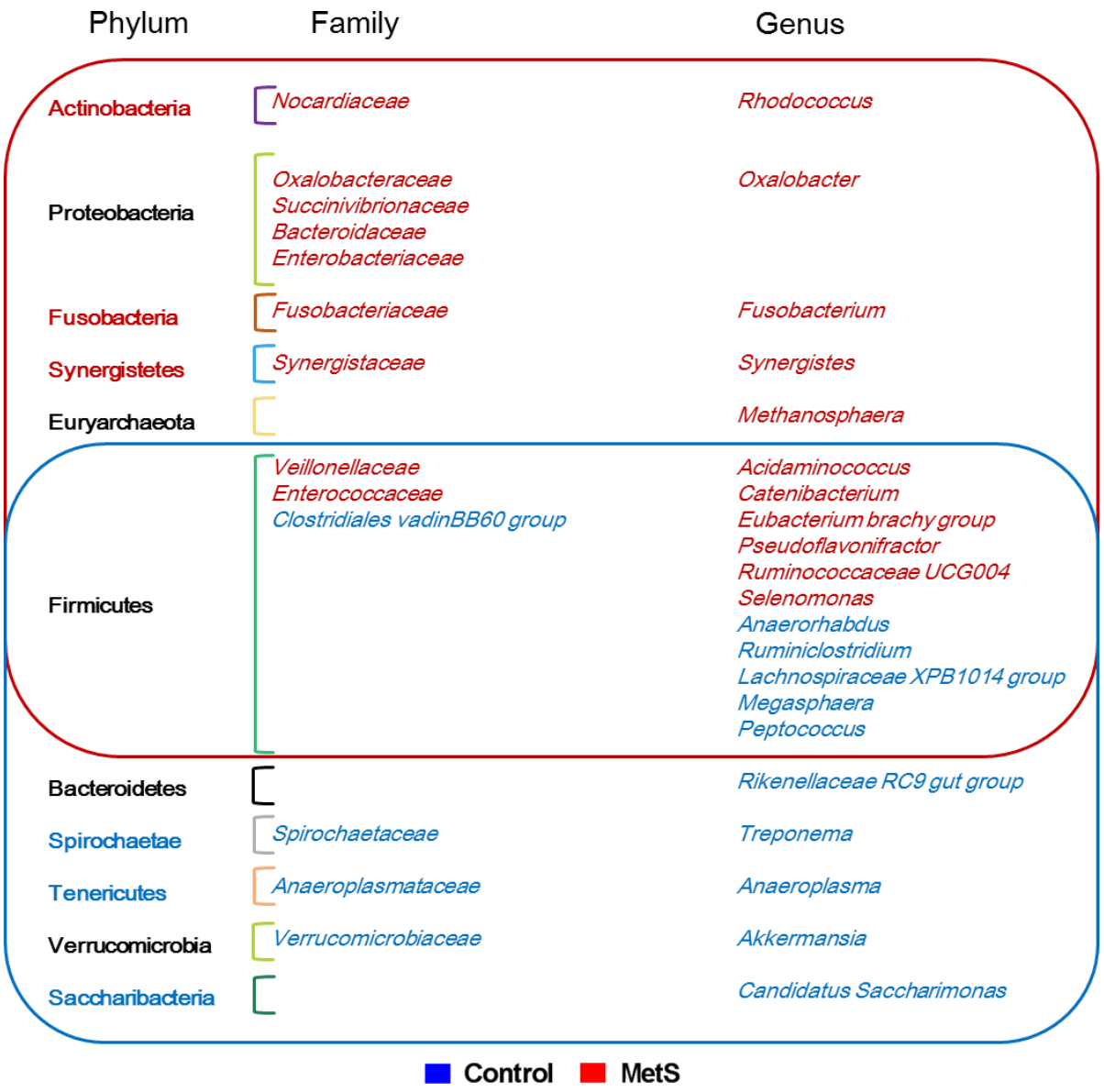

Supplemental FigS7: Relative abundance of Phylum, Family and Genus significantly increased in Control (blue) and MetS (red), samples at T6 and T12. Black describes bacteria that remain unchanged when compared between groups.

Supplemental FigS8

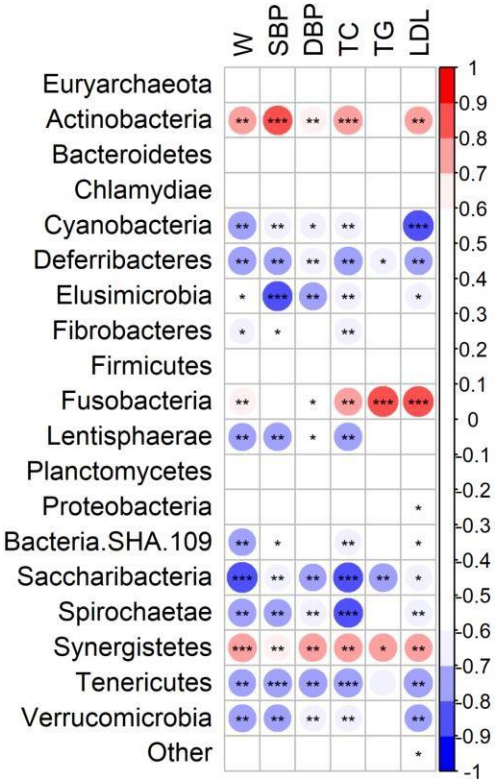

Supplemental FigS8: Association between gut microbial phyla and MetS-associated symptoms at T12. Gut microbial phyla prevalence was correlated with pigs weight (W, kg), Systolic Blood Pressure (SBP, mmHg), Diastolic Blood Pressure (DBP, mmHg), Total Cholesterol (TC, mg/dL), Triglycerides (TG, mg/dL) and Low Density Lipoproteins (LDL, mg/dL) blood concentrations. Red indicates positive associations and blue negative associations. Brighter colours indicate that the association was significant at false discovery rate (FDR) 0.05 level. Larger circle indicates a small p-value. Spearman correlation test was run using pairwise "corr.test" function, adjusted according to Benjamini-Hochberg procedure, in Rstudio (Version 1.0.136 – © 2009-2016 RStudio, Inc). Correlation plot depicts correlation relationships depending on their Spearman's rho values (colour scale) and their p-values ($P < 0.05$ (*), 0.01 (**), 0.001 (***)).

Supplemental FigS9

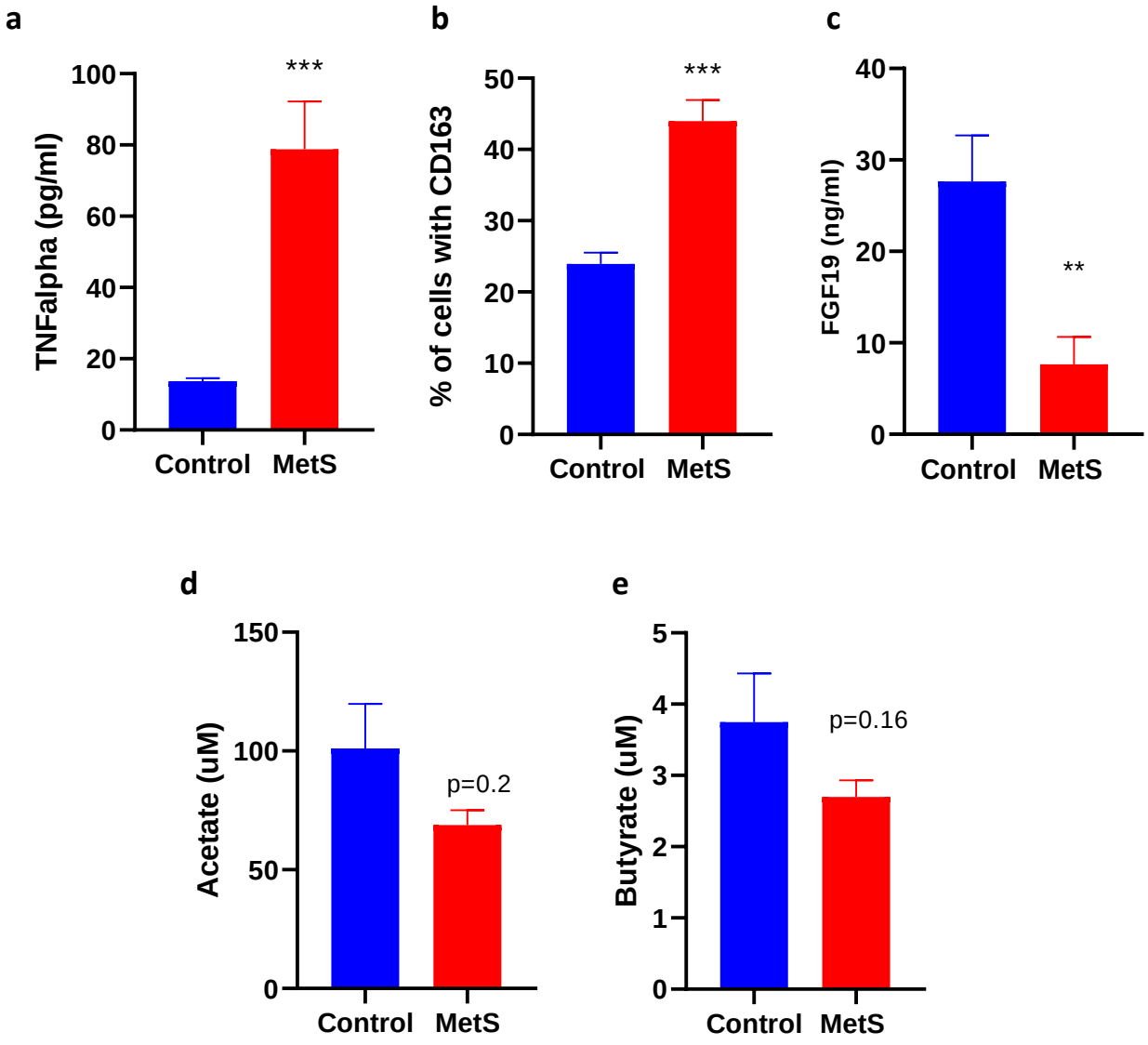

Supplemental FigS9: TNF-α and CD163, FGF19 and SCFAs in MetS compared to control animals after 12 weeks fed with HFD. (a) Serum concentrations of TNF alpha Control N=9, MetS N=8 and (b) CD163 in pigs liver Control N= 7, MetS N=7 (c) Serum concentrations of FGF19, Control N=8, MetS N=8 and (d) Serum concentrations of Acetate (e) Butyrate Controls N=10, MetS N=9. Significant difference was calculated using Mann-Whitney test using PRISM. $P < 0.01$(**), $P < 0.001$ (***).

Chapter 5.

Investigating the efficacy of orally administered Lactobacillus mucosae DPC 6426 and fibre singly or in combination on the gut microbiome in a porcine model of Metabolic Syndrome

Noel Caplice, Catherine Stanton and Paul Ross designed the study, Dr. Florence Herisson performed body weight analysis, Aoife O Donovan and Dr. Florence Herisson performed microbiome analysis together, Dr. Kiera Murphy performed bioinformatic analysis and MS-Omics performed short-chain fatty acid analysis.

5.1 Abstract

The gut microbiome has been suggested to act as a major player in the development of risk factors associated with Metabolic Syndrome (MetS) and with MetS being identified as one of the major global health challenges of the 21st century, the development of new therapeutic strategies is necessary. In this current study, a previously established porcine model of MetS was used to investigate the effects of daily oral administration of *Lactobacillus mucosae* DPC 6426, and fibre, singly and in combination on the gut microbiome over a 12-week period. Following dietary supplementation with *Lactobacillus mucosae* DPC 6426, and fibre singly, all animals developed obesity. However, following supplementation with *Lb. mucosae* DPC 6426 and fibre in combination, the percentage of body weight gained was significantly decreased at week 12 (T12) compared to pigs receiving *Lb. mucosae* DPC 6426, and fibre singly or no supplementation. Overall results of this study have indicated that the supplementation with fibre alone and in combination with *Lb. mucosae* DPC 6426 have significant effects on specific gut microbiota, demonstrating that supplementation with the combination of *Lb. mucosae* DPC 6426 and fibre resulted in significant increases in *Porphyromonadaceae, Parabacteroides* and *Ruminiclostridium* 5 ($p < 0.05$) compared to supplementation with *Lb. mucosae* DPC 6424 and fibre singly and no supplementation at all, whilst *Succinivibrio* was significantly decreased in the HFD+Fib group only ($p < 0.05$). Furthermore, results have also indicated that fibre acts in combination with *Lb. mucosae* DPC 6426 to affect existing anti-inflammatory gut microbiota, suggesting that supplementation of a combination of *Lb. mucosae* DPC 6426 and fibre could provide a new, novel therapeutic approach in the treatment of gut microbiota composition alterations associated with MetS.

5.2 Introduction

Metabolic syndrome (MetS) is a cluster of risk factors including obesity, insulin resistance and low-grade inflammation, and has been identified as a major global health challenge [287], and is increasingly viewed as a chronic inflammatory disease, in which alterations in the gut microbiota composition contribute to disease development, including obesity, type 2 diabetes, cardiovascular disease and non-alcoholic fatty liver disease (NAFLD) [288]. Several studies have suggested that the gut microbiome plays a major role in the development of obesity, and is an essential part of energy balance in the host [289, 290]. The earliest evidence supporting this was from a study that demonstrated that germ-free mice were leaner compared with mice that had an intact microbiota since birth, and following conventionalisation of germ-free mice with a gut microbiota from conventionally raised animals, a 60% increase in fat mass and insulin resistance was observed [124]. Additionally, Rabot *et al*. [291] demonstrated that germ-free mice were resistant to diet-induced obesity following the feeding of a high fat diet, in which germ-free mice gained significantly less body weight compared to conventional mice consuming the same diet ($p < 0.001$). The authors also demonstrated that germ-free mice were resistant to high-fat diet-induced insulin resistance [291]. Subsequently, in humans, metabolic syndrome has been associated with alterations in gut microbiota composition, ultimately resulting in low-grade inflammation [292]. Additionally, societal changes in dietary habits, in particular the increased consumption of processed foods which lack dietary fibre, negatively impact the gut microbiota composition and subsequently contribute to the increased occurrence of chronic inflammatory diseases, including MetS [293].

Obesity is considered a risk factor in the development of MetS, and recent studies have shown a significantly different gut microbiome composition when compared to

lean subjects [197]. Currently, the understanding of the mechanistic link between the gut microbiota alterations associated with MetS is limited due to inadequacies of existing pre-clinical animal models in translating reproducible results to humans, as there is still currently no animal model which exactly replicates human disease, and limited access to *ex vivo* tissues in the case of human clinical trial subjects [198]. An example of a limitation associated with using pre-clinical rodent models is that the gut microbiome is significantly different to that of humans, with only a total of 4% of bacterial genes found to share considerable identity, in addition to rodent MetS models requiring additional genetic alteration, thus reducing their relevance to the causes of specific alterations in the gut microbiota composition, biochemical and metabolic functions in humans [199].

The use of larger animal models, which have closer structural uniformity to human gastrointestinal, immune and metabolic systems, is essential to carry out further investigations on the microbiome-metabolic syndrome interaction. The pig is an excellent example of a potential large pre-clinical animal model as it fulfils many of these criteria, including having a similar body mass and physiology to humans as well as consuming an omnivorous diet, thus offering the potential opportunity to mimic human responses to diet with respect to investigating the alterations in the gut microbiota composition, its function and the role it plays in metabolic syndrome development [200]. In a recent study by O Donovan et al. [77] (Chapter 4), we investigated diet-induced MetS and the temporal alterations in the taxa composition and functional taxonomic changes in a large pig model following the feeding of a high fat, sugar and salt diet, and whether these microbiome changes mimic those seen in human subjects with metabolic syndrome, whilst also demonstrating the potential clinical relevance of the porcine model for investigation the role of the gut

microbiota in the development of metabolic syndrome. This model demonstrated a reduction in α-diversity and specific microbiota changes at phylum, family and genus levels. In particular, there were increases observed in the abundance of pro-inflammatory bacteria, coupled with a significant decrease in enteroprotective bacteria and a reduction in short-chain fatty acid (SCFA) producing bacteria *Lachnospiraceae, Rikenellaceae* and *Akkermansia.* Additionally, temporal shifts in β-diversity were seen as early as week 2 of dietary intervention and this difference was maintained to week 12 of the study. Together these data have suggested that diet- and mineralocorticoid-induced metabolic syndrome in pigs results in alterations to the gut microbiota composition which closely mimic those seen in human metabolic syndrome [77].

It has previously been shown that supplementation with probiotics may re-establish the gut microbiome composition and introduce beneficial functions to the gut microbiota, resulting in the improvement or prevention of inflammation and other intestinal and systemic diseases [146]. Probiotics have been defined by the FAO/WHO as "live microorganisms which, when administered in adequate amounts, confer a health benefit on the host" [144]. In a study which investigated the effects of dietary supplementation with *Lactobacillus mucosae* DPC 6426, an exopolysaccharide (EPS)-producing lactic acid (LAB) bacteria, on the enteric microbiota in an ApoE-deficient mouse model, found that supplementation with *Lb. mucosae* DPC 6426 had an effect on the composition of the gut microbiota. Furthermore, that study also found that supplementation with *Lb. mucosae* DPC 6426 significantly changed the composition of the content microbiota in the caecal content, resulting in significant reductions in *Clostridiaceae* ($p < 0.05$), *Peptococcaceae* ($p < 0.001$) and *Staphylococcaceae* (< 0.01) compared to the

controls [1].

Poor intake of dietary fibre has been associated with gut microbiome dysbiosis, resulting in reduced diversity and a decreased abundance of beneficial bacteria. The health benefits associated with dietary fibre intake have been known for over 200 years, and in the late 1960's it was proposed that low dietary fibre intake was linked with increased risk of developing a variety of diseases, including obesity, diabetes, heart disease and bowel diseases such as cancer, appendicitis and diverticulosis [294]. Increasing dietary fibre intake has been shown to improve many of the risk factors associated with MetS, including the reduction of body fat and insulin resistance [295]. In a recent review by Koç *et al.* [296], the authors summarised the benefits of increased dietary fibre intake on non-communicable diseases such as cardiovascular disease, diabetes and obesity, all of which are associated with the development of MetS. To date, the benefits of increased dietary fibre intake have been considered as general associations rather than causal effects, however, with our increased knowledge and understanding of the impact of increased dietary fibre intake on gut microbiota composition, along with scientific evidence to support the underlying mechanisms, it should be possible to establish the causal links between increased dietary fibre intake and the gut microbiota composition and its effects on the overall health of the host.

Synbiotics are described as a combination of prebiotics and probiotics which when administered can provide greater benefits than prebiotics or probiotics alone. Recently, the International Scientific Association for Probiotics and Prebiotics (ISAPP) redefined the concept of synbiotics as "a mixture comprising of live microorganisms and substrate(s) selectively utilised by host microorganisms that confers a health benefit on the host" [297]. The most common probiotic strains used

in synbiotics are *Lactobacillus, Bifidobacterium* spp*, S. boulardii and B. coagulans*, whilst the most common prebiotics used are oligosaccharaides, such as fructooligosaccharides (FOS), galactooligosaccharides (GOS) and xyloseoligosaccharides (XOS), and inulin [298]. However, even though there are *in vitro* and animal studies which suggest that synbiotics may improve MetS associated parameters, these associations are not as clear in human clinical trials [299], and further clinical investigations are needed in order to clarify their relevance and verify their effects in the prevention and treatment of MetS, however, they do still remain a potential therapeutic strategy for the treatment of MetS associated alterations in the gut microbiota composition.

We hypothesis that daily oral administration of *Lactobacillus mucosae* DPC singly, or in combination with fibre will positively affect the gut microbiome, which in turn may positively affect MetS associated parameters. Thus, the aim of this current study was to investigate alterations in the gut microbiome composition using a porcine model of MetS (as described in Chapter 4) as a result of daily oral supplementation with fibre, a probiotic strain (*Lactobacillus mucosae* DPC 6426), at a minimum concentration of 10^{10} CFU/g, and a combination of both.

5.3 Materials and Methods

5.3.1 Ethics Statement

All experimental procedures used during the study were reviewed and approved by the University College Cork Ethics Committee, under a licence issued by the Health Products Regulatory Authority (HPRA) (reference number: AE19130/P097). Effect size was calculated on G Power (version 3.1.9.2 University Kiel, Germany) using our previous experiment [77]: N= 5 per group, and sample-size estimation was calculated. As this was experimental work generating new data, a 10% observed

difference in means was assumed with an estimated standard deviation of 5.2 for each group. This required a sample size of 6 animals in each group to detect a statistically significant difference in the gut microbiome composition between the experimental groups and reject the null hypothesis. Calculations were based on an effect size of 0.83, α probability 0.05 with a power of 0.95.

5.3.2 Production of Freeze-Dried *Lactobacillus mucosae* DPC 6426 Powder

Production of freeze-dried *Lb. mucosae* DPC 6426 powder was carried out according to the optimised cultivation and pilot scale freeze-drying protocol which was developed previously (Chapter 2). This protocol included the use of a 1% inoculum, anaerobic incubation of 10ml and 200ml inoculations for 6.5 hours, followed by anaerobic incubation of ~16-18 hours for 5L inoculations combined with the addition of 10% trehalose acting as a cryoprotectant and a 90-95 hour freeze-drying program (shelf freeze temperature: -45°C; condenser set point: -85°C and vacuum set point; 0.02mBar) in the Labconco™ FreeZone™ 12L -84°C Console Freeze dryer with stoppering tray dryer (Labconco Corporation, Kansas, USA). This protocol resulted in a minimum concentration of 10^{10} CFU/g and the use of 10% trehalose as a cryoprotectant was shown to aid in maintaining viability and survival of freeze- dried *Lb. mucosae* DPC 6426 during storage at -30°C.

5.3.3 Study Design and Sampling

This study used the porcine model of metabolic syndrome and heart failure with preserved ejection fraction [77], as previously described in Chapter 4, to investigate the effects of daily oral supplementation of fibre, *Lb. mucosae* DPC 6426 singly or in combination, with particular focus being placed on the alterations to the gut microbiome. Three-month old Landrace female piglets, with a starting weight of 20-25kg were acquired and housed in individual stalls in the Biological Service Unit,

University College Cork. Animals were separated into 4 groups: HFD (*n* = 6) were fed 0.5kg/day Connolly's Redmills normal chow (20% Hi-Density Weaner Pellets; 20% protein, 3.5% fibre, 6% oil) supplemented with 1kg/day 4% salt, 4% cholesterol, 25% crude fat, 0.5% cholate and 26% sugar (high fat, salt and sugar diet – HFD), from SAFE, Augy R8620 version 0011), HFD + *Lb. mucosae* DPC 6426 (*n* = 6) fed with 0.5kg/day Connolly's Redmills normal chow supplemented with 1kg/day of HFD and 1g of *Lb. mucosae* DPC 6426 (HFD+LB) at 10^{10} CFU/g, HFD + Fibre (HFD+Fib) (*n* = 6) fed with 0.5kg/day Connolly's Redmills normal chow supplemented with 1kg/day of HFD and 43g of fibre and HFD + *Lb. mucosae* DPC 6426 + Fibre (HFD+LB+Fib) (*n* = 6) fed with 0.5kg/day Connolly's Redmills normal chow supplemented with 1kg/day of HFD, 1g of *Lb. mucosae* DPC 6426 at 10^{10} CFU/g and 43g of fibre. All animals had free access to water at all times. In conjunction with the supplemented diets, all animals underwent surgical implantation of a subcutaneous mineralocorticoid deoxycorticosterone acetate (DOCA) depot (200mg/kg, 90 days release pellets from Innovative Research of America) in the inguinal region prior to trial initiation to induce sodium and water retention, ultimately resulting in hypertension. All groups were fed the aforementioned diets over a 12-week period. Faecal samples were collected every two weeks for a total of seven time points; at baseline prior to study diet initiation (Baseline – n = 6 HFD + Fib and HFD + LB + Fib, n = 5 HFD and HFD + LB), as well as two weeks (T2 – n = 6 per group), four weeks (T4 – n = 6 HFD, HFD + LB and HFD + LB + Fib, n = 5 HFD + Fib), six weeks (T6 – n = 6 HFD + LB, HFD + Fib and HFD + LB + Fib, n = 5 HFD), eight weeks (T8 – n = 6 HFD, HFD + LB and HFD + LB + Fib, n = 5 HFD + Fib), ten weeks (T10 – n = 6 HFD, HFD + LB and HFD + LB + Fib, n = 5 HFD + Fib) and twelve weeks (T12 – n = 6 HFD + LB, HFD + Fib and HFD + LB + Fib, n = 5 HFD) post diet commencement. Following 12

weeks of feeding, the animals were fasted for 24 hours, at which point body weight was measured. Animals were sacrificed through bolus IV injection of pentobarbitone (50mg/kg, Dolethal Vetaquinol). The caecum and faecal samples were collected from the pigs and were stored at 4°C for a maximum of two hours prior to faecal water preparation and bacterial genomic DNA extraction.

5.3.4 Faecal Short Chain Fatty Acid Analysis

Sample extraction: Between 200 and 400mg of faecal material was placed into sterile microcentrifuge tubes and 2x wt/vol of sterile PBS was added and the samples were homogenised using a benchtop vortex for 15 minutes. Following homogenisation, samples were centrifuged at 16,000 x g for 30 minutes. The supernatant was removed and centrifuged at 16,000 x g for a further 30 minutes. The supernatant was removed again and a final centrifugation was carried out at 16,000 x g for a further 30 minutes. The final supernatant was then filtered through Corning® CoStar® Spin-X® centrifuge filter tubes (cellulose acetate membrane, pore size 0.22µm) (Sigma Aldrich, Germany) at a top speed of 10,000 x g until the supernatant was clear in colour. The filters was removed and the faecal water samples were stored at -20°C until analysis.

Quantification of Faecal Short Chain Fatty Acids: Sample analysis was carried out by MS-Omics as follows. Samples were acidified using hydrochloride acid, and deuterium labelled internal standards were added. All samples were analysed in a randomised order. For quality control, a mixed pooled sample (QC sample) was created by taking a small aliquot from each sample. The QC sample was analysed at regular intervals throughout the sequence. Matrix effects were tested for quantified compounds by spiking the QC sample in a minimum of two levels. Analysis was performed using a high polarity column (Zebron™ ZB-FFAP, GC Cap. Column 30m

x 0.25 mm x 0.25 μm) installed in a GC (7890B, Agilent) coupled with a quadropole detector (5977B, Agilent). The system was controlled by ChemStation (Agilent). Raw data were converted to netCDF format using ChemStation before the data were imported and processed in Matlab R2014b (Mathworks, Inc.) using the PARADISe software as described by Johnsen *et al.* [300].

5.3.5 Microbiome analysis

DNA Extraction: Bacterial genomic DNA was extracted from 0.25g of faecal and caecal material using the repeat bead beating plus column (RBB+C) method as described by Yu *et al.* [190], combined with the QIAamp Fast DNA Stool Mini Kit (Qiagen, UK) as described by Fouhy *et al.* [301] with slight modifications: 1.0mm and 2.3mm sterile zirconia beads were used during the homogenizing step instead of 0.5mm sterile zirconia beads, in order to prevent sedimentation of the 0.1mm beads and the faecal material. Bacterial genomic DNA was eluted in 200μl of Buffer AE (QIAamp Fast DNA Stool Mini Kit, Qiagen, UK) and stored at -80°C [84].

16S rRNA sequencing and analysis: Following on from DNA extraction, the V3-V4 regions of the 16S rRNA gene were amplified though 30 cycles of PCR reactions the DNA using the primer pair TCGT CGGC AGCG TCAG ATGT GTAT AAGA GACA GCCT ACGG GNGG CWGC AG-3' and 5'-GTCT CGTG GGCT CGGA GATG TGTA TAAG AGAC AGGA CTAC HVGG GTAT CTAA TCC-3', according to the 16S Metagenomic Sequencing preparation protocol for Illumina MiSeq and as previously described by Fouhy *et al* [301]. The indexed products were then visualised using gel electrophoresis and cleaned using Beckman Coulter™ Agencourt AMPure XP magnetic beads (Fisher Scientific, Ireland) prior to DNA quantification using the Qubit (BioSciences, Dublin, Ireland), with the Qubit High Sensitivity DNA kit (ThermoFisher Scientific, Ireland). Following cleaning and

quantification, samples were pooled at equal concentrations and high-throughput sequencing was carried out on the Illumina MiSeq platform in the Teagasc sequencing facility using a 2 x 300 cycle kit, following the standard Illumina sequencing protocols.

Bioinformatic analysis: The 300-bp paired ends which arose from the sequencing were assembled using FLASH (fast length adjustment of short reads to improve genome assemblies). QIIME (Quantitative Insights into Microbial Ecology; version 1.8.0) was used for quality control filtering of pair-end reads, based on a quality score of >25 and the removal of mismatching barcodes [192]. As part of the quality control process, prior to analysis sequences which had produced less than 40,000 reads were manually removed, which accounts for the differences in animal numbers between groups and between time points. USEARCH (version 7, 64-bit) was used for deionisation, detection of chimeras and clustering into operational taxonomic units (OTU's; 97% identity). PyNAST (Python Nearest Alignment Space Termination) was used for alignment of OTUs and assignment of taxonomy of 97% similarity identity against the SILVA SSURef database release v123.

Statistical analysis: Data are presented as mean ± SEM and analysed by ANOVA test using PRISM (GraphPad Software, Inc.), where $p < 0.05$ was used to reject the null hypothesis. Estimations of α-diversities were developed with QIIME and visualised using principal co-ordinate analysis (PCoA) plots which were generated using the web-based software Calypso (version 8.72). Multiple β-diversities were also calculated using Calypso, including Bray Curtis UniFrac PCoA plots, which highlighted the alterations based on supplementation and time point. In order to assess the phylum, family and genus level changes in the pigs, all significant taxa which were analysed by the Mann Whitney-U test, were graphically represented as

relative abundance with the means ± SEM, *P* values and confidence intervals. All significant taxa were analysed by an ANOVA test using PRISM (GraphPad Software, Inc.) and were adjusted by a false discovery rate (FDR) and a *q* value of less than 0.5 was considered statistically significant.

5.4 Results

This study investigated the effects of daily oral supplementation of *Lb. mucosae* DPC 6426, at a minimum concentration of 10^{10} CFU/g, and fibre alone, or in combination on temporal alterations in the gut microbiome during the development of MetS in a previously established porcine model of diet- and mineralocorticoid-MetS (as described in Chapter 4).

5.4.1 Body weight

The percentage of weight gained was measured bi-weekly over the 12-week study period. At T0 (baseline), there were no differences observed between the four dietary intervention groups. Similar to our previous publication, [77] (Chapter 4), all animals developed obesity. However, the percentage of weight gained was seen to be reduced from the mid-point of the study (week 6) onwards, and was significantly decreased at week 12 in pigs supplemented with *Lb. mucosae* DPC 6426 and fibre in combination compared to pigs receiving *Lb. mucosae* DPC 6426, and fibre singly or no supplementation ($p < 0.05$).

5.4.2 Impact of Dietary Intervention on the Faecal SCFA profile in MetS

SCFA analysis was carried out on week 12 (T12) faecal water samples from all four dietary intervention groups by MS-Omics (Denmark). The SCFA method used to analyse the faecal water samples is a targeted method which analyses the samples for 10 different compounds (acetic acid, formic acid, propanoic acid, 2-methylpropanoic

acid, butanoic acid, 3-methylbutanoic acid, pentanoic acid, 4-methylpentatoic acid, hexanoic acid and heptanoic acid). Out of all samples analysed, formic acid, 4-methlypantanoic acid and heptanoic acid were only detected in a few samples (Supplementary Table 1), in which concentrations undetectable as they were below the limit of detection (< LOD), while all other compounds were detected in all samples analysed (Supplementary Table 2).

The score plot from a principal component analysis (PCA) model calculated on the reduced dataset is shown in Figure 1a and in this plot the QC samples are tightly grouped indicating that the analytical variance, which is represented by the spread of QC samples, are greatly exceeded by the biological variance. It should also be noted that the QC samples are in the centre of the plot, indicating that matrix effects are not a major issue with these samples. There was no distinct separation between the four dietary intervention groups, but rather a high degree of variance between and within the four dietary intervention groups. The loading plot, which is shown in Figure 1b, shows which compounds are responsible for the patterns observed in the score plot.

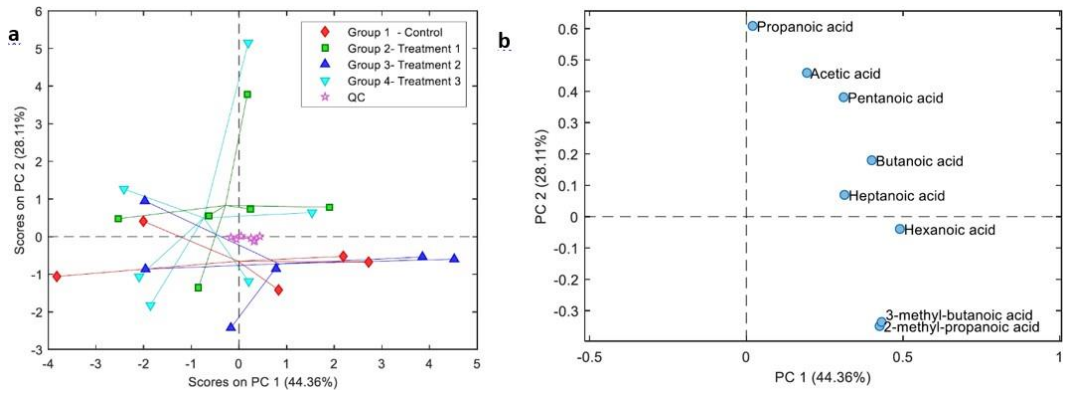

Figure 1. Faecal Short Chain Fatty Acid Analysis (a) Score plot from PCA model calculated on the relative concentrations of the variables in the reduced dataset; Group 1 – Control = HFD, Group 2 – Treatment 1 = HFD+LB, Group 3 – Treatment 2 = HFD+Fib and Group 4 –Treatment 3 = HFD+LB+Fib. (b) Loading plot from PCA model calculated on the relative concentrations of the compounds in the reduced dataset.

Figure 2 shows bar charts of the individual SCFA compounds (acetic acid, propionic acid, 2-methyl-propioic acid, butanoic acid, 3-methyl-butanoic acid, pentanoic acid, hexanoic acid and heptanoic acid) in the reduced dataset. Samples have been grouped according to dietary intervention and data are presented as the mean concentration for each group.

Dietary intervention with *Lb. mucosae* DPC 6426 and fibre, singly or in combination had no significant effects on the concentrations of SCFA in the T12 faecal samples. Analyses of SCFA concentrations showed that the following SCFA compounds were higher, but without significance,; propionic acid in the HFD+LB and HFD+LB+Fib groups, 2-methyl-propionic acid in the HFD and HFD+Fib groups, butanoic acid in the HFD+LB group, 3-methyl-butanoic acid in the HFD+Fib group, pentanoic acid

in the HFD+LB group, hexanoic acid in the HFD and HFD+LB groups and heptanoic acid in the HFD+Fib and HFD+LB+Fib groups, however, none of these were significant (Figure 2).

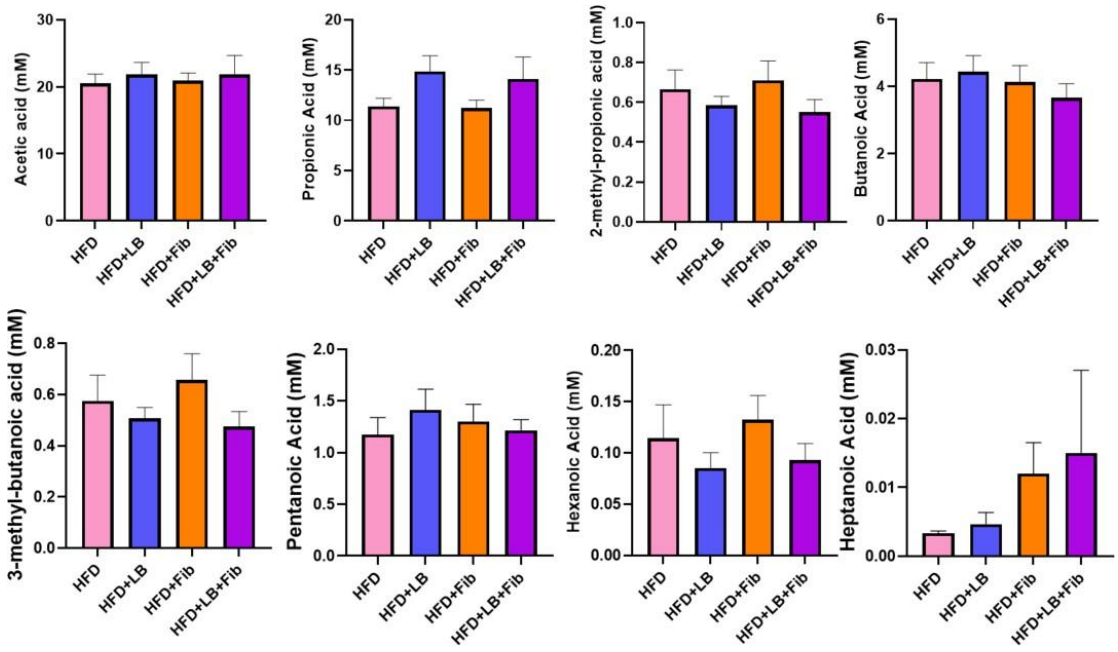

Figure 2. Concentration of individual faecal SCFAs in T12 faecal samples of MetS pigs in response to different dietary interventions. (A) Acetic acid, (B) Propionic acid, (C) 2-methyl-propionic acid, (D) Butanoic acid, (E) 3-methyl-butanoic acid, (F) Pentanoic acid, (G) Hexanoic acid and (H) Heptanoic acid. (Dietary intervention: HFD – Pink, HFD+LB – Blue, HFD+Fib – Orange and HFD+LB+Fib – Purple). Significant difference was calculated using ANOVA followed by Tukey's multiple comparisons test using GraphPad Prism.

5.4.3 Alterations in Microbiome following Diet-Induced Metabolic Syndrome

Chao1, Shannon, Simpson and Phylogenetic Diversity (PD Whole Tree) indices were used to measure the α-diversity of the gut microbiota composition following the feeding of a HFD, with or without intervention with *Lb. mucosae* DPC 6426 and fibre, singly and in combination. A significant decrease in α-diversity of the gut

microbiota was seen in all dietary intervention groups between baseline (T0) and T12 (Figure 3A, HFD, HFD+LB, and HFD+LB+Fib $p < 0.001$ and HFD+Fib $p < 0.05$, Figure 3C: Shannon $p < 0.001$, Figure 3D: Chao1 $p < 0.001$, and Figure 3E: Simpson $p = 0.017$), and this significant decrease in α-diversity was seen as early on a week 2 (T2), and was maintained until the end of the 12-week study (Figure 3A), similar to what was observed in our previous study (Chapter 4). However, there were no statistically significant differences observed in α-diversity between the four groups at each time point (Figure 3B).

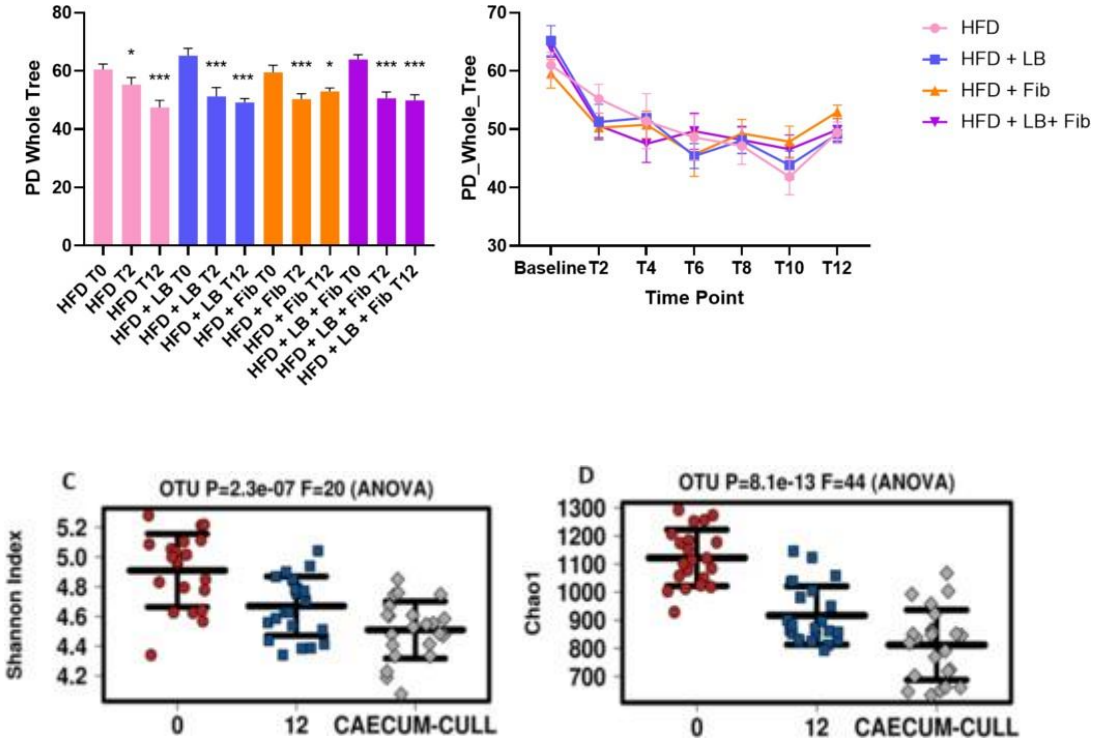

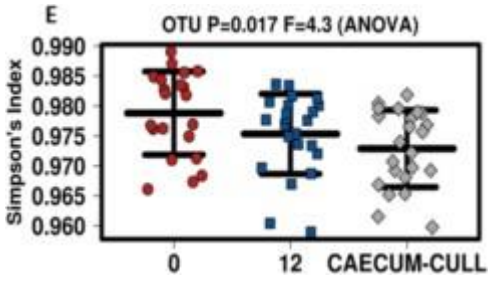

Figure 3. Alterations in α-diversity in response to different dietary interventions. (A) Phylogenetic distance (PD) compared between diet interventions at baseline (T0), 2 weeks (T2) and 12 weeks (T12) and (B) compare over time from baseline to T12. (Dietary intervention: HFD (Pink), HFD+LB (Blue), HFD+Fibre (Orange) and HFD+LB+Fibre (Purple)). Community diversity is represented by Shannon, Chao1 and Simpson (C-E) and is compared between baseline (0) and week 12 (12) in faecal samples and week 12 in caecum samples (caecum-cull) for all groups. Significant differences were calculated using ANOVA followed by Original FDR method of Benjamini and Hochberg multiple comparisons test using GraphPad PRISM (A, B) and calypso online platform $P < 0.05$ (*), $P < 0.01$ (**), $P < 0.001$ (***).

A PCoA plot based on Bray-Curtis distance matrices found distinct separation in the composition of the gut microbiota between all animal groups at baseline (T0) compared to T12 (Figure 4A), however there was no separation observed between the four dietary intervention groups between T0 and T12 (Figure 4B). Similar to the results from our previous study (Chapter 4), a temporal shift in the beta diversity between the groups was observed early on at week 2 (T2) in this study, however, there were no distinct separations observed between the four dietary intervention groups at T0, T2, T6 or T12 (Figure 4C).

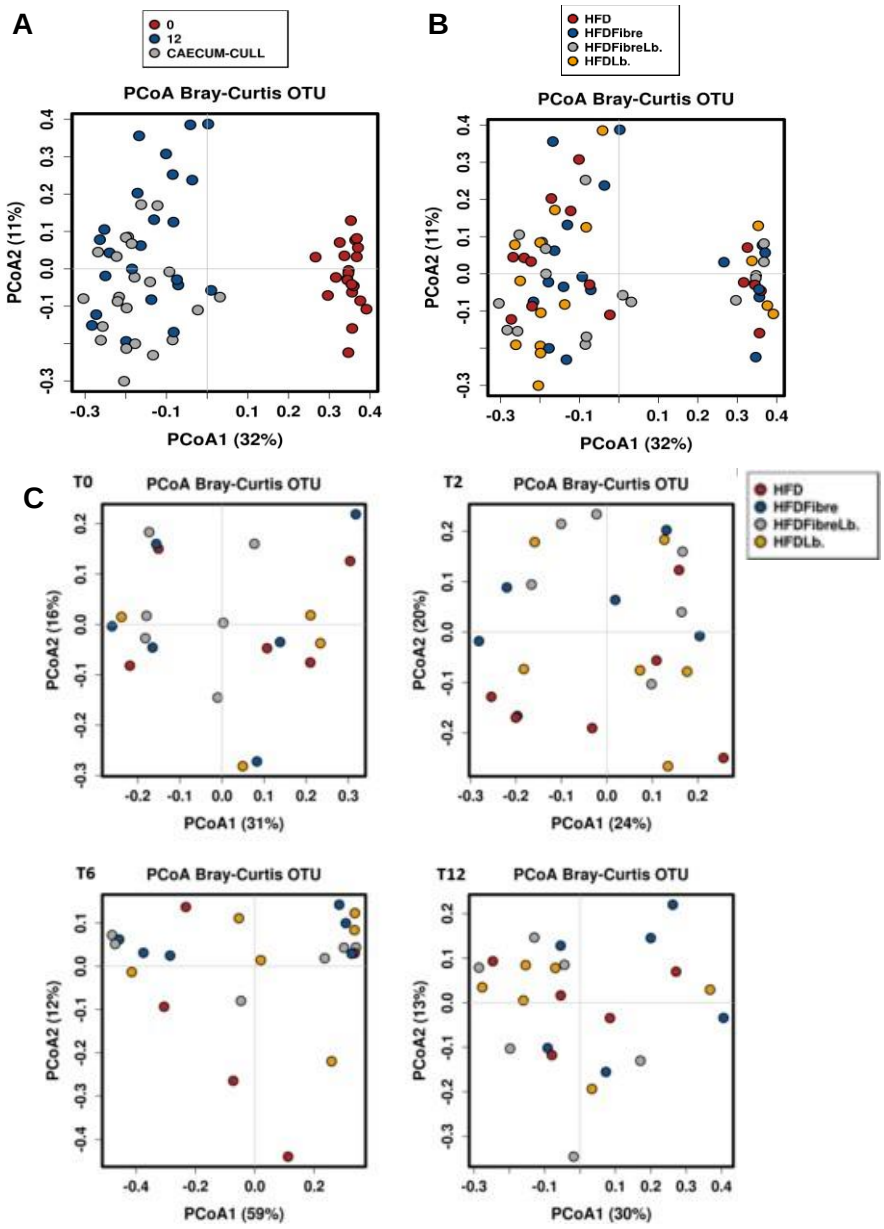

Figure 4: Temporal shift in β-diversity in response to different dietary interventions. (A) PCoA plot based on Bray-Curtis distance matrices of β-diversity of pig faecal microbiota composition at baseline (0) and week 12 (12) and week 12 in caecum samples (caecum-cull). (B) Temporal shift of pig faecal microbiome β-diversity in response to different diet intervention at baseline (T0), week 2 (T2), week 6 (T6) and week 12 (T12). (HFD – red, HFD+LB – orange, HFD+Fibre – blue and HFD+LB+Fibre – grey).

5.4.4 Microbiome Analysis at Phylum, Family and Genus Levels.

At T0 (baseline), the microbiome composition at Phylum, Family and Genus levels showed no differences between the four dietary intervention groups (Figure 5, 6, 7). Additionally, there were no significant differences observed at phylum level at T2, T6 and T12 between the four dietary intervention groups (Supplementary Figure 1).

At family level, the top fourteen most abundant families were *Veillonellaceae*, *Streptococcaceae, Ruminococcaceae, Prevotellaceae*, *Porphyromonadaceae*, *Lactobacillaceae, Lachnospiraceae, Erysipelotrichaceae, Enterobacteriaceae, Clostridiaceae 1, Christensenellaceae, Bacteroidales* S247 group, *Bacteroidaceae* and *Acidaminococcaceae* (Figure 6). The one family observed at T12 to be significantly increased, *Porphyromonadaceae* was significantly increased in the HFD+LB+Fib group compared to the HFD, HFD+LB and HFD+Fib groups ($p < 0.05$) (Figure 8A). Furthermore, a trend towards significance was observed at T12 in *Ruminococcaceae* in the HFD+Fib group compared to the HFD and HFD+LB+Fib groups ($p = 0.06$) (Figure 8B).

At genus level, the top ten most abundant genera were uncultured bacterium, uncultured, *Streptococcus, Roseburia, Prevotellaceae* NK3B31 group, *Prevotella* 9, *Phascolarctobacterium, Megasphaera, Lactobacillus* and *Christensenellaceae* R7 group (Figure 7). There were three significant changes observed at genus level at T12, *Parabacteroides* was significantly increased in the HFD+LB+Fib group compared to the HFD, HFD+LB and the HFD+Fib groups ($p < 0.05$) (Figure 9A), *Succinivibrio* was significantly decreased only in the HFD+Fib group ($p < 0.05$) (Figure 9B) and *Ruminiclostridium* 5 was significantly increased in the HFD+LB+Fib group only compared to the HFD, HFD+LB and HFD+Fib groups (p

< 0.05) (Figure 9C). Furthermore, a trend towards significance was observed at T2 in *Prevotellaceae* NK3B31 group in the HFD+Fib and HFD+LB+Fib groups (p = 0.06) (Figure 9D).

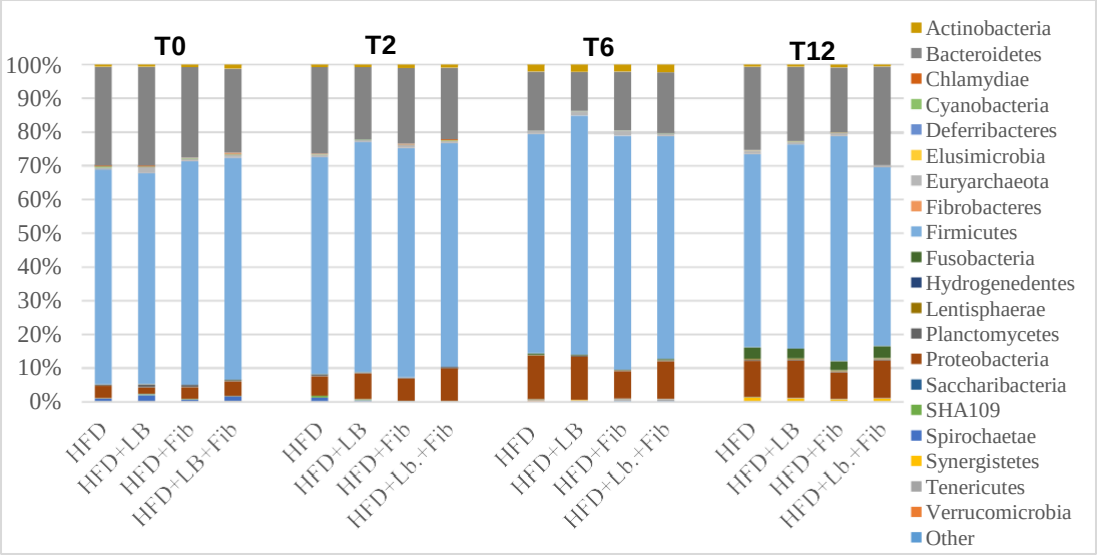

Figure 5. Phylum-level analysis. 100% stacked bar charts showing the relative abundance of specified Phyla in pig faeces at Baseline (T0), T2, T6 and T12 between the four dietary interventions.

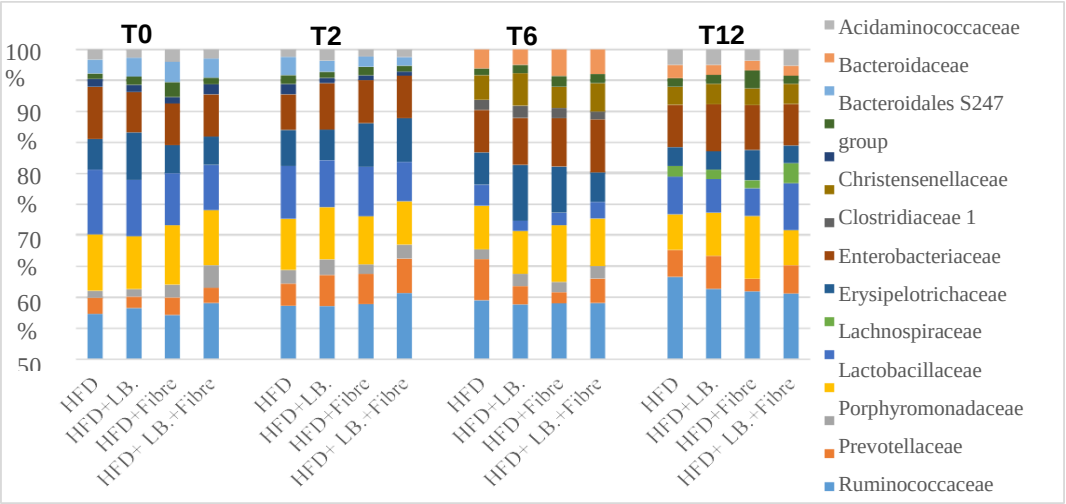

Figure 6. Family-level analysis. 100% stacked bar charts showing the 10 most abundant families in pig faeces at Baseline (T0), T2, T6 and T12 between the four dietary interventions.

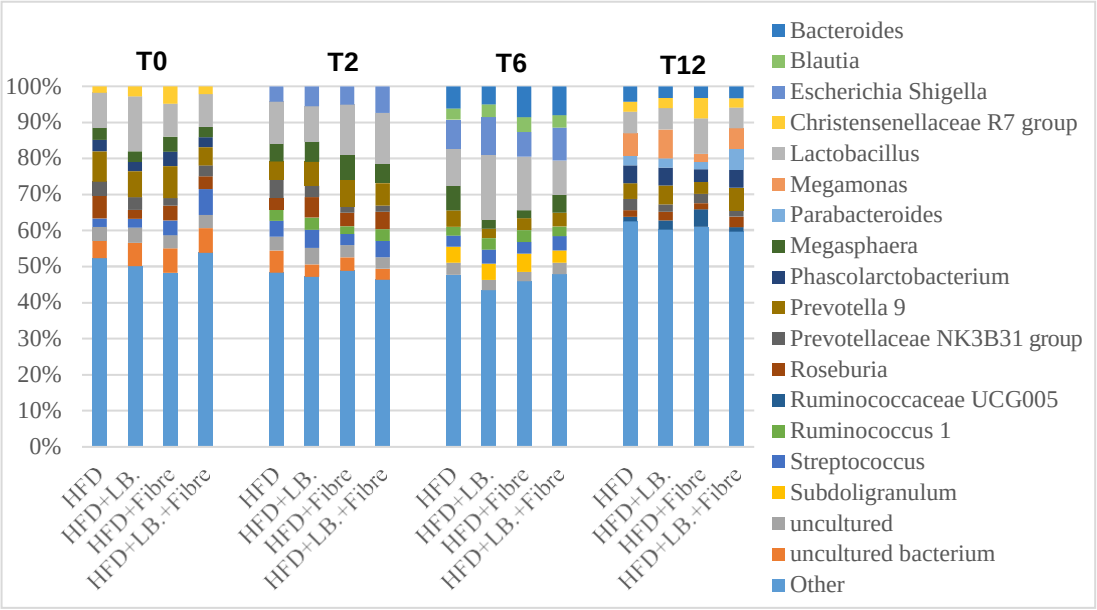

Figure 7. Genus-level analysis. 100% stacked bar charts showing 10 most abundant genera in pig faeces at Baseline (T0), T2, T6 and T12 between the four dietary interventions.

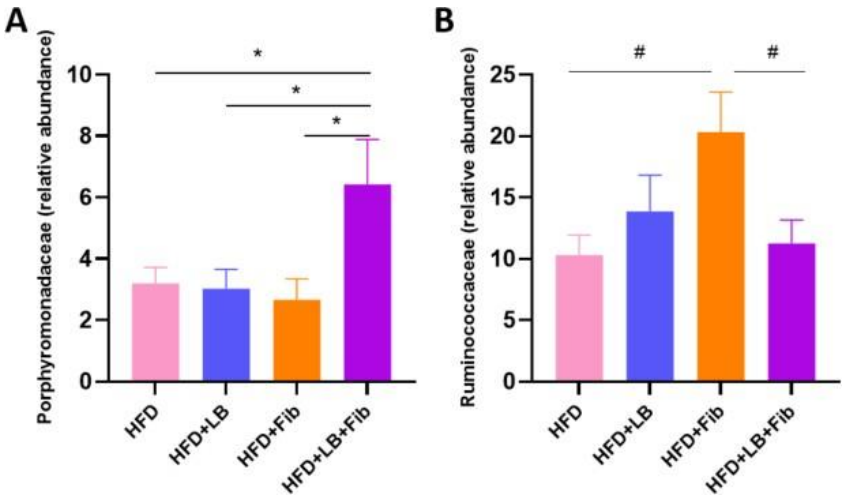

Figure 8. Family-level analysis - Extended error bar plot identifying significantly different families between the four dietary intervention groups at T12. (Dietary intervention: HFD – Pink, HFD+LB – Blue, HFD+Fibre – Orange, HFD+LB+Fib – Lavender). Significant difference was calculated using ANOVA followed by Original FDR method of Benjamini and Hochberg multiple comparisons test using GraphPad PRISM. P = 0.06 (#), P < 0.05 (*).

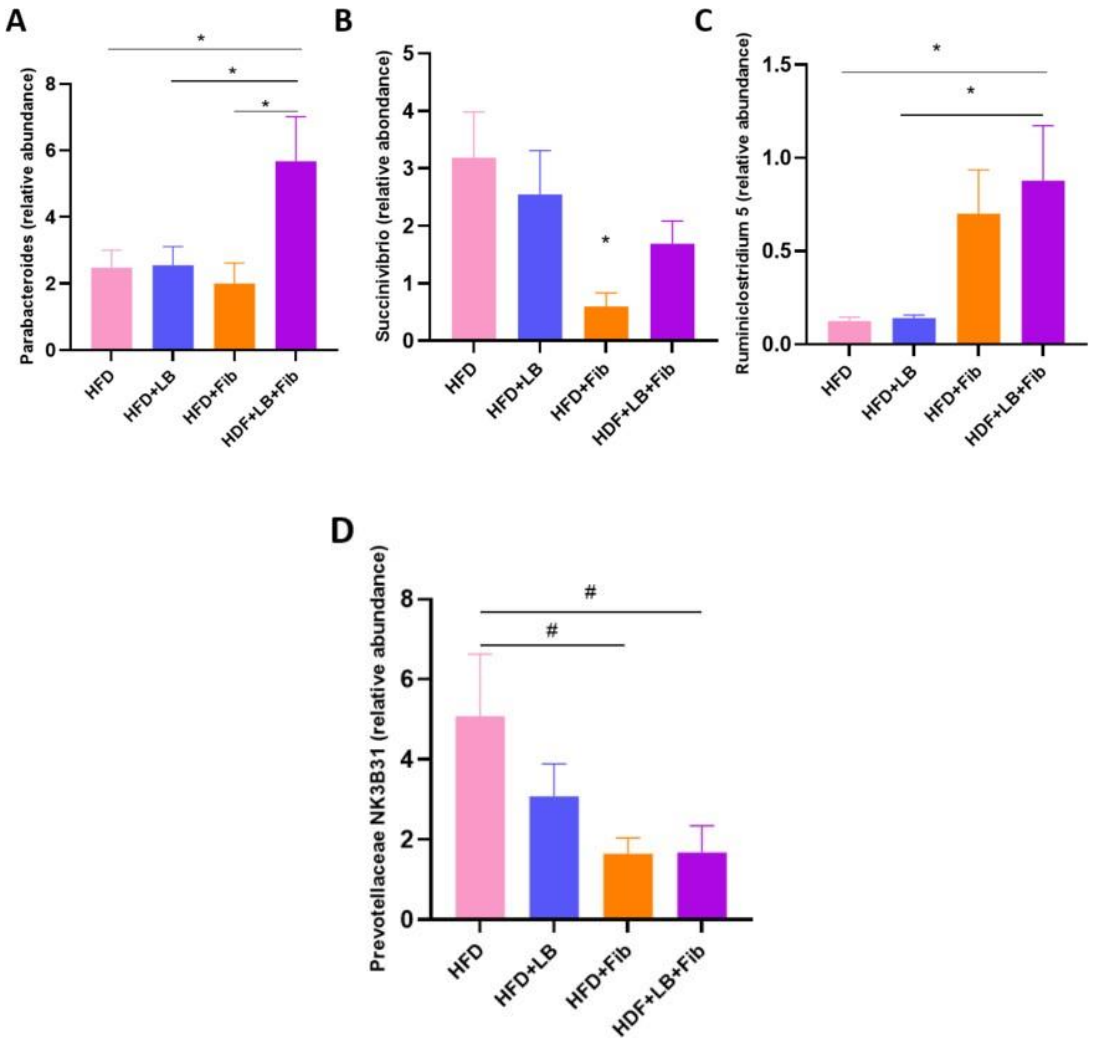

Figure 9. Genus-level analysis - Extended error bar plot identifying significantly different genera between the four dietary intervention groups at T12 (A-C), and the reduction observed in *Prevotellaceae* NK3B31 group at T2 (D). (Dietary intervention: HFD – Pink, HFD+LB – Blue, HFD+Fibre – Orange, HFD+LB+Fib – Purple). Significant difference was calculated using ANOVA followed by Original FDR method of Benjamini and Hochberg multiple comparisons test using GraphPad PRISM. P = 0.06 (#), P < 0.05 (*).

5.5 Discussion

Metabolic syndrome (MetS) is increasingly viewed as a chronic inflammatory disease, where changes in the gut microbiome contribute to disease development,

including obesity, type-2 diabetes, cardiovascular disease and non-alcoholic fatty liver disease (NAFLD) [288]. Numerous studies have suggested that the gut microbiome plays a major role in the development of fat mass and homeostatic control of energy [124, 230, 289, 290, 302] and subsequently, in humans, metabolic syndrome has been associated with alterations in the gut microbiota composition, most of which are caused by diet [292, 303, 304]. Additionally, societal changes in dietary habits, in particular the increased consumption of processed foods, which lack dietary fibre, are thought to negatively impact the gut microbiota composition and subsequently contribute to the increased occurrence of chronic inflammatory diseases, including MetS [293, 305]. Increased dietary fibre intake, in which fibre fermentation by the gut microbiota results in the production of SCFA, has been shown to have important effects on host health [306]. Additionally, it has also been reported that higher faecal SCFA concentrations have been associated with gut microbiome dysbiosis and obesity [307]. Furthermore, supplementation with probiotics may restore the composition of the gut microbiome [146]. In particular, *Lactobacillus mucosae* DPC 6426, has been previously shown to positively impact the composition of the gut microbiota *in vivo* in ApoE-deficient mice, which are prone to the development lipid-rich pro-inflammatory atherosclerotic plaque [1]. Furthermore, that study also found that supplementation with *Lb. mucosae* DPC 6426 significantly changed the composition of the microbiota in the caecal content, resulting in significant reductions in *Clostridiaceae* ($p < 0.05$), *Peptococcaceae* ($p < 0.001$) and *Staphylococcaceae* (< 0.01) compared to the un-supplemented controls and supplementation also led to an increase in *Prevotellaceae* and *Prevotella* at family and genus levels, respectively, compared to the un-supplemented mice [1].

This current study investigated the effects of daily oral supplementation of *Lb.*

mucosae DPC 6426, at a minimum concentration of 10^{10} CFU/g/day, and fibre, singly and in combination on the gut microbiome composition and faecal short chain fatty acid concentrations in a previously established porcine model of MetS (Chapter 4).

Short-chain fatty acid analysis indicated that there were no significant changes observed between the four dietary intervention groups at T12. In a recent study by Oliver *et al,* [308], the authors indicated that although short term (two weeks) high fibre intake resulted in changes to the gut microbiome composition, there were no significant changes observed in the abundance of SCFAs [308]. Furthermore, in a study by Alexander *et al.* [309], the fermentation of dietary fibre results was reported to result in the production of SCFAs that positively affect the glycaemic response, satiety and weight loss, whilst also decreasing biomarkers associated with inflammation, and improved intestinal health [309]. The results of the current study indicated the supplementation with *Lb. mucosae* DPC 6426 and fibre in combination act independently of faecal SCFA on risk factors associated with MetS.

There were no significant changes observed at phylum level at T0, T2, T6 and T12 in any of the four dietary intervention groups. In a study by Tomas *et al.* [310], in which mice were fed a high-fat diet for 30 days, alterations in the gut microbiota were reported, including significant increases observed in the abundance of *Firmicutes, Proteobacteria* and *Verrucomicrobia* and a reduction in the abundance of *Bacteroidetes,* indicating that obesity may be associated with alterations to the gut microbiota composition [310]. Nobel *et al.* [311] reported a strong correlation between dietary fibre intake and the relative abundance of *Firmicutes* in the human gut. Furthermore, the authors also reported a significant inverse correlation between dietary fibre and *Proteobacteria* [311]. However, in the current study,

there were no significant differences observed in the relative abundance of *Firmicutes* and *Proteobacteria* across the four dietary intervention groups.

At family level, there were no significant differences observed at T2 and T6, however at T12, *Porphyromonadaceae* was significantly increased in the HFD+LB+Fib group compared to the other three dietary intervention groups, and there was a trend towards significance in *Ruminococcaceae* in the HFD+Fib group compared to the HFD and HFD+LB+Fib groups ($p = 0.06$).

At genus level, there were no significant differences observed at T2 and T6, however there were three significant changes observed at T12. *Parabacteroides* was increased in the HFD+LB+Fib group compared to the other three groups ($p < 0.05$), while *Succinivibrio* was significantly decreased in the HFD+Fib group only ($p < 0.05$) and *Ruminiclostrodium* 5 was significantly increased in the HFD+LB+Fib group compared to the HFD, HFD+LB and HFD+Fib groups ($p < 0.05$). Additionally, there was a trend towards significance observed at T2 in *Prevotellaceae* NK3B31 group in HFD+Fib and HFD+LB+Fib compared to HFD ($p = 0.06$). In a previous study by Yamamura *et al.* [312], the relative abundance of *Ruminococcus* was found to be positively associated with faecal SCFA concentration and in particular, *Ruminiclostridium* was positively associated with faecal acetate concentrations [312]. However, the increase observed in the relative abundance of *Ruminiclostridium* 5 in the current study was moderate and could explain, in part, why there were no significant differences observed in the concentrations of faecal SCFA in any of the four dietary intervention groups. Further studies need to be carried out to elucidate the link between the relative abundance of specific gut microbiota and their effects on the concentrations of faecal SCFAs. Furthermore, a study by Tavella *et al.* [313], in which the link between abdominal fat and the gut

microbiome composition was investigated in old age in a cohort of elderly Italians, the authors hypothesised that increased amounts of *Porphyromonadaceae,* along with *Christensenallaceae* and *Rikenellaceae,* may play a protective role in metabolic diseases which are associated with abdominal organ fat [313]. In this current study, *Porphyromonadaceae* was significantly increased in the HFD+LB+Fib group, which may also explain the significant decrease observed in the percentage weight gain at T12 in this group. *Parabacteroides* has been reported to be a beneficial gut bacteria, in which administration has been shown to affect experimental murine colitis [314], as well as mitigating obesity and metabolic dysfunction in *ob/ob* and HFD fed mice [315], however, it has also been negatively associated with IBD, in particular there is evidence suggesting that *Parabacteroides distasonis* may potentially contribute to IBD, [316] and was the most abundant gut bacteria seen in Crohn's disease [317].

On the other hand, there was a significant decrease observed in the abundance of *Succinivibrio* in the HFD+Fib group only. In a study by Murugesan *et al.* [318], it was demonstrated that *Succinivibrio* spp. was present in higher abundance in normal weight children compared to obese children [318]. Additionally, it has been shown that *Succinivibrio* spp. are involved in the regulation of energy balance in normal weight children [318] and this may explain, in part, the significant decrease observed in the percentage weight gain in the animals that received supplementation *Lb. mucosae* DPC 6426 and fibre in combination. In a recent study by Iljazovic *et al.* [319], it was demonstrated that colonisation of mice with a member of the *Prevotella* genus resulted in heightened intestinal inflammation [319]. Furthermore, *Prevotella* has been associated with a number of host diseases, including rheumatoid arthritis, metabolic diseases and low-grade inflammation [320]. In this current study, there were no significant differences in the relative abundance of *Prevotella* 9 and *Prevotellaceae* NK3B31 group across the four dietary intervention groups.

In conclusion, results of this study suggest that the synbiotic combination of dietary fibre and *Lb. mucosae* DPC 6426 work in combination leading to an increased anti-inflammatory gut microbiota, indicating that the synbiotic intervention could be a promising, novel therapeutic approach for the treatment of the alterations in the gut microbiota composition as a result of MetS. However, further investigations are required to identify and understand the exact mechanisms by which this combination therapy addresses these alterations.

5.6 Acknowledgements

We thank Dr. Cara Hueston for technical support; MS-Omics in SCFA analysis; Vincent Mehigan and Kerry Carlile for technical support with animal husbandry and care. We acknowledge the Teagasc Moorepark sequencing team, Dr. Paul Cotter, Dr. Fiona Crispie, Laura Finnegan and Amanda Brechon. The authors are supported in part by Science Foundation Ireland in the form of a centre grant for APC Microbiome Ireland Grant No. SFI/12/RC/2273-P2.

Supplementary Material

Supplementary Table 1: Concentration of SCFA compounds detected in only a few samples.

SCFA Compound	Formic Acid	4-methyl-pentanoic acid	Heptanoic acid
	mM	mM	mM
HFD			
Pig 1	<LOD	0.011	0.004
Pig 2	<LOD	<LOD	<LOD
Pig 3	0.09	0.009	0.003
Pig 4	<LOD	<LOD	<LOD
Pig 5	0.11	<LOD	0.003
HFD+LB			
Pig 1	0.12	<LOD	<LOD
Pig 2	0.09	0.011	<LOD
Pig 3	0.10	<LOD	0.003
Pig 4	<LOD	<LOD	0.008
Pig 5	0.09	<LOD	<LOD
Pig 6	<LOD	<LOD	0.003
HFD+Fib			
Pig 1	0.09	<LOD	<LOD
Pig 2	0.09	<LOD	<LOD
Pig 3	0.08	<LOD	<LOD
Pig 4	0.09	<LOD	0.007
Pig 5	<LOD	<LOD	0.021
Pig 6	<LOD	<LOD	0.008
HFD+LB+Fib			
Pig 1	0.08	<LOD	<LOD
Pig 2	0.11	<LOD	<LOD
Pig 3	0.10	<LOD	<LOD
Pig 4	0.08	<LOD	0.027
Pig 5	<LOD	<LOD	0.003
Pig 6	0.08	<LOD	<LOD

< LOD – Below limit of detection.

Supplementary Table 2: Concentration of SCFA compounds detected in all samples.

SCFA Compound	Acetic Acid	Propionic Acid	2-methyl-propionic acid	Butanoic acid	3-methyl-butanoic acid	Pentanoic acid	Hexanoic acid
	mM	mM	mM	mM	mM	mM	mM
HFD							
Pig 1	24.9	9.82	0.80	5.38	0.71	1.31	0.217
Pig 2	22.1	12.80	0.50	3.44	0.38	1.14	0.053
Pig 3	19.8	13.82	0.88	4.99	0.81	1.64	0.136
Pig 4	16.6	10.02	0.38	2.74	0.30	0.62	0.034
Pig 5	19.0	10.40	0.77	4.51	0.68	1.16	0.131
HFD+LB							
Pig 1	18.9	11.72	0.73	4.10	0.62	0.88	0.057
Pig 2	29.7	11.42	0.69	6.70	0.63	1.21	0.132
Pig 3	20.7	14.94	0.61	4.54	0.53	1.52	0.112
Pig 4	24.2	21.84	0.47	3.74	0.41	2.25	0.089
Pig 5	19.8	15.02	0.48	3.49	0.38	1.01	0.031
Pig 6	17.5	14.28	0.53	4.04	0.47	1.60	0.090
HFD+Fib							
Pig 1	19.3	10.03	0.85	2.52	0.78	0.94	0.099
Pig 2	19.0	13.32	0.37	3.81	0.32	1.44	0.075
Pig 3	23.5	7.93	0.50	3.65	0.41	0.72	0.074
Pig 4	18.4	12.28	0.68	3.68	0.65	1.29	0.160
Pig 5	20.1	11.41	0.86	5.82	0.79	1.64	0.178
Pig 6	25.2	12.27	1.00	5.26	0.99	1.78	0.209
HFD+LB+ Fib							
Pig 1	16.0	8.84	0.47	2.72	0.42	1.27	0.083
Pig 2	15.8	9.33	0.58	2.60	0.52	0.95	0.082
Pig 3	19.8	11.48	0.78	4.45	0.70	1.13	0.083
Pig 4	21.7	15.10	0.66	3.56	0.53	1.34	0.155
Pig 5	34.6	22.69	0.35	5.27	0.29	1.63	0.118
Pig 6	23.2	17.24	0.46	3.34	0.39	0.97	0.036

Supplementary Figure 1: Phylum level analysis – response to dietary intervention

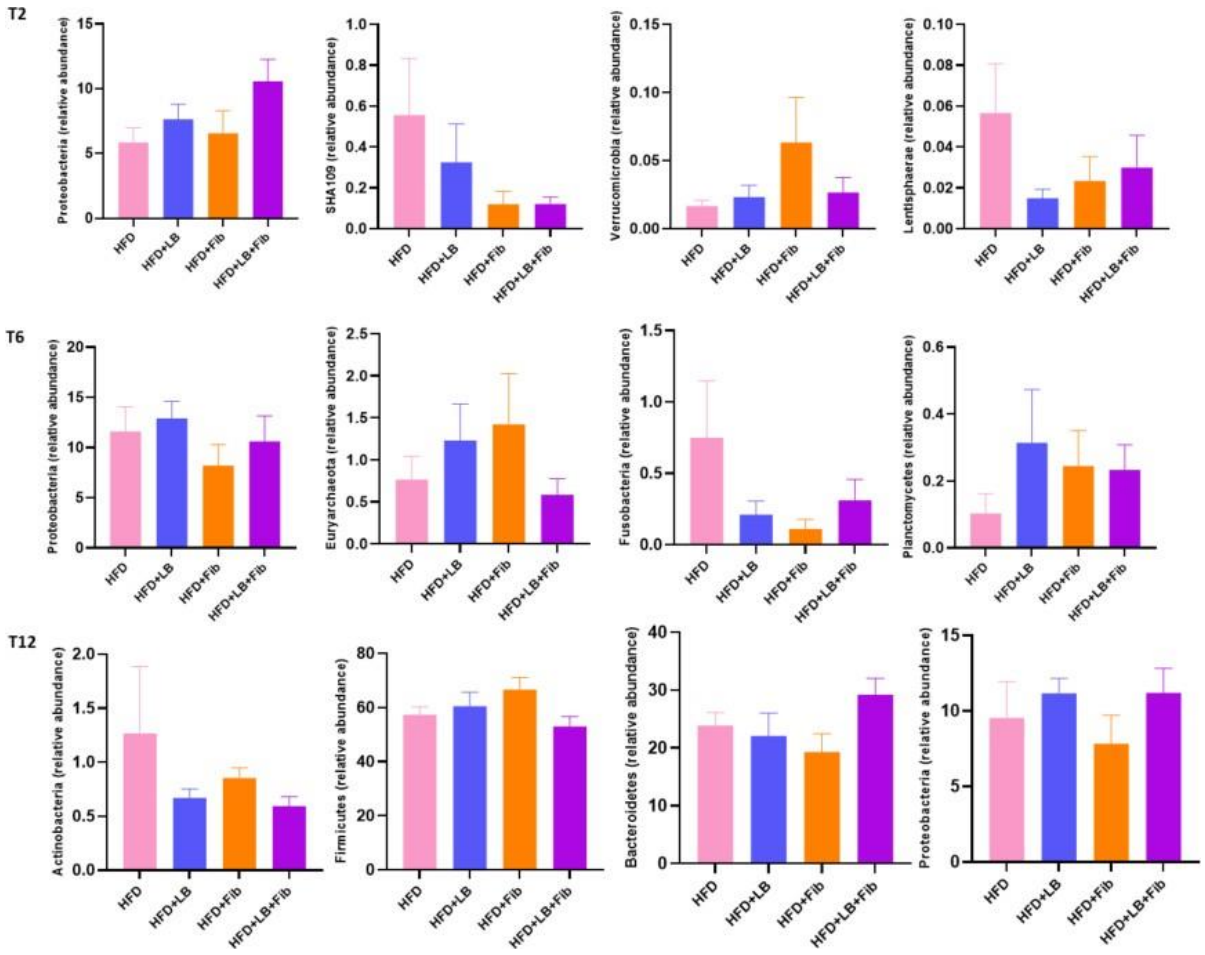

Supplementary Figure 1: Extended error bar plots showing increases and decreases observed between T2, T6 and T12 at phylum level in response to dietary intervention. (Dietary intervention: HFD – Pink, HFD+LB – Blue, HFD+Fib – Orange, HFD+LB+Fib – Lavender). Significant difference was calculated using ANOVA followed by Original FDR method of Benjamini and Hochberg multiple comparisons test using GraphPad Prism.

Chapter 6.
General Discussion

With the increased adoption of westernised dietary patterns and lifestyles, the incidence of Metabolic Syndrome (MetS) has increased worldwide, with its worldwide prevalence ranging between 10% and 84% depending on age, race, gender, ethnicity and definition of MetS [198]. It is estimated that approximately 20-25% of the global adult population have MetS and are thus three times as likely to have a heart attack or stroke compared with those without MetS [321]. An opportunity for the development of new therapeutic strategies, through the use functional foods and probiotics, has arisen due to low consumer compliance in relation to dietary recommendations and the expense and negative side effects associated with drug therapy for many consumers. Additionally, increased consumer acceptance of foods with additional health benefits has led to the opportunity for functional foods in the area of heart health. Furthermore, increased consumption of processed foods, in dietary fibre, has resulted in reduced gut microbiota diversity and decreased abundance of beneficial bacteria, and has also been linked with the increased risk of developing a variety of diseases associated with MetS, including obesity, heart disease, and diabetes [294]. Studies have shown that increasing dietary fibre intake has resulted in the improvement of many of the risk factors associated with MetS, including reduction in body fat and insulin resistance [295]. In addition to the use of functional foods and increased fibre intake, probiotics have been proposed as an approach to target the gut microbiota alterations which have been associated with a number of disease states, by restoring the composition of the gut microbiome back to its "healthy" state prior to disease onset and through the introduction of beneficial functions to the gut microbiota communities, resulting in the improvement or prevention of inflammation and other disease phenotypes [146].

In Chapter 1, the need for appropriate pre-clinical models, the link between the gut microbiota and cardiovascular disease and the use of probiotics in the treatment of

cardiovascular disease is discussed. Pre-clinical models are essential for studying and understanding the underlying mechanisms of disease development as well as in the use of developing therapeutic strategies in order to treat disease. The development of suitable animal models has been shown to be a very challenging task for scientists and there is still currently no “gold-standard” animal model which exactly replicates cardiovascular disease in humans. Therefore, when moving from the lab bench to the bedside, it is essential to test procedures and treatment methods in the most relevant animal model that will result in the highest reproducible results. With the constant emergence of evidence which points to the association between alterations in the gut microbiota composition and microbial metabolites with the development of cardiovascular disease, the use of probiotic interventions provide a promising alternative therapeutic strategy in cardiovascular disease risk prevention. However, further investigations, including the use of more translatable pre-clinical animal models, large multicentre trials, combined with information on doses and frequency of administration and specific strains investigated must be carried out in order to generate more convincing data and confirm the hypotheses regarding probiotic use and risk prevention.

Growing scientific evidence has indicated that the gut microbiome plays an important role in the physiological functions of the host, and dysbiosis of the gut microbiota has been shown to cause physiological changes resulting in an increased risk of developing MetS [322]. Evidence of the link between the gut microbiome and MetS first emerged in 2007 following studies carried out in rodents [323] and humans [324], which showed that the consumption of a high fat diet resulted in defects in the intestinal barrier which in turn facilitated the transfer of intestinal luminal contents, such as food antigens, bacteria and their by-products, as well and

LPS, into circulation, resulting in low-grade inflammation causing insulin resistance [325]. Another study carried out by Backhed *et al* [124] demonstrated that conventionalisation of adult germ-free mice with normal microbiota from lean mice resulted in a 60% increase in body fat and insulin resistance within two weeks regardless of reduced food intake [124]. Furthermore, studies carried out in the leptin gene-deficient obese mouse model (*ob/ob*) have shown that *Firmicutes* and *Bacteroidetes* are the predominant bacterial species in the gut [326]. Alterations in the ratio of *Firmicutes* and *Bacteroidetes* results in a change in fermentation patterns and may explain weight gain [326], and it also seems that alterations in the function and composition of the gut microbiota populations is also linked with the development of atherosclerosis [327]. Moreover, in a study by Turnbaugh *et al.* [324], the authors showed that individuals with a gut microbiome that is more efficient at extracting energy from the diet, or those who possess an increased ability to promote adiposity, caused by changes in host gene expression and metabolism, may possess a predisposition to the development of obesity [324], and this hypothesis predicts that lean and obese individuals have significantly different gut microbiota compositions. The proposed mechanisms by which the gut microbiota may contribute to obesity and MetS include energy harvest from the diet, fat deposition promotion and by triggering systemic inflammation [328]. As a result of the emerging evidence linking the gut microbiota and incidence of MetS, the gut microbiota has emerged as a target for new therapeutic strategies such as the use of probiotics and prebiotics.

Probiotics have been defined by the FAO/WHO as “live microorganisms, which when administered in adequate amounts, confer a health benefit on the host” [144]. The use of freeze-drying is considered an important and effective technique to maintain the viability, integrity and functionality of probiotic cultures, whilst also

playing a key role in the stabilisation of heat sensitive products, such as lactic acid bacteria (LAB), therefore it is a commonly used approach for the preservation of probiotic strains. One downside of the freeze-drying process is that it can result in a proportion of cell viability loss as a result of ice crystal formation resulting in irreversible damage to the cell [179]. To minimise the loss in viability, a variety of cryoprotectants have been used in order to give freeze-dried bacterial strains additional structural support, as aiding in the rehydration process, ultimately helping in maintaining the viability of the probiotic strain during frozen storage, resulting in a higher level of survival of the freeze-dried bacterial strain [179].

Lactobacillus spp. are known facultative anaerobes, however there are several *Lactobacillus* species that are known to be unable to thrive in aerobic conditions. In Chapter 2, it was important to investigate whether *Lactobacillus mucosae* DPC 6426, an exopolysaccharide (EPS)-producing LAB strain which was originally isolated from bovine faecal samples at Teagasc Moorepark Food Research Centre (MRFC), Fermoy, Cork [172], could grow optimally under aerobic conditions. This strain demonstrated poor tolerance to and low growth under aerobic conditions. Therefore, due to the strains poor tolerance to aerobic conditions, it was determined that anaerobic conditions are required in order to ensure optimal growth and EPS production. Additionally, it was seen that the use of extended incubation times, 24 hours for both 10ml and 200ml inoculations, and ~60 hours for 5L inoculations, for the cultivation of the bacterial strain, resulted in cell death and in turn sub-optimal CFU/ml values, and are likely attributed to the production and accumulation of metabolic by-products such as lactic acid and acetic acid [179, 180]. It was also observed that a 48 hour freeze-drying program (shelf freeze temperature: -45°C; condenser set point: -84°C and vacuum set point; 0.02mBar), using the Labconco™ FreeZone™ 12L -84°C Console Freeze dryer with

stoppering tray dryer (Labconco Corporation, Kansas, USA), was insufficient in terms of fully drying the entire bacterial culture and cryoprotectant mix. Based on the results from the methods investigating aerobic conditions (method 1) and extended incubation periods (methods 1 and 2) as well as the results from both freeze-drying methods, a method was developed which resulted in high concentrations of between 10^{10} and 10^{11} CFU/g of freeze-dried powder, and included the use of a 1% inoculum, anaerobic incubation of the 10ml and 200ml inoculations for 6.5 hours, and ~16-18 hours for the 5L inoculations, combined with the use of 10% trehalose as a cryoprotectant and an extended freeze-drying program of between 90-95 hours. Significant changes were seen with regards to the concentrations of cells when the optimised cultivation method (Method 3) and freeze-drying method (Method 2) were used in combination. In order to optimise culture viability during fermentation, it was important to maintain anaerobic conditions through the growth phase. As seen in Method 1, the use of aerobic conditions during cultivation resulted in sub-optimal growth of the bacterial strain. Furthermore, the use of 10% trehalose as a cryoprotectant during freeze-drying and subsequent storage at -30°C, for both short term (1 and 2 weeks) and long term (1 month) storage, was shown to be an effective method for maintaining culture viability and aiding in the survival of the freeze-dried strain during sub-zero storage.

A growing body of evidence has demonstrated the beneficial health effects of probiotic supplementation and could be considered as a therapeutic option for the treatment of cardiovascular disease. It has been shown that elevated levels of serum cholesterol, in particular LDL-cholesterol, is a known risk factor for the development of cardiovascular disease and probiotic bacteria have been studied as a therapeutic approach to improve serum lipid profiles. It has been shown that probiotic bacteria

which possess bile salt hydrolase activity have potential to reduce serum cholesterol levels through the deconjugation of bile acids and increasing their excretion [114]. In Chapter 3, the efficacy of *Lactobacillus mucosae* DPC 6426 was investigated in humans for its cholesterol lowering effects. *Lactobacillus mucosae* DPC 6426 had previously been shown to alter the composition of the bile pool and immune system tone [329], and therefore has potential as a therapeutic for cardiovascular disease. The main aim of the study was to investigate the effect of daily dietary supplementation of *Lactobacillus mucosae* DPC 6426 on cholesterol levels and on the gut microbiota composition over a 12-week period in healthy, mildly hypercholesterolaemic ($\geq$ 5.5 mmol/L and < 8 mmol/L) adults using a randomised, double-blind, placebo controlled clinical trial, carried out by Atlantia Food CRO. Results of blood lipid analysis indicated that there were no statistically significant changes observed between treatment groups (active and placebo) from baseline (week 0 (V2)) to visit 5 (week 12), baseline to visit 4 (week 8), or baseline to visit 3 (week 4) for total cholesterol, LDL-cholesterol, HDL-cholesterol or total triglyceride concentrations. Analysis of the change in total cholesterol concentrations revealed that, on average, total cholesterol concentrations at baseline were slightly higher in the placebo group compared to the active group, however it was not considered statistically significant ($p = 0.054$). Additionally, analysis of the gut microbiota indicated no significant differences observed between the treatment groups at phylum, family and genus levels. Dietary supplementation of *Lactobacillus mucosae* DPC 6426, at a minimum concentration of 10^9 CFU/g daily, did not significantly alter the gut microbiota between baseline and the end of the study. Furthermore, analysis of both plasma and urine metabolites showed no clear separation between treatment groups and based on the permutation test statistic, it was also not statistically significant ($p = 0.6615$ for plasma metabolites and $p = 0.385$ for urine

metabolites). Four plasma metabolites, kynurenic acid, xanthurenic acid, kynurenine and tyrosine, were identified to be present in higher concentrations in the placebo group, and additionally, L-valine was >1.5 fold higher in the probiotic group compared to the placebo group, however this was not statistically significant ($p > 0.05$). In a study by Lund *et al.* [330], the authors showed that higher levels of plasma kynurenine, 3-hydroxykynurenine (HK), quinolinic acid (QA), the kynurenine-tryptophan ratio (KTR) and the ratio of HK to xanthurenic acid (HK/XA) were identified in heart failure patients compared to the control groups [330]. It was also shown that QA, HK, HK/XA and KTR were associated with increased mortality in patients with heart failure, whilst HK and HK/XA demonstrated weak associations with coronary artery disease (CAD) [330]. Furthermore, Mohorko *et al.* [331] demonstrated that changes in the blood concentrations of leucine, tyrosine and phenylalanine were associated with obesity and insulin resistance, and have proposed the use of elevated serum levels of cysteine and tyrosine as early biomarkers in asymptomatic patients at increased risk of developing MetS [331]. In this study there were slight decreases observed in the concentrations of leucine and tyrosine between V2 and V5 for the probiotic group, with slight increases being observed in the placebo group. Furthermore, there was also a slight increase observed in the concentration of phenylalanine in both the treatment and placebo groups, however this increase was not significant. Moreover, in a study by Mitrega *et al.* [332], the authors provided evidence of the anti-arrhythmic activity of L-valine in decreasing incidence of arrhythmias in a model of induced ischemia and reperfusion, and have shown the potential role of L-valine as an additional therapy for cardiovascular diseases combined with an increased risk of arrhythmias [332]. In this study, there was an increase in the concentration of L- valine between V2 and V5 in the treatment group, but it was not significant (p

> 0.0.5). Three urine metabolites, indole-3-acetic acid, indole-3-acetamide and 3-hydroxyanthranilic acid, were identified to be present in higher concentrations in the placebo group compared to the active group but without statistical significance. Dou *et al.* [333] carried out a study which investigated the cardiovascular effects of indole-3-acetic acid in patients with chronic kidney disease (CKD) and found that serum indole-3-acetic acid may act as a predictor of cardiovascular events and mortality in patients with CKD. Additionally, the authors also demonstrated *in vitro* that indole-3-acetic acid resulted in the induction of endothelial inflammation and oxidative stress and the activation of an inflammatory pathway [333]. Furthermore, it has been shown that 3-hydroxyanthranilic acid levels in CKD patients have been associated with the CC-chemokine family, markers of macrophage inflammation in atherosclerotic lesions [334]. In contrast to the results of the pre-clinical animal trial on the ApoE-deficient mouse model [1], daily supplementation with *Lactobacillus mucosae* DPC 6426, at a minimum concentration of 10^9 CFU/g, did not significantly alter the blood lipid profiles or the gut microbiota of mildly hypercholesterolaemic adults. The negative effect of the probiotic supplementation on blood lipids in the human study may be as a result of the dose use (10^9 CFU/g daily) and may also have been insufficient to result in significant changes to the gut microbiota composition. Results of this study warrant further investigations using larger pre-clinical animal models and increased concentrations of *Lactobacillus mucosae* DPC 6426 to verify the efficacy of *Lb. mucosae* DPC 6426.

In order to understand and explain the pathophysiology of MetS in humans, an animal model of similar scale and physiology that mimics the complex nature of MetS is essential. In Chapter 4, we confirmed in our porcine model the cardiometabolic features of heart failure with preserved ejection fractions (HF-pEF) which was first described by Schwarzl *et al.* [202]. Furthermore, it was also shown

that this model demonstrated fatty liver disease and early insulin resistance. With the growing body of scientific evidence supporting the gut microbiome as a key player between the diet and biochemical and cardiometabolic changes which characterise obesity, insulin resistance, hyperlipidaemia, hypertension and HF-pEF [196, 217], identifying the microbial changes which occur during MetS development in a human scale porcine model may offer additional insight into the underlying mechanisms of MetS and the opportunity for assessment of additional therapeutic approaches for future gut microbiome targeted interventional studies. The changes observed in body weight, blood pressure, and insulin and glucose levels in MetS Landrace pigs were similar to those observed in other porcine models of obesity in other pig breeds, however, both lipid and insulin levels were higher in the current model [220-222]. As seen in humans with MetS, serum levels of total cholesterol, LDL-cholesterol and triglycerides are all increased [223], and in the current porcine model these lipids were significantly elevated compared to the control animals. Additionally insulin resistance has been identified as a risk factor for the development of MetS, and in a study carried out by Ghasemi *et al.* [335] the authors suggested that the homeostatic model of assessment of insulin resistance (HOMA-IR) cut off was 2.17 for males and 1.85 for females [335], and in this porcine model of MetS, HOMA-IR was significantly elevated compared to the control animals, indicating the onset of insulin resistance. Furthermore, the development of non-alcoholic fatty liver disease (NAFLD) is an established feature of human MetS [225, 336], and in MetS pigs fed a high fat, sugar and salt diet (HFD) over a 12-week period, an increased liver weight was observed and histopathology identified excess hepatic lipid deposition compared to the control animals. This combination of increased hepatic lipid deposition and dyslipidaemia in the MetS pigs mimics what has been observed in humans with MetS-associated NAFLD [226]. Moreover, a reduction in α-diversity and specific

microbiota changes were observed at phylum, family and genus levels in this model. In particular, this model displayed increased abundance of pro- inflammatory bacteria coupled with a significant decrease in enteroprotective bacteria, as well as a reduction of short-chain fatty acid-producing bacteria, namely *Lachnospiraceae*, *Rikenellaceae*, and *Akkermansia*. Together, these results suggest that diet- and mineralocorticoid-induced development of MetS in pigs leads to temporal gut microbiome changes that mimic significant gut microbiota composition alterations in human cardiometabolic disease. This clinical scale model may facilitate the design of future interventional studies to investigate the casual relationships between altered gut microbiota populations and cardiometabolic syndrome at systemic and organ levels.

The use of the porcine model of MetS and HF-pEF has provided a way to bridge the gap between rodent models, most of which require genetic alterations, and humans, and also the opportunity to investigate the efficacy of specific therapeutics, such as prebiotics, probiotics or synbiotics, and to determine the optimum dose required to elicit the desired effect of the therapeutic.

In Chapter 5, using the previously established porcine model of MetS (Chapter 4) we investigated the effect of daily oral supplementation of *Lactobacillus mucosae* DPC 6426 (at a minimum concentration of 10^{10} CFU/g) and fibre, singly and in combination on the composition of the gut microbiome over a 12-week period of high fat diet feeding. Analysis of the gut microbiome composition indicated that there were no significant differences observed between the four dietary intervention groups, HFD. HFD+LB, HFD+Fib and HFD+LB+Fib, at T0, T2, T6 and T12 at phylum level, indicating that supplementation did not have a significant effect on the composition of the gut microbiota. In a recent study by Singh *et al.* [337], it was found that both *Proteobacteria* and *Firmicutes* were in higher abundance in gut

microbiome of mice fed a high-fat diet for eight weeks compared to the normal diet controls [337]. Furthermore in a study by Tomas *et al.* [310], a reduction in the abundance of *Verrucomicrobia* and *Bacteroidetes* was found in mice fed a high-fat diet for 30 days, suggesting that obesity may be associated with alteration in the gut microbiota composition [310]. At family and genus levels, there were no significant differences observed between the four dietary intervention groups at T2 and T6. At T12 *Porphyromonadaceae* was significantly increased in the HFD+LB+Fib group only ($p < 0.05$) compared to the other three intervention groups. Tavella *et al.* [313] have suggested that increased abundances of *Porphyromonadaceae* may act in a protective role in abdominal organ fat associated metabolic diseases [313]. At genus level, there were three significant alterations observed at T12, *Parabacteroides* and *Ruminiclostridium* 5 were significantly increased in the HFD+LB+Fib group ($p < 0.05$) and *Succinivibrio* was significantly decreased in the HFD+Fib group only ($p < 0.05$). Additionally, although not significant, *Prevotellaceae* NK3B31 was shown to be decreased in the HFD+Fib and HFD+LB+Fib groups compared to the HFD group ($p = 0.06$). In a study by Yamamura *et al.* [312], which investigated the associations between the gut microbiota, dietary intake, and serum SCFA with faecal SCFA, the authors indicated that the relative abundance of *Ruminococcus* was positively associated with faecal SCFA concentrations, and in particular, *Ruminiclostridium* abundance was positively associated with faecal acetate concentrations, however dietary intake was not found to be associated with faecal SCFA concentrations [312]. Furthermore, this study highlighted the potential use of faecal SCFAs as an indicator of the state of the gut microbiome health [312]. However, these associations fail to explain the lack of significant changes observed in the concentrations of faecal SCFAs in our study, and further investigations need to be carried out in order to understand the link between the abundance of specific gut

microbiota and their effects on faecal SCFAs. *Succinivibrio* spp. has been shown to be present in higher amounts in normal weight children compared to their obese counterparts, and it has also been shown that *Succinivibrio* spp. have been involved in energy balance regulation in normal weight children [318]. Furthermore, increased *Prevotella* abundance has been linked with a number of host diseases, including metabolic disease and low-grade inflammation, which is a considered a marker of MetS [320].

Dietary intervention with *Lb. mucosae* DPC 6426 and fibre, singly or in combination appeared to have no significant effects on the concentrations of faecal SCFAs at T12. Despite some of the faecal SCFAs appearing increased in the HFD+Fib and HFD+LB+Fib groups, none were statistically significant. In a recent study by Oliver *et al.* [308] it was seen that short term (2 weeks) increased dietary fibre intake resulted in alterations to the gut microbiota compositions, but did not significantly alter abundance of faecal SCFAs [308], however, given that our study was carried out over a 12-week period, this may explain the increased concentrations observed in the HFD+Fib and HFD+LB+Fib groups.

Overall results of this study appear to indicate that supplementation of *Lb. mucosae* DPC 6426 in combination with fibre has an effect on the existing anti-inflammatory gut microbiota. Furthermore, these results show combination therapy as a promising novel therapeutic approach for the treatment of gut microbiota composition alterations in MetS, however, extensive investigations are needed to identify and understand the mechanisms by which combination therapy mitigate these alterations.

Further investigations are needed in order to advance the causative links between alterations in gut microbiota composition and development and progression of MetS-associated risk factors. Investigations should include the use of larger pre-clinical

animal models which would result in more translatable and reproducible results with regards to the development of novel therapeutic strategies as well as the verification of the effects of novel strategies, such as probiotics and combination therapies, which have only been assessed in pre-clinical rodent models prior to human clinical trials.

This thesis contributes to the current knowledge on metabolic syndrome, the underlying mechanisms of the disease, and the potential advantages of using probiotics and combination therapies which target the gut microbiome and have a positive impact on the associated risk factors for the development of metabolic syndrome.

Bibliography

1. London, L.E., et al., *Exopolysaccharide-producing probiotic Lactobacilli reduce serum cholesterol and modify enteric microbiota in ApoE-deficient mice.* J Nutr, 2014. **144**(12): p. 1956-62.
2. Stewart, J., G. Manmathan, and P. Wilkinson, *Primary prevention of cardiovascular disease: A review of contemporary guidance and literature.* JRSM Cardiovasc Dis, 2017. **6**: p. 2048004016687211.
3. Xu, H., et al., *The gut microbiota and its interactions with cardiovascular disease.* Microb Biotechnol, 2020. **13**(3): p. 637-656.
4. Tang, W.H., T. Kitai, and S.L. Hazen, *Gut Microbiota in Cardiovascular Health and Disease.* Circ Res, 2017. **120**(7): p. 1183-1196.
5. WHO. *The challenge of cardiovascular disease – quick statistics*. 2016; Available from: https://www.euro.who.int/en/health-topics/noncommunicable-diseases/cardiovascular-diseases/data-and-statistics.
6. Zhou, W., et al., *Implication of Gut Microbiota in Cardiovascular Diseases.* Oxid Med Cell Longev, 2020. **2020**: p. 5394096.
7. Cannon, C.P., *Cardiovascular disease and modifiable cardiometabolic risk factors.* Clinical Cornerstone, 2007. **8**(3): p. 11-28.
8. Olshansky, S.J., et al., *A potential decline in life expectancy in the United States in the 21st century.* N Engl J Med, 2005. **352**(11): p. 1138-45.
9. Razak, F., et al., *Defining obesity cut points in a multiethnic population.* Circulation, 2007. **115**(16): p. 2111-8.
10. Chowdhury, B., H. Lantz, and L. Sjöström, *Computed tomography—determined body composition in relation to cardiovascular risk factors in Indian and matched Swedish males.* Metabolism, 1996. **45**(5): p. 634-644.

11. Chang, C.J., et al., *Low body mass index but high percent body fat in Taiwanese subjects: implications of obesity cutoffs.* Int J Obes Relat Metab Disord, 2003. **27**(2): p. 253-9.

12. Shabir, O., et al., *Preclinical models of disease and multimorbidity with focus upon cardiovascular disease and dementia.* Mech Ageing Dev, 2020. **192**: p. 111361.

13. Camacho, P., et al., *Large Mammalian Animal Models of Heart Disease.* J Cardiovasc Dev Dis, 2016. **3**(4).

14. Simon, F., A. Oberhuber, and H. Schelzig, *Advantages and Disadvantages of Different Animal Models for Studying Ischemia/Reperfusion Injury of the Spinal Cord.* European Journal of Vascular and Endovascular Surgery, 2015. **49**(6): p. 744.

15. Milani-Nejad, N. and P.M. Janssen, *Small and large animal models in cardiac contraction research: advantages and disadvantages.* Pharmacol Ther, 2014. **141**(3): p. 235-49.

16. Valdes, A.M., et al., *Role of the gut microbiota in nutrition and health.* BMJ, 2018. **361**: p. k2179.

17. Fan, Y. and O. Pedersen, *Gut microbiota in human metabolic health and disease.* Nat Rev Microbiol, 2021. **19**(1): p. 55-71.

18. Schiattarella, G.G., et al., *Diagnostics and therapeutic implications of gut microbiota alterations in cardiometabolic diseases.* Trends Cardiovasc Med, 2019. **29**(3): p. 141-147.

19. Tindall, A.M., K.S. Petersen, and P.M. Kris-Etherton, *Dietary Patterns Affect the Gut Microbiome-The Link to Risk of Cardiometabolic Diseases.* J Nutr, 2018. **148**(9): p. 1402-1407.

20. Novakovic, M., et al., *Role of gut microbiota in cardiovascular diseases.* World J Cardiol, 2020. **12**(4): p. 110-122.

21. Ahmad, A.F., et al., *The gut microbiome and cardiovascular disease: current knowledge and clinical potential.* Am J Physiol Heart Circ Physiol, 2019. **317**(5): p. H923-H938.

22. Lavelle, A. and H. Sokol, *Gut microbiota-derived metabolites as key actors in inflammatory bowel disease.* Nat Rev Gastroenterol Hepatol, 2020. **17**(4): p. 223-237.

23. McCarville, J.L., et al., *Microbiota Metabolites in Health and Disease.* Annu Rev Immunol, 2020. **38**: p. 147-170.

24. Koeth, R.A., et al., *Intestinal microbiota metabolism of L-carnitine, a nutrient in red meat, promotes atherosclerosis.* Nat Med, 2013. **19**(5): p. 576-85.

25. Wang, Z., et al., *Gut flora metabolism of phosphatidylcholine promotes cardiovascular disease.* Nature, 2011. **472**(7341): p. 57-63.

26. Tang, W.H., et al., *Intestinal microbial metabolism of phosphatidylcholine and cardiovascular risk.* N Engl J Med, 2013. **368**(17): p. 1575-84.

27. Dawber, T.R., G.F. Meadors, and F.E. Moore, Jr., *Epidemiological approaches to heart disease: the Framingham Study.* Am J Public Health Nations Health, 1951. **41**(3): p. 279-81.

28. Keys, A., et al., *The diet and 15-year death rate in the seven countries study.* Am J Epidemiol, 1986. **124**(6): p. 903-15.

29. Mozaffarian, D., et al., *Heart Disease and Stroke Statistics-2016 Update: A Report From the American Heart Association.* Circulation, 2016. **133**(4): p. e38-360.

30. Vilahur, G., et al., *Perspectives: The burden of cardiovascular risk factors and coronary heart disease in Europe and worldwide.* European Heart Journal Supplements, 2014. **16**(suppl_A): p. A7-A11.

31. Yusuf, S., et al., *Effect of potentially modifiable risk factors associated with myocardial infarction in 52 countries (the INTERHEART study): case-control study.* Lancet, 2004. **364**(9438): p. 937-52.

32. Canto, J.G., et al., *Number of coronary heart disease risk factors and mortality in patients with first myocardial infarction.* JAMA, 2011. **306**(19): p. 2120-7.

33. Killip, T., 3rd and J.T. Kimball, *Treatment of myocardial infarction in a coronary care unit. A two year experience with 250 patients.* Am J Cardiol, 1967. **20**(4): p. 457-64.

34. Antman, E.M., et al., *The TIMI risk score for unstable angina/non-ST elevation MI: A method for prognostication and therapeutic decision making.* JAMA, 2000. **284**(7): p. 835-42.

35. Khot, U.N., et al., *Prevalence of conventional risk factors in patients with coronary heart disease.* JAMA, 2003. **290**(7): p. 898-904.

36. Barrett-Connor, E.L., et al., *Why Is Diabetes Mellitus a Stronger Risk Factor for Fatal Ischemic Heart Disease in Women Than in Men?: The Rancho Bernardo Study.* JAMA, 1991. **265**(5): p. 627-631.

37. Willett, W.C.M.D., et al., *Relative and Absolute Excess Risks of Coronary Heart Disease among Women Who Smoke Cigarettes.* The New England Journal of Medicine, 1987. **317**(21): p. 1303-1309.

38. Forouhi, N.G. and N. Sattar, *CVD risk factors and ethnicity—A homogeneous relationship?* Atherosclerosis Supplements, 2006. **7**(1): p. 11-19.

39. Getz, G.S. and C.A. Reardon, *Diet and murine atherosclerosis.* Arterioscler Thromb Vasc Biol, 2006. **26**(2): p. 242-9.

40. Whitman, S.C., *A practical approach to using mice in atherosclerosis research.* Clin Biochem Rev, 2004. **25**(1): p. 81-93.

41. Allayee, H., A. Ghazalpour, and A.J. Lusis, *Using mice to dissect genetic factors in atherosclerosis.* Arterioscler Thromb Vasc Biol, 2003. **23**(9): p. 1501-9.

42. Zadelaar, S., et al., *Mouse models for atherosclerosis and pharmaceutical modifiers.* Arterioscler Thromb Vasc Biol, 2007. **27**(8): p. 1706-21.

43. Zaragoza, C., et al., *Animal models of cardiovascular diseases.* J Biomed Biotechnol, 2011. **2011**: p. 497841.

44. van Vlijmen, B.J., et al., *Diet-induced hyperlipoproteinemia and atherosclerosis in apolipoprotein E3-Leiden transgenic mice.* J Clin Invest, 1994. **93**(4): p. 1403-10.

45. Knowles, J.W. and N. Maeda, *Genetic modifiers of atherosclerosis in mice.* Arterioscler Thromb Vasc Biol, 2000. **20**(11): p. 2336-45.

46. Ishibashi, S., et al., *Hypercholesterolemia in low density lipoprotein receptor knockout mice and its reversal by adenovirus-mediated gene delivery.* J Clin Invest, 1993. **92**(2): p. 883-93.

47. Sanan, D.A., et al., *Low density lipoprotein receptor-negative mice expressing human apolipoprotein B-100 develop complex atherosclerotic lesions on a chow diet: no accentuation by apolipoprotein(a).* Proc Natl Acad Sci U S A, 1998. **95**(8): p. 4544-9.

48. Chen, Z., et al., *Simvastatin reduces neointimal thickening in low-density lipoprotein receptor-deficient mice after experimental angioplasty without changing plasma lipids.* Circulation, 2002. **106**(1): p. 20-3.

49. Wilson, C., et al., *Salt bridge relay triggers defective LDL receptor binding by a mutant apolipoprotein.* Structure, 1994. **2**(8): p. 713-8.

50. Zhang, S.H., et al., *Spontaneous hypercholesterolemia and arterial lesions in mice lacking apolipoprotein E.* Science, 1992. **258**(5081): p. 468-71.

51. Plump, A.S., et al., *Severe hypercholesterolemia and atherosclerosis in apolipoprotein E-deficient mice created by homologous recombination in ES cells.* Cell, 1992. **71**(2): p. 343-53.

52. Davignon, J., *Apolipoprotein E and atherosclerosis: beyond lipid effect.* Arterioscler Thromb Vasc Biol, 2005. **25**(2): p. 267-9.

53. van den Maagdenberg, A.M., et al., *Transgenic mice carrying the apolipoprotein E3-Leiden gene exhibit hyperlipoproteinemia.* J Biol Chem, 1993. **268**(14): p. 10540-5.

54. Koopal, C., A.D. Marais, and F.L. Visseren, *Familial dysbetalipoproteinemia: an underdiagnosed lipid disorder.* Curr Opin Endocrinol Diabetes Obes, 2017. **24**(2): p. 133-139.

55. Golforoush, P., D.M. Yellon, and S.M. Davidson, *Mouse models of atherosclerosis and their suitability for the study of myocardial infarction.* Basic Res Cardiol, 2020. **115**(6): p. 73.

56. Larsson, M., et al., *Apolipoproteins C-I and C-III inhibit lipoprotein lipase activity by displacement of the enzyme from lipid droplets.* J Biol Chem, 2013. **288**(47): p. 33997-34008.

57. Mahley, R.W. and S.C. Rall, Jr., *Apolipoprotein E: far more than a lipid transport protein.* Annu Rev Genomics Hum Genet, 2000. **1**: p. 507-37.

58. Hofker, M.H., B.J. van Vlijmen, and L.M. Havekes, *Transgenic mouse models to study the role of APOE in hyperlipidemia and atherosclerosis.* Atherosclerosis, 1998. **137**(1): p. 1-11.

59. Leppanen, P., et al., *Characterization of atherosclerotic lesions in apo E3-leiden transgenic mice.* Atherosclerosis, 1998. **136**(1): p. 147-52.

60. Oppi, S., T.F. Luscher, and S. Stein, *Mouse Models for Atherosclerosis Research-Which Is My Line?* Front Cardiovasc Med, 2019. **6**: p. 46.

61. Ignatowski, A., *Influence of animal food on the organsim of rabbits.* Izvest Imper Voennomed Akad St Petersburg, 1908. **16**: p. 154-173.

62. Steinberg, D., *Thematic review series: the pathogenesis of atherosclerosis. An interpretive history of the cholesterol controversy: part I.* J Lipid Res, 2004. **45**(9): p. 1583-93.

63. Fan, J., et al., *Rabbit models for the study of human atherosclerosis: from pathophysiological mechanisms to translational medicine.* Pharmacol Ther, 2015. **146**: p. 104-19.

64. Aikawa, M., et al., *Lipid lowering reduces oxidative stress and endothelial cell activation in rabbit atheroma.* Circulation, 2002. **106**(11): p. 1390-6.

65. Bustos, C., et al., *HMG-CoA reductase inhibition by atorvastatin reduces neointimal inflammation in a rabbit model of atherosclerosis.* J Am Coll Cardiol, 1998. **32**(7): p. 2057-64.

66. Largo, R., et al., *Chronic arthritis aggravates vascular lesions in rabbits with atherosclerosis: a novel model of atherosclerosis associated with chronic inflammation.* Arthritis Rheum, 2008. **58**(9): p. 2723-34.

67. Shimizu, T., et al., *Simple rabbit model of vulnerable atherosclerotic plaque.* Neurol Med Chir (Tokyo), 2009. **49**(8): p. 327-32; discussion 332.

68. Kobayashi, T., T. Ito, and M. Shiomi, *Roles of the WHHL rabbit in translational research on hypercholesterolemia and cardiovascular diseases.* J Biomed Biotechnol, 2011. **2011**: p. 406473.

69. Kita, T., et al., *Delayed clearance of very low density and intermediate density lipoproteins with enhanced conversion to low density lipoprotein in WHHL rabbits.* Proc Natl Acad Sci U S A, 1982. **79**(18): p. 5693-7.

70. Kita, T., et al., *Hepatic uptake of chylomicron remnants in WHHL rabbits: a mechanism genetically distinct from the low density lipoprotein receptor.* Proc Natl Acad Sci U S A, 1982. **79**(11): p. 3623-7.

71. Helft, G., et al., *Atherosclerotic aortic component quantification by noninvasive magnetic resonance imaging: an in vivo study in rabbits.* J Am Coll Cardiol, 2001. **37**(4): p. 1149-54.

72. Shiomi, M., et al., *Development of an animal model for spontaneous myocardial infarction (WHHLMI rabbit).* Arterioscler Thromb Vasc Biol, 2003. **23**(7): p. 1239-44.

73. Shiomi, M., et al., *Cell compositions of coronary and aortic atherosclerotic lesions in WHHL rabbits differ. An immunohistochemical study.* Arterioscler Thromb, 1994. **14**(6): p. 931-7.

74. Tsang, H.G., et al., *Large animal models of cardiovascular disease.* Cell Biochem Funct, 2016. **34**(3): p. 113-32.

75. Granada, J.F., et al., *Porcine models of coronary atherosclerosis and vulnerable plaque for imaging and interventional research.* EuroIntervention, 2009. **5**(1): p. 140-8.

76. Hamada, N., et al., *Tacrolimus-eluting stent inhibits neointimal hyperplasia via calcineurin/NFAT signaling in porcine coronary artery model.* Atherosclerosis, 2010. **208**(1): p. 97-103.

77. O'Donovan, A.N., et al., *Gut microbiome of a porcine model of metabolic syndrome and HF-pEF.* Am J Physiol Heart Circ Physiol, 2020. **318**(3): p. H590-H603.

78. Alviar, C.L., et al., *Impact of adventitial neovascularisation on atherosclerotic plaque composition and vascular remodelling in a porcine model of coronary atherosclerosis.* EuroIntervention, 2010. **5**(8): p. 981-8.

79. Turnbaugh, P.J., et al., *The human microbiome project.* Nature, 2007. **449**(7164): p. 804-10.

80. Mariat, D., et al., *The Firmicutes/Bacteroidetes ratio of the human microbiota changes with age.* BMC Microbiol, 2009. **9**: p. 123.

81. Ley, R.E., et al., *Microbial ecology: human gut microbes associated with obesity.* Nature, 2006. **444**(7122): p. 1022-3.

82. Dreyer, J.L. and A.L. Liebl, *Early colonization of the gut microbiome and its relationship with obesity.* Human Microbiome Journal, 2018. **10**: p. 1-5.

83. Sirisinha, S., *The potential impact of gut microbiota on your health:Current status and future challenges.* Asian Pac J Allergy Immunol, 2016. **34**(4): p. 249-264.

84. Hill, C.J., et al., *Evolution of gut microbiota composition from birth to 24 weeks in the INFANTMET Cohort.* Microbiome, 2017. **5**(1): p. 4.

85. Pastori, D., et al., *Gut-Derived Serum Lipopolysaccharide is Associated With Enhanced Risk of Major Adverse Cardiovascular Events in Atrial Fibrillation: Effect of Adherence to Mediterranean Diet.* J Am Heart Assoc, 2017. **6**(6).

86. Li, J., et al., *Akkermansia Muciniphila Protects Against Atherosclerosis by Preventing Metabolic Endotoxemia-Induced Inflammation in Apoe-/- Mice.* Circulation, 2016. **133**(24): p. 2434-46.

87. Claesson, M.J., et al., *Gut microbiota composition correlates with diet and health in the elderly.* Nature, 2012. **488**(7410): p. 178-84.

88. Woodmansey, E.J., *Intestinal bacteria and ageing.* J Appl Microbiol, 2007. **102**(5): p. 1178-86.

89. Sanduzzi Zamparelli, M., et al., *The Metabolic Role of Gut Microbiota in the Development of Nonalcoholic Fatty Liver Disease and Cardiovascular Disease.* Int J Mol Sci, 2016. **17**(8).

90. Muegge, B.D., et al., *Diet drives convergence in gut microbiome functions across mammalian phylogeny and within humans.* Science, 2011. **332**(6032): p. 970-4.

91. De Filippo, C., et al., *Impact of diet in shaping gut microbiota revealed by a comparative study in children from Europe and rural Africa.* Proc Natl Acad Sci U S A, 2010. **107**(33): p. 14691-6.

92. Arora, T. and F. Bäckhed, *The gut microbiota and metabolic disease: current understanding and future perspectives.* Journal of Internal Medicine, 2016. **280**(4): p. 339-349.

93. Walker, A.W., et al., *Dominant and diet-responsive groups of bacteria within the human colonic microbiota.* ISME J, 2011. **5**(2): p. 220-30.

94. Gregory, J.C., et al., *Transmission of atherosclerosis susceptibility with gut microbial transplantation.* J Biol Chem, 2015. **290**(9): p. 5647-60.

95. Bale, B.F., A.L. Doneen, and D.J. Vigerust, *High-risk periodontal pathogens contribute to the pathogenesis of atherosclerosis.* Postgrad Med J, 2017. **93**(1098): p. 215-220.

96. Hyvarinen, K., et al., *A common periodontal pathogen has an adverse association with both acute and stable coronary artery disease.* Atherosclerosis, 2012. **223**(2): p. 478-84.

97. Koren, O., et al., *Human oral, gut, and plaque microbiota in patients with atherosclerosis.* Proc Natl Acad Sci U S A, 2011. **108 Suppl 1**: p. 4592-8.

98. Emoto, T., et al., *Analysis of Gut Microbiota in Coronary Artery Disease Patients: a Possible Link between Gut Microbiota and Coronary Artery Disease.* J Atheroscler Thromb, 2016. **23**(8): p. 908-21.

99. Jie, Z., et al., *The gut microbiome in atherosclerotic cardiovascular disease.* Nat Commun, 2017. **8**(1): p. 845.

100. Emoto, T., et al., *Characterization of gut microbiota profiles in coronary artery disease patients using data mining analysis of terminal restriction fragment length polymorphism: gut microbiota could be a diagnostic marker of coronary artery disease.* Heart Vessels, 2017. **32**(1): p. 39-46.

101. Kasahara, K. and F.E. Rey, *The emerging role of gut microbial metabolism on cardiovascular disease.* Curr Opin Microbiol, 2019. **50**: p. 64-70.

102. Velmurugan, G., et al., *Blood Microbiota and Circulating Microbial Metabolites in Diabetes and Cardiovascular Disease.* Trends Endocrinol Metab, 2020. **31**(11): p. 835-847.

103. Liu, Y. and M. Dai, *Trimethylamine N-Oxide Generated by the Gut Microbiota Is Associated with Vascular Inflammation: New Insights into Atherosclerosis.* Mediators Inflamm, 2020. **2020**: p. 4634172.

104. Fennema, D., I.R. Phillips, and E.A. Shephard, *Trimethylamine and Trimethylamine N-Oxide, a Flavin-Containing Monooxygenase 3 (FMO3)-Mediated Host-Microbiome Metabolic Axis Implicated in Health and Disease.* Drug Metab Dispos, 2016. **44**(11): p. 1839-1850.

105. Dumas, M.-E., et al., *Metabolic profiling reveals a contribution of gut microbiota to fatty liver phenotype in insulin-resistant mice.* Proceedings of the national academy of sciences, 2006. **103**(33): p. 12511-12516.

106. Koh, A., et al., *From Dietary Fiber to Host Physiology: Short-Chain Fatty Acids as Key Bacterial Metabolites.* Cell, 2016. **165**(6): p. 1332-1345.

107. Yan, Q., et al., *Alterations of the Gut Microbiome in Hypertension.* Front Cell Infect Microbiol, 2017. **7**: p. 381.

108. Ridlon, J.M., et al., *Consequences of bile salt biotransformations by intestinal bacteria.* Gut Microbes, 2016. **7**(1): p. 22-39.

109. Brown, J.M. and S.L. Hazen, *Microbial modulation of cardiovascular disease.* Nat Rev Microbiol, 2018. **16**(3): p. 171-181.

110. Muzio, M., et al., *Toll like receptor family (TLT) and signalling pathway.* Eur Cytokine Netw, 2000. **11**(3): p. 489-90.

111. Ghanim, H., et al., *Orange juice neutralizes the proinflammatory effect of a high-fat, high-carbohydrate meal and prevents endotoxin increase and Toll-like receptor expression.* Am J Clin Nutr, 2010. **91**(4): p. 940-9.

112. Wiedermann, C.J., et al., *Association of endotoxemia with carotid atherosclerosis and cardiovascular disease: prospective results from the Bruneck Study*. J Am Coll Cardiol, 1999. **34**(7): p. 1975-81.

113. FAO/WHO, *Health and Nutritional Properties of Probiotics in Food including Powder Milk with Live Lactic Acid Bacteria. Report of a Joint FAO/WHO Expert Consultation on Evalutation of Health and Nutritional Properties of Probiotics in food including Powder Milk with Live Lactic Acid Bacteria. Córdoba, Argentina*. 1-4 October 2001.

114. Tsai, C.C., et al., *Cholesterol-lowering potentials of lactic acid bacteria based on bile-salt hydrolase activity and effect of potent strains on cholesterol metabolism in vitro and in vivo.* ScientificWorldJournal, 2014. **2014**: p. 690752.

115. Kumar, M., et al., *Cholesterol-lowering probiotics as potential biotherapeutics for metabolic diseases.* Exp Diabetes Res, 2012. **2012**: p. 902917.

116. Ishimwe, N., et al., *The perspective on cholesterol-lowering mechanisms of probiotics.* Mol Nutr Food Res, 2015. **59**(1): p. 94-105.

117. Pereira, D.I. and G.R. Gibson, *Cholesterol assimilation by lactic acid bacteria and bifidobacteria isolated from the human gut.* Appl Environ Microbiol, 2002. **68**(9): p. 4689-93.

118. Ahn, H.Y., et al., *The triglyceride-lowering effect of supplementation with dual probiotic strains, Lactobacillus curvatus HY7601 and Lactobacillus plantarum KY1032: Reduction of fasting plasma lysophosphatidylcholines in nondiabetic and hypertriglyceridemic subjects.* Nutr Metab Cardiovasc Dis, 2015. **25**(8): p. 724-33.

119. Cavallini, D.C., et al., *Probiotic Soy Product Supplemented with Isoflavones Improves the Lipid Profile of Moderately Hypercholesterolemic Men: A Randomized Controlled Trial.* Nutrients, 2016. **8**(1).

120. Rerksuppaphol, S. and L. Rerksuppaphol, *A Randomized Double-blind Controlled Trial of Lactobacillus acidophilus Plus Bifidobacterium bifidum versus Placebo in Patients with Hypercholesterolemia.* J Clin Diagn Res, 2015. **9**(3): p. KC01-4.

121. Davis, C.D., *The Gut Microbiome and Its Role in Obesity.* Nutr Today, 2016. **51**(4): p. 167-174.

122. Schwiertz, A., et al., *Microbiota and SCFA in lean and overweight healthy subjects.* Obesity (Silver Spring), 2010. **18**(1): p. 190-5.

123. Kalliomaki, M., et al., *Early differences in fecal microbiota composition in children may predict overweight.* Am J Clin Nutr, 2008. **87**(3): p. 534-8.

124. Backhed, F., et al., *The gut microbiota as an environmental factor that regulates fat storage.* Proc Natl Acad Sci U S A, 2004. **101**(44): p. 15718-23.

125. He, J., et al., *Short-Chain Fatty Acids and Their Association with Signalling Pathways in Inflammation, Glucose and Lipid Metabolism.* Int J Mol Sci, 2020. **21**(17).

126. Psichas, A., et al., *The short chain fatty acid propionate stimulates GLP-1 and PYY secretion via free fatty acid receptor 2 in rodents.* Int J Obes (Lond), 2015. **39**(3): p. 424-9.

127. Christiansen, C.B., et al., *The impact of short-chain fatty acids on GLP-1 and PYY secretion from the isolated perfused rat colon.* Am J Physiol Gastrointest Liver Physiol, 2018. **315**(1): p. G53-G65.

128. Qi, D., X.L. Nie, and J.J. Zhang, *The effect of probiotics supplementation on blood pressure: a systemic review and meta-analysis.* Lipids Health Dis, 2020. **19**(1): p. 79.

129. Ehlers, P.I., et al., *High blood pressure-lowering and vasoprotective effects of milk products in experimental hypertension.* Br J Nutr, 2011. **106**(9): p. 1353-63.

130. Seppo, L., et al., *A fermented milk high in bioactive peptides has a blood pressure-lowering effect in hypertensive subjects.* Am J Clin Nutr, 2003. **77**(2): p. 326-30.

131. Shakerian, M., et al., *Proteolytic and ACE-inhibitory activities of probiotic yogurt containing non-viable bacteria as affected by different levels of fat, inulin and starter culture.* J Food Sci Technol, 2015. **52**(4): p. 2428-33.

132. Sharafedtinov, K.K., et al., *Hypocaloric diet supplemented with probiotic cheese improves body mass index and blood pressure indices of obese hypertensive patients--a randomized double-blind placebo-controlled pilot study.* Nutr J, 2013. **12**: p. 138.

133. Kadooka, Y., et al., *Effect of Lactobacillus gasseri SBT2055 in fermented milk on abdominal adiposity in adults in a randomised controlled trial.* Br J Nutr, 2013. **110**(9): p. 1696-703.

134. Sanchez, M., et al., *Effect of Lactobacillus rhamnosus CGMCC1.3724 supplementation on weight loss and maintenance in obese men and women.* Br J Nutr, 2014. **111**(8): p. 1507-19.

135. Hoppu, U., et al., *Maternal dietary counseling reduces total and LDL cholesterol postpartum.* Nutrition, 2014. **30**(2): p. 159-64.

136. Asemi, Z., et al., *Effect of daily consumption of probiotic yoghurt on lipid profiles in pregnant women: a randomized controlled clinical trial.* J Matern Fetal Neonatal Med, 2012. **25**(9): p. 1552-6.

137. Tenorio-Jimenez, C., et al., *Lactobacillus reuteri V3401 Reduces Inflammatory Biomarkers and Modifies the Gastrointestinal Microbiome in Adults with Metabolic Syndrome: The PROSIR Study.* Nutrients, 2019. **11**(8).

138. Malik, M., et al., *Lactobacillus plantarum 299v Supplementation Improves Vascular Endothelial Function and Reduces Inflammatory Biomarkers in Men With Stable Coronary Artery Disease.* Circ Res, 2018. **123**(9): p. 1091-1102.

139. Tripolt, N.J., et al., *Effect of Lactobacillus casei Shirota supplementation on trimethylamine-N-oxide levels in patients with metabolic syndrome: An open-label, randomized study.* Atherosclerosis, 2015. **242**(1): p. 141-4.

140. Tenore, G.C., et al., *Lactofermented Annurca Apple Puree as a Functional Food Indicated for the Control of Plasma Lipid and Oxidative Amine Levels: Results from a Randomised Clinical Trial.* Nutrients, 2019. **11**(1).

141. Sun, J. and N. Buys, *Effects of probiotics consumption on lowering lipids and CVD risk factors: a systematic review and meta-analysis of randomized controlled trials.* Ann Med, 2015. **47**(6): p. 430-40.

142. Mo, R., X. Zhang, and Y. Yang, *Effect of probiotics on lipid profiles in hypercholesterolaemic adults: A meta-analysis of randomized controlled trials.* Med Clin (Barc), 2019. **152**(12): p. 473-481.

143. Dixon, A., et al., *Efficacy of Probiotics in Patients of Cardiovascular Disease Risk: a Systematic Review and Meta-analysis.* Curr Hypertens Rep, 2020. **22**(9): p. 74.

144. FAO/WHO, *Health and Nutritional Properties of Probiotics in Food including Powder Milk with Live Lactic Acid Bacteria. Report of a Joint FAO/WHO Expert Consultation on Evalutation of Health and Nutritional Properties of Probiotics in food including Powder Milk with Live Lactic Acid Bacteria. Córdoba, Argentina. 1-4 October 2001.*

145. Metchnikoff, E., *The prolongation of life*. 1908: Putnam.

146. Hemarajata, P. and J. Versalovic, *Effects of probiotics on gut microbiota: mechanisms of intestinal immunomodulation and neuromodulation.* Therap Adv Gastroenterol, 2013. **6**(1): p. 39-51.

147. Jalali, M., et al., *Stability evaluation of freeze-dried Lactobacillus paracasei subsp. tolerance and Lactobacillus delbrueckii subsp. bulgaricus in oral capsules.* Res Pharm Sci, 2012. **7**(1): p. 31-6.

148. Fijan, S., *Microorganisms with claimed probiotic properties: an overview of recent literature.* Int J Environ Res Public Health, 2014. **11**(5): p. 4745-67.

149. Thomas, C.M. and J. Versalovic, *Probiotics-host communication: Modulation of signaling pathways in the intestine.* Gut Microbes, 2010. **1**(3): p. 148-63.

150. Cani, P.D. and N.M. Delzenne, *The role of the gut microbiota in energy metabolism and metabolic disease.* Curr Pharm Des, 2009. **15**(13): p. 1546-58.

151. Hooper, L.V. and J.I. Gordon, *Commensal host-bacterial relationships in the gut.* Science, 2001. **292**(5519): p. 1115-8.

152. Preidis, G.A. and J. Versalovic, *Targeting the human microbiome with antibiotics, probiotics, and prebiotics: gastroenterology enters the metagenomics era.* Gastroenterology, 2009. **136**(6): p. 2015-31.

153. Kukkonen, K., et al., *Probiotics and prebiotic galacto-oligosaccharides in the prevention of allergic diseases: a randomized, double-blind, placebo-controlled trial.* J Allergy Clin Immunol, 2007. **119**(1): p. 192-8.

154. Pena, J.A., et al., *Probiotic Lactobacillus spp. diminish Helicobacter hepaticus-induced inflammatory bowel disease in interleukin-10-deficient mice.* Infect Immun, 2005. **73**(2): p. 912-20.

155. Cavalcanti Neto, M.P., et al., *Gut microbiota and probiotics intervention: A potential therapeutic target for management of cardiometabolic disorders and chronic kidney disease?* Pharmacol Res, 2018. **130**: p. 152-163.

156. Traina, G., et al., *Probiotic mixture supplementation in the preventive management of trinitrobenzenesulfonic acid-induced inflammation in a murine model.* Journal of Biological Regulators and Homeostatic Agents, 2016. **30**(3): p. 895-901.

157. Resta-Lenert, S. and K.E. Barrett, *Probiotics and commensals reverse TNF-alpha- and IFN-gamma-induced dysfunction in human intestinal epithelial cells.* Gastroenterology, 2006. **130**(3): p. 731-46.

158. Amaretti, A., et al., *Antioxidant properties of potentially probiotic bacteria: in vitro and in vivo activities.* Appl Microbiol Biotechnol, 2013. **97**(2): p. 809-17.

159. Wang, Y., et al., *Antioxidant Properties of Probiotic Bacteria.* Nutrients, 2017. **9**(5).

160. Kobatake, E., et al., *Protective effects and functional mechanisms of Lactobacillus gasseri SBT2055 against oxidative stress.* PLoS One, 2017. **12**(5): p. e0177106.

161. Thomas, L.V., K. Suzuki, and J. Zhao, *Probiotics: a proactive approach to health. A symposium report.* British Journal of Nutrition, 2015. **114**(S1): p. S1-S15.

162. Caggianiello, G., M. Kleerebezem, and G. Spano, *Exopolysaccharides produced by lactic acid bacteria: from health-promoting benefits to stress tolerance mechanisms.* Appl Microbiol Biotechnol, 2016. **100**(9): p. 3877-86.

163. Chapot-Chartier, M., V. Monnet, and L. De Vuyst. *Cell walls and exopolysaccharides of lactic acid bacteria*. in *The 10th LAB Symposium. Thirty Years Research on Lactic Acid Bacteria*. 2011. Media Labs Rotterdam.

164. Donot, F., et al., *Microbial exopolysaccharides: Main examples of synthesis, excretion, genetics and extraction.* Carbohydrate polymers., 2012. **87**(2): p. 951-962.

165. Broadbent, J.R., et al., *Biochemistry, Genetics, and Applications of Exopolysaccharide Production in Streptococcus thermophilus: A Review1.* Journal of Dairy Science, 2003. **86**(2): p. 407-423.

166. Ruas-Madiedo, P., J. Hugenholtz, and P. Zoon, *An overview of the functionality of exopolysaccharides produced by lactic acid bacteria.* International Dairy Journal, 2002. **12**(2): p. 163-171.

167. Maeda, H., et al., *Effects of an exopolysaccharide (kefiran) on lipids, blood pressure, blood glucose, and constipation.* Biofactors, 2004. **22**(1-4): p. 197-200.

168. Ryan, P.M., et al., *Sugar-coated: exopolysaccharide producing lactic acid bacteria for food and human health applications.* Food Funct, 2015. **6**(3): p. 679-93.

169. Vinderola, G., et al., *Effects of the oral administration of the exopolysaccharide produced by Lactobacillus kefiranofaciens on the gut mucosal immunity.* Cytokine, 2006. **36**(5-6): p. 254-60.

170. Matsuzaki, C., et al., *Immunomodulating activity of exopolysaccharide-producing Leuconostoc mesenteroides strain NTM048 from green peas.* J Appl Microbiol, 2014. **116**(4): p. 980-9.

171. Nishimura, J., *Exopolysaccharides Produced from Lactobacillus delbrueckii subsp. bulgaricus.* Advances in Microbiology, 2014. **4**(14): p. 1017.

172. London, L.E.E., et al., *Use of Lactobacillus mucosae DPC 6426, an exopolysaccharide-producing strain, positively influences the techno-functional properties of yoghurt.* International Dairy Journal, 2015. **40**: p. 33-38.

173. Ruas-Madiedo, P. and C.G. de los Reyes-Gavilan, *Invited review: methods for the screening, isolation, and characterization of exopolysaccharides produced by lactic acid bacteria.* J Dairy Sci, 2005. **88**(3): p. 843-56.

174. London, L.E., et al., *Characterization of a bovine isolate Lactobacillus mucosae DPC 6426 which produces an exopolysaccharide composed predominantly of mannose residues.* J Appl Microbiol, 2014. **117**(2): p. 509-17.

175. Montel Mendoza, G., et al., *Survival and beneficial properties of lactic acid bacteria from raniculture subjected to freeze-drying and storage.* J Appl Microbiol, 2014. **116**(1): p. 157-66.

176. Berner, D. and H. Viernstein, *Effect of protective agents on the viability of Lactococcus lactis subjected to freeze-thawing and freeze-drying.* Scientia Pharmaceutica, 2006. **74**(3): p. 137-149.

177. Zamora, L.M., C. Carretero, and D. Parés, *Comparative Survival Rates of Lactic Acid Bacteria Isolated from Blood, Following Spray-drying and Freeze-drying.* Food Science and Technology International, 2006. **12**(1): p. 77-84.

178. Fonseca, F., S. Cenard, and S. Passot, *Freeze-drying of lactic acid bacteria.* Methods Mol Biol, 2015. **1257**: p. 477-88.

179. Ren, H., J. Zentek, and W. Vahjen, *Optimization of Production Parameters for Probiotic Lactobacillus Strains as Feed Additive.* Molecules (Basel, Switzerland), 2019. **24**(18): p. 3286.

180. Zacharof, M., R. Lovitt, and K. Ratanapongleka, *Optimization of Growth Conditions for Intensive Propagation, Growth Development and Lactic Acid Production of Selected Strains of'Lactobacilli'.* Engineering Our Future: Are We up to the Challenge?: 27-30 September 2009, Burswood Entertainment Complex, 2009: p. 1830.

181. FAO/WHO. *Interim summary of conclusions and dietary recommendations on total fat & fatty acids. From the Joint FAO/WHO Expert Consultation on Fats and Fatty Acids in Human Nutrition,10–14 November 2008, WHO, Geneva. Available from: http://www.who.int/nutrition/topics/FFA_summary_rec_conclusion.pdf?ua=1*

182. WHO. *Cardiovascular diseases (CVDs) Fact Sheet, Geneva, Switzerland*. May 2017; Available from: https://www.who.int/news-room/fact-sheets/detail/cardiovascular-diseases-(cvds).

183. CDC. *Know Your Risk for Heart Disease*. December 2019; Available from: https://www.cdc.gov/heartdisease/risk_factors.htm.

184. Brinks, J., et al., *Lifestyle Modification in Secondary Prevention: Beyond Pharmacotherapy.* Am J Lifestyle Med, 2017. **11**(2): p. 137-152.

185. Gibson, G.R., et al., *Expert consensus document: The International Scientific Association for Probiotics and Prebiotics (ISAPP) consensus statement on the definition and scope of prebiotics.* Nat Rev Gastroenterol Hepatol, 2017. **14**(8): p. 491-502.

186. John, G.K. and G.E. Mullin, *The Gut Microbiome and Obesity.* Curr Oncol Rep, 2016. **18**(7): p. 45.

187. Ooi, L.G. and M.T. Liong, *Cholesterol-lowering effects of probiotics and prebiotics: a review of in vivo and in vitro findings.* Int J Mol Sci, 2010. **11**(6): p. 2499-522.

188. Wang, L., et al., *The effects of probiotics on total cholesterol: A meta-analysis of randomized controlled trials.* Medicine (Baltimore), 2018. **97**(5): p. e9679.

189. Ryan, P.M., et al., *Microbiome and metabolome modifying effects of several cardiovascular disease interventions in apo-E(-/-) mice.* Microbiome, 2017. **5**(1): p. 30.

190. Yu, Z. and M. Morrison, *Improved extraction of PCR-quality community DNA from digesta and fecal samples.* Biotechniques, 2004. **36**(5): p. 808-12.

191. Fouhy, F., et al., *The effects of freezing on faecal microbiota as determined using MiSeq sequencing and culture-based investigations.* PLoS One, 2015. **10**(3): p. e0119355.

192. Caporaso, J.G., et al., *QIIME allows analysis of high-throughput community sequencing data.* Nat Methods, 2010. **7**(5): p. 335-6.

193. Anesi, A., et al., *Metabolic Profiling of Human Plasma and Urine, Targeting Tryptophan, Tyrosine and Branched Chain Amino Acid Pathways.* Metabolites, 2019. **9**(11).

194. Rinninella, E., et al., *What is the Healthy Gut Microbiota Composition? A Changing Ecosystem across Age, Environment, Diet, and Diseases.* Microorganisms, 2019. **7**(1).

195. Watanabe, H., et al., *Metabolic syndrome and risk of development of atrial fibrillation: the Niigata preventive medicine study.* Circulation, 2008. **117**(10): p. 1255-1260.

196. Sanz, Y., et al., *Understanding the role of gut microbiome in metabolic disease risk.* Pediatr Res, 2015. **77**(1-2): p. 236-44.

197. Hansen, T.H., et al., *The gut microbiome in cardio-metabolic health.* Genome Med, 2015. **7**(1): p. 33.

198. Wong, S.K., et al., *Animal models of metabolic syndrome: a review.* Nutr Metab (Lond), 2016. **13**: p. 65.

199. Hugenholtz, F. and W.M. de Vos, *Mouse models for human intestinal microbiota research: a critical evaluation.* Cell Mol Life Sci, 2018. **75**(1): p. 149-160.

200. Meurens, F., et al., *The pig: a model for human infectious diseases.* Trends Microbiol, 2012. **20**(1): p. 50-7.

201. Aigner, B., et al., *Transgenic pigs as models for translational biomedical research.* J Mol Med (Berl), 2010. **88**(7): p. 653-64.

202. Schwarzl, M., et al., *A porcine model of hypertensive cardiomyopathy: implications for heart failure with preserved ejection fraction.* Am J Physiol Heart Circ Physiol, 2015. **309**(9): p. H1407-18.

203. Lang, R.M., et al., *Recommendations for cardiac chamber quantification by echocardiography in adults: an update from the American Society of Echocardiography and the European Association of Cardiovascular Imaging.* J Am Soc Echocardiogr, 2015. **28**(1): p. 1-39 e14.

204. Lang, R.M., et al., *Recommendations for chamber quantification: a report from the American Society of Echocardiography's Guidelines and Standards Committee and the Chamber Quantification Writing Group, developed in conjunction with the European Association of Echocardiography, a branch of the European Society of Cardiology.* J Am Soc Echocardiogr, 2005. **18**(12): p. 1440-63.

205. Nagueh, S.F., et al., *Recommendations for the evaluation of left ventricular diastolic function by echocardiography.* Eur J Echocardiogr, 2009. **10**(2): p. 165-93.

206. Pellikka, P.A., et al., *American Society of Echocardiography recommendations for performance, interpretation, and application of stress echocardiography.* J Am Soc Echocardiogr, 2007. **20**(9): p. 1021-41.

207. MS-Omics, *GC-MS Metabolomics with Methyl Chloroformate (MCF) (Online).*

208. Xia, J. and D.S. Wishart, *Using MetaboAnalyst 3.0 for Comprehensive Metabolomics Data Analysis.* Curr Protoc Bioinformatics, 2016. **55**: p. 14 10 1-14 10 91.

209. Le Cao, K.A., S. Boitard, and P. Besse, *Sparse PLS discriminant analysis: biologically relevant feature selection and graphical displays for multiclass problems.* BMC Bioinformatics, 2011. **12**: p. 253.

210. Duvallet, C., et al., *Meta-analysis of gut microbiome studies identifies disease-specific and shared responses.* Nat Commun, 2017. **8**(1): p. 1784.

211. Everard, A., et al., *Cross-talk between Akkermansia muciniphila and intestinal epithelium controls diet-induced obesity.* Proc Natl Acad Sci U S A, 2013. **110**(22): p. 9066-71.

212. Hildebrandt, M.A., et al., *High-fat diet determines the composition of the murine gut microbiome independently of obesity.* Gastroenterology, 2009. **137**(5): p. 1716-24 e1-2.

213. Shin, N.R., T.W. Whon, and J.W. Bae, *Proteobacteria: microbial signature of dysbiosis in gut microbiota.* Trends Biotechnol, 2015. **33**(9): p. 496-503.

214. Athyros, V.G., et al., *Dyslipidaemia of obesity, metabolic syndrome and type 2 diabetes mellitus: the case for residual risk reduction after statin treatment.* Open Cardiovasc Med J, 2011. **5**: p. 24-34.

215. Cornier, M.A., et al., *The metabolic syndrome.* Endocr Rev, 2008. **29**(7): p. 777-822.

216. Gayoso-Diz, P., et al., *Insulin resistance (HOMA-IR) cut-off values and the metabolic syndrome in a general adult population: effect of gender and age: EPIRCE cross-sectional study.* BMC Endocr Disord, 2013. **13**: p. 47.

217. Ryan, P.M., C. Stanton, and N.M. Caplice, *Bile acids at the cross-roads of gut microbiome-host cardiometabolic interactions.* Diabetol Metab Syndr, 2017. **9**: p. 102.

218. Wilck, N., et al., *Salt-responsive gut commensal modulates TH17 axis and disease.* Nature, 2017. **551**(7682): p. 585-589.

219. Xiao, L., et al., *A reference gene catalogue of the pig gut microbiome.* Nat Microbiol, 2016. **1**: p. 16161.

220. Al-Mashhadi, A.L., et al., *Diet-Induced Abdominal Obesity, Metabolic Changes, and Atherosclerosis in Hypercholesterolemic Minipigs.* J Diabetes Res, 2018. **2018**: p. 6823193.

221. Li, S.J., et al., *Development of a dietary-induced metabolic syndrome model using miniature pigs involvement of AMPK and SIRT1.* Eur J Clin Invest, 2015. **45**(1): p. 70-80.

222. Neeb, Z.P., et al., *Metabolic syndrome and coronary artery disease in Ossabaw compared with Yucatan swine.* Comp Med, 2010. **60**(4): p. 300-15.

223. Nordestgaard, B.G. and A. Varbo, *Triglycerides and cardiovascular disease.* Lancet, 2014. **384**(9943): p. 626-635.

224. Miccoli, R., et al., *Prevalence of the metabolic syndrome among Italian adults according to ATP III definition.* Nutr Metab Cardiovasc Dis, 2005. **15**(4): p. 250-4.

225. Angulo, P., *Nonalcoholic fatty liver disease.* N Engl J Med, 2002. **346**(16): p. 1221-31.

226. Chatrath, H., R. Vuppalanchi, and N. Chalasani, *Dyslipidemia in patients with nonalcoholic fatty liver disease.* Semin Liver Dis, 2012. **32**(1): p. 22-9.

227. Mai, V., et al., *Monitoring of stool microbiota in subjects with diarrhea indicates distortions in composition.* J Clin Microbiol, 2006. **44**(12): p. 4550-2.

228. Manichanh, C., et al., *Reduced diversity of faecal microbiota in Crohn's disease revealed by a metagenomic approach.* Gut, 2006. **55**(2): p. 205-11.

229. Murphy, S.F., J.H. Kwon, and D.L. Boone, *Novel players in inflammatory bowel disease pathogenesis.* Curr Gastroenterol Rep, 2012. **14**(2): p. 146-52.

230. Turnbaugh, P.J., et al., *A core gut microbiome in obese and lean twins.* Nature, 2009. **457**(7228): p. 480-4.

231. Le Chatelier, E., et al., *Richness of human gut microbiome correlates with metabolic markers.* Nature, 2013. **500**(7464): p. 541-6.

232. Lu, D., et al., *Host contributes to longitudinal diversity of fecal microbiota in swine selected for lean growth.* Microbiome, 2018. **6**(1): p. 4.

233. Fitzmaurice, C., et al., *The Global Burden of Cancer 2013.* JAMA Oncol, 2015. **1**(4): p. 505-27.

234. Musigdilok, V.V., et al., *Assessing American Red Cross First Aid mobile app user trends: Implications for resilience.* Am J Disaster Med, 2015. **10**(4): p. 273-83.

235. Pallister, T., et al., *Hippurate as a metabolomic marker of gut microbiome diversity: Modulation by diet and relationship to metabolic syndrome.* Sci Rep, 2017. **7**(1): p. 13670.

236. Zhang, C., et al., *Interactions between gut microbiota, host genetics and diet relevant to development of metabolic syndromes in mice.* ISME J, 2010. **4**(2): p. 232-41.

237. Fu, J., et al., *The Gut Microbiome Contributes to a Substantial Proportion of the Variation in Blood Lipids.* Circ Res, 2015. **117**(9): p. 817-24.

238. He, Y., et al., *Linking gut microbiota, metabolic syndrome and economic status based on a population-level analysis.* Microbiome, 2018. **6**(1): p. 172.

239. Ferrer, M., et al., *Microbiota from the distal guts of lean and obese adolescents exhibit partial functional redundancy besides clear differences in community structure.* Environ Microbiol, 2013. **15**(1): p. 211-26.

240. Pu, S., et al., *Interactions between Obesity Status and Dietary Intake of Monounsaturated and Polyunsaturated Oils on Human Gut Microbiome Profiles in the Canola Oil Multicenter Intervention Trial (COMIT).* Front Microbiol, 2016. **7**: p. 1612.

241. Feng, W., H. Ao, and C. Peng, *Gut Microbiota, Short-Chain Fatty Acids, and Herbal Medicines.* Front Pharmacol, 2018. **9**: p. 1354.

242. Lippert, K., et al., *Gut microbiota dysbiosis associated with glucose metabolism disorders and the metabolic syndrome in older adults.* Benef Microbes, 2017. **8**(4): p. 545-556.

243. Gargari, G., et al., *Consumption of a Bifidobacterium bifidum Strain for 4 Weeks Modulates Dominant Intestinal Bacterial Taxa and Fecal Butyrate in Healthy Adults.* Appl Environ Microbiol, 2016. **82**(19): p. 5850-9.

244. Anderson, J.W. and S.E. Gilliland, *Effect of fermented milk (yogurt) containing Lactobacillus acidophilus L1 on serum cholesterol in hypercholesterolemic humans.* J Am Coll Nutr, 1999. **18**(1): p. 43-50.

245. Cani, P.D., et al., *Selective increases of bifidobacteria in gut microflora improve high-fat-diet-induced diabetes in mice through a mechanism associated with endotoxaemia.* Diabetologia, 2007. **50**(11): p. 2374-83.

246. Derrien, M., C. Belzer, and W.M. de Vos, *Akkermansia muciniphila and its role in regulating host functions.* Microb Pathog, 2017. **106**: p. 171-181.

247. Schneeberger, M., et al., *Akkermansia muciniphila inversely correlates with the onset of inflammation, altered adipose tissue metabolism and metabolic disorders during obesity in mice.* Sci Rep, 2015. **5**: p. 16643.

248. Dhiman, R.K., *Gut microbiota, inflammation and hepatic encephalopathy: a puzzle with a solution in sight.* J Clin Exp Hepatol, 2012. **2**(3): p. 207-10.

249. Gevers, D., et al., *The treatment-naive microbiome in new-onset Crohn's disease.* Cell Host Microbe, 2014. **15**(3): p. 382-392.

250. Blais Lecours, P., et al., *Increased prevalence of Methanosphaera stadtmanae in inflammatory bowel diseases.* PLoS One, 2014. **9**(2): p. e87734.

251. Yun, Y., et al., *Comparative analysis of gut microbiota associated with body mass index in a large Korean cohort.* BMC Microbiol, 2017. **17**(1): p. 151.

252. Zhang, H., et al., *Human gut microbiota in obesity and after gastric bypass.* Proc Natl Acad Sci U S A, 2009. **106**(7): p. 2365-70.

253. Ciubotaru, I., et al., *Significant differences in fecal microbiota are associated with various stages of glucose tolerance in African American male veterans.* Transl Res, 2015. **166**(5): p. 401-11.

254. Mohammadi, M., et al., *Clinical Significance of Serum IL-6 and TNF-alpha Levels in Patients with Metabolic Syndrome.* Rep Biochem Mol Biol, 2017. **6**(1): p. 74-79.

255. Fang, L., et al., *Systemic inflammation is associated with myocardial fibrosis, diastolic dysfunction, and cardiac hypertrophy in patients with hypertrophic cardiomyopathy.* Am J Transl Res, 2017. **9**(11): p. 5063-5073.

256. Gullestad, L., et al., *Inflammatory cytokines in heart failure: mediators and markers.* Cardiology, 2012. **122**(1): p. 23-35.

257. Gonzalez-Dominguez, E., et al., *CD163L1 and CLEC5A discriminate subsets of human resident and inflammatory macrophages in vivo.* J Leukoc Biol, 2015. **98**(4): p. 453-66.

258. Bieghs, V., et al., *Role of scavenger receptor A and CD36 in diet-induced nonalcoholic steatohepatitis in hyperlipidemic mice.* Gastroenterology, 2010. **138**(7): p. 2477-86, 2486 e1-3.

259. Marra, F. and F. Tacke, *Roles for chemokines in liver disease.* Gastroenterology, 2014. **147**(3): p. 577-594 e1.

260. Tacke, F., *Targeting hepatic macrophages to treat liver diseases.* J Hepatol, 2017. **66**(6): p. 1300-1312.

261. Stojsavljevic, S., et al., *Adipokines and proinflammatory cytokines, the key mediators in the pathogenesis of nonalcoholic fatty liver disease.* World J Gastroenterol, 2014. **20**(48): p. 18070-91.

262. Staels, B. and V.A. Fonseca, *Bile acids and metabolic regulation: mechanisms and clinical responses to bile acid sequestration.* Diabetes Care, 2009. **32 Suppl 2**: p. S237-45.

263. Fukiya, S., et al., *Conversion of cholic acid and chenodeoxycholic acid into their 7-oxo derivatives by Bacteroides intestinalis AM-1 isolated from human feces.* FEMS Microbiol Lett, 2009. **293**(2): p. 263-70.

264. Niu, Q., et al., *Dynamic distribution of the gut microbiota and the relationship with apparent crude fiber digestibility and growth stages in pigs.* Sci Rep, 2015. **5**: p. 9938.

265. Gerard, P., *Metabolism of cholesterol and bile acids by the gut microbiota.* Pathogens, 2013. **3**(1): p. 14-24.

266. Everard, A., et al., *Microbiome of prebiotic-treated mice reveals novel targets involved in host response during obesity.* ISME J, 2014. **8**(10): p. 2116-30.

267. Geurts, L., et al., *Altered gut microbiota and endocannabinoid system tone in obese and diabetic leptin-resistant mice: impact on apelin regulation in adipose tissue.* Front Microbiol, 2011. **2**: p. 149.

268. Luo, Y., et al., *Microbiota from Obese Mice Regulate Hematopoietic Stem Cell Differentiation by Altering the Bone Niche.* Cell Metab, 2015. **22**(5): p. 886-94.

269. Bhatnagar, S., H.A. Damron, and F.B. Hillgartner, *Fibroblast growth factor-19, a novel factor that inhibits hepatic fatty acid synthesis.* J Biol Chem, 2009. **284**(15): p. 10023-33.

270. Holt, J.A., et al., *Definition of a novel growth factor-dependent signal cascade for the suppression of bile acid biosynthesis.* Genes Dev, 2003. **17**(13): p. 1581-91.

271. Potthoff, M.J., S.A. Kliewer, and D.J. Mangelsdorf, *Endocrine fibroblast growth factors 15/19 and 21: from feast to famine.* Genes Dev, 2012. **26**(4): p. 312-24.

272. Inagaki, T., et al., *Fibroblast growth factor 15 functions as an enterohepatic signal to regulate bile acid homeostasis.* Cell Metab, 2005. **2**(4): p. 217-25.

273. Bodogai, M., et al., *Commensal bacteria contribute to insulin resistance in aging by activating innate B1a cells.* Sci Transl Med, 2018. **10**(467).

274. Murray, C.J., et al., *Global, regional, and national disability-adjusted life years (DALYs) for 306 diseases and injuries and healthy life expectancy (HALE) for 188 countries, 1990-2013: quantifying the epidemiological transition.* Lancet, 2015. **386**(10009): p. 2145-91.

275. Hopkins, M.J. and G.T. Macfarlane, *Changes in predominant bacterial populations in human faeces with age and with Clostridium difficile infection.* J Med Microbiol, 2002. **51**(5): p. 448-454.

276. Li, Y., et al., *Antibiotic-Induced Elevations of Plasma Bile Acids in Rats Independent of Bsep Inhibition.* Toxicol Sci, 2017. **157**(1): p. 30-40.

277. Zhou, M., et al., *Engineered FGF19 eliminates bile acid toxicity and lipotoxicity leading to resolution of steatohepatitis and fibrosis in mice.* Hepatol Commun, 2017. **1**(10): p. 1024-1042.

278. Gallego-Escuredo, J.M., et al., *Opposite alterations in FGF21 and FGF19 levels and disturbed expression of the receptor machinery for endocrine FGFs in obese patients.* Int J Obes (Lond), 2015. **39**(1): p. 121-9.

279. Hao, Y., et al., *Serum levels of fibroblast growth factor 19 are inversely associated with coronary artery disease in chinese individuals.* PLoS One, 2013. **8**(8): p. e72345.

280. Mulla, C.M., et al., *Plasma FGF-19 Levels are Increased in Patients with Post-Bariatric Hypoglycemia.* Obes Surg, 2019. **29**(7): p. 2092-2099.

281. Moon, J., et al., *Alterations in Circulating Amino Acid Metabolite Ratio Associated with Arginase Activity Are Potential Indicators of Metabolic Syndrome: The Korean Genome and Epidemiology Study.* Nutrients, 2017. **9**(7).

282. Aglago, E.K., et al., *Association between serum phospholipid fatty acid levels and adiposity in Mexican women.* J Lipid Res, 2017. **58**(7): p. 1462-1470.

283. Lovejoy, J.C., et al., *Relationship of dietary fat and serum cholesterol ester and phospholipid fatty acids to markers of insulin resistance in men and women with a range of glucose tolerance.* Metabolism, 2001. **50**(1): p. 86-92.

284. Palomer, X., et al., *Palmitic and Oleic Acid: The Yin and Yang of Fatty Acids in Type 2 Diabetes Mellitus.* Trends Endocrinol Metab, 2018. **29**(3): p. 178-190.

285. Ebbesson, S.O., et al., *Fatty acids linked to cardiovascular mortality are associated with risk factors.* Int J Circumpolar Health, 2015. **74**: p. 28055.

286. Rodriguez-Carrio, J., et al., *Free Fatty Acids Profiles Are Related to Gut Microbiota Signatures and Short-Chain Fatty Acids.* Front Immunol, 2017. **8**: p. 823.

287. Afshin, A., et al., *Health Effects of Overweight and Obesity in 195 Countries over 25 Years.* N Engl J Med, 2017. **377**(1): p. 13-27.

288. Zou, J., et al., *Fiber-Mediated Nourishment of Gut Microbiota Protects against Diet-Induced Obesity by Restoring IL-22-Mediated Colonic Health.* Cell Host Microbe, 2018. **23**(1): p. 41-53 e4.

289. Everard, A. and P.D. Cani, *Diabetes, obesity and gut microbiota.* Best Pract Res Clin Gastroenterol, 2013. **27**(1): p. 73-83.

290. Schele, E., et al., *Regulation of body fat mass by the gut microbiota: Possible mediation by the brain.* Peptides, 2016. **77**: p. 54-9.

291. Rabot, S., et al., *Germ-free C57BL/6J mice are resistant to high-fat-diet-induced insulin resistance and have altered cholesterol metabolism.* FASEB J, 2010. **24**(12): p. 4948-59.

292. Chassaing, B., et al., *Colonic Microbiota Encroachment Correlates With Dysglycemia in Humans.* Cell Mol Gastroenterol Hepatol, 2017. **4**(2): p. 205-221.

293. Sonnenburg, E.D. and J.L. Sonnenburg, *Starving our microbial self: the deleterious consequences of a diet deficient in microbiota-accessible carbohydrates.* Cell Metab, 2014. **20**(5): p. 779-786.

294. Cummings, J.H. and A. Engineer, *Denis Burkitt and the origins of the dietary fibre hypothesis.* Nutr Res Rev, 2018. **31**(1): p. 1-15.

295. Chen, J.P., et al., *Dietary Fiber and Metabolic Syndrome: A Meta-Analysis and Review of Related Mechanisms.* Nutrients, 2017. **10**(1).

296. Koç, F., et al., *The public health rationale for increasing dietary fibre: Health benefits with a focus on gut microbiota.* Nutrition Bulletin, 2020. **45**(3): p. 294-308.

297. Swanson, K.S., et al., *The International Scientific Association for Probiotics and Prebiotics (ISAPP) consensus statement on the definition and scope of synbiotics.* Nat Rev Gastroenterol Hepatol, 2020. **17**(11): p. 687-701.

298. Pandey, K.R., S.R. Naik, and B.V. Vakil, *Probiotics, prebiotics and synbiotics- a review.* J Food Sci Technol, 2015. **52**(12): p. 7577-87.

299. Núñez-Sánchez, M.A., et al., *Metabolic syndrome and synbiotic targeting of the gut microbiome.* Current Opinion in Food Science, 2021. **41**: p. 60-69.

300. Johnsen, L.G., et al., *Gas chromatography - mass spectrometry data processing made easy.* J Chromatogr A, 2017. **1503**: p. 57-64.

301. Fouhy, F., et al., *The effects of freezing on faecal microbiota as determined using MiSeq sequencing and culture-based investigations.* PLoS One, 2015. **10**(3): p. e0119355.

302. Turnbaugh, P.J., et al., *An obesity-associated gut microbiome with increased capacity for energy harvest.* Nature, 2006. **444**(7122): p. 1027-31.

303. David, L.A., et al., *Diet rapidly and reproducibly alters the human gut microbiome.* Nature, 2014. **505**(7484): p. 559-63.

304. Haro, C., et al., *The gut microbial community in metabolic syndrome patients is modified by diet.* J Nutr Biochem, 2016. **27**: p. 27-31.

305. Kim, K. and Y. Chang, *Association of dietary fiber intake with metabolic syndrome among adult cancer survivors: a population-based cross-sectional study.* Sci Rep, 2021. **11**(1): p. 11794.

306. Flint, H.J., et al., *Microbial degradation of complex carbohydrates in the gut.* Gut Microbes, 2012. **3**(4): p. 289-306.

307. de la Cuesta-Zuluaga, J., et al., *Higher Fecal Short-Chain Fatty Acid Levels Are Associated with Gut Microbiome Dysbiosis, Obesity, Hypertension and Cardiometabolic Disease Risk Factors.* Nutrients, 2018. **11**(1).

308. Oliver, A., et al., *High fiber, whole foods dietary intervention alters the human gut microbiome but not fecal short-chain fatty acids.* bioRxiv, 2021: p. 2021.02.04.429869.

309. Alexander, C., et al., *Perspective: Physiologic Importance of Short-Chain Fatty Acids from Nondigestible Carbohydrate Fermentation.* Adv Nutr, 2019. **10**(4): p. 576-589.

310. Tomas, J., et al., *High-fat diet modifies the PPAR-gamma pathway leading to disruption of microbial and physiological ecosystem in murine small intestine.* Proc Natl Acad Sci U S A, 2016. **113**(40): p. E5934-E5943.

311. Nobel, Y.R., et al., *Increasing Dietary Fiber Intake Is Associated with a Distinct Esophageal Microbiome.* Clin Transl Gastroenterol, 2018. **9**(10): p. 199.

312. Yamamura, R., et al., *Associations of gut microbiota, dietary intake, and serum short-chain fatty acids with fecal short-chain fatty acids.* Biosci Microbiota Food Health, 2020. **39**(1): p. 11-17.

313. Tavella, T., et al., *Elevated gut microbiome abundance of Christensenellaceae, Porphyromonadaceae and Rikenellaceae is associated with reduced visceral adipose tissue and healthier metabolic profile in Italian elderly.* Gut Microbes, 2021. **13**(1): p. 1-19.

314. Kverka, M., et al., *Oral administration of Parabacteroides distasonis antigens attenuates experimental murine colitis through modulation of immunity and microbiota composition.* Clin Exp Immunol, 2011. **163**(2): p. 250-9.

315. Wang, K., et al., *Parabacteroides distasonis Alleviates Obesity and Metabolic Dysfunctions via Production of Succinate and Secondary Bile Acids.* Cell Rep, 2019. **26**(1): p. 222-235 e5.

316. Yang, F., et al., *Complete Genome Sequence of a Parabacteroides distasonis Strain (CavFT hAR46) Isolated from a Gut Wall-Cavitating Microlesion in a Patient with Severe Crohn's Disease.* Microbiol Resour Announc, 2019. **8**(36).

317. Lopetuso, L.R., et al., *Gut Microbiota in Health, Diverticular Disease, Irritable Bowel Syndrome, and Inflammatory Bowel Diseases: Time for Microbial Marker of Gastrointestinal Disorders.* Dig Dis, 2018. **36**(1): p. 56-65.

318. Murugesan, S., et al., *Study of the diversity and short-chain fatty acids production by the bacterial community in overweight and obese Mexican children.* Eur J Clin Microbiol Infect Dis, 2015. **34**(7): p. 1337-46.

319. Iljazovic, A., et al., *Perturbation of the gut microbiome by Prevotella spp. enhances host susceptibility to mucosal inflammation.* Mucosal Immunol, 2021. **14**(1): p. 113-124.

320. Larsen, J.M., *The immune response to Prevotella bacteria in chronic inflammatory disease.* Immunology, 2017. **151**(4): p. 363-374.

321. Alberti, G., et al., *The IDF consensus worldwide definition of the metabolic syndrome.* Brussels: International Diabetes Federation, 2006. **23**(5): p. 469-80.

322. Wang, P.X., et al., *Gut microbiota and metabolic syndrome.* Chin Med J (Engl), 2020. **133**(7): p. 808-816.

323. Cani, P.D., et al., *Metabolic endotoxemia initiates obesity and insulin resistance.* Diabetes, 2007. **56**(7): p. 1761-72.

324. Turnbaugh, P.J. and J.I. Gordon, *The core gut microbiome, energy balance and obesity.* J Physiol, 2009. **587**(Pt 17): p. 4153-8.

325. Dabke, K., G. Hendrick, and S. Devkota, *The gut microbiome and metabolic syndrome.* J Clin Invest, 2019. **129**(10): p. 4050-4057.

326. Arora, T. and R. Sharma, *Fermentation potential of the gut microbiome: implications for energy homeostasis and weight management.* Nutr Rev, 2011. **69**(2): p. 99-106.

327. Drosos, I., A. Tavridou, and G. Kolios, *New aspects on the metabolic role of intestinal microbiota in the development of atherosclerosis.* Metabolism, 2015. **64**(4): p. 476-81.

328. Tsai, F. and W.J. Coyle, *The microbiome and obesity: is obesity linked to our gut flora?* Curr Gastroenterol Rep, 2009. **11**(4): p. 307-13.

329. Ryan, P.M., et al., *Lactobacillus mucosae DPC 6426 as a bile-modifying and immunomodulatory microbe.* BMC Microbiol, 2019. **19**(1): p. 33.

330. Lund, A., et al., *Plasma kynurenines and prognosis in patients with heart failure.* PLoS One, 2020. **15**(1): p. e0227365.

331. Mohorko, N., et al., *Elevated serum levels of cysteine and tyrosine: early biomarkers in asymptomatic adults at increased risk of developing metabolic syndrome.* Biomed Res Int, 2015. **2015**: p. 418681.

332. Mitrega, K., et al., *Beneficial effects of l-leucine and l-valine on arrhythmias, hemodynamics and myocardial morphology in rats.* Pharmacol Res, 2011. **64**(3): p. 218-25.

333. Dou, L., et al., *The cardiovascular effect of the uremic solute indole-3 acetic acid.* J Am Soc Nephrol, 2015. **26**(4): p. 876-87.

334. Konje, V.C., et al., *Tryptophan levels associate with incident cardiovascular disease in chronic kidney disease.* Clin Kidney J, 2021. **14**(4): p. 1097-1105.

335. Ghasemi, A., et al., *Cut-off points of homeostasis model assessment of insulin resistance, beta-cell function, and fasting serum insulin to identify future type 2 diabetes: Tehran Lipid and Glucose Study.* Acta Diabetol, 2015. **52**(5): p. 905-15.

336. Cusi, K., *Role of obesity and lipotoxicity in the development of nonalcoholic steatohepatitis: pathophysiology and clinical implications.* Gastroenterology, 2012. **142**(4): p. 711-725 e6.

337. Singh, R.P., et al., *High-Fat Diet Induced Alteration of Mice Microbiota and the Functional Ability to Utilize Fructooligosaccharide for Ethanol Production.* Front Cell Infect Microbiol, 2020. **10**: p. 376.

Acknowledgements

Thank you to all my supervisors for providing me with support and guidance throughout the PhD process. In particular to Professor Catherine Stanton and Professor Paul Ross, for giving me the opportunity to pursue this PhD with them and for all your help and support you have provided throughout the years.

To Professor Noel Caplice and all the members of the Centre for Research in Vascular Biology team, thank you for giving me the opportunity to work with an extremely talented group of people.

To my APC2 and Teagasc lab colleagues, both past and present, thank you for the continued guidance and support you all gave to me throughout the years, I would not have been able to do it without you all.

Finally, to my family and friends, thank you for the overwhelming support you have given me throughout the whole PhD process. It has been tough, but with all of your continued support and encouragement, we got there in the end.